UNIVERSIDAD NACIONAL AUTÓNOMA DE MÉXICO

DOCTORADO EN CIENCIAS BIOMÉDICAS
INSTITUTO DE INVESTIGACIONES BIOMÉDICAS

ESTUDIO DE LOS MECANISMOS INVOLUCRADOS EN LA LESIÓN RENAL AGUDA Y SU PROGRESIÓN A ENFERMEDAD RENAL CRÓNICA: DIAGNÓSTICO Y TERAPÉUTICA

TESIS
QUE PARA OPTAR POR EL GRADO DE:
DOCTOR EN CIENCIAS

PRESENTA:
JONATAN BARRERA CHIMAL

DIRECTOR DE TESIS:
DRA. NORMA ARACELI BOBADILLA SANDOVAL
INSTITUTO DE INVESTIGACIONES BIOMÉDICAS

COMITÉ TUTOR:
DRA. MARÍA EUGENIA GONSEBATT BONAPARTE
INSTITUTO DE INVESTIGACIONES BIOMÉDICAS

DR. JULIO EDUARDO ROQUE MORÁN ANDRADE
INSTITUTO DE FISIOLOGÍA CÉLULAR

MÉXICO, D. F. MAYO DE 2013

R E C O N O C I M I E N T O S

El presente trabajo se realizó bajo la asesoría de la Dra. Norma Araceli Bobadilla Sandoval en la Unidad de Fisiología Molecular del Departamento de Medicina genómica y Toxicología Ambiental del Instituto de Investigaciones Biomédicas de la Universidad Nacional Autónoma de México y el Departamento de Nefrología y Metabolismo Mineral del Instituto Nacional de Ciencias Médicas y Nutrición "Salvador Zubirán". Periodo: Agosto 2009 – Abril 2013.

El comité tutor que asesoró el desarrollo de ésta tesis estuvo formado por:

Dra. Norma A. Bobadilla Sandoval	Instituto de Investigaciones Biomédicas
Dra. Ma. Eugenia Gonsebatt Bonaparte	Instituto de Investigaciones Biomédicas
Dr. Julio Morán Andrade	Instituto de Fisiología Celular

Al programa de Doctorado en Ciencias Biomédicas del Instituto de Investigaciones Biomédicas de la UNAM, por todas las facilidades otorgadas.

A los miembros del Jurado:

Dr. Federico Martínez Montes	Facultad de Medicina
Dr. Juan Carlos Gómora Martínez	Instituto de Fisiología Celular
Dr. Diego Ricardo Félix Grijalva	CINVESTAV
Dr. Alfonso León del Río	Instituto de Investigaciones Biomédicas
Dra. Norma A. Bobadilla Sandoval	Instituto de Investigaciones Biomédicas

Este trabajo fue realizado con los apoyo otorgados a la Dra. Norma A. Bobadilla Sandoval por el Consejo Nacional de Ciencia y Tecnología (CONACyT) No. 48483, 101030 y 112780 y por la UNAM-DGAPA IN2009-09-3 y IN203412-3.

Durante la realización de mis estudios de doctorado recibí una beca otorgada por el CONACyT con el número de registro 229325.

A la Q.F.B. Rosalba Pérez Villalva por su asesoría técnica durante la realización de este trabajo.

Al LIBB Miguel Tapia por su asesoría en la Unidad de Microscopía del Instituto de Investigaciones Biomédicas.

Parte del trabajo realizado en esta tesis se encuentra como solicitud de patente nacional con número de solicitud Mx/a/2009/012633 y como solicitud de patente internacional con número de publicación WO 2011/062469 A2.

A G R A D E C I M I E N T O S

*A mis padres **Esther y Rafael**: Gracias por todas las enseñanzas que me han aportado a lo largo de mi vida. Por impulsarme a lograr mis objetivos. Sin su apoyo esto no sería posible. Los amo.*

*A mi hermano **Helí**: Por estar siempre al pendiente, por cuidarme, se que puedo contar con tu apoyo.*

*A **Norma Bobadilla**: Por confiar en mí para el desarrollo de este trabajo, las innumerables enseñanzas académicas y personales, por ser un gran ejemplo e inspiración para mí. Por todo el apoyo. Gracias.*

*A mis tíos **Carlos, Antonia, Ana, Beatriz, Sandra y Reyna:** Por todas las atenciones, sus sabios consejos, las largas horas de plática y ser un ejemplo de dedicación.*

*A mis abuelitas **Senorina García Fábila y María Torrescano**: Por ser el mejor ejemplo de que el amor, la paciencia y la perseverancia lo pueden todo.*

*A **Benjamín**: Gracias por la paciencia, los consejos, por las inyecciones de ánimo cuando lo necesitaba y por todo el apoyo.*

*A **Rosy:** Por la valiosa colaboración para el desarrollo de esta tesis, las palabras siempre oportunas y por tu amistad.*

*A **Emmanuel**: Por todo lo compartido a lo largo de estos años. Por ser tan comprensivo y por tu valiosa amistad. Gracias.*

*A **Paulette**: Por dibujar siempre una sonrisa en mi rostro. Por los excelentes consejos.*

*A **Juan Reyna, Roxana Rodríguez, César Cortés, Juan Antonio Ortega y Marcos Ojeda**: Por su colaboración en el desarrollo de este trabajo.*

*A **Everardo, Juan Carlos, Leslie, Juan, Ana, Susana, Layla y Betty**: Gracias por su amistad y por contagiarme de entusiasmo y alegría.*

A todos mis compañeros de la Unidad de Fisiología Molecular.

A todos los que han contribuido a mi crecimiento personal y profesional.

*A la **UNAM.***

Í N D I C E

ABREVIATURAS

TFG	Tasa de filtración glomerular
I/R	Isquemia/reperfusión
LRA	Lesión renal aguda
ERC	Enfermedad renal crónica
ERCT	Enfermedad renal crónica terminal
NO	Óxido nítrico
VEGF	Factor de crecimiento vascular endotelial
HSP	Proteína de choque térmico
kDa	Kilodaltones
HSE	Elemento de Choque térmico
HSF-1	Factor de choque térmico
eNOS	Sintasa de óxido nítrico endotelial
Hsp90	Proteína de choque térmico de 90 kilodaltones
O2-	Anión superóxido
Hsp72	Proteína de choque térmico de 72 kilodaltones
TGF-β	Factor de crecimiento transformante β
HEK	Células epiteliales de riñón humano
BUN	Nitrógeno ureico en sangre
NGAL	Lipocalina asociada a la gelatinasa de neutrófilos
KIM-1	Molécula de daño renal-1
IL-18	Interleucina-18
NAG	N-acetil-β-glucosaminidasa

L-FABP	Proteína de unión a ácidos grasos de hígado
RNAm	Ácido ribonucleico mensajero
UTI	Unidad de terapia intensiva
TCA	Ácido tricloroácetico
PCNA	Antígeno nuclear de proliferación celular
RT	Transcripción reversa
PCR	Reacción en cadena de la polimerasa
α-SMA	Actina de músculo liso
Gpx	Glutatión peroxidasa
ANOVA	Análisis de varianza
GFP	Proteína verde fluorescente
TAM	Tensión arterial media
FSR	Flujo sanguíneo renal
Uprot	Excreción urinaria de proteínas
Nx	Nefrectomía
h	Horas
TonEBP	Proteína de unión a elementos de respuesta de tonicidad
17-AAG	17-N-Alilamino-17-demetoxigeldanamicina

RESUMEN

El daño renal por isquemia-reperfusión (I/R) es la principal causa de lesión renal aguda en riñones nativos y trasplantados. Esta enfermedad resulta de una disminución en el flujo sanguíneo renal con subsecuente reducción en la llegada de oxígeno y nutrientes al epitelio tubular renal. A pesar de los avances en la estrategias preventivas, la LRA continúa con alta morbilidad y mortalidad que no se han modificado en las últimas cuatro décadas, debido a que se conoce poco sobre los mecanismos moleculares involucrados y también porque las herramientas disponibles para establecer un diagnóstico temprano de LRA no son lo suficientemente sensibles y específicas. Aunado a esto, recientemente se ha reconocido a la LRA como un factor de riesgo para el desarrollo de enfermedad renal crónica o bien como responsable de acelerar la aparición de la enfermedad renal crónica terminal.

El presente proyecto afrontó este problema de salud pública desde tres abordajes: el primero se enfocó a caracterizar si la proteína de choque térmico de 72 kDa (Hsp72) puede servir como biomarcador de LRA en un modelo de daño renal por I/R en la rata y en pacientes diagnosticados con LRA; el segundo se diseñó para profundizar en el conocimiento sobre el papel que juegan las proteínas de choque térmico de 90 kDa (Hsp90α y Hsp90β) en la fisiopatología de la lesión renal aguda inducida por I/R en la rata; y el tercero se diseñó para estudiar los mecanismos por los cuales un episodio de LRA pueden llevar al desarrollo de la ERC y evaluar si el tratamiento con espironolactona puede prevenir el desarrollo de la ERC provocada por un episodio de I/R en la rata.

En la primera parte mostramos que Hsp72 es un biomarcador urinario capaz de estratificar diferentes grados de daño renal, además de ser un biomarcador

temprano ya que esta proteína se detectó en la orina desde 3 h después de la inducción de isquemia. Otra característica no menos importante de este biomarcador fue su capacidad para monitorear la eficacia de una maniobra renoprotectora. En concordancia con nuestros estudios experimentales, uno o dos días antes del diagnóstico de LRA en pacientes críticamente enfermos, se observó un incremento significativo en los niveles urinarios de Hsp72, sugiriendo que efectivamente Hsp72 puede ser un biomarcador temprano de LRA en humanos.

En la segunda parte del proyecto encontramos que la sobre-expresión de Hsp90α o de Hsp90β tienen el mismo efecto renoprotector al ser transfectadas 48 h antes de la inducción de la isquemia renal en la rata. El efecto renoprotector se asoció con la preservación de la síntesis de óxido nítrico y del estado de fosforilación de la serina 1177 de la sintasa de óxido nítrico endotelial. Además demostramos que la técnica de transfección intra-renal es eficiente para que el material genético se introduzca en las células de la vasculatura y del epitelio tubular.

Finalmente en la tercera parte de este estudio caracterizamos un modelo experimental de ERC inducida por un periodo de LRA en la rata. Diversos mecanismos fueron los responsables del desarrollo de ERC, entre ellos se encuentran: una mayor proliferación celular tubular, la activación de la vía de TGF-β, el desarrollo de fibrosis túbulo-intersticial, mayor estrés oxidante y una mayor respuesta inflamatoria. Además mostramos que el prevenir la LRA con espironolactona previno el desarrollo de ERC.

Por lo tanto este trabajo contribuye de manera importante al entendimiento de los mecanismos involucrados en la LRA, a resolver la problemática de establecer un diagnóstico oportuno de LRA y a la prevención de la ERC inducida por un episodio de LRA.

I. I N T R O D U C C I Ó N

Los riñones son dos órganos que se localizan detrás del peritoneo a cada lado de la columna vertebral. Se encuentran desde la vértebra torácica número 12 hasta la tercera vértebra lumbar. Los riñones llevan a cabo diversas funciones en nuestro organismo, varias de ellas son indispensables para la vida. Dentro de estas funciones se encuentran: la regulación de los equilibrios hídrico y electrolítico, la excreción de los deshechos metabólicos y de sustancias bioactivas que afectan la función corporal, la regulación de la presión arterial, la producción de vitamina D y eritropoyetina y realizar una parte de la gluconeogénesis durante el ayuno prolongado [1].

La unidad funcional del riñón se conoce como nefrona. Cada riñón consiste de 800,000 a 1,200,000 nefronas; cada una de ellas es una entidad independiente hasta el punto en que su túbulo colector se une con los túbulos colectores de otras nefronas. La nefrona consiste de un componente vascular que es el penacho capilar o glomérulo en el cual se lleva a cabo el proceso de filtración (el agua y los solutos de la sangre dejan el sistema vascular) y un componente de epitelio tubular o túbulo, en el cual, se llevan a cabo los procesos de reabsorción y secreción que formarán la orina final. El túbulo renal se divide en túbulo proximal, asa de Henle, túbulo distal y túbulo colector. La mayor parte del filtrado glomerular se reabsorbe en los túbulos renales. Cada segmento es específico para diferentes sustancias o iones que se van a reabsorber [1].

La formación de orina comienza con la filtración glomerular (flujo de líquido de los capilares glomerulares a la cápsula de Bowman). Al volumen del filtrado que se forma por unidad de tiempo se conoce como tasa de filtración glomerular (TFG). Típicamente la función renal se cuantifica mediante la TFG, siendo normal cuando es alrededor 180 litros/día o 125 ml/min en el humano [1] [2].

Los riñones son los órganos que reciben la mayor cantidad de sangre por

gramo de peso. Una forma de expresar el flujo de sangre renal es considerando la fracción del gasto cardíaco que pasa por los riñones. Por ejemplo, en un sujeto de unos 60 kg de peso, el gasto cardíaco es de unos 6 litros/min, de este gasto cardiaco el riñón recibe el 21% (1.6 litros/min). Dividiendo este volumen por el peso de ambos riñones, se obtiene un flujo de sangre de 420 ml/min/100 gr de tejido, flujo sustancialmente mayor que el del hígado, o del músculo en reposo [1] [2]. Esto refleja que el riñón es un órgano metabólicamente muy activo, por lo que las consecuencias de que la sangre no llegue adecuadamente al riñón pueden ser muy importantes para la función de este órgano.

LESIÓN RENAL AGUDA

El daño renal por isquemia/reperfusión (I/R) es la principal causa de lesión renal aguda en riñones nativos y trasplantados y resulta de una disminución en el flujo sanguíneo renal con una subsecuente reducción en la llegada de oxígeno y nutrientes al epitelio tubular renal [3]. Aunque la reperfusión es esencial para que sobreviva el tejido isquémico, hay evidencia de que la reperfusión por sí misma causa daño celular adicional [4]. La lesión renal aguda es un síndrome que se caracteriza por la pérdida rápida de la función renal, dentro de las primeras 48 h que se produjo el evento isquémico. A pesar de los avances en las estrategias preventivas, la LRA continúa con alta morbilidad y mortalidad que no se han modificado en las últimas cuatro décadas [5]. Se conoce que la LRA afecta al 15% de los pacientes hospitalizados, siendo su incidencia entre el 40 y 60% en los pacientes en terapia intensiva y alrededor del 40% de estos pacientes fallece por esta causa. La LRA también es frecuente en los pacientes que son sometidos a cirugía cardiaca o abdominal, los que presentan shock séptico, hemorragia o deshidratación o bien pacientes que son tratados con medicamentos nefrotóxicos o

que reciben medios de contraste [6]. Por lo tanto, la LRA constituye un problema de salud pública por su frecuencia creciente, su asociación con graves complicaciones y altos costos, así como su elevada mortalidad a corto y a largo plazo. Dos razones por las que la mortalidad de la LRA no ha sido mejorada de manera sustancial es porque no se conocen con detalle los mecanismos moleculares involucrados y porque las herramientas disponibles para establecer un diagnóstico temprano de LRA no son lo suficientemente sensibles y específicas [5]. En la práctica medica actual, la LRA se diagnostica mediante la detección de un incremento en los niveles de creatinina sérica [7], sin embargo, este parámetro no es confiable ya que es un marcador tardío de daño renal y esto puede ser claramente explicado por el hecho de que una cantidad importante del tejido renal puede sufrir daño sin reflejar cambios en la concentración de creatinina sérica y por lo tanto no se observan cambios en la tasa de filtración glomerular, por ejemplo, los donadores de riñón pierden el 50% de la masa renal total sin presentar elevación en los niveles de creatinina sérica. Además la elevación de la creatinina en suero ocurre hasta 48 h después de que la lesión en el tejido renal ha ocurrido [8] [9]. Es importante resaltar que el inicio temprano del tratamiento contra la LRA mejora de manera sustancial el pronóstico de los pacientes con LRA, por lo que el desarrollo de un biomarcador de daño renal temprano y sensible es crucial [10].

Aunado a la falta de biomarcadores sensibles y tempranos para el diagnóstico oportuno de LRA, anteriormente se pensaba que las personas que se recuperaban de un episodio de LRA, no tenían ninguna consecuencia posterior en la función y estructura renal. Sin embargo, evidencia reciente basada en observaciones epidemiológicas en pacientes que sufrieron LRA indican que esto no es así. Por lo que, se ha propuesto que la LRA es un factor de riesgo para desarrollar enfermedad renal crónica, además de que puede promover la transición de ERC a enfermedad

renal crónica terminal, es decir cuando los riñones prácticamente ya no funcionan y para que el paciente sobreviva debe someterse a terapia sustitutiva (hemodiálisis o diálisis peritoneal) o bien recibir un trasplante de riñón [11, 12, 13, 14, 15]. También, se ha descrito que la probabilidad de desarrollar ERC o ERCT es proporcional a la severidad y a la duración de la LRA [16]. Además estudios epidemiológicos muestran que la incidencia y la prevalencia de la ERC y de la ERCT ha aumentado considerablemente en las últimas tres décadas, al igual que los gastos generados en el cuidado de estos pacientes. En Estados Unidos el programa de ERCT ocupa el 6.7 % del total de los gastos médicos [11]. Tomado todo en consideración, resulta indispensable el estudio de los mecanismos por los cuales un episodio de LRA puede desencadenar y conducir a la afectación de la función y la estructura renal en forma progresiva, así mismo, es de vital importancia encontrar maniobras farmacológicas que eviten la LRA con lo que, se evitará el desarrollo de la ERC y de la ERCT. A pesar de la gran importancia que tiene la LRA como factor de riesgo para desarrollar ERC, no se han estudiado a fondo los mecanismos responsables, lo que además permitiría estudiar estrategias farmacológicas para reducir o prevenir la progresión a ERC.

MECANISMOS DE DAÑO DURANTE LA LESIÓN RENAL AGUDA

Durante el curso de la LRA, una de las regiones afectadas es el endotelio vascular [4]. En el riñón post-isquémico las pequeñas arteriolas presentan mayor vasoconstricción que aquellas de un riñón normal, esto se debe principalmente a un desbalance en la producción de factores vasoactivos. Después de la isquemia se incrementan los niveles de endotelina-1, angiotensina II, tromboxano A2, prostaglandinas, leucotrienos, adenosina y de la aldosterona [17, 18, 19, 20]. Además, la vasoconstricción se potencia debido a una reducción en la producción de

óxido nítrico (NO) [21]. Estos efectos son aumentados por un incremento en la adhesión de leucocitos al endotelio, lo que ocluye a los pequeños vasos y compromete la microcirculación vascular renal. Además del proceso isquémico, esta vasoconstricción propicia aun más una disminución en la llegada de oxígeno y nutrientes al endotelio. El número de vasos en la medula externa disminuye después de la I/R, fenómeno conocido como rarefacción capilar [22]. Este fenómeno puede facilitarse debido a la regulación a la baja de factores pro-angiogénicos como el factor de crecimiento vascular (VEGF) [23]. La reducción en el número de vasos genera hipoxia crónica que puede conducir al desarrollo de daño al epitelio tubular y generación de fibrosis túbulo-intersticial a largo plazo.

Otro de los factores que contribuye de manera importante en la patogénesis de la LRA es la activación de la respuesta inmune. Los neutrófilos, monocitos/macrófagos, células dendríticas y células T son importantes actores durante un fenómeno de isquemia/reperfusión renal [24]. Los neutrófilos se adhieren al endotelio activado y se acumulan en los riñones de pacientes con LRA, particularmente en la red capilar peritubular [25]. Producen proteasas, mieloperoxidasa, especies reactivas de oxígeno y diferentes citocinas, lo que lleva a un incremento en la permeabilidad vascular y reducción en la integridad del epitelio tubular y de las células endoteliales, agravando así la lesión renal [26]. A pesar de que el infiltrado inflamatorio se ha reconocido como deletéreo durante la LRA, estudios recientes han mostrado que el factor de estimulación de colonias-1 (CSF-1) promueve la proliferación de los macrófagos y células dendríticas residentes, así como, su diferenciación hacia un fenotipo de macrófagos reparadores de tejido tipo M2. Sin embargo durante la LRA el endotelio se ve afectado y hay infiltración de macrófagos inflamatorios tipo M1 que, en vez de promover la reparación perpetúan el daño por inflamación [27].

Uno de los principales sitios donde se presenta muerte celular durante la LRA es en el epitelio del túbulo proximal, específicamente en el segmento S3 [28]. La aparición de cilindros y de células tubulares en la orina es una evidencia de que existe muerte celular por apoptosis y necrosis acompañada de desprendimiento de las células tubulares [29]. El proceso de lesión y de reparación en el epitelio tubular se esquematiza en la figura 1. La isquemia resulta en pérdida de la polaridad y de la integridad del citoesqueleto, desaparece el borde en cepillo característico de la porción luminal de las células epiteliales y se des-localizan las moléculas de adhesión y otras proteínas como la sodio-potasio-ATPasa [30] [31]. Con este tipo de daño, tanto células viables como no-viables se desprenden de la membrana basal y se proyectan hacia la orina. Las células y los restos celulares que se proyectan hacia la orina se combinan con fibronectina y la uromodulina (proteína Tamm Horsfall) para formar cilindros que obstruirán el flujo urinario hasta que la presión intra-tubular se incremente, los cilindros lleguen a la vejiga y se puedan detectar en la orina. En condiciones donde la LRA no ha sido tan severa, las células viables migran y cubren la membrana basal. Estas células se dividen y reemplazan a las células que se desprendieron, se diferencian y restablecen la polaridad normal del epitelio [32] [33] [34] [35]. Dentro de las proteínas sobre-reguladas en el túbulo proximal y que se han propuesto como moléculas citoprotectoras contra la LRA están la hemo-oxigenasa y las proteínas de choque térmico [36] [37] [38]. Sin embargo, es frecuente que la reparación no sea adecuada y esta respuesta mal adaptada puede conducir al desarrollo de fibrosis crónica [14]. Por lo tanto, la LRA puede llevar a una reparación tubular incompleta, inflamación túbulo-intersticial persistente, proliferación de fibroblastos y deposición de matriz extracelular.

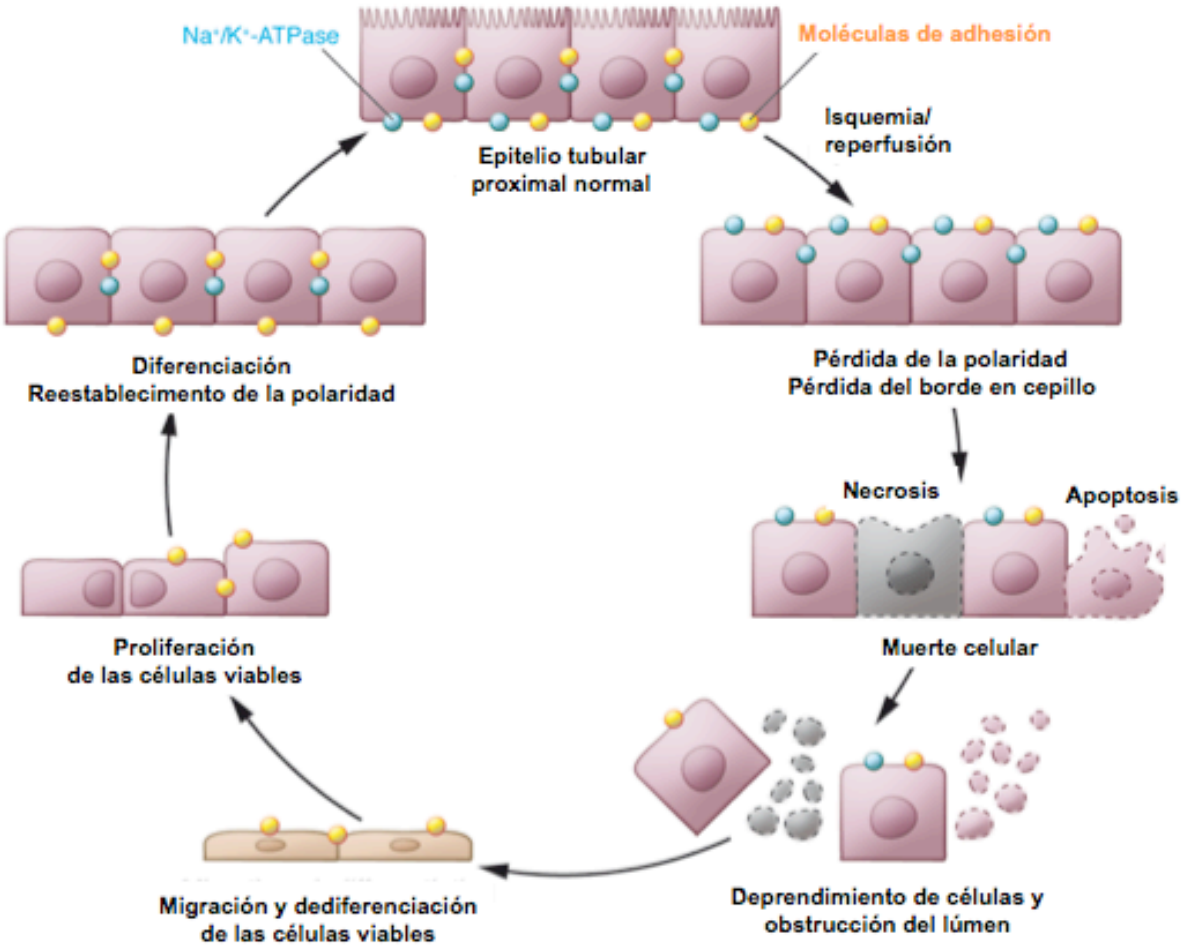

Figura 1. Daño tubular y reparación normal después de la LRA. Después de la I/R, las células epiteliales pierden su polaridad y el borde en cepillo que las caracteriza. Se presenta muerte celular por necrosis o apoptosis y desprendimiento de las células de la membrana basal tubular. Las células viables migran, proliferan y remplazan a las células que se desprendieron, restableciendo así la polaridad normal del epitelio. Figura modificada de Bonventre and Yang, 2011 [4].

LAS PROTEÍNAS DE CHOQUE TÉRMICO

En situaciones de estrés celular como en la LRA, la síntesis proteica se ve afectada dando lugar a proteínas mal plegadas o con una conformación inadecuada, lo que puede propiciar la formación de agregados proteicos no funcionales y comprometer la viabilidad celular. En estas condiciones se activa la transcripción de genes que principalmente están dirigidos hacia proteínas reparadoras conocidas como proteínas de choque térmico (Hsp), lo que inicia la reparación proteica y la

activación de vías de señalización que permiten una mejor adaptación al estado de estrés en el que se encuentra la célula [39] [40] [41].

La familia de proteínas de choque térmico esta formada por varios genes que codifican para proteínas con peso molecular que varía desde los 10 hasta los 160 kDa y se han clasificado de acuerdo a su peso molecular en seis subfamilias conocidas como: las Hsp de 100-110 KDa, la de 90 KDa, la de 70 KDa, la de 60 KDa, la de 40 KDa, y la subfamilia de Hsp con peso molecular de 18-30kDa [42]. Una de las subfamilias mas abundantes es la de Hsp90 que está conformada por 5 isoformas: Grp94, Hsp90N, TRAP1, Hsp90α y Hsp90β; que se diferencian básicamente por su localización intracelular. Las isoformas citosólicas Hsp90α y Hsp90β ocupan el 80% de esta subfamilia y conforman del 1 al 2% de la proteína citosólica total en la mayoría de las células [43].

Tanto la Hsp90α como la Hsp90β son genes multicopia y se han identificado en diferentes cromosomas; el gen que codifica para HSP90 alfa está ubicado en los cromosomas 1, 3, 4, 11 y 14 con un tamaño de 7393 pb generando un transcrito de 2912 pb que traduce una proteína de 733 aminoácidos, sin embargo únicamente la copia del gen ubicada en el cromosoma 14 presenta actividad. En cambio, el gen que codifica para HSP90 beta se encuentra en los cromosomas 4, 6, 10, 13, 14 y 15 con un tamaño de 8210 pb y un RNAm de 2567 pb, que traduce una proteína de 726 aminoácidos; la copia que presenta actividad es la que se localiza en el cromosoma 6 [44] [45].

La transcripción de los genes de HSP90 se regula principalmente por los elementos de respuesta a choque térmico (HSE). En células Jurkat (células T en leucemia) se demostró que Hsp90α es altamente regulada por al menos 3 secuencias HSE con el motivo ‘nGAAn’ localizadas en la región 5’ y que son de vital importancia para la expresión constitutiva e inducible de la proteína. En cambio, en

Hsp90β los elementos de respuesta a estrés térmico se localizan en dos regiones diferentes: en la región 5' no transcrita (responsable de la expresión constitutiva) y en el primer intrón, donde se regula la trascripción inducible funcionando como potenciador de la trascripción en condiciones celulares adversas [46].

Ambas isoformas son reguladas por el factor de transcripción de choque térmico-1 (*Heat Shock Factor*, HSF-1). En condiciones normales HSF-1 se localiza en el citoplasma en estado inactivo unido a diferentes chaperonas incluyendo Hsp90, cuando se produce estrés celular, ya sea físico o químico, HSF-1 es liberado del complejo, fosforilado y se transloca al núcleo, en donde forma un trímero activo que se une a los elementos de respuesta HSE, lo que activa la transcripción de los genes de choque térmico [47] [48] [49].

Hsp90 se compone de cuatro dominios (Figura 2), el primer dominio es el amino terminal donde se localiza el sitio de unión de ATP, también conocido como dominio ATPasa, aquí el ATP es hidrolizado en ciclos de asociación y disociación entre Hsp90 y sus proteínas cliente [50]. Este dominio es particularmente importante porque es aquí donde se unen los inhibidores de Hsp90, como geldanamicina, radiciol y 17-AAG que compiten por el sitio de unión a ATP y de esta forma impiden que Hsp90 se una a sus proteínas cliente. El segundo dominio es el denominado "cargado", por la presencia de aproximadamente 30 aminoácidos con carga negativa y este segmento parece ser importante para que la Hsp90 realice los cambios conformacionales durante el ciclo ATPasa y recientemente se reportó que ha evolucionado para sufrir modificaciones post-traduccionales que modifican la actividad chaperona de Hsp90 [51] [52]. El tercer dominio es el llamado "dominio medio" en donde se unen proteínas cliente, entre ellas eNOS y cinasas como la Akt y por último el dominio carboxilo terminal donde se realiza la dimerización de Hsp90, la cual es una unión flexible y producto de cambios en el ambiente celular. Estudios

bioquímicos recientes muestran que en el extremo carboxilo hay un segundo sitio de unión a ATP, sensible a novomicina y cis-platino [53]. La función de este sitio aún se desconoce, pero algunos autores sugieren que ambos sitios de unión a ATP pueden funcionar de forma cooperativa. Recientemente ha tomado importancia las modificaciones pos-traduccionales que sufre Hsp90, como la fosforilación, la cual puede afectar su actividad de chaperona. Por ejemplo, se ha demostrado que la fosforilación de Hsp90 en la treonina 22 es importante para mantener la habilidad de esta proteína para dimerizar y en consecuencia para realizar la hidrólisis de ATP y su función de chaperona y además para discriminar entre sus proteínas blanco específicas [54].

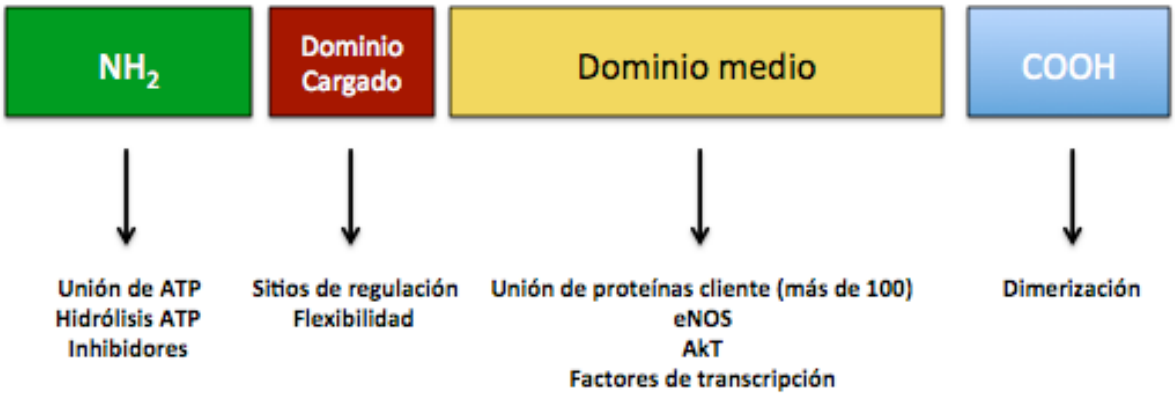

Figura 2. Dominios en la estructura proteica de Hsp90.

Hsp90 modula la actividad y estabilidad de un amplio rango de proteínas cliente. La unión a estas proteínas le permite participar en diferentes procesos celulares como lo son: la regulación del ciclo celular, la respuesta inmune, el estrés celular, la apoptosis, la remodelación del citoesqueleto y participar en procesos cancerígenos [55]. Entre las mas de 100 proteínas cliente conocidas de Hsp90 se encuentran: la familia de los receptores de hormonas esteroideas, algunos factores

de transcripción, cinasas de tirosina, subunidades de proteínas G y las sintasas de óxido nítrico neuronal, inducible y endotelial (eNOS) [56] [57] [58].

Se conoce que la asociación entre Hsp90 y eNOS es un paso crítico para la producción de NO y por lo tanto para la regulación del tono vascular [56]. Hsp90 participa en el plegamiento de las sintasas de oxido nítrico y también se ha reportado que determina la inserción del grupo hemo dentro de la proteína inmadura. Además, Hsp90 se puede asociar con eNOS en células endoteliales en estado basal y en células endoteliales estimuladas con el factor de crecimiento vascular endotelial e incrementar la producción de NO. Se ha descrito que diferentes estímulos como, la presencia de Angiotensina II, el incremento en los niveles de calcio intracelular, el VEGF o cambios en las fuerzas de rozamiento en los vasos sanguíneos por vasoconstricción, son capaces de incrementar la síntesis de NO mediada por la eNOS [59] [60].

El NO producido difunde a la célula de músculo liso y activa a la guanilato ciclasa soluble GCs. La GCs promueve la conversión de GTP a CMPc, el cual tiene tres efectos: 1) inhibe la entrada de calcio a la célula, 2) activa los canales de potasio favoreciendo así la hiperpolarización y 3) activa a la fosfatasa de las cadenas ligeras de miosina, asistiendo la defosforilación de cadenas ligeras de miosina: En conjunto estos tres efectos producen un efecto relajador del músculo liso y por ende se produce vasodilatación [61] [62].

La asociación entre Hsp90 y eNOS se mostró por primera vez en 1998 [56] en un estudio en el que se observó mediante ensayos de inmunoprecipitación que Hsp90 establece una interacción directa con eNOS, además de que esta interacción produce un aumento en la actividad de esta enzima, generando mayor producción de NO. Para conocer el papel fisiológico de esta interacción, se incubaron anillos de aorta con un inhibidor de Hsp90: la geldanamicina y se encontró que la producción

de NO disminuía, así como la relajación dependiente de endotelio, por lo que se concluyó que la interacción Hsp90-eNOS tiene un papel preponderante en la regulación del tono vascular a través de regular el efecto vasodilatador del NO.

Recientemente se caracterizó el sitio de unión de Hsp90 a eNOS [63], mediante el uso de péptidos "señuelo" de la eNOS que fueron diseñados en la región de unión a Hsp90 (aa 291-400). Los péptidos fueron incubados con lisados de células de endotelio de bovino y se determinó cuál de estos péptidos inhibía la asociación de Hsp90 con eNOS. Se mostró que el péptido B2 (diseñado del aa 301 al 320) disminuyó la producción de NO y la asociación de Hsp90, concluyendo así que eNOS se une a Hsp90 en los aminoácidos 301 a 320.

Posteriormente se demostró que el desacople de la interacción de Hsp90 con eNOS, mediante la inhibición farmacológica de Hsp90 con geldanamicia, no solo resulta en una disminución en la generación de NO, sino también aumenta la producción del $O^{2\bullet-}$, por lo que concluyeron que la interacción Hsp90-eNOS es esencial para la producción de NO y que la inhibición de Hsp90 desacopla la actividad de la eNOS para producir NO, en cambio incrementa la producción de $O^{2\bullet-}$ dependiente de eNOS [64].

Existen varios sitios de fosforilación en la estructura proteica de eNOS, sin embargo se conoce que dos de ellos son lo que tienen mayor consecuencia sobre la actividad de eNOS, son las fosforilaciones que ocurren en los residuos de Ser1177 en el dominio de reductasa y la fosforilación en la Tre495 que ocurre en el dominio de unión a calmodulina. Hsp90 facilita la fosforilación de eNOS en la Ser1177 y promueve la generación de NO, en cambio cuando esta interacción se pierde, se fosforila la Tre495 y se promueve la generación de $O^{2\bullet-}$ [65] [66] [67]. Las cinasas que se ha reportado pueden fosforilar a la Tre495 incluyen a Rho cinasa y PKC-β.

Las cinasas reportadas que fosforilan al residuo de Ser1177 son Akt, PKA, AMPK y PKC-α [68].

En resumen, la Hsp90 activa a eNOS a través de tres mecanismos diferentes: 1) Favorecer que el calcio y la calmodulina se unan a eNOS, 2) Mantener la forma dimérica activa de la eNOS y 3) Facilitar la fosforilación de la serina 1177 (Ser-1177) de la eNOS por la cinasa Akt.

En forma contraria, el desacople entre Hsp90 y eNOS propicia la fosforilación de la treonina 497 (Tre-497) de eNOS, con lo que no solo se inactiva, sino que también se favorece que eNOS ahora produzca el anión superóxido. Sin embargo, pocos de estos estudios especifican cuál isoforma de Hsp90 ejerce estos efectos (Figura 3).

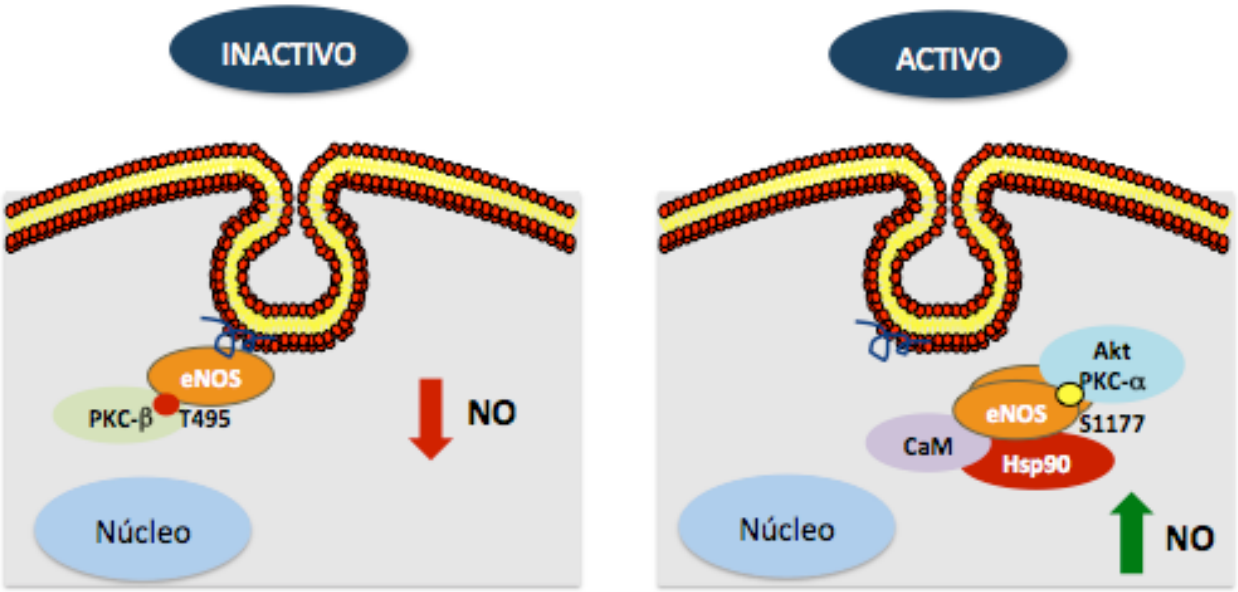

Figura 3. En condiciones basales la eNOS se localiza en la caveola unida a caveolina-1 y es fosforilada en la treonina 495 previniendo su unión a calmodulina, manteniendo a eNOS en un estado inactivo. En respuesta a un estímulo celular, se disocia la interacción de eNOS con caveolina-1 y ahora interactúa con Hsp90, la cual facilita la unión de calmodulina, la dimerización de eNOS y la fosforilación en el residuo de serina 1177 por AkT ó PKC-α, lo que en conjunto propiciará la activación de eNOS para la producción adecuada de óxido nítrico. Figura modificada de Fleming I, 2010 [68].

ÓXIDO NÍTRICO E ISQUEMIA/REPERFUSIÓN (I/R)

El óxido nítrico que proviene de la sintasa de oxido nítrico endotelial (eNOS) resulta de gran importancia durante la fisiopatología de la I/R. Este hecho se ha evidenciado en diferentes estudios, uno de ellos donde se demostró que la I/R induce una disminución en la expresión de la eNOS en células endoteliales, efecto que se observa desde las 3 h después de la reperfusión. En este mismo estudio se demostró que la inhibición de eNOS se debe al reclutamiento de des-acetilasas de histonas hacia la región promotora del gen de eNOS, inhibiendo así su transcripción referencia [69]. Otro estudio evidenció que las ratas de la cepa Norway (BN/Mcw) son mas resistentes a la I/R del miocardio que las ratas de la cepa Dahl S (SS/Mcw) y que esta característica se debe a que presentan mayor cantidad de NO secundario a una mayor asociación de eNOS con Hsp90 y a una mayor biodisponibilidad de la tetrahidrobiopterina, un cofactor importante en la síntesis de NO [70].

La implicación de eNOS en la regulación del tono vascular sugiere que maniobras que estimulen la producción de óxido nítrico pudieran prevenir o mejorar el daño por I/R. A este respecto, estudios recientes en rata han mostrado que el pre-acondicionamiento con periodos cortos de isquemia protege contra el daño inducido por I/R. Interesantemente, esta protección es mediada por la activación de Akt y de eNOS, promoviendo así una mayor generación de NO. Además el impacto benéfico que tiene el pre-acondicionamiento isquémico puede ser eliminado cuando se inhibe la producción de NO antes del pre-acondicionamiento [71]. En este mismo sentido la importancia de Hsp90 se evidenció en un estudio en donde se efectuó isquemia intestinal en donde las ratas fueron tratadas con geldanamicina (inhibidor de la actividad de Hsp90) o bien con LY-294002 (inhibidor de la PI3K, enzima que inicia la fosforilación de Akt y en consecuencia la fosforilación de la Ser 1177 de eNOS). Los animales se estudiaron 30 minutos después de inducir la isquemia y se observó que

la inhibición de Hsp90 o de PI3k revirtió la activación de eNOS y de Akt que se observa normalmente en la isquemia intestinal y además empeoró el daño inducido por la isquemia [72]. En el riñón, un estudio pretendió evaluar el papel de Hsp90 en la isquemia renal, para lo cual, se indujo la expresión de las proteínas de choque térmico a través de la administración de dosis altas de geldanamicina y sus análogos, con el fin de liberar el factor de transcripción HSF1. En este estudio se utilizó el modelo de I/R renal en el ratón y se observó que la administración de geldanamicina protegió a nivel funcional y morfológico contra el daño por I/R, sin embargo esta protección fue mediada principalmente por la inducción de Hsp70 y no de Hsp90 por lo tanto en ese estudio no se logró disecar el papel específico que juega Hsp90 en la lesión renal aguda inducida por I/R [73].

Dentro de la funciones conocidas de Hsp90 en la fisiología renal se encuentran: La participación en la estabilización, activación y translocación del receptor de mineralocorticoides, a través de formar un heterocomplejo con Hsp70, Hip (p48), Hop (p56) y Hsp40, su implicación en regular la actividad del cotransportador de sodio, potasio y 2 cloros (NKCC) en el asa de Henle y su colaboración en la adaptación a la hiperosmolaridad en la médula renal a través de su interacción con la proteína encargada de sensar el estrés osmótico TonEBP [55]. Finalmente también se ha mostrado que los inhibidores de Hsp90 pueden reprimir la señalización de TGF-β1 e inhibir el desarrollo de fibrosis renal. En un modelo de obstrucción unilateral ureteral se demostró que la administración de 17-AAG disminuyó la expresión de alfa-SMA, fibronectina y colágena I y además restableció la expresión de E-caderina. El 17-AAG inhibió la fosforilación de Smad2, Akt, GSK3-β y ERK. Estos efectos anti-fibróticos fueron mediados por el bloqueo en la interacción entre Hsp90 y el receptor de TGF-β tipo II, promoviendo su ubiquitinación y de esta manera disminuyendo la señalización a través de este receptor [74].

Desde hace varios años en nuestro laboratorio hemos estado interesados en ahondar en el conocimiento sobre el papel que juegan estas proteínas a nivel renal, por lo que en un primer trabajo, caracterizamos la expresión y localización de Hsp90α y Hsp90β en la nefrona de la rata. Encontramos que estas proteínas se expresan en forma abundante, siendo mayor su expresión en la medula renal que en la corteza. Mediante inmunohistoquímica, también se observó que se encuentran localizadas en la mayoría de las estructuras de la nefrona, pero no se observó diferencia en el patrón de localización de cada isoforma [75]. En un estudio posterior, observamos que la inhibición farmacológica de Hsp90α y Hsp90β con radicicol produce una reducción en el FSR y la tasa de filtrado glomerular en la rata. Este efecto fue mediado por la disminución de la síntesis de NO y por cambios en la fosforilación y dimerización de la sintasa de NO endotelial, lo que sugiere que Hsp90 regula la vía de eNOS/NO en el riñón [76]. Para establecer el papel específico de cada isoforma, evaluamos el efecto de la sobre-expresión de Hsp90α y Hsp90β *in vitro*, mediante su clonación y transfección en células HEK-293. En el cultivo celular, la sobre-expresión de Hsp90α produjo un aumento significativo en la síntesis de NO, lo que se asoció con un incremento en la fosforilación activante de eNOS, mientras que la sobre-expresión de Hsp90β no solo redujo la síntesis de NO sino que también produjo un incremento en los niveles de anión superóxido y esto se asoció con un incremento en la fosforilación inactivante de eNOS [77]. Debido a que se observó que en células HEK-293, la sobre-expresión de ambas isoformas de Hsp90 modifica la regulación de la producción de NO y del anión superóxido (radicales libres que participan en la regulación del tono vascular renal), en este trabajo se pretende evaluar cuál es el efecto que tendría la transfección de Hsp90α y de Hsp90β sobre la función renal y en un proceso fisiopatológico tan relevante como lo es la LRA

inducida por isquemia-reperfusión. A pesar de que se conoce que Hsp90 interactúa con eNOS también se sabe que establece interacción con más de 300 proteínas cliente, por lo que, no se sabe si su sobre-expresión puede llegar a ser benéfica o deletérea en un fenómeno de I/R. Un ejemplo es el caso de la Hsp27, la cual al ser sobre-expresada sistémicamente en ratones, promovió que en respuesta a I/R renal, los ratones transgénicos presentaran menor función renal comparada con los ratones silvestres, este efecto se asoció con mayor muerte celular por necrosis y además por una mayor cantidad de citocinas pro-inflamatorias e infiltrado inflamatorio. Cuando se transfirieron esplenocitos o neutrófilos de los ratones transgénicos a ratones normales se observó que estos últimos tenían mayor cantidad de daño renal. Estas observaciones sugieren que a pesar de que Hsp27 se asocie con protección contra la muerte celular, cuando se sobre-expresa de manera sistémica promueve una mayor respuesta inflamatoria debida a la I/R [78]. Es por lo anterior que en este trabajo se utilizó la técnica de transfección intra-renal para evaluar específicamente el efecto de la sobre-expresión renal de ambas isoformas de Hsp90 frente a la lesión renal aguda inducida por isquemia.

BIOMARCADORES DE LESIÓN RENAL AGUDA

Como ya se mencionó, se conoce que el inicio temprano del tratamiento para la LRA mejora de manera importante el pronóstico de los pacientes. Además es necesario encontrar marcadores que puedan estratificar el grado del daño renal que cada paciente tiene y de esta manera poder monitorear a aquellos pacientes que estén en alto riesgo de progresar a enfermedad renal crónica. Durante varias décadas el diagnóstico de la LRA se ha basado en la elevación de la concentración de creatinina sérica, del nitrógeno ureico en sangre (BUN) o por la presencia de oliguria. Sin embargo estos no son buenos biomarcadores de LRA [8]. En el caso de

la creatinina, su concentración puede ser influenciada por factores no-renales como la actividad muscular, el peso corporal, la edad, el género, la raza y la ingesta proteica. Además, la elevación de creatinina ocurre después de 48 h que ocurrió el insulto, por lo que difícilmente se puede establecer un diagnóstico temprano utilizando este parámetro [79]. En el caso del BUN también puede ser influenciado por otros factores como una dieta alta en proteínas, la terapia con glucocorticoides o un trauma. Así mismo se ha reportado que un gran número de pacientes pueden padecer LRA sin pérdida de la función excretora, por lo que tomando en cuenta la oliguria se subestimaría el numero de pacientes con daño tubular agudo [80]. Es por ello que la identificación de nuevos biomarcadores de LRA es una necesidad imperante. Durante el desarrollo de un nuevo biomarcador se deben cubrir 5 fases diferentes: 1) Estudios experimentales que identifiquen moléculas cuya expresión o concentración se modifique durante la LRA en la rata o el ratón; 2) la identificación de un método reproducible y confiable para cuantificar al biomarcador en cuestión en muestras de orina o sangre; 3) ensayos clínicos para detectar el biomarcador en muestras de pacientes diagnosticados con LRA y la evaluación de la utilidad del biomarcador para detectar la LRA en comparación con los métodos convencionales, 4) validación en gran escala para determinar las propiedades del biomarcador tal como la sensibilidad y especificidad y 5) verificar que el uso del biomarcador tenga un efecto benéfico en una población a nivel del tratamiento, evolución de la enfermad y del pronóstico de estos pacientes [81]. En los últimos años, muchos estudios se han enfocado en el desarrollo de biomarcadores sensibles y tempranos para la LRA. Con el advenimiento de las herramientas genómicas y proteómicas, varias moléculas cuya concentración en suero u orina se modifica durante la LRA se han identificado y se han propuesto como biomarcadores de LRA. Dentro de las moléculas mas estudiadas y que han mostrado resultados más prometedores se

encuentran la gelatinasa de neutrófilos asociada a lipocalina 2 (NGAL), la molécula de daño renal-1 (kim-1), la interleucina 18 (IL-18), la cistatina C, la N-acetil-β-glucosaminidasa (NAG) y la proteína de unión a ácidos grasos de hígado (L-FABP).

NGAL es una proteína de 25 kDa que se encuentra unida covalentemente a la gelatinasa de los neutrófilos y que se expresa en niveles bajos en diferentes tejidos incluyendo los pulmones, estómago, colon y las células epiteliales localizadas en el túbulo proximal [82] [83]. NGAL es una de las proteínas que se sobre-expresan después de un insulto isquémico con mayor rapidez (2 h) y se ha mostrado que se eleva hasta 100 veces en pacientes diagnosticados con LRA en unidades de terapia intensiva (UTI), además los niveles plasmáticos de NGAL son útiles para diagnosticar la LRA hasta con 48 h previas a la elevación de la creatinina sérica, con un área baja la curva de 0.78 [84]. También se ha mostrado que NGAL puede ser un biomarcador temprano en humanos, ya que en un estudio de una población pediátrica sometida a bypass cardiopulmonar se observó que la elevación de NGAL ocurría entre 2 a 6 h después de la cirugía, mientras que la elevación de creatinina se observó entre 1 a 3 días después [85] [20]. Una de las desventajas del uso de este biomarcador es que el NGAL, que no se produce en el riñón, se eleva en respuesta a estrés sistémico y por lo tanto la excreción urinaria de NGAL se eleva en otras condiciones patológicas o en pacientes con enfermedad renal crónica, sin que esto refleje la presencia de LRA. A pesar de que NGAL es un biomarcador temprano, su baja especificidad limita su consistencia como un biomarcador ideal de LRA [86] [87].

Kim-1 es una glicoproteína trans-membranal con dominios de inmunoglobulina y de mucina. Esta proteína es un receptor de fosfatidilserina que reconoce células en apoptosis y confiere a las células epiteliales la capacidad de reconocer y fagocitar células muertas que están presentes después de la isquemia renal [88] [89]. Kim-1

se expresa mínimamente en el riñón de la rata y se sobre-expresa dramáticamente en las células del segmento S3 del túbulo proximal después de I/R o por el daño renal asociado a fármacos nefrotóxicos [90]. Un ectodominio procesado proteolíticamente puede ser fácilmente detectado en la orina [91]. En pacientes con LRA diagnosticada por la elevación de la creatinina sérica, se observó que la presencia de Kim-1 es mucho mayor que en los pacientes con otro tipo de daño renal o de ERC [92] [93]. Sin embargo Kim-1 ha demostrado tener un bajo desempeño como biomarcador temprano de LRA [94].

La IL-18 es una citocina pro-inflamatoria que no solo sufre un procesamiento proteolítico en el túbulo proximal durante la LRA, sino que además su expresión aumenta en esta condición. Esta proteína, se expresa en las células intercaladas del túbulo contorneado distal, túbulo conector y colector. Se co-expresa con P2X7 y la caspasa-1 que convierten a la pro-IL-18 en su forma activa. Posteriormente la IL-18 sale de la célula y drena en la orina [95] [96]. Se ha visto que su concentración en orina es mayor en los pacientes con LRA. Sin embargo para establecer un diagnóstico temprano parece tener una baja sensibilidad pero alta especificidad aunque se han observado resultados inconsistentes en estudios con diversas cohortes de pacientes [97] [98].

La cistatina C es una proteína inhibidora de proteasas que se produce en todas las células nucleadas, se libera al torrente sanguíneo de forma constante y aparentemente no es influenciada por otros factores ajenos a la tasa de filtración glomerular (TFG). La cistatina C se considera como un marcador de la TFG ya que posee las características ideales de un marcador de TGF: se filtra libremente, se reabsorbe completamente y no se secreta en los túbulos renales [99]. Para establecer un diagnóstico temprano de LRA se ha observado que en pacientes hospitalizados predice desde 24 h hasta con 48 h de anticipación el desarrollo de

LRA, sin embargo lo hace 10 h más tarde que NGAL. Por lo tanto la cistatina C parece tener mejor desempeño que la creatinina sérica, pero no cuando se compara con otros marcadores descritos recientemente [100].

NAG es una enzima lisosomal que se encuentra en los túbulos proximales y cuya actividad en la orina sugiere la presencia de daño en las células tubulares. NAG ha sido efectivo para el diagnóstico de nefrotoxicidad, función retardada del injerto y la LRA inducida por isquemia antes que la elevación de la creatinina sérica, sin embargo la actividad de NAG puede ser inhibida por la urea y se ha reportado que también se incrementa en una variedad de patologías aún en la ausencia de LRA por lo que su insensibilidad y no-especificidad pueden limitar su uso como biomarcador de LRA [101] [102] [103].

L-FABP se encuentra normalmente en el citoplasma de las células del túbulo proximal en humanos. Se une a los ácidos grasos y los transporta a la mitocondria o a los peroxisomas, donde los ácidos grasos son β-oxidados. L-FABP se reabsorbe en el túbulo proximal por endocitosis mediada por megalina [104] [105]. Se ha mostrado que es un marcador de LRA más temprano que NGAL y NAG en pacientes sometidos a cirugía cardiovascular, sin embargo no se ha estudiado más a fondo su comportamiento en humanos [106].

Diversos estudios han mostrado que las proteínas de choque térmico son inducidas en túbulos dañados después de lesión isquémica o por fármacos nefrotóxicos [107]. En particular la subfamilia de proteínas de choque térmico de 70 kDa (Hsp70) se compone de cuatro isoformas: Hsc70 (isoforma constitutiva), Hsp72 (isoforma inducible), mHsp75 y Grp78. La Hsp72 es una de las proteínas cuya inducción es mayor durante la LRA. Dada su inducción en los túbulos proximales y que el desprendimiento de células del túbulo tanto viables, como no viables se proyecta hacia el espacio urinario; propusimos que los niveles urinarios de Hsp72

podrían servir como biomarcador para detectar, monitorear y estratificar a los pacientes con LRA. En este sentido, el contar con un biomarcador temprano y capaz de estratificar el grado de daño renal que un paciente ha sufrido, permitirá ofrecer un tratamiento farmacológico para evitar el daño por isquemia y también permitirá detectar aquellos pacientes que estén en riesgo de desarrollar enfermedad renal crónica inducida por LRA y de esta forma observar cuidadosamente a estos pacientes para prevenir o retrasar la aparición de la ERC.

PROGRESIÓN DE LESIÓN RENAL AGUDA A ENFERMEDAD RENAL CRÓNICA.

Como ya se mencionó, evidencia epidemiológica reciente muestra que la LRA es un factor de riesgo para el desarrollo de ERC y que además acelera la transición de ERC a ERCT. De hecho, la probabilidad de desarrollar ERC o ERCT es proporcional a la severidad y la duración del evento de LRA. Además resulta alarmante que se ha demostrado que el 6.6% de los pacientes que tuvieron un episodio de LRA y que recuperaron por completo la función renal, presentaron un mayor riesgo de muerte y de ERC *de novo* en un seguimiento de 2 a 4 años [15].

Una de las teorías sobre cómo la lesión renal aguda puede conducir al desarrollo de ERC tiene que ver con una reparación incompleta o defectuosa después del proceso de LRA y se esquematiza en la figura 4.

Uno de los factores involucrados en el desarrollo de ERC posterior a un epidodio de LRA es la pérdida en la densidad capilar que ocurre posterior a la I/R, esto lleva a una disminución del FSR y por lo tanto a una hipoxia crónica que se convertirá en un círculo vicioso de hipoxia y pérdida de capilares peri-tubulares con activación de la respuesta inflamatoria.

Basile y cols. [108] mostraron que después de la I/R renal en la rata no hay proliferación de las células endoteliales y además hay transición endotelio a

mesénquima y esto se evidenció por la co-localización del marcador de células endoteliales CD31 con el marcador de fibroblastos S100A4. Es decir, la disminución en la densidad vascular que ocurre después de la LRA resulta en parte por la transición fenotípica que sufren las células endoteliales que se combina con la capacidad impedida de regeneración, lo que pudiera contribuir al desarrollo de ERC.. Este mismo grupo de trabajo mostró que los capilares peritubulares medulares se ven afectados a largo plazo y que este efecto se asociaba con problemas de concentración de orina [109]. Además, Conger et al. mostraron que el riñón post-isquémico de la rata pierde la capacidad de autorregular adecuadamente el flujo sanguíneo renal. Estas condiciones en conjunto perpetúan los ciclos continuos de daño por hipoxia e inflamación que eventualmente conducen al desarrollo de ERC [110].

Como ya se señaló, después de la LRA es esencial que las células tubulares proliferen para restablecer la estructura tubular normal, sin embargo dos estudios recientes sugieren que las células epiteliales de los túbulos renales también tienen un papel crítico en el desarrollo de fibrosis túbulo intersticial característica de la ERC, a través de un arresto en el ciclo celular y modificaciones epigenéticas. En el primer trabajo, Yang L. et al. demostraron que después de daño renal por I/R, por nefrotóxicos o por obstrucción ureteral, las células epiteliales sufren un arresto en el ciclo celular en la fase G_2/M, lo que resulta en un fenotipo que facilita la producción de factores pro-fibróticos como el TGF-β. Esto se debe a que en las células del túbulo proximal que se encuentran arrestadas, la cinasa JNK se activa y sobre-regula la producción de citocinas pro-inflamatorias [111]. En el segundo trabajo, Bechtel W et al. (2010) infirieron que el mantenimiento de la fibrosis puede representar que los fibroblastos activados no pueden regresar a su estado basal. Para ello realizaron una búsqueda de cambios en la metilación del genoma e

identificaron varias modificaciones que ocurren en el patrón de metilación y que son únicas para fibroblastos obtenidos de riñones de humano con fibrosis y los compararon con riñones sin fibrosis. La metilación es una modificación epigenética que reduce la expresión de genes y que se puede heredar a través de la división celular, por ello se considera como una transformación estable del patrón de expresión de genes para una población celular en particular. Los autores identificaron 12 genes candidatos, pero demostraron que la metilación en el gen RASAL1 por la metiltransferasa Dnmt1.5, es esencial para la activación crónica de los fibroblastos [112].

Tomado todo en consideración, resulta indispensable el estudio de los mecanismos por los cuales un episodio de LRA puede desencadenar y conducir a la afectación de la función y la estructura renal en forma progresiva, así mismo, es de vital importancia encontrar maniobras farmacológicas que eviten la LRA con lo que se evitará el desarrollo de la ERC y de la ERCT. Hasta este momento la progresión de LRA a ERC en ratas con dos riñones intactos no se ha explorado. Tal modelo permitiría estudiar los mecanismos que causan la progresión a ERC y para identificar estrategias farmacológicas que puedan prevenir ó retrasar el desarrollo de ERC.

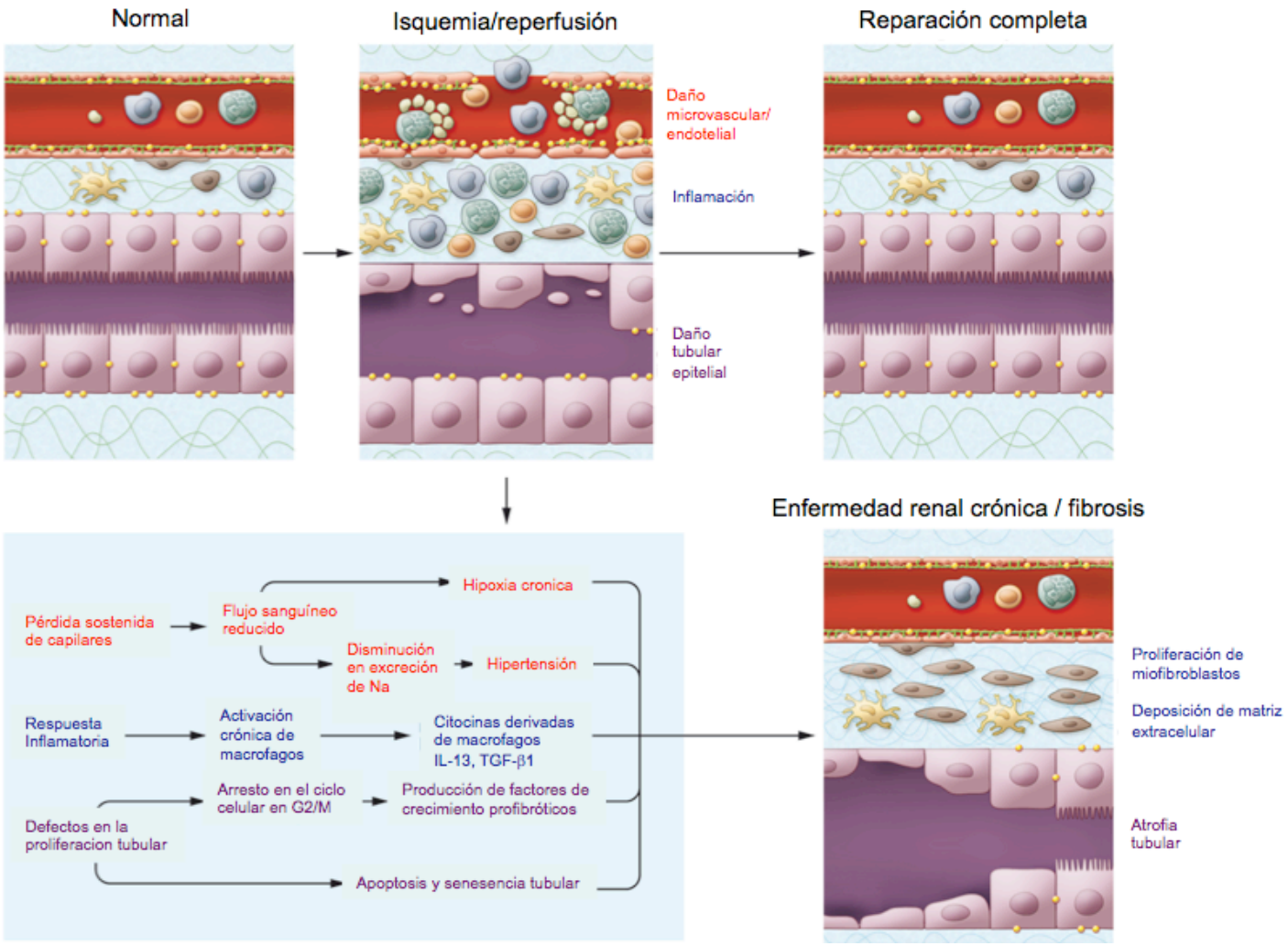

Figura 4. Mecanismos propuestos por los que la LRA puede conducir al desarrollo de ERC. Figura modificada de Bonventre and Yang, 2011 [4].

Con el objetivo de encontrar una maniobra farmacológica para prevenir la progresión de LRA a ERC, estudios de nuestro laboratorio han mostrado que el bloqueo de las acciones de aldosterona por la administración profiláctica de espironolactona (fármaco antagonista de los receptores de mineralocorticoides) o el retiro de las glándulas suprarrenales previene el daño funcional y estructural inducido por un fenómeno de I/R. Además la administración de espironolactona a diferentes periodos de tiempo post-isquemia previno o redujo el daño funcional y estructural lo que sugiere fuertemente que la aldosterona juega un papel preponderante en el daño renal que se observa después de un episodio de LRA

[113, 114, 115, 116, 117, 118]. A este respecto, se ha propuesto que la aldosterona tiene un papel importante en la regulación del tono vascular, específicamente a través de su unión con los receptores a mineralocorticoides presentes en la vasculatura a través muy probablemente de mediar vasoconstricción [119]. De hecho, la participación del receptor de mineralocorticoides en la regulación del tono vascular ha sido evidenciada en un estudio donde se utilizaron ratones deficientes de este receptor, específicamente en las células de músculo liso vascular, observando que estos ratones presentaban una menor presión arterial durante el envejecimiento en comparación con los ratones silvestres. Este efecto se asoció con una reducción en el tono miogénico y la contracción vascular, así como, menor expresión de canales de calcio tipo L [120]. Con estos antecedentes en este trabajo nos propusimos también, desarrollar un modelo de ERC inducida por LRA para estudiar los mecanismos moleculares involucrados y evaluar si el bloqueo de los receptores a mineralocorticoides con espironolactona antes o después de la I/R puede prevenir el desarrollo de ERC.

En resumen, dado que la morbilidad y la mortalidad de la lesión renal aguda no se ha mejorado en las últimas cuatro décadas debido a diferentes factores, el presente proyecto pretende abordar este problema de salud pública desde tres abordajes: el primero se enfoca a caracterizar si Hsp72 puede servir como biomarcador de LRA, el segundo se diseñó para profundizar en el conocimiento sobre el papel que juegan Hsp90α y Hsp90β en la fisiología y en un modelo de fisiopatología renal; y el tercero se diseñó para estudiar los mecanismos por los cuales un episodio de LRA puede llevar al desarrollo de la ERC y evaluar si el tratamiento con espironolactona puede prevenir el desarrollo de la ERC provocada por un episodio de LRA.

II. O B J E T I V O S

1. **Establecer si la detección de la proteína Hsp72 en la orina puede ser utilizada como biomarcador del daño renal inducido por I/R.**
   1.1. Determinar los niveles de RNAm y de proteína Hsp72 en el tejido renal de animales sometidos a diferentes periodos de isquemia**.**
   1.2. Estudiar si los niveles urinarios de Hsp72 se incrementan en forma proporcional ante los diferentes grados de daño renal inducido por diferentes periodos de isquemia.
   1.3. Correlacionar la cantidad urinaria de Hsp72 con el daño funcional y estructural inducido por diferentes periodos de isquemia.
   1.4. Determinar si la detección urinaria de Hsp72 es un biomarcador temprano de daño renal.
   1.5. Estudiar el comportamiento de Hsp72 sobre el monitoreo de una intervención farmacológica que prevenga el daño renal inducido por I/R.
   1.6. Investigar si la detección urinaria de Hsp72 es un biomarcador sensible de LRA en humanos, mediante el análisis de la orina de pacientes con LRA en la unidad de terapia intensiva.

2. **Evaluar el efecto de la sobre-expresión de Hsp90α y de Hsp90β en la fisiología renal normal y en un modelo de daño renal por isquemia/reperfusión.**
   2.1. Evaluar si la sobre expresión de Hsp90α o de Hsp90β modifica la función renal normal, mediante la transfección intra-renal del cDNA de las isoformas Hsp90α y Hsp90β clonadas.
   2.2. Determinar si la sobre-expresión de Hsp90α o de Hsp90β mejora o empeora el daño renal inducido por I/R, mediante estudios fisiológicos, histopatológicos y moleculares.

2.3. Investigar el efecto de la sobre expresión de Hsp90α o de Hsp90β sobre la vía de eNOS/NO en el tejido renal de las ratas sometidas a I/R.

3. Estudiar si el tratamiento con espironolactona es una maniobra útil para la prevención de la enfermedad renal crónica inducida por un periodo de LRA.

3.1. Desarrollar un modelo de enfermedad renal crónica inducida por un periodo de lesión renal aguda.

3.2. Estudiar los mecanismos por los que la lesión renal aguda conduce al desarrollo de enfermedad renal crónica.

3.3. Evaluar si la espironolactona previene el desarrollo de enfermedad renal crónica inducida por un episodio de LRA.

III. MATERIALES Y MÉTODOS

Modelo de Isquemia/Reperfusión renal

Se incluyeron ratas Wistar macho de 270 a 300 g. Las ratas se anestesiaron con pentobarbital sódico (30 mg/kg) y se colocaron en una mesa termo-regulada para mantener la temperatura corporal a 37ºC. Se realizó una incisión abdominal y se expusieron ambos riñones. Se disecaron los pedículos renales y se indujo isquemia bilateral (o unilateral cuando se especifique) mediante la colocación de clips no traumáticos para interrumpir el flujo sanguíneo a los riñones por el tiempo indicado en cada experimento. La reperfusión se logró al retirar los clips y se confirmó mediante el cambio de coloración de los riñones. La incisión se cerró en dos capas con suturas 3-0 y las ratas se dejaron evolucionar por 24 horas o por el tiempo indicado en cada experimento. Las ratas con cirugía falsa (sham) sostuvieron el mismo procedimiento, excepto por la colocación de los clips.

Transfección intra-renal de los plásmidos pcDNA3.1/Hsp90α y pcDNA3.1/Hsp90β

La inducción de Hsp90α ó Hsp90β se realizó mediante la estrategia de transfección intra-renal izquierda 48 horas antes de inducir la isquemia. Las isoformas Hsp90α ó Hsp90β fueron previamente clonadas en el vector de expresión pcDNA3.1-(+). Se disecó perfectamente la arteria renal izquierda y se colocó un clip no-traumático en la arteria y uno en la vena izquierda para poder inyectar 50 μg del plásmido correspondiente en conjunto con lipofectamina 2000 (100 μL) utilizando agujas para insulina de 31mm y de 31 G. La correcta colocación de los liposomas en el tejido renal se corroboró visualmente por el cambio de coloración en el riñón. Después de 2 minutos se retiraron los clips para permitir nuevamente el paso del

flujo sanguíneo al riñón. Después de 48 horas los animales fueron sometidos a isquemia-reperfusión.

Protocolo experimental derivado del primer objetivo

Para inducir diferentes grados de daño renal, se incluyeron 30 ratas que se dividieron en 6 grupos: el control y los grupos con isquemia renal bilateral de 10, 20, 30, 45 y 60 min, todos con reperfusión de 24 horas. Para evaluar si Hsp72 es un biomarcador temprano de daño renal se incluyeron 30 ratas que se sometieron a isquemia de 30 min y se dividieron en 10 grupos de diferentes tiempos de reperfusión: 3, 6, 9, 12, 18, 24, 48, 72, 96 y 120 horas. Para determinar si Hsp72 es un marcador capaz de monitorear la eficacia de una estrategia reno-protectora se incluyeron 30 ratas que se sometieron a I/R de 30 min. y se dividieron en 5 grupos: un grupo de ratas no recibió tratamiento y los otro cuatro grupos recibieron un tratamiento profiláctico de espironolactona a una dosis de 20, 10, 5 y 2.5 mg/kg respectivamente. Finalmente para evaluar la utilidad clínica de Hsp72 como biomarcador de LRA, se estudió la concentración de Hsp72 en pacientes sanos y en pacientes que se diagnosticaron con LRA mediante elevación de creatinina sérica durante su estancia en la UTI del Instituto Nacional de Ciencias Médicas y Nutrición Salvador Zubirán.

Protocolo experimental derivado del segundo objetivo

Se incluyeron 85 ratas Wistar macho (270-300 g) divididas en 17 grupos:

PROTOCOLO 1

1) Sham o de cirugía falsa
2) Transfección con vector vacío (pcDNA3.1)

3) Transfección con pcDNA3.1/Hsp90α

4) Transfección con pcDNA3.1/Hsp90β

PROTOCOLO 2

5) I/R bilateral de 30 min.

6) I/R bilateral de 30 min. + vector vacío (pcDNA3.1)

7) I/R bilateral de 30 min. + pcDNA3.1/Hsp90α

8) I/R bilateral de 30 min. + pcDNA3.1/Hsp90β

PROTOCOLO 3

9) I/R unilateral de 30 min.

10)I/R unilateral de 30 min. + vector vacío (pcDNA3.1)

11)I/R unilateral de 30 min. + pcDNA3.1/Hsp90α

12)I/R unilateral de 30 min. + pcDNA3.1/Hsp90β

PROTOCOLO 4

13)Nefrectomía derecha

14)Nefrectomía derecha + I/R de 30 min. Izquierda

15) Nefrectomía derecha + I/R de 30 min. Izquierda + vector vacío (pcDNA3.1)

16)Nefrectomía derecha + I/R de 30 min + pcDNA3.1/Hsp90α

17)Nefrectomía derecha + I/R de 30 min + pcDNA3.1/Hsp90β

En estos animales se evaluó: la presión arterial media, el flujo sanguíneo renal, la creatinina sérica y la excreción urinaria de peróxido de hidrógeno y de nitritos y nitratos. Una porción del riñón transfectado y/o sometido a isquemia se extrajo y se fijo en formaldehído al 4% para el análisis histológico del grado de daño renal mediante morfometría. Como marcadores de daño renal, se evaluó la excreción urinaria de Hsp72 y de proteínas. La otra fracción del riñón se separó

macroscópicamente en corteza y médula renal y se congeló a -80°C para los estudios moleculares.

Protocolo experimental derivado el tercer objetivo

Se incluyeron 75 ratas. Las ratas se sometieron a isquemia bilateral de 45 min, se suturaron y se dejaron evolucionar por 10 ó 270 días hasta su sacrificio. La espironolactona se administró por una sonda gástrica a una dosis de 20 mg/kg/día durante tres días antes de inducir I/R y se suspendió el tratamiento el día de la isquemia o 20 mg/kg inmediatamente después de la isquemia, 1.5 ó 3 horas después de la isquemia. Para estudiar el efecto de la administración de espironolactona antes de inducir la isquemia, se incluyeron cuatro grupos (n=10): 1) ratas sometidas a cirugía falsa (S), 2) el grupo que recibió espironolactona 3 días antes de ser sometido a cirugía falsa (Sp), 3) ratas que se sometieron a isquemia bilateral de 45 min (A-a-C), y 4) el grupo que recibió espironolactona 3 días antes de la isquemia (A-a-C+Sp). Cuatro animales de cada grupo se estudiaron después de 10 días de reperfusión y el resto después de 270 días. Cada 30 días se realizó recolección de orina de 24 h para la determinación de la excreción urinaria de proteínas. Al final del periodo experimental se registró el flujo sanguíneo renal, la presión arterial media y se calculó la depuración de creatinina. Para determinar el efecto de la administración de espironolactona después de inducir la isquemia se incluyeron 7 grupos adicionales como se muestra en la figura 5 (n=5): ratas sometidas a cirugía falsa (S), ratas que se sometieron a I/R bilateral de 45 min (A-a-C) y ratas sometidas a I/R bilateral de 45 min y tratamiento con dosis baja de espironolactona (20mg/kg) a las 0, 1.5 ó 3 horas después de la I/R y con dosis alta de espironolactona (80mg/kg) a las 0 y 1.5 h después de la I/R. Se extrajo el riñón

izquierdo para estudios moleculares de PCR y Western blot y el riñón derecho se utilizó para el análisis histológico y de microscopía electrónica.

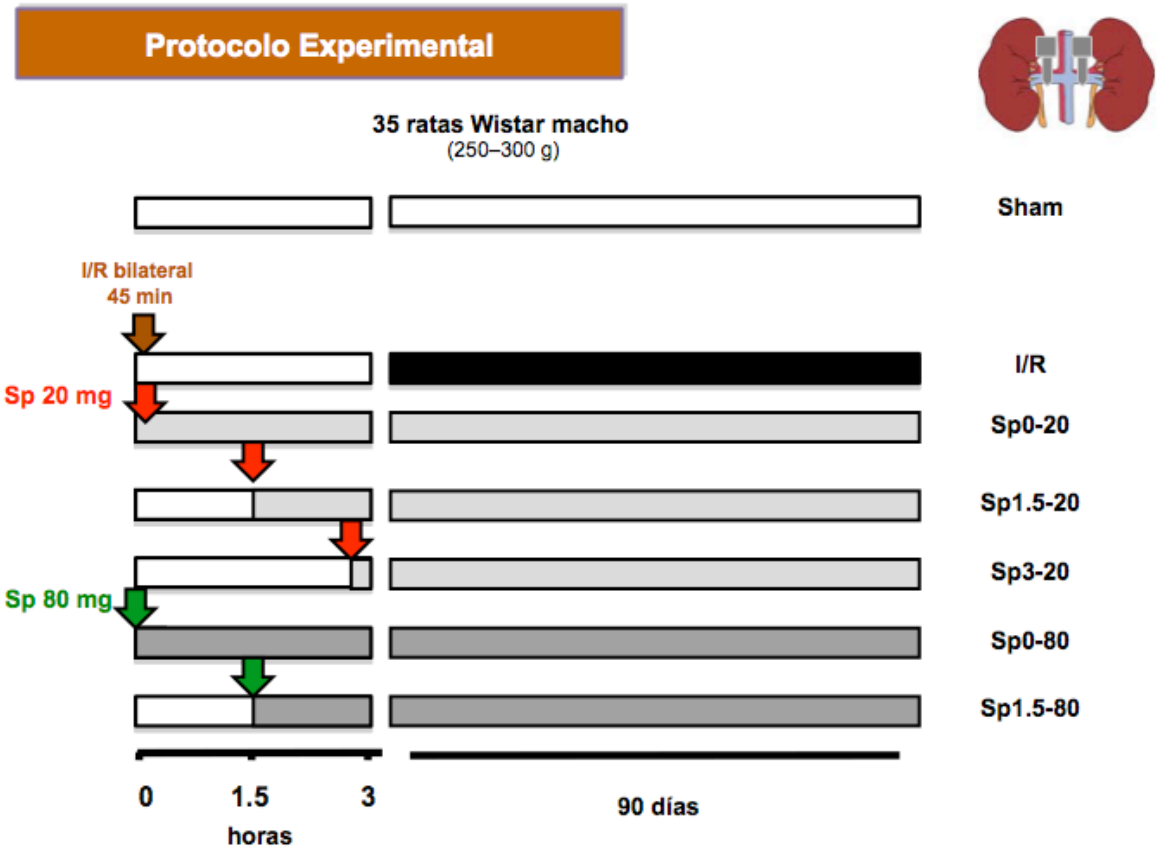

Figura 5. Protocolo experimental para evaluar la eficacia del tratamiento con espironolactona después de inducir la I/R.

Estudios Fisiológicos

Cada 30 días, las ratas se colocaron en jaulas metabólicas para recolección de orina de 24 h para determinar el volumen urinario, la excreción urinaria de proteínas y la depuración de creatinina. La concentración de creatinina en suero y en orina se determinó con un auto-analizador (Technicon RA-1000, Bayer Co. Tarrytown, NY). La depuración de creatinina se calculó mediante la fórmula C=(UxV)/P, donde U es la concentración de creatinina en orina, V es el flujo urinario y P es la concentración de creatinina en orina. La excreción urinaria de

proteínas se determinó mediante el método de turbidimetría con acido tricloroácetico (TCA) y se cuantificó en el espectrofotómetro a 420nm.

Al finalizar el periodo experimental, las ratas fueron anestesiadas con pentobarbital sódico (30 mg/kg) y puestas en una mesa termo-regulada. Se cateterizó la arteria femoral izquierda con tubo de polietileno PE-50. La presión arterial media fue registrada con un transductor de presión (Model p23 db, Gould. Puerto Rico) y almacenada con un polígrafo (Grass Instruments, Quincy, MA). A través de una incisión media, la arteria renal izquierda fue expuesta y con una sonda de ultrasonido (1RB, Transonic, Ithaca, NY) puesta alrededor de la arteria renal izquierda se registró el flujo sanguíneo renal.

Estudios histopatológicos

Al finalizar el experimento, el riñón derecho se extrajo y se congeló para los estudios moleculares y el riñón izquierdo se perfundió a través del catéter de la arteria femoral con solución salina, preservando la presión arterial media de cada animal. Una vez que se limpió el riñón del contenido de sangre, se perfundió con formaldehído al 4% y se continuó la perfusión hasta que se completó la fijación. Los riñones se sumergieron en parafina, se realizaron secciones de 4μm de grosor y se tiñeron con ácido per-yódico de Schiff (PAS) o rojo de sirio. El análisis de las laminillas fue ciego. Se evaluó el tamaño glomerular mediante la determinación del diámetro del mismo. Para ello se capturaron de 10 a 15 campos de corteza renal de las ratas utilizando una cámara digital incorporada en un microscopio marca Nikon y se midieron al menos 500 glomérulos en las microfotografías digitalizadas. Además en 10 campos subcorticales se evaluó el porcentaje de área tubular afectada mediante morfometría. En este caso el daño tubular se caracterizó por una pérdida del borde en cepillo, dilatación tubular y desprendimiento de las células de la

membrana basal tubular. En las secciones teñidas con rojo de Sirio se capturaron 10 campos subcorticales de los riñones de diferentes grupos para evaluar el porcentaje de fibrosis túbulo-intersticial mediante morfometría. La fibrosis túbulo-intesrticial consistió en expansión de la matriz extracelular, deposición de colágena junto con distorsión o colapso de los túbulos. Se capturaron 15 imágenes y se delimitó el área afectada. El porcentaje de fibrosis se calculó al dividir el área fibrótica entre el área total excluyendo el área glomerular. Para evaluar la proliferación celular se realizó inmunohistoquímica para el antígeno nuclear de proliferación celular (PCNA) utilizando el anticuerpo DAKO monoclonal mouse anti-PCNA antibody, clone PC10. Se realizó el conteo de células positivas para PCNA además del porcentaje de túbulos dilatados. Para evaluar la integridad de los podocitos se efectúo microscopía electrónica de transmisión. Para ello un fragmento de 1x1 mm de cada corteza renal se fijó en glutaraldehído al 2.5%, se seccionó en fragmentos de 50-100nm y se analizaron en un microscopio electrónico Carl Zeiss (EM-19C).

Estudios Moleculares

Extracción de RNA: El RNA total se extrajo de los tejidos almacenados a -80 ºC mediante homogenización en TRIZoL (Invitrogen). Para determinar la calidad del RNA se midió su concentración por espectrofotometría de UV (280 nm/260 nm) y se analizó su integridad mediante electroforesis en gel de agarosa al 1%.

RT (Transcripción Reversa): La transcripción reversa (RT) se llevó a cabo con 1 μg de RNA total del tejido. Primero se llevó el RNA a 65 ºC por 10 min. La reacción se realizó utilizando 200 U de transcriptasa reversa del virus de la leucemia en el mono (Moloney murine leukemia virus reverse transcriptase, MMLV, Stratagene), 100 pmol de hexámeros al azar (random primers, Life Technologies), 0.5 mM de

cada dNTP (una mezcla de dCTP, dATP, dGTP, dTTP, Sigma), y 1X de buffer de TR (75 mM KCl; 50 mM Tris-HCl; 3 mM MgCl2; 10 mM DTT, pH 8.3), se incubó a 37ºC por 60 min, a un volumen final de 20 μl. Una vez transcurrido el tiempo de reacción, las muestras se llevaron a 95ºC por 5 min para inactivar la transcriptasa reversa.

PCR en tiempo real: Se utilizaron sondas TaqMan específicas para amplificar fragmentos de DNAc de Applied Biosystems marcadas con FAM (6-carboxyfluoresceina) o VIC, para el análisis de TGF-β, ICAM-1, IL-6, TNF-α, MCP-1, Hsp72 y 18S RNAr como amplificación control. FAM y VIC son colorantes fluorescentes utilizados para detectar la amplificación de productos. De esta forma la cantidad de FAM o VIC, liberada por la degradación de la sonda TaqMan por exonucleasa en la reacción de PCR, es medida en función del cada ciclo de amplificación por reacción PCR mediante el uso de un termociclador en tiempo real ABI 7000 Prism (Applied Biosystems). La expresión de cada gene se cuantificó en forma relativa usando el método comparativo de Ct [121]. Los números de catálogo de las sondas utilizadas son los siguientes: TGF-β (Rn00572010_m1), IL-6 (Rn01410330_m1), TNF-α (Rn01753871_m1), MCP-1 (Rn00580555_m1), ICAM (Rn00446234_m1), Kim-1 (Rn00597703_m1) y Hsp72 (Rn00583013_s1).

Análisis de Western Blot: La corteza renal de cada rata se homogenizó en buffer de lisis (50mM HEPES pH 7.4, 250mM NaCl, 5mM EDTA, 0.1% NP-40) más un cocktail de inhibidores de proteasas Complete (Roche), en el sobrenadante se determinó la concentración de proteínas por el método de Lowry (BIO-RAD). Posteriormente las muestras se sometieron a electroforesis, se cargaron 50 μg de proteína total en un gel SDS-PAGE al 7.5% con buffer de carga 2X en relación 1:1

con un volumen final de 20 μl. Las proteínas se transfirieron a una membrana de difloruro de polivinilo, (PVDF, Millipore), previamente equilibrados con buffer de transferencia 1X (190 mM glicina, 2 mM Tris base, SDS 0.1%) en un trans-blot (SD cell, BioRad) durante 60 min a 9 volts, después las membranas fueron bloqueadas por 90 min en TBS-t (buffer Tris-salina) con 5% de agente bloqueante (BioRad) y posteriormente incubadas con el anticuerpo primario correspondiente. Se utilizaron anticuerpos específicos para Smad2 (1:500), Smad3 (1:500), fibronectina (1:200), colágena I (1:100), α-SMA (1:15000), Hsp72 (1:5000), Hsp90α (1:5000), Hsp90β (1:5000), eNOS (1:500) y fosfo-anticuerpos específicos para detectar la fosforilación en Ser423 de Smad3 (1:500), Ser465 de Smad2 (1:500), Ser1177 de eNOS (1:500) y Tre495 de eNOS (1:500). Después de la incubación con cada anticuerpo primario, las membranas se lavaron y se incubaron con el anticuerpo secundario "HRP-conjugated rat anti-rabbit IgG" (Alpha Diagnostics, San Antonio, TX) utilizando una dilución 1:2500. Para controlar la cantidad de proteína cargada y transferida, la parte inferior de todas las membranas se cuantificó la cantidad de actina, utilizando el anticuerpo primario diluido a 1:2500 y el secundario 1:10000 (donkey anti-goat IgG-HRP, Santa Cruz Biotechnology, Santa Bárbara, CA). Las proteínas se detectaron utilizando un estuche comercial de quimioluminiscencia (Millipore) y autoradiografía, siguiendo las recomendaciones del fabricante. Todos los análisis de Western blot se realizaron dentro del rango lineal de la carga de proteína y del anticuerpo utilizado. Se determinó la densidad óptica de cada banda para analizar la concentración de la proteína analizada.

Análisis de la relación dímero/monómero de Hsp90: La relación dímero/monómero de Hsp90 se evaluó en proteínas no-desnaturalizadas. Las proteínas se sometieron a electroforesis en gel de acrilamida sin SDS al 7.5% a 4ºC,

utilizando buffer de corrida y de carga sin SDS. Se transfirieron a una membrana de PVDF (Millipore) y se realizó el análisis de Western blot para Hsp90α y Hsp90β como se describió anteriormente en este trabajo.

Estudio de Inmunoprecipitación: Las proteína de Hsp90α, Hsp90β o eNOS se inmunoprecipitó utilizando el kit de inmunoprecipitación con proteína G (Sigma Aldrich). Cada inmunoprecipitación se optimizó utilizando 5 μg de anticuerpo anti-Hsp90α, Hsp90β o eNOS y 1 mg de proteína total. Las proteínas inmunoprecipitadas se eluyeron por calentamiento con buffer Laemmli y se realizó electroforesis en geles de SDS-PAGE al 8.5% para la detección de las proteínas mediante western blot como se mencionó anteriormente.

ELISA: Los niveles urinarios de Hsp72, NGAL, Kim-1 e IL-18 así como los niveles en tejido de TNF-α, MCP-1 e IL-6 fueron cuantificados utilizando estuches comerciales de ELISA. Todos los procedimientos se llevaron a cabo de acuerdo a las instrucciones del fabricante. La densidad óptica de las muestras se leyó a 450 nm y se extrapoló en la curva estándar correspondiente. Los kits utilizados fueron los siguientes: Hsp72 (Assay Designs EKS-715), NGAL (Innovative Research IRNGALKT), kim-1 (CosmoBIO Co CSB-E08808r), IL-18 (Invitrogen KRC2341), TNF-α (Ray Bio ELR-TNF alpha-001C), MCP-1 (Ray Bio ELR-MCP1-001C) e IL-6 (Ray Bio ELR-IL-6-001C).

Estudios bioquímicos

Evaluación del estrés oxidante: Para evaluar el estrés oxidante se determinó la excreción urinaria de peróxido de hidrógeno. La cantidad de peróxido de hidrógeno (H_2O_2), se determinó utilizando el estuche comercial "Amplex® Red Hydrogen Peroxide/Peroxidase Assay" siguiendo las instrucciones del fabricante. La determinación se basa en que en presencia de peroxidasa, el reactivo "Amplex Red" reacciona con el H_2O_2 produciendo un producto de oxidación rojo-fluorescente; la resurfina, la cual puede ser cuantificada espectrofotométricamente. Se mezclaron 50 μl de orina con 50 μl del reactivo del estuche comercial, las muestras se incubaron por 30 minutos a temperatura ambiente protegidos de la luz, se obtuvo la densidad óptica a 560 nm y la absorbancia fue extrapolada con la curva estándar para determinar la concentración de H_2O_2.

Excreción urinaria de nitritos y nitratos: La producción de NO se determinó en muestras de orina de recolección de 24 h de manera indirecta al cuantificar los metabolitos estables de la síntesis de óxido nítrico: los nitritos y los nitratos. Para ello se utilizó un ensayo comercial colorimétrico (Oxford Biomedical Research), el cual consiste en la conversión de los nitratos a nitritos utilizando la enzima *Nitrato Reductasa.* Posterior a la reducción, los nitritos totales se cuantificaron espectrofotométricamente mediante la reacción de Griess a una absorbancia de 540nm, dando así de una determinación confiable de la producción de NO.

Actividad de catalasa y de glutatión peroxidasa (GpX): La corteza renal se homogenizó en una solución de buffer de fosfatos 50 mM, pH 7.0 y 0.1% de Tritón. El homogenizado se centrifugó a 15000 g por 30 min a 4ºC y se utilizó para evaluar la actividad antioxidante de las enzimas. La actividad de catalasa se determinó de

acuerdo a el método de Aebi [122] y la actividad de Gpx se detectó de manera indirecta mediante un método reportado previamente por Lawrence y Burk [123]. Se determinó la concentración total de proteína mediante el método de Lowry [124] para normalizar la actividad enzimática.

Análisis estadístico

Los resultados se presentan como el promedio ± el error estándar (SE). Las diferencias entre los grupos se evaluaron por análisis de varianza (ANOVA) y la prueba de Bonferroni para comparaciones múltiples. Las diferencias en los diámetros glomerulares se evaluó mediante análisis de contingencia y las diferencias se evaluaron con la prueba de chi-cuadrada y la corrección de Yates. La diferencia se consideró significativa cuando el valor de p fue <0.05. Para la representación gráfica de los datos se utilizó el programa Sigma Plot 10.0.

IV. R E S U L T A D O S

RESULTADOS DEL PROTOCOLO I: Hsp72 como biomarcador sensible y temprano de lesión renal aguda.

Hsp72 como biomacardor para estratificar la LRA

Como se mencionó en la introducción, la mortalidad de la LRA no se ha disminuido en las últimas cuatro décadas debido a que no se cuenta con un método diagnóstico temprano que detecte este padecimiento de manera oportuna para intervenir al paciente eficientemente y mejorar el pronóstico. Es por ello que nuestro primer objetivo se enfocó en investigar si Hsp72 puede ser un biomarcador sensible y temprano de lesión renal aguda. Para ello, primero evaluamos si Hsp72 se encuentra en la orina de los animales con LRA inducida por I/R y si esta proteína puede estratificar la severidad del daño renal inducido. Para ello, se indujeron diferentes grados de lesión renal en cinco grupos de ratas sometidos a varios periodos de isquemia: 10, 20, 30, 45 y 60 minutos y se compararon con el grupo control sometido a cirugía falsa; todos los grupos se estudiaron 24 h después de la reperfusión. En la figura 6 se muestran los parámetros de función renal de los seis grupos estudiados junto con la cuantificación de dos marcadores clásicos de lesión tubular. Aunque los incrementos en creatinina fueron significativos únicamente después de los 30 minutos de isquemia bilateral (Figura 6A), todas las ratas sometidas a I/R mostraron disfunción renal caracterizada por una reducción gradual en la depuración de creatinina (Figura 6B) y en el flujo sanguíneo renal (Figura 6C). Estas alteraciones no se asociaron con cambios en la presión arterial media (Figura 6D). Como se esperaba, los animales sometidos a 60 min de isquemia bilateral fueron los que presentaron mayor grado de disfunción renal. El daño tubular inducido por diferentes periodos de isquemia fue evaluado por la elevación urinaria de NAG y de las proteínas en la orina. De forma similar al comportamiento de la creatinina sérica, el incremento en el NAG urinario solamente fue significativo

después de 30 minutos de isquemia, lo que sugiere que NAG no es un marcador sensible para detectar diferentes grados de lesión renal.

Para evaluar el grado de daño renal, se cuantificó el daño tubular por microscopía de luz e histomorfometría y se utilizó como el “estándar de oro" para determinar el grado de lesión renal aguda inducido por los diferentes tiempos de isquemia. En el panel izquierdo de la figura 7 se muestran las imágenes representativas de secciones de riñón de ratas sometidas a diferentes periodos de isquemia y en el panel derecho se muestra la cuantificación de los cilindros, así como el porcentaje del área tubular afectada cuantificada mediante estudios morfométricos. El daño tubular inducido por la I/R se caracterizó por perdida del borde en cepillo, dilatación o colapso del lumen tubular y desprendimiento celular de la membrana basal del túbulo (Figuras 7A - 7F). Como se aprecia en las figuras 7G y 7H hubo un incremento gradual y proporcional al periodo de isquemia inducido. Como era de esperarse, después de 24 h de reperfusión, el menor grado de daño tubular se observó en ratas que se sometieron a isquemia bilateral de 10 min y el peor daño se observó en ratas sometidas a 60 min de isquemia.

Posteriormente, para evaluar si Hsp72 se induce de forma proporcional al daño isquémico renal inducido, se evaluaron los niveles de RNAm y de proteína de Hsp72 en la corteza renal de ratas sometidas a diferentes periodos de isquemia. Como se muestra en la figura 8A los niveles de RNAm de Hsp72 se incrementaron de manera significativa y progresiva desde los 20 minutos de isquemia bilateral. Estos hallazgos fueron reflejados a nivel de proteína, como se muestra en la figura 8B. Es decir, el daño renal inducido por diferentes periodos de isquemia se asoció con un incremento gradual y significativo en los niveles de RNAm y de proteína de Hsp72 en comparación con las ratas sometidas a cirugía falsa. La mayor expresión de Hsp72 se observó en el grupo con el daño tubular más severo, siendo el incremento de 15 veces con respecto al grupo control. Estos resultados muestran que la expresión de Hsp72 es gradual y proporcionalmente incrementada de acuerdo a la intensidad del daño renal inducido. Por lo anterior, decidimos evaluar si la aparición en la orina de Hsp72 se pudiera utilizar como un biomarcador de daño renal inducido por I/R.

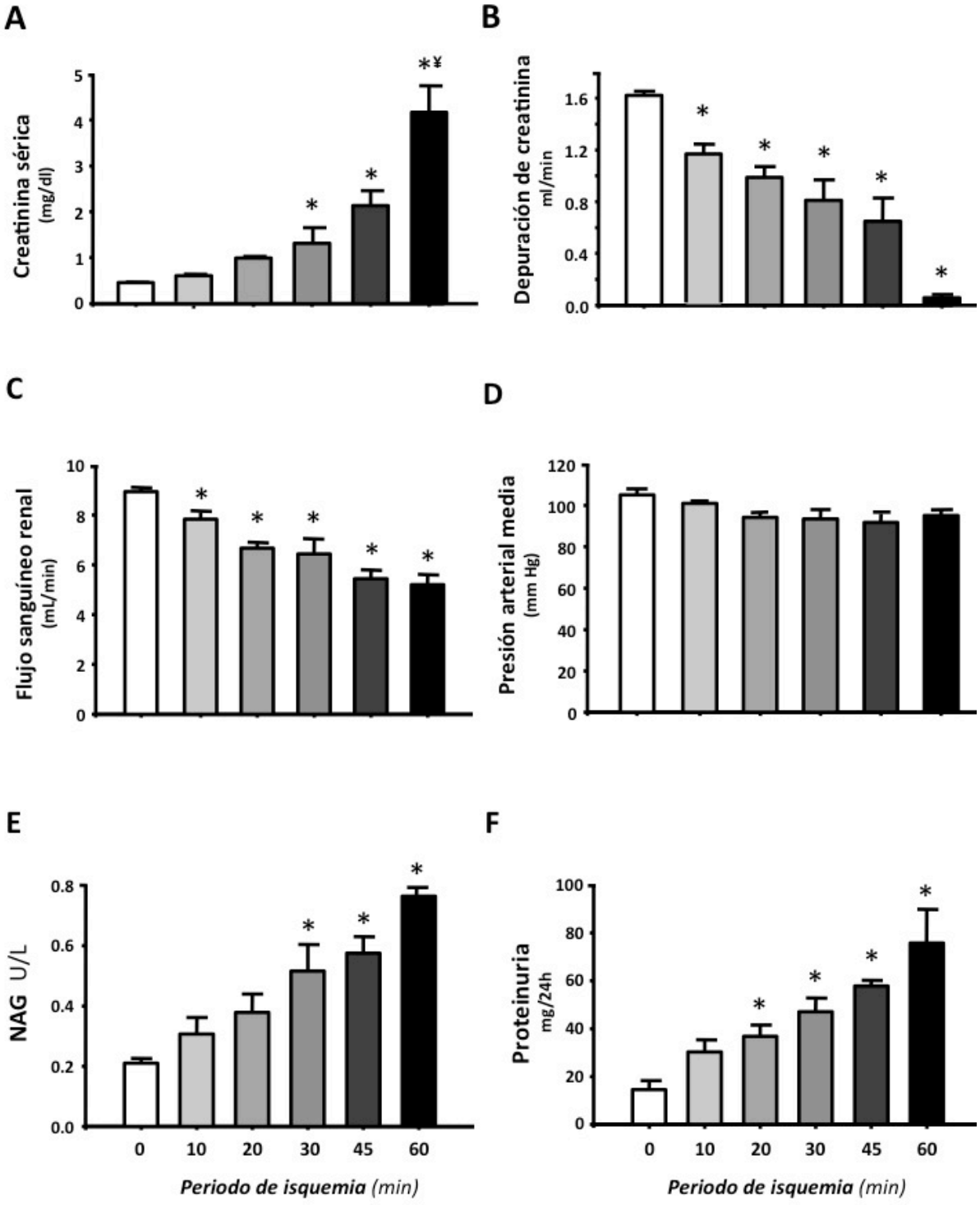

Figura 6. Parámetros de función renal en ratas sometidas a diferentes periodos de isquemia bilateral (10,20,30,45 y 60 min) y 24 h de reperfusión comparadas con ratas con cirugía sham (Barras blancas). El daño renal inducido por I/R se determinó mediante incrementos en la creatinina sérica (A) y reducciones en la depuración de creatinina (B) y flujo sanguíneo renal (C) sin cambios en la presión arterial media (D). La excreción urinaria de NAG y de proteínas se evaluaron como marcadores de daño tubular (E y F). n=6 animales por grupo. *p<0.05 vs. y ¥ p<0.05 vs. 45 min de isquemia .

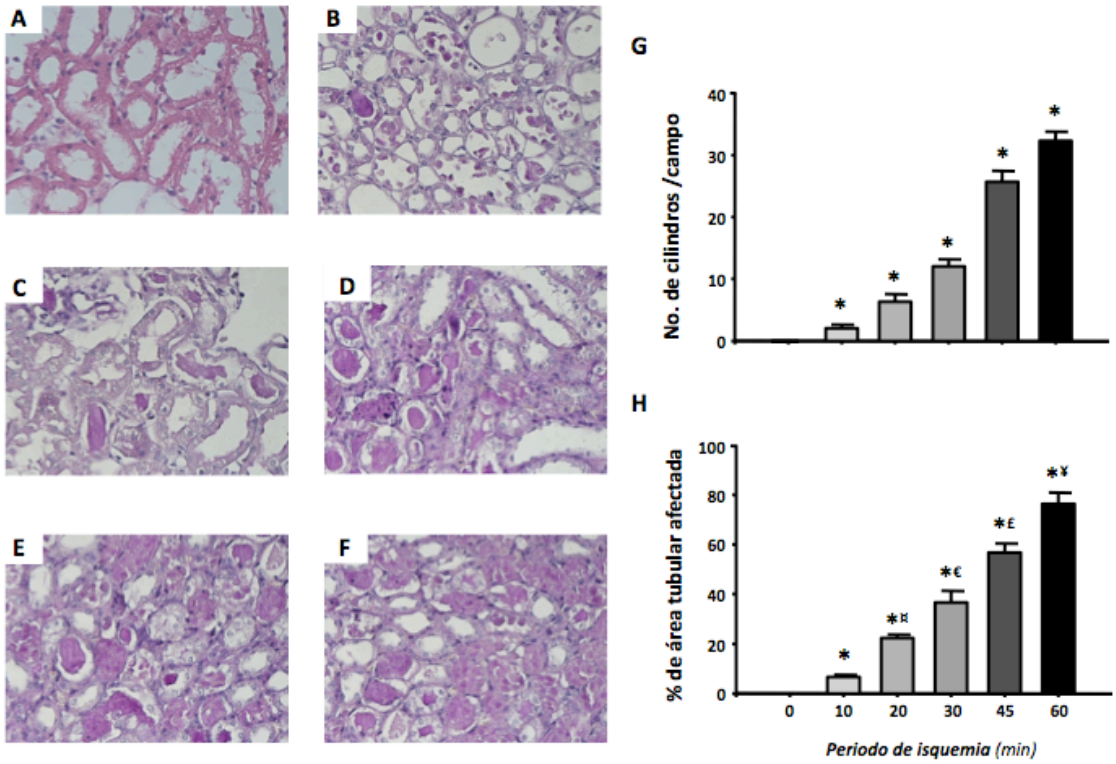

Figura 7. Secciones subcorticales de riñón teñidas con la técnica de PAS (periodic acid.Schiff) de A) sham, B) 10 min, C) 20 min, D) 30 min, E) 45 min y F) 60 min de isquemia bilateral. En las imágenes se puede observar el daño tubular caracterizado por el desprendimiento de las células epiteliales y la formación de cilindros que obstruyen el lumen tubular. G) Número de cilindros por campo y H) cuantificación morfométrica del porcentaje del área tubular afectada. n=6 animales por grupo. *p<0.05 vs. sham, ¤p<0.05 vs. 10 min, €p<0.05 vs. 20 min, £p<0.05 vs. 30 min, and ¥ p<0.05 vs. 45 min.

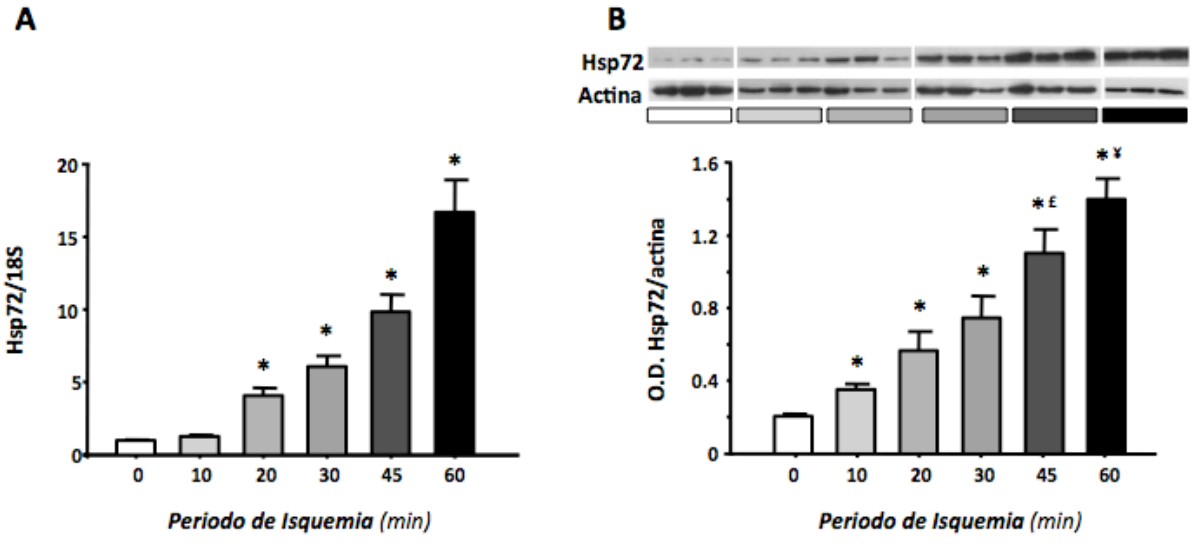

Figura 8. Expresión renal de Hsp72 en ratas sometidas a diferentes periodos de isquemia, determinados por PCR en tiempo real y análisis de western blot. A y B muestran la expresión de RNAm y proteína de Hsp72, respectivamente. n=6 animales por grupo. *p<0.05 vs. sham, £p<0.05 vs. 30 min, y ¥ p<0.05 vs. 45 min de isquemia.

Para demostrar si la Hsp72 podría ser detectada en la orina de animales que sufrieron LRA, primero analizamos los niveles de RNAm de Hsp72 en la orina colectada de los diferentes grupos estudiados. Como se muestra en la figura 9A, los niveles de RNAm de Hsp72 se incrementaron en el grupo de 10 minutos de isquemia comparado con el grupo control, este incremento fue mayor y proporcional a la duración de la isquemia en los otros grupos. Cuando estos valores fueron comparados con el número de cilindros, se encontró una correlación significativa, como se muestra en la figura 9B, con una r de Pearson de 0.8509 y $p<0.0001$. En la figura 9C, se muestran resultados similares cuando la correlación se hizo entre los niveles urinarios de RNAm de Hsp72 y el porcentaje de área tubular afectada (Pearson $r=0.9075$ y $p<0.0001$).

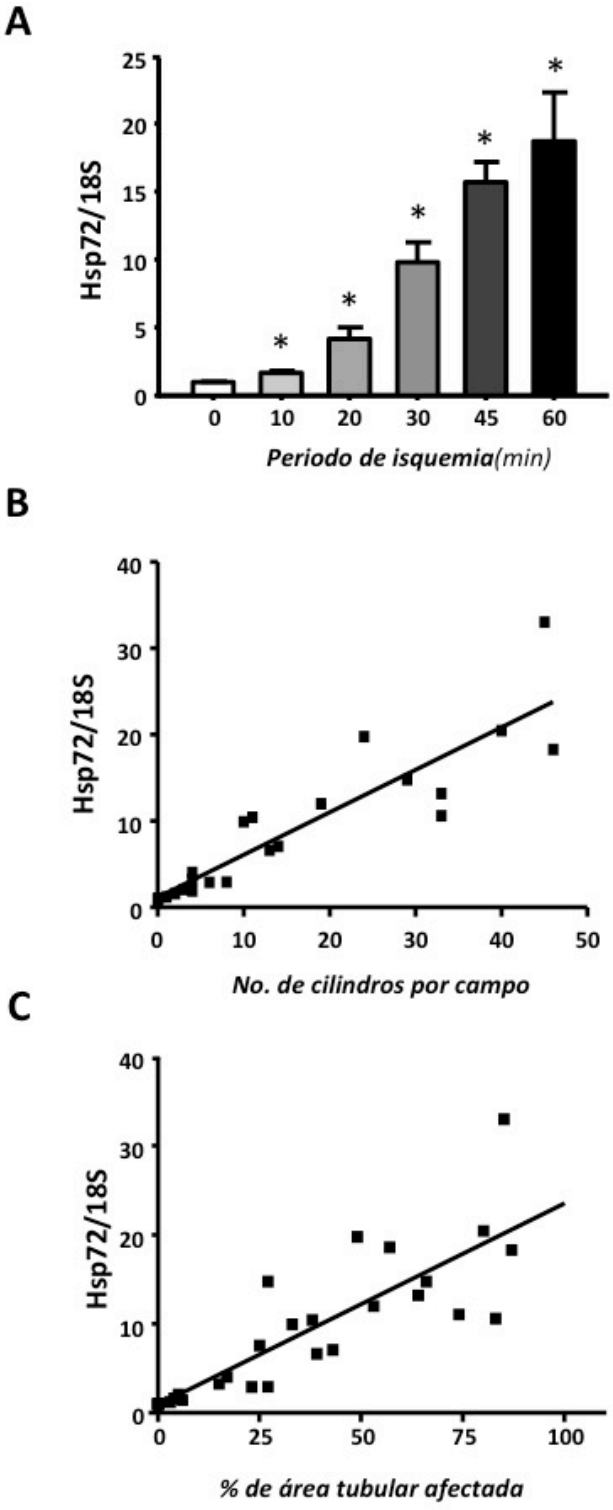

Figura 9. Niveles urinarios de RNAm de Hsp72 en ratas sometidas a diferentes periodos de isquemia. A) El RNA total fue extraído individualmente de la orina de las ratas estudiadas y los niveles de RNAm se determinaron mediante RT-PCR en tiempo real. B) Correlación entre los niveles urinarios de RNAm de Hsp72 y el número de cilindros por campo. C) Correlación entre los niveles urinarios de Hsp72 y el área tubular afectada. n=6 animales por grupo.*p<0.05 vs. sham.

Se determinaron los niveles urinarios de proteína de Hsp72 mediante dos inmunoensayos: ELISA y análisis de Western blot. La determinación de Hsp72 urinaria mediante ELISA, como se muestra en la figura 10A, reveló que esta proteína puede ser detectada en la orina y que es un excelente marcador de LRA dada su capacidad de diferenciar la severidad del daño, desde ligero (10 min), moderado (20 y 30 min) y severo (45 y 60 min de isquemia). La presencia de Hsp72 correlacionó con la extensión del daño tubular inducido por diferentes periodos de isquemia. La mayor cantidad de Hsp72 fue detectada en el grupo que se sometió a 60 min de isquemia y el incremento fue de 23 veces comparado con el grupo control. Como se muestra en la figura 10B y 10C, la elevación progresiva de la cantidad urinaria de Hsp72 correlacionó con la intensidad del daño renal, determinado por el número de cilindros y el área tubular afectada con $r= 0.8337$ y 0.7929 respetivamente ($p<0.0001$). Se observaron cambios similares cuando los niveles urinarios de Hsp72 se analizaron mediante Western blot. El panel superior de la figura 10D muestra las autoradiografías de este análisis en la orina de 4 diferentes ratas de cada grupo estudiado. Como se aprecia, la Hsp72 fue casi indetectable en la orina de las ratas controles, en contraste, los niveles de proteína de Hsp72 en la orina aumentaron progresivamente en las ratas que sufrieron periodos de isquemia crecientes. Como se aprecia en la figura 10D, los niveles de Hsp72 determinados por Western blot, se incrementaron significativamente desde los 10 minutos de isquemia y se elevaron en animales sometidos a periodos de isquemia más prolongados. La sensibilidad para detectar diferentes grados de daño renal fue mayor con el análisis de Western blot que con ELISA. Por Western blot, la elevación urinaria de Hsp72 fue de 40 veces en el grupo sometido a 10 minutos de isquemia y de 535 veces en el grupo con daño renal severo (60 min de isquemia), comparado con el grupo control. Como se muestra en la figura 10E y 10F, se encontraron correlaciones mayores entre la

cantidad urinaria de Hsp72 en la orina y la formación de cilindros o el % de área tubular afectada, r=0.9254 y r=0.9433, respectivamente ($p<0.0001$). ***Estos hallazgos muestran que Hsp72 puede ser detectada en la orina de ratas sometidas a isquemia y su detección urinaria es suficientemente sensible para estratificar la extensión del daño tubular***.

Hsp72 como biomacardor temprano de la LRA

La siguiente pregunta a contestar fue si Hsp72 es un biomarcador temprano de LRA y si es capaz de detectar la regeneración tubular que ocurre después de un fenómeno de isquemia. Para resolver esta interrogante se determinaron los niveles urinarios de Hsp72 en la orina de animales sometidos a 30 min de isquemia seguido de periodos de reperfusión de 3 hasta 120 h. En la figura 11 se muestran fotografías representativas de cortes histológicos de corteza renal después de periodos de reperfusión de 3, 6, 9, 12, 18, 24, 48, 72, 96 y 120 h (11A – 11J). En el panel derecho, se muestra la cuantificación del porcentaje de área tubular afectada y el conteo de cilindros por campo. Como muestra el análisis morfométrico en la figura 11K, hubo un incremento progresivo en el daño tubular, alcanzando un pico máximo de daño después de 18 h de reperfusión; en este punto el 50 % del área tubular se vio afectada. Después de las 18 h de reperfusión se observó una recuperación tubular progresiva hasta las 120 h de reperfusión, tiempo en el cual solamente el 12% del área tubular estaba afectada. El mismo patrón se observó cuando se cuantificó el número de cilindros por campo, como se muestra en la figura 11L.

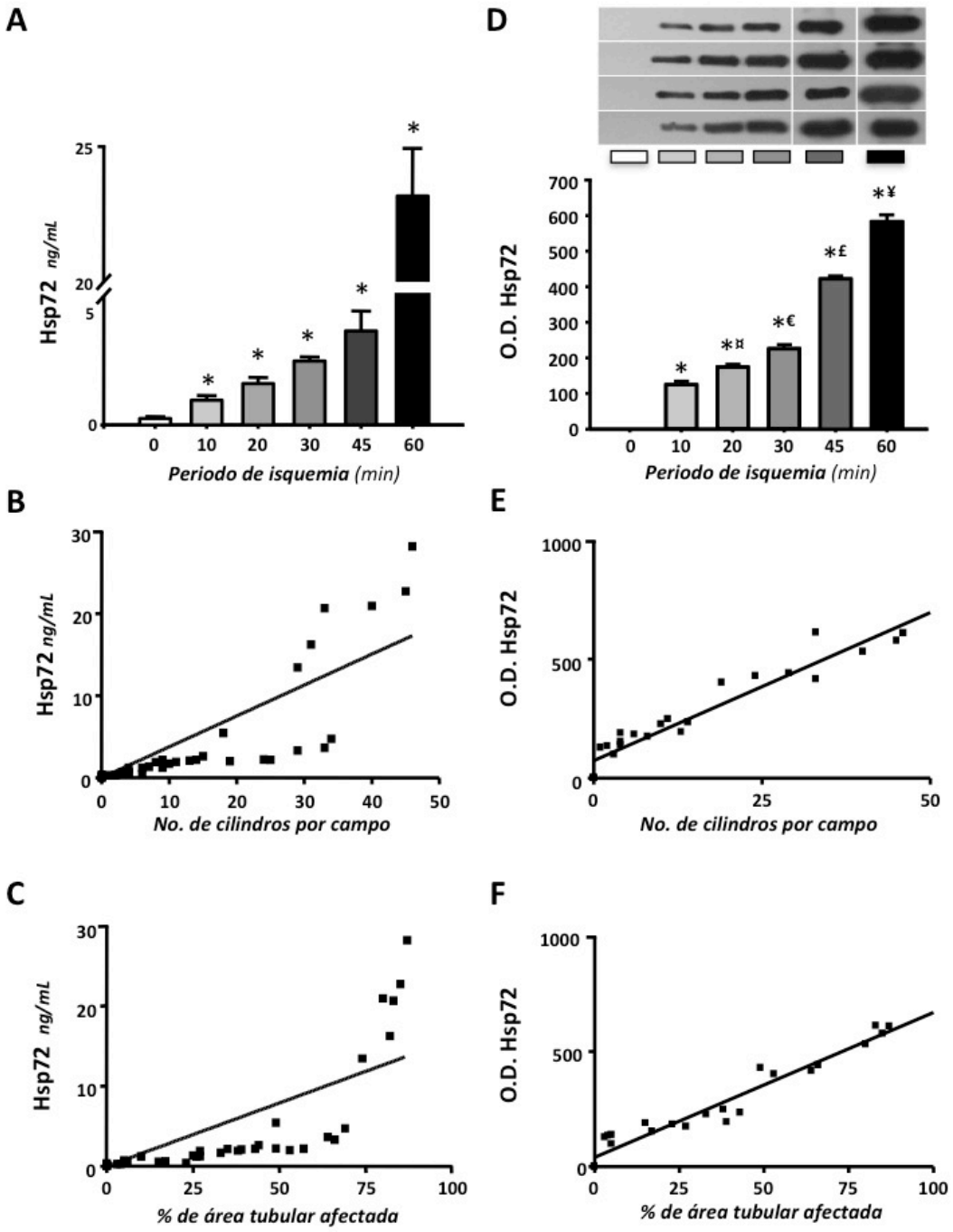

Figura 10. Niveles urinarios de Hsp72 de ratas sometidas a diferentes periodos de isquemia. A) Niveles urinarios de Hsp72 determinados por ELISA. B y C) muestran la correlación entre los niveles urinarios de Hsp72 y el número de cilindros o el % de área tubular afectada, respectivamente. D) Niveles urinarios de Hsp72 determinados pro análisis de western blot. E y F) muestran la correlación entre los niveles urinarios de Hsp72 y el número de cilindros o el % de área tubular afectada, respectivamente. n=6 animales por grupo. n=6 animales por grupo *p<0.05 vs. sham, ¤p<0.05 vs. 10 min, €p<0.05 vs. 20 min, £p<0.05 vs. 30 min, and ¥ p<0.05 vs. 45 min de isquemia.

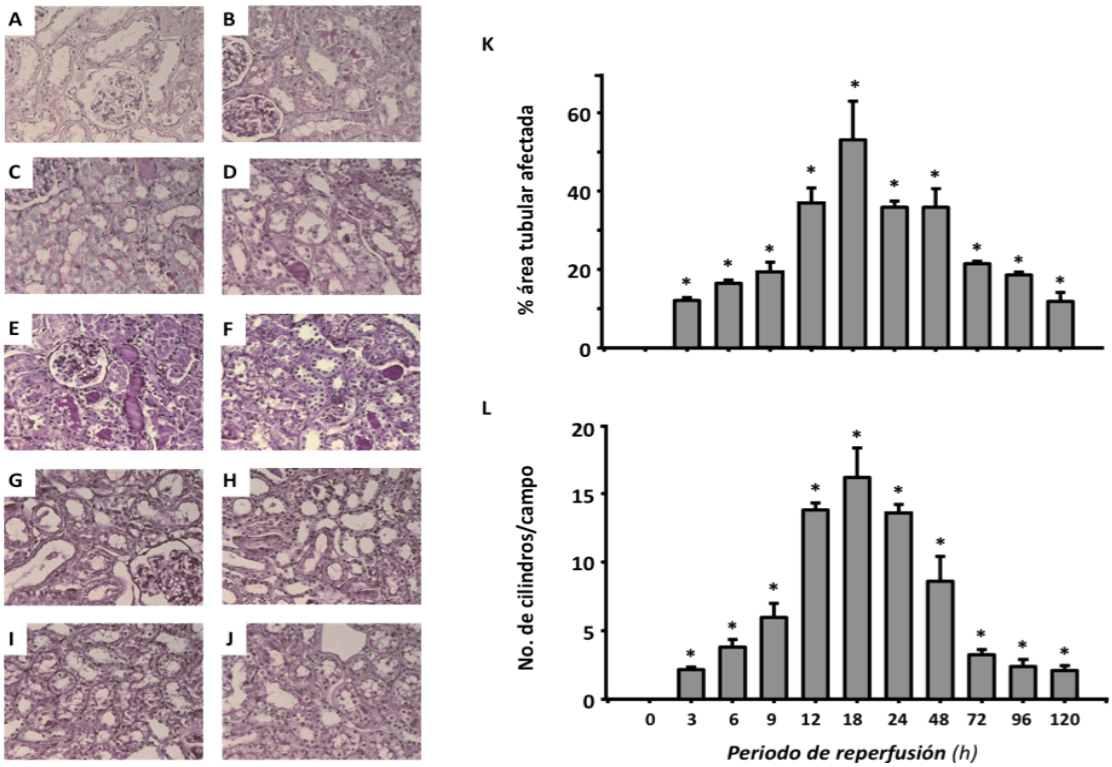

Figura 11. A-J) Cortes histológicos de corteza renal de rata teñidos con PAS. K) Cuantificación del porcentaje del área tubular afectada. L) Conteo del No. de cilindros por campo. n=3 animales por grupo *p<0.05 vs. Sham.

En la figura 12A, se muestra la detección urinaria de Hsp72 por ELISA donde se observó una elevación significativa en Hsp72 desde las 3 h después de la reperfusión. De forma similar al daño histológico, la mayor cantidad de Hsp72 se observó a las 18 h y regresó a valores basales después de 96 h de reperfusión. Nuevamente se observó una correlación significativa entre la cantidad urinaria de Hsp72 y el % del área tubular afectada r^2=0.65 (p<0.0001). En la figura 12C, se muestran las autoradiografías del análisis de Western blot de 3 ratas de cada grupo y el análisis densitométrico se muestra debajo. La cantidad urinaria de Hsp72 fue casi indetectable en las ratas con cirugía falsa, en contraste, se observó un incremento significativo en Hsp72 en los grupos sometidos a isquemia renal seguidos desde las 3 h de reperfusión y que se fue incrementando la cantidad detectada de Hsp72, teniendo un pico máximo a las 18 h y con un subsecuente disminución en la excreción urinaria de esta proteína. Interesantemente, se observó

una correlación entre Hsp72 y el % de área tubular afectada r^2= 0.55 (p<0.0001). ***Estos resultados demuestran que Hsp72 es un biomarcador temprano para detectar la LRA y sugiere que la cantidad detectada de Hsp72 en la orina puede revelar el estado tubular de daño y recuperación.***

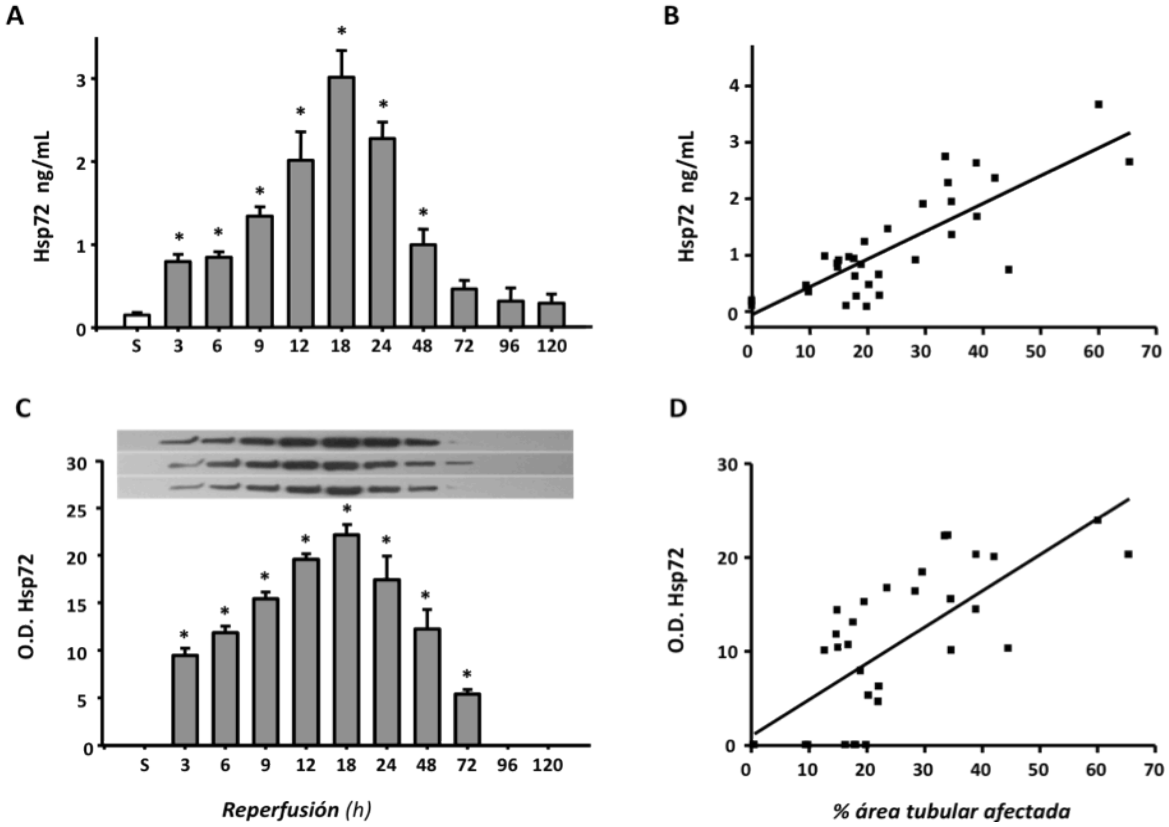

Figura 12. Niveles urinario de Hsp72 mediante ELISA (A) y western Blot (C) en ratas de diferentes tiempos de reperfusión y sus correlaciones con el % de área tubular afectada. n=3 animales por grupo *p<0.05 vs. Sham.

Hsp72 como biomarcador de la efectividad de una intervención renoprotectora en la LRA

Previamente reportamos que el bloqueo de los receptores de mineralocorticoides es una herramienta útil para prevenir el daño renal inducido por I/R, por lo que decidimos determinar si este efecto renoprotector podría ser reflejado por los niveles urinarios de Hsp72. La figura 13A y 13B muestran la creatinina sérica

y la depuración de creatinina en dos grupos de ratas, las sometidas a I/R sin tratamiento y las que se sometieron a I/R pero que recibieron el pre-tratamiento con espironolactona durante 3 días antes de la I/R (I/R + Sp). La administración de la espironolactona previno la disfunción renal, este efecto renoprotector se asoció con una reducción significativa en los niveles urinarios de Hsp72 detectados tanto por ELISA como por Western blot, como se muestra en las figuras 13C y 13D, respectivamente.

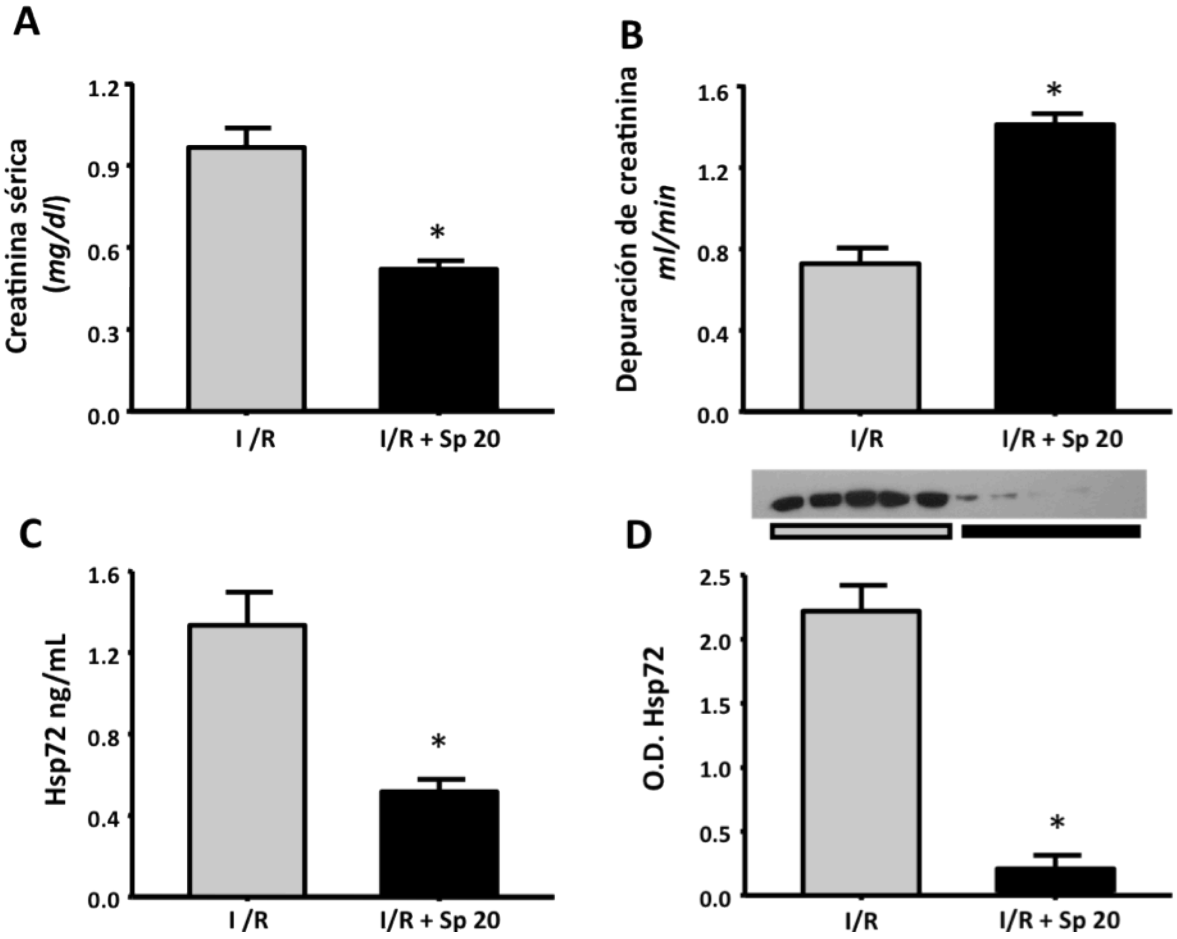

Figura 13. A y B) Creatinina sérica y depuración de creatinina respectivamente. C) Niveles urinarios de Hsp72 determinados por ELISA y D) Niveles urinarios de Hsp72 determinados por western blot. N= 4 ratas por grupo*p<0.05 vs. Sham.

Para evaluar si Hsp72 nos permite monitorear diferentes grados de renoproteción en ausencia de elevación de creatinina, se incluyeron diferentes

grupos pre-tratados con dosis menores de espironolactona. Como se muestra en la Figura 14A, las ratas pre-tratadas con espironolactona a 10 y 5 mg/kg mostraron valores normales de creatinina sérica que contrastaron con los niveles obtenidos en las ratas con 2.5 mg/kg, las cuales fueron prácticamente iguales a las ratas con I/R no tratadas. Interesantemente, los niveles urinarios de Hsp72 se incrementaron significativamente desde la dosis de 10 mg/kg y se elevaron aun más con las menores dosis de espironolactona empleada, como se ilustra en la figura 14B. ***Estos hallazgos sugieren que a menor dosis de espironolactona, menor es el grado de renoprotección y que esto puede ser detectado eficientemente por los niveles urinarios de Hsp72.***

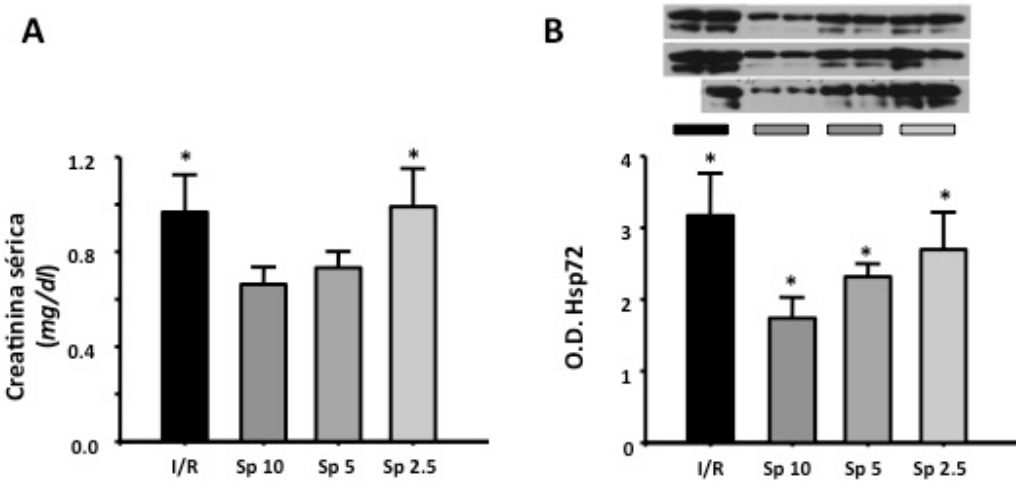

Figura 14. Niveles urinarios de Hsp72 como biomarcador de diferentes grados de renoprotección. A) Creatinina sérica en el grupo de I/R y en los animales tratados con dosis menores de espironolactona (10, 5 y 2.5 mg/kg) B) Análisis de western blot en las ratas pre-tratadas con diferentes dosis de espironolactona. N= 6 ratas por grupo. *p<0.05 vs I/R

Hsp72 como biomarcador sensible y temprano de LRA en el humano

Finalmente, para investigar si Hsp72 es un biomarcador sensible para detectar la LRA en humanos, se determinaron los niveles de esta proteína en la orina de sujetos sanos y se compararon con los de pacientes que desarrollaron LRA durante su estancia en la Unidad de Terapia Intensiva (UTI) del Instituto Nacional de

Ciencias Médicas y Nutrición Salvador Zubirán (INNSZ) mediante análisis de Western blot. Como se aprecia en la figura 15A, los niveles de Hsp72 fueron muy bajos en la orina de los individuos sanos, mientras que en los pacientes con LRA, se observó un aumento de 17 veces. Estos resultados también se confirmaron por ELISA (15B). La variabilidad en los resultados puede deberse a los diferentes grados de LRA que cada paciente tuvo, de hecho dos de los pacientes con la mayor cantidad de Hsp72 en la orina fallecieron durante su estancia en la UTI. Para identificar si Hsp72 es un biomarcador temprano de LRA en los humanos, se tomaron muestras diarias de orina de pacientes que ingresaron a la UCI y que tuvieron falla respiratoria complicada con alguna otra falla orgánica. Estos pacientes tenían función renal normal al momento de su admisión a la UTI. Se incluyeron 5 pacientes que desarrollaron LRA y 5 que no tenían evidencia clínica de LRA. En la figura 15C y 15D se muestran los niveles promedio de creatinina sérica y volumen urinario de estos pacientes respectivamente. El día cero representa el día que se realizó el diagnóstico de LRA por la elevación de creatinina. En la figura 15E se presenta el análisis de Western blot que muestra los niveles de Hsp72 en la orina recolectada desde el día -3 hasta el día 5 en aquellos pacientes con LRA, donde se puede apreciar un incremento significativo en los niveles de Hsp72 comparado con la orina de los días 1, 3, 5, 8 y 10 de los pacientes que no la desarrollaron (Figura 15F). Los niveles basales de Hsp72 fueron mínimos en los pacientes sin LRA y 3 días antes de aquellos diagnosticados con LRA. ***En concordancia con nuestros estudios experimentales, uno o dos días antes del diagnóstico de LRA se observó un incremento significativo en los niveles urinarios de Hsp72, sugiriendo que efectivamente Hsp72 puede ser un biomarcador temprano de LRA en humanos.***

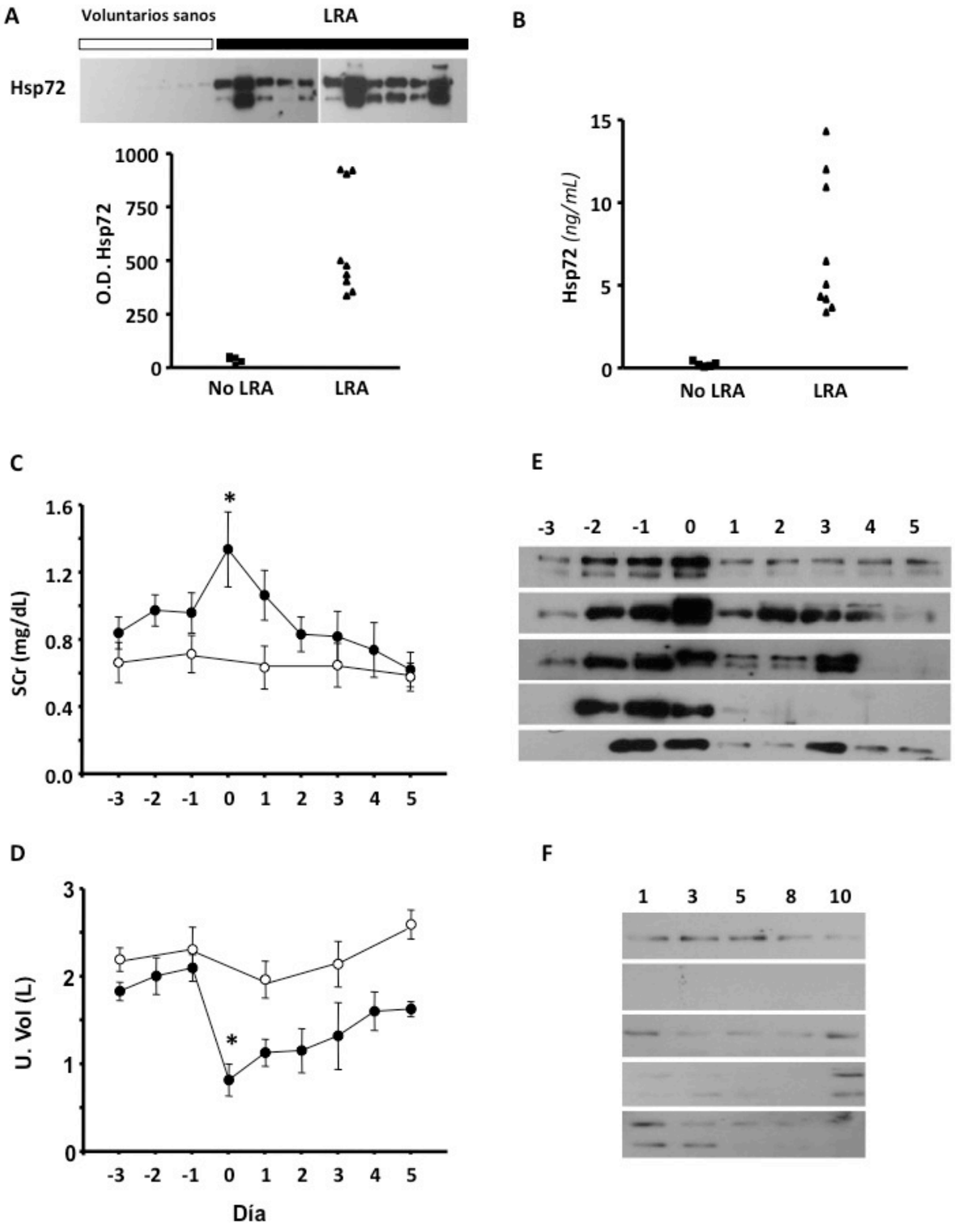

Figura 15. Niveles urinarios de Hsp72 como biomarcador de LRA en humanos determinados mediante A) Western blot y B) ELISA. C) Niveles de creatinina sérica y D) Volumen urinario en los pacientes con LRA (círculos negros) y sin LRA (círculos blancos) E,F) Niveles de Hsp72 urinaria en pacientes con y sin LRA, respectivamente. En los pacientes con LRA se analizaron las orinas del día -3 al día 5 y en los pacientes sin LRA se analizaron las muestras de orina de los días 1, 3, 5, 8 y 10 de su estancia en la UTI. *p<0.05 vs. -3.

RESULTADOS DEL PROTOCOLO II: EFECTO DE LA SOBRE-EXPRESION DE Hsp90α y Hsp90β EN UN MODELO DE LESIÓN RENAL AGUDA.

Validación de la sobre-expresión de Hsp90α y Hsp90β mediante la transfección intra-renal de los plásmidos con las isoformas clonadas en la rata

Para establecer el tiempo óptimo en el que ocurre la mayor sobre-expresión de Hsp90α o Hsp90β después de la transfección intra-renal del plásmido con el cDNA clonado, se realizó una curva temporal para analizar la expresión de Hsp90α y Hsp90β después de 24, 48 y 72 h de haber realizado la transfección. Como se observa en la figura 16A y 16B, la transfección intra-renal de cada plásmido indujo un incremento significativo en los niveles de proteína de Hsp90α y Hsp90β, respectivamente en el tejido renal. En ambos casos, el pico de sobre-expresión se detectó a las 48 h post-transfección. Por este motivo todos los experimentos que serán presentados a continuación fueron llevados a cabo 48 h después de la transfección de los plásmidos.

¿A qué región de la nefrona llega el material genético transfectado mediante la técnica de transfección intra-renal?

Para conocer en qué región de la nefrona se localiza la sobre-expresión de las proteínas transfectadas a través de la técnica reportada en este estudio, se procedió a la transfección intra-renal del vector que codifica para la proteína verde fluorescente (GFP). La detección de esta proteína en el tejido renal se realizó mediante inmunofluorescencia contra GFP y se analizó por microscopía confocal. Como se puede observar en la figura 16, la transfección del vector vacío no generó fluorescencia inespecífica (Figura 17A) ni fluorescencia en la longitud de onda de GFP (17B). En cambio en las ratas transfectadas con el vector de GFP se detectó fluorescencia en la longitud de onda esperada (668 nm) (Figuras 18B y 19B). Al

realizar la co-localización de la señal de fluorescencia con la imagen de campo claro se puede observar que la señal de GFP se encuentra en la vasculatura (Figura 18D) y en el epitelio tubular (Figura 19D).

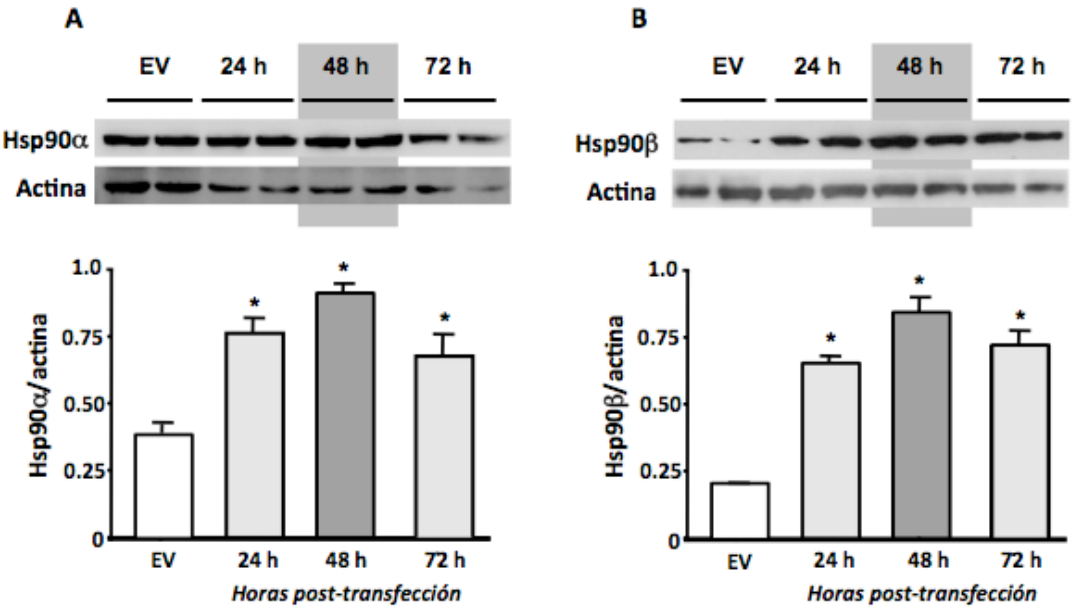

Figura 16. A) Niveles de proteína de Hsp90α en la corteza renal de ratas transfectadas con vector vacío (EV) ó Hsp90α a las 24, 48 y 72 h después de la transfección. B) Niveles de proteína de Hsp90β en la corteza renal de ratas transfectadas con vector vacío (EV) ó Hsp90β a las 24, 48 y 72 h después de la transfección. n = 4 ratas por grupo. *p<0.05 vs. EV.

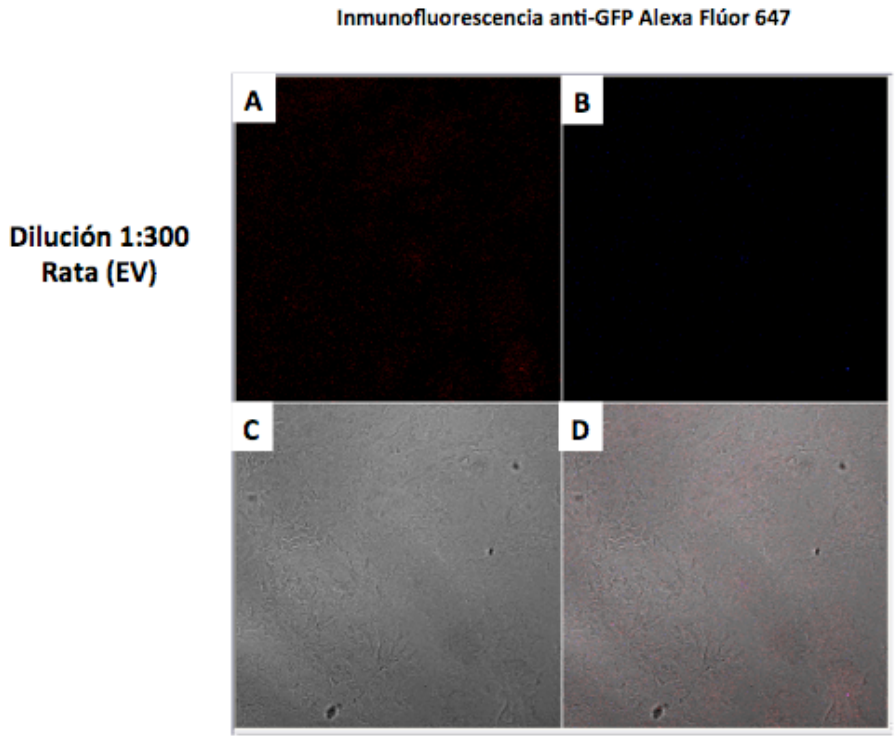

Figura 17. Microscopía confocal de un corte de riñón de rata transfectada con el vector vacío. A) longitud de onda inespecífica (640 nm), B) longitud de onda esperada (668nm), C) campo claro y D) co-localización de campo claro con la imagen obtenida en la longitud de onda esperada (668 nm).

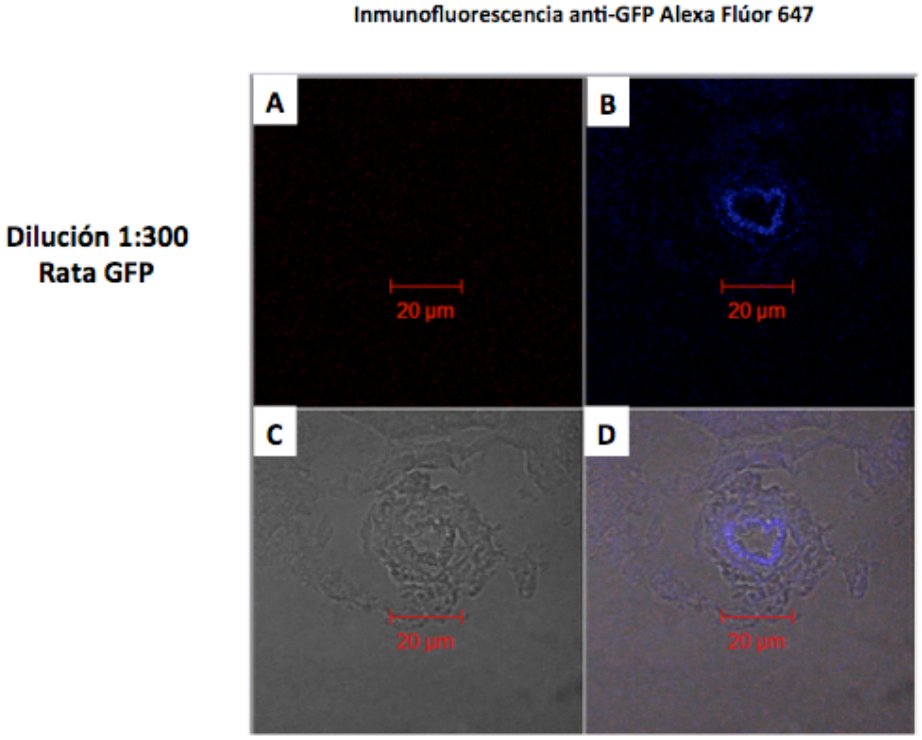

Figura 18. Microscopía confocal de un corte de riñón de rata transfectada con el vector que codifica para GFP. A) longitud de onda inespecífica (640 nm), B) longitud de onda esperada (668nm), C) campo claro y D) co-localización de campo claro con la imagen obtenida en la longitud de onda esperada (668 nm).

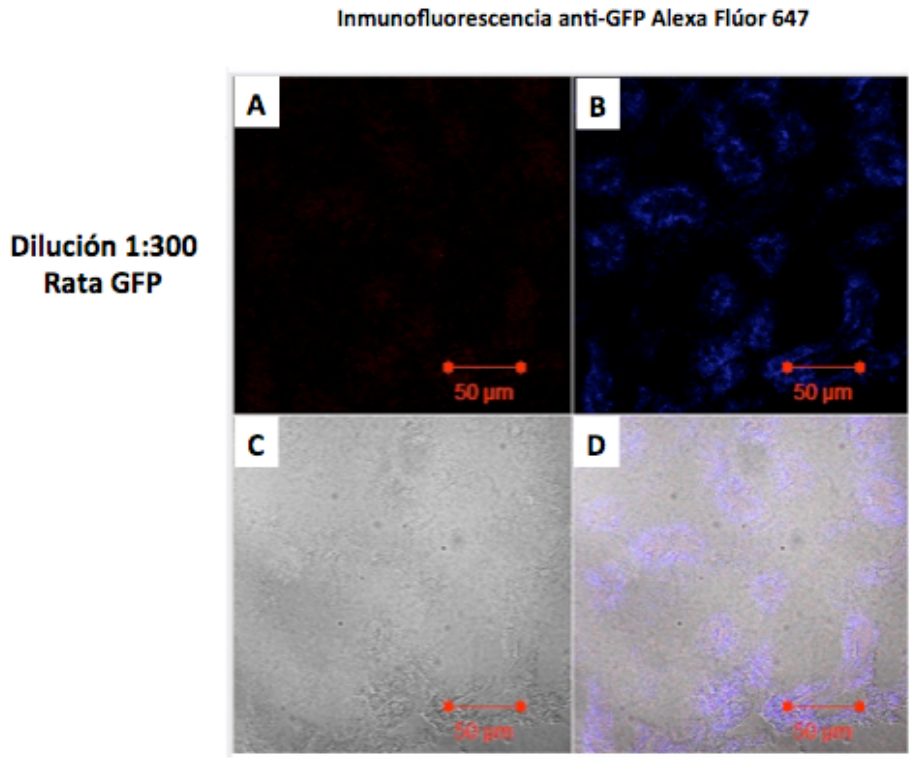

Figura 19. Microscopía confocal de un corte de riñón de rata transfectada con el vector que codifica para GFP. A) longitud de onda inespecífica (640 nm), B) longitud de onda esperada (668nm), C) campo claro y D) co-localización de campo claro con la imagen obtenida en la longitud de onda esperada (668 nm).

Efecto de la sobre-expresión de Hsp90α y Hsp90β sobre la función renal normal

Para determinar si la sobre-expresión de Hsp90α y/o Hsp90β producía algún efecto sobre los niveles de presión arterial media (PAM) o sobre algunos de los principales parámetros de función renal en las ratas normales, se incluyeron cuatro grupos: 1) Sham o de cirugía falsa (S), 2) transfección con vector vacío (EV), 3) transfección intra-renal izquierda con el plásmido de Hsp90α y 4) transfección intra-renal izquierda con el plásmido de Hsp90β. Después de 48-h se determinó la PAM, el flujo sanguíneo renal (FSR), los niveles de creatinina sérica y la excreción urinaria de proteínas. Como podemos apreciar en la figura 19, la transfección de Hsp90α ó de Hsp90β, no modificó las cifras de PAM, ni el FSR, ni la proteinuria en las ratas control. Los resultados anteriores sugieren que la sobre-expresión de Hsp90α y

Hsp90β no propicia cambios en el funcionamiento renal. Esto es importante porque evidencia que la inyección intra-renal no daña la perfusión renal, ni altera la fisiología renal de estos animales.

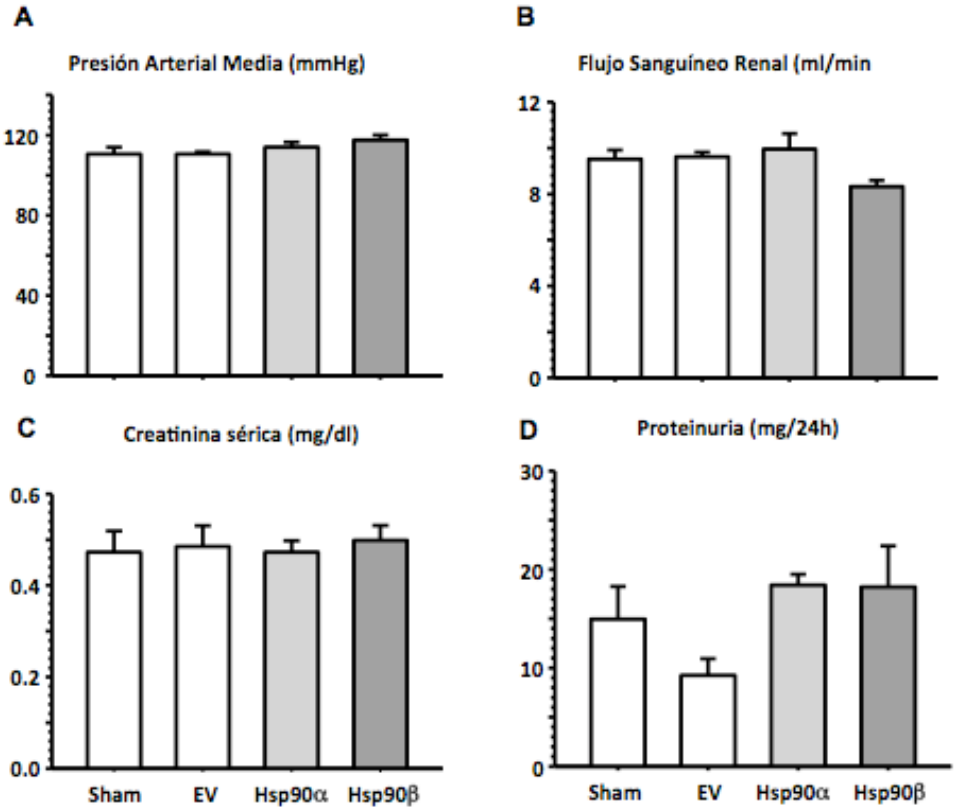

Figura 20. Efecto de la transfección de Hsp90α ó de Hsp90β en el rinón izquierdo sobre la presión arterial media (PAM) y algunos parámetros de función renal en animales normales. Sham = ratas con cirugía falsa, EV= ratas que recibieron el vector vacío, Hsp90α y Hsp90β=ratas normales transfectadas con los plásmidos correspondientes de cada isoforma de Hsp90. n = 5 ratas por grupo.

Efecto de la transfección intra-renal de Hsp90α y Hsp90β sobre la isquemia/reperfusión

Para conocer si la sobre-expresión de cada una de las isoformas de Hsp90 protege o empeora el daño por isquemia-reperfusión, se procedió a someter a un grupo de animales a isquemia renal bilateral de 30 min y reperfusión de 24 h (I/R), otro grupo que se transfectó con el vector vacío (EV) 48 h antes de inducir la

isquemia y los grupos de ratas a las cuales se les transfectó Hsp90α o Hsp90β, también 48 h antes de inducir la isquemia renal bilateral. Todos los animales se estudiaron 24 h después de la reperfusión. Como se observa en la figura 21A, la PAM no se modificó ni como resultado de la isquemia bilateral, ni como resultado de la transfección de Hsp90α o de Hsp90β. Como era de esperarse, el daño por la I/R se caracterizó por una caída en el flujo sanguíneo renal (Fig. 21B), por un aumento significativo de la creatinina sérica (Fig. 21C) y por un aumento de la proteinuria (Fig. 21D). Interesantemente, la transfección del riñón izquierdo con el plásmido de Hsp90α o de Hsp90β previamente a la isquemia bilateral, previno la caída del FSR pero no evitó la elevación de creatinina sérica. Así mismo, la elevación de la excreción urinaria de proteínas que se observa en los animales sometidos a I/R fue parcialmente prevenida por la transfección de Hsp90α o de Hsp90β. Estos resultados nos hicieron pensar que el efecto renoprotector de la sobre-expresión de cada isoforma de Hsp90 no lo estábamos observando tan claramente debido a que estos animales se sometieron a isquemia bilateral y la transfección de una u otra isoforma de Hsp90 solo se realizó en el riñón izquierdo. Por lo tanto, cuando medimos la función renal, se refleja la función de los dos riñones, por lo que el riñón derecho (el no transfectado) estaba enmascarando el efecto real de la sobre-expresión de las isoformas de Hsp90 frente a un fenómeno de I/R. Para discernir si este era el caso se decidió incluir a otros grupos de ratas que solo fueron sometidas a isquemia unilateral.

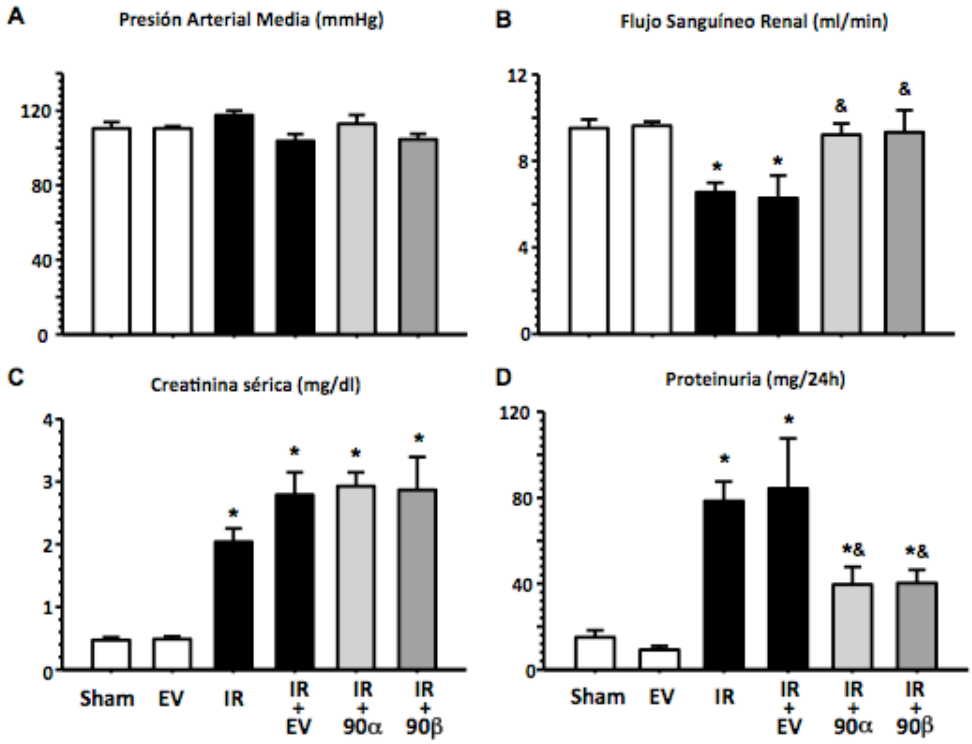

Figura 21. Efecto de la transfección de Hsp90α ó de Hsp90β en el riñón izquierdo en el modelo de isquemia bilateral por 30 min y 24h de reperfusión. Sham = ratas con cirugía falsa, EV= ratas que recibieron vector vacío, IR= isquemia renal bilateral, IR+EV= ratas con isquemia bilateral transfectadas con vector vacío, IR + 90α ó 90β=ratas transfectadas con los plásmidos correspondientes a cada isoforma 48-h antes de inducir la isquemia renal bilateral. n = 5 ratas por grupo. *p<0.05 vs. S, &p<0.05 vs. IR.

Para este fin, se incluyeron tres grupos que se sometieron a isquemia unilateral del riñón izquierdo y fueron transfectados con el vector vacío, Hsp90α o Hsp90β en este mismo riñón izquierdo, 48 h antes de inducir la isquemia. En estos grupos de animales se corroboró que la transfección de Hsp90α o Hsp90β previno la caída del flujo sanguíneo renal en comparación con el grupo que recibió el vector vacío como se muestra en la figura 22B. Así mismo, observamos que la proteinuria (22D) se revertía casi a niveles normales con la transfección de Hsp90α ó Hsp90β.

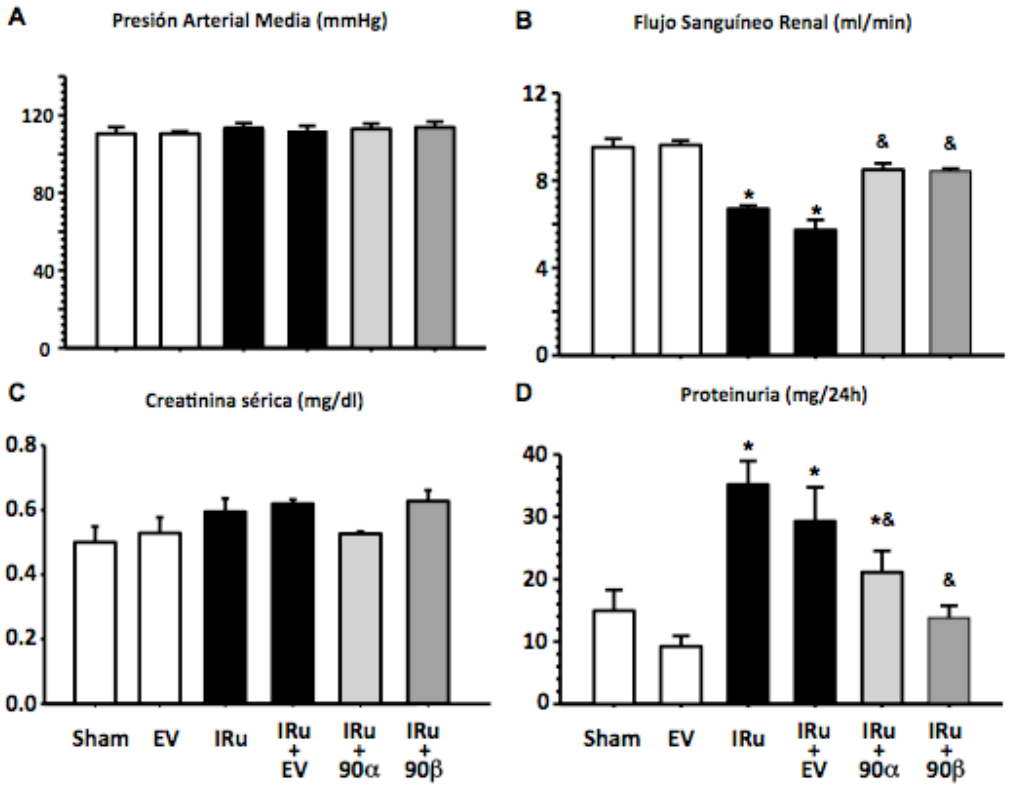

Figura 22. Efecto de la transfección de Hsp90α ó de Hsp90β en el riñón izquierdo en el modelo de isquemia unilateral por 30 min y 24h de reperfusión. Sham = ratas con cirugía falsa, EV = ratas que recibieron vector vacío, IRu = isquemia unilateral, IRu + EV = isuqmia unilateral transfectadas con vector vacío, Hsp90α y Hsp90β=ratas transfectadas con los plásmidos correspondientes a cada isoforma 48-h antes de inducir la isquemia renal bilateral. n = 5 ratas por grupo. *p<0.05 vs. Sham, &p<0.05 vs. IRu.

Sin embargo, como se muestra en la figura 22C, no se observaron cambios en la concentración sérica de creatinina en ninguno de los grupos estudiados, es decir no hubo una elevación de la creatinina sérica en los grupos de ratas sometidas a I/R. Esto puede explicarse porque el riñón no afectado por la isquemia compensó la función renal de una forma eficiente que no permitió detectar el daño renal por I/R en el riñón izquierdo.

Por estos resultados y como estrategia para evitar que el riñón contra-lateral no-isquémico o no transfectado compensara o enmascarara el efecto renoprotector conferido por la sobre-expresión de Hsp90α o de Hsp90β, se incluyeron cuatro

grupos de animales que ahora fueron sometidos a nefrectomía del riñón derecho y en el riñón izquierdo se realizaron las siguientes maniobras; 1) isquemia de 30 min (Nx+IR), 2) transfección con vector vacío mas isquemia de 30 min (Nx+EV+IR), 3) transfección con Hsp90α mas isquemia de 30 min (Nx+IR+α) y 4) transfección con Hsp90β mas isquemia (Nx+IR+β).

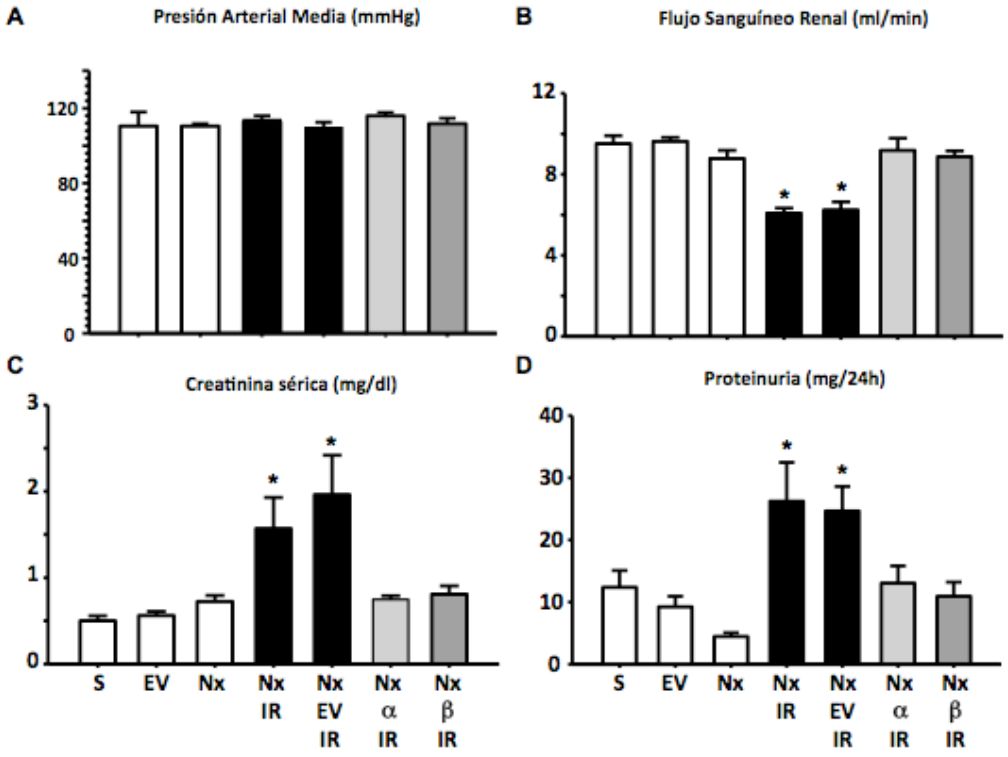

Figura 23. Efecto de la transfección de Hsp90α o de Hsp90β en el riñón izquierdo en el modelo de nefectomía e isquemia unilateral por 30 min y 24h de reperfusión. S = ratas con cirugía falsa, EV= ratas que recibieron vector vacío, Nx = ratas sometidas a nefrectomía, NX+IR= ratas con nefrectomía mas isquemia renal unilateral, Nx+IR+EV= ratas con nefrectomía e isquemia unilateral transfectadas con vector vacío, Hsp90α y Hsp90β=ratas transfectadas con los plásmidos correspondientes a cada isoforma 48-h antes de inducir la isquemia renal bilateral. n = 5 ratas por grupo. *p<0.05 vs. S

Como se muestra en la figura 23 los animales sometidos a isquemia unilateral posterior a la nefrectomía del riñón derecho presentaron una reducción significativa del FSR (23B) y una elevación significativa de los niveles de creatinina sérica (23C), junto con un aumento en la excreción urinaria de proteínas (23D). En esta ocasión el efecto renoprotector de Hsp90α y Hsp90β fue claramente disecado como se

evidenció por la prevención de la hipoperfusión renal y de la elevación de los niveles séricos de creatinina y de la excreción urinaria de proteínas.

La renoprotección conferida por la sobre-expresión de Hsp90α o de Hsp90β también se corroboró con el estándar de oro, para determinar el grado de lesión renal, que es el análisis histopatológico. En la figura 24 se observan fotografías de microscopía de luz representativas de cada grupo. Como era de esperarse, la I/R ocasionó daño tubular severo en los animales no transfectados y en los transfectados con el vector vacío (24 A y B). En cambio la transfección de Hsp90α o Hsp90β fue capaz de prevenir el desarrollo de daño tubular (24 C y D). Este efecto renoprotector también fue corroborado a través de la cuantificación del porcentaje del área tubular afectada cuantificado por morfometría (24 E) y los niveles urinarios de Hsp72 como marcador sensible del daño tubular inducido por la isquemia renal. Como se muestra en la figura 24F, los animales sometidos a isquemia sin transfección y transfectadas con el vector vacío tuvieron un aumento significativo en los niveles urinarios de Hsp72. Este incremento no se observó en los animales transfectados con una u otra de las isoformas de Hsp90.

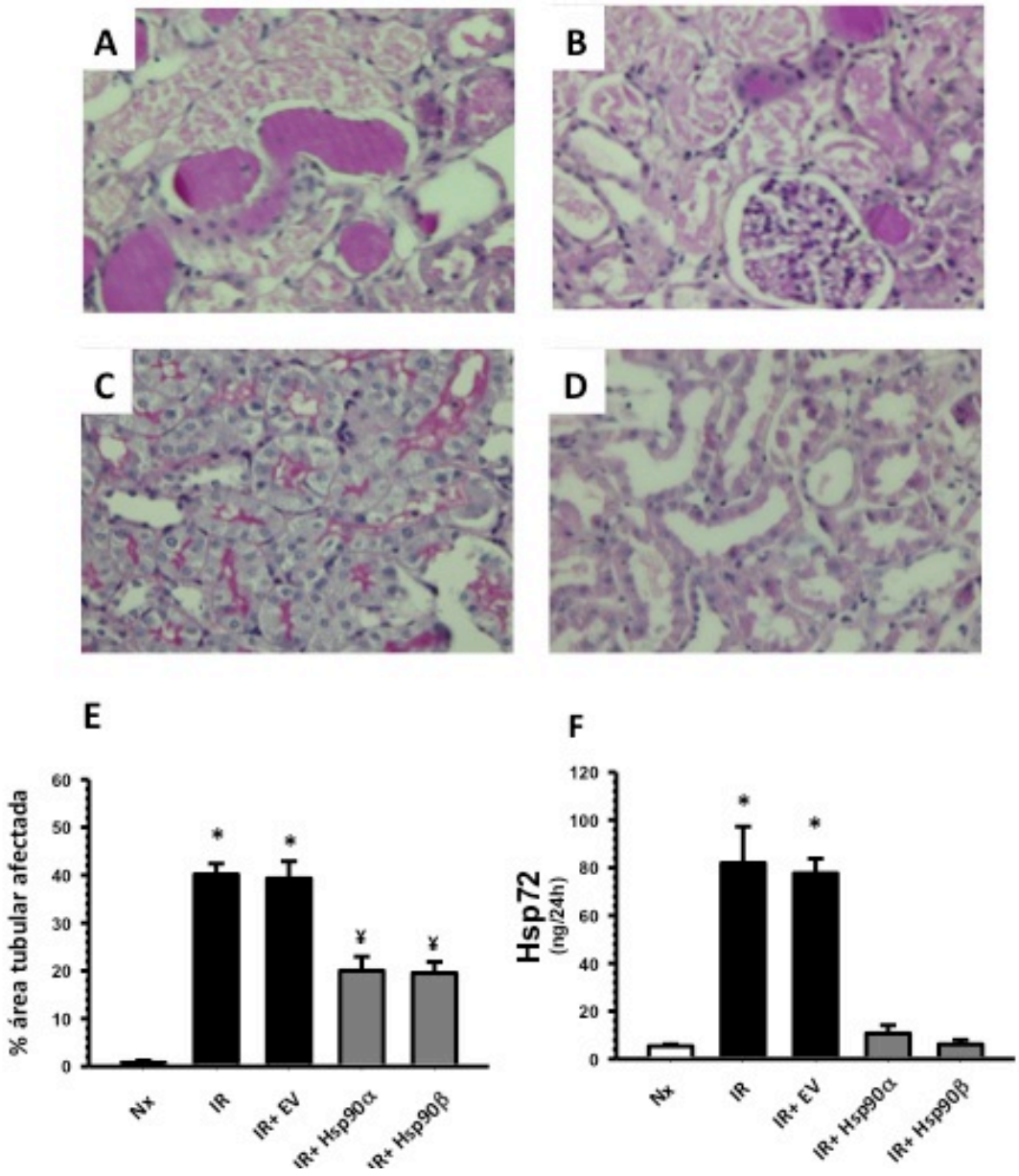

Figura 24. Fotografías representativas de microscopía de luz de cortes histológicos de corteza renal teñidos mediante la tinción de PAS en A) Nx + I/R, B) Nx + EV + IR, C) Nx + Hsp90α + I/R y D) Nx + Hsp90β + I/R. E) Porcentaje de área tubular afectada y E) niveles urinarios de Hsp72. n = 5 ratas por grupo. *p<0.05 vs.Nx, &p<0.05 vs. Nx + IR.

Posteriormente evaluamos si la corrección del FSR conferida por la sobre-expresión de Hsp90α o de Hsp90β se relacionaba con una mayor generación de NO, para ello, determinamos la excreción urinaria de los metabolitos estables de este radical vasodilatador. Como se aprecia en la figura 25A, la sobre-expresión de Hsp90α o de Hsp90β se asoció con la preservación de la excreción urinaria de NO_2/NO_3. Además el incremento en el estrés oxidante que se observó en los

animales sometidos a isquemia, se previno completamente con la transfección de ambas isoformas de Hsp90 (Figura 25B).

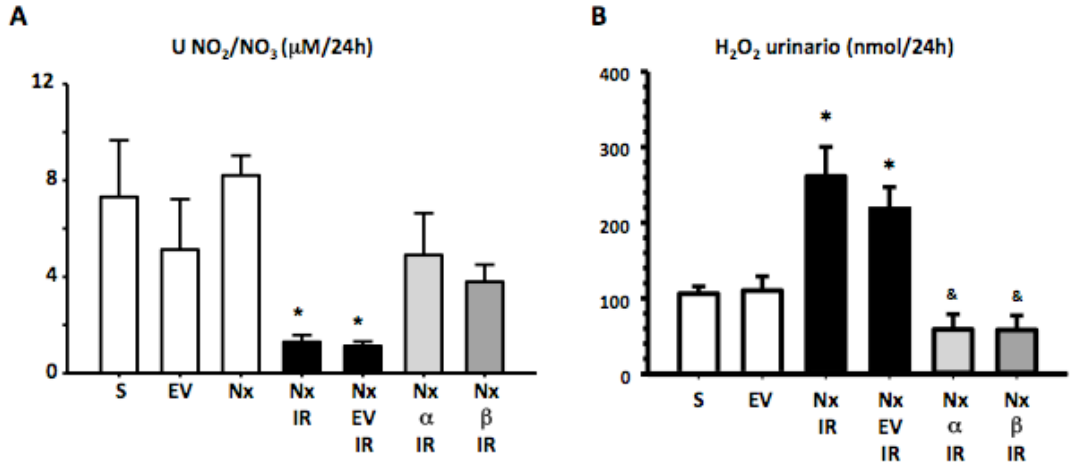

Figura 25. A) Excreción urinaria de los metabolitos estables de la síntesis de NO; los nitritos y los nitratos. B) Como índice del estrés oxidante se determino la excreción urinaria de peróxido de hidrógeno. n = 5 ratas por grupo. *p<0.05 vs. Sham y &p<0.05 vs. Nx + IR.

Debido a que observamos que la transfección de Hsp90α ó de Hsp90β se asoció con la preservación de la síntesis de óxido nítrico y a que una de las proteínas clientes de Hsp90 es la sintasa de óxido nítrico endotelial, decidimos evaluar el estado de fosforilación de eNOS en la Treonina 495 que se asocia con la inactivación de eNOS y en la serina 1177 que se relaciona con la activación de eNOS. Como se observa en la figura 25, la reducción en la síntesis de óxido nítrico en los animales sometidos a I/R sin transfección o con el vector vacío, se asoció con un incremento en la fosforilación de la Treonina 495 (Figura 26A) y con reducción en la fosforilación de la serina 1177 (Figura 26B). Interesantemente la transfección de ambas isoformas de Hsp90, previno el incremento en la fosforilación inactivante de eNOS y la reducción de la fosforilación activante de eNOS.

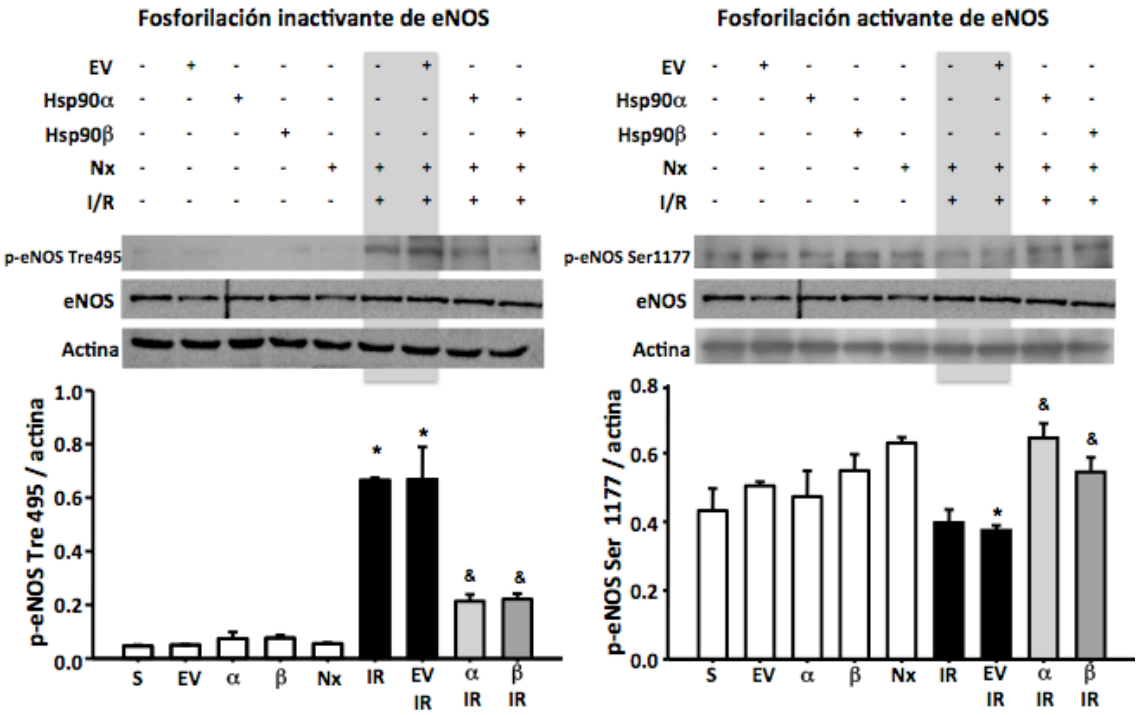

Figura 26. Efecto de la isquemia/reperfusión y de la transfección de Hsp90α ó de Hsp90β sobre la fosforilación de eNOS en la Tre- 495 y en la Ser-1177. n = 5 ratas por grupo. *p<0.05 vs. S, & p<0.05 vs Nx + IR.

Para estudiar si la disfunción de eNOS se debía a una menor presencia de Hsp90 en su conformación dimérica y si esto se podía revertir con la transfección de Hsp90, se evaluó la relación dímero/monómero en geles no-desnaturalizantes. Como se puede observar en la figura 27, la relación dímero/monómero no se afectó ni por la I/R ni por la transfección de Hsp90. Al no ver efecto en este parámetro decidimos evaluar qué ocurre con la interacción entre Hsp90 y eNOS cuando se transfectan ambas isoformas de Hsp90. Para ello se inmunoprecipitó eNOS y se detectó a Hsp90α ó Hsp90β. Como se aprecia en la figura 28 ambas isoformas interactúan con eNOS en condiciones normales, pero esta interacción se ve incrementada en los animales transfectados con cada isoforma de Hsp90, lo que puede explicar el efecto reno-protector mediado por una mayor activación de eNOS y generación de NO.

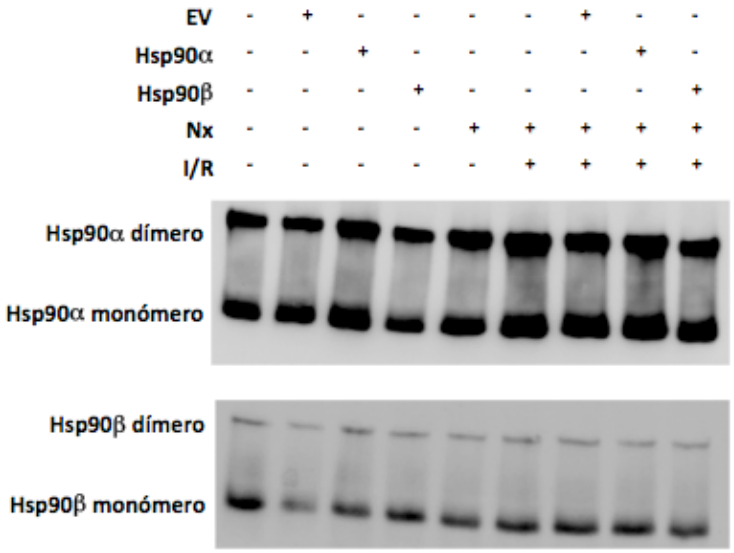

Figura 27. Relación dímero/monómero de Hsp90α ó Hsp90β.

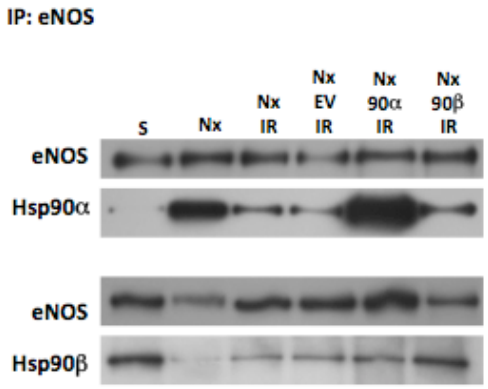

Figura 28. Inmunoprecipitación de eNOS y Western blot con eNOS, Hsp90α y Hsp90β.

Para conocer si también se modificaba la expresión de las cinasas responsables de las fosforilaciones de eNOS, se evaluó la expresión de PKC-β que fosforila a la treonina 495 y de PKC-α que fosforila a serina 1177 de eNOS. Como se observa en la figura 29 la expresión de PKC-β no se modificó ni por la isquemia ni por la transfección de Hsp90α o de Hsp90β. En cambio se observó una reducción significativa en la expresión de PKC-α que fue prevenida por completo por la transfección intra-renal de cada una de las isoformas de Hsp90. Como se mencionó

anteriormente, PKC-α fosforila a eNOS en la serina 1177 por lo que, la disminución en su expresión parece dar como resultado una disminución en la fosforilación de la serina 1177.

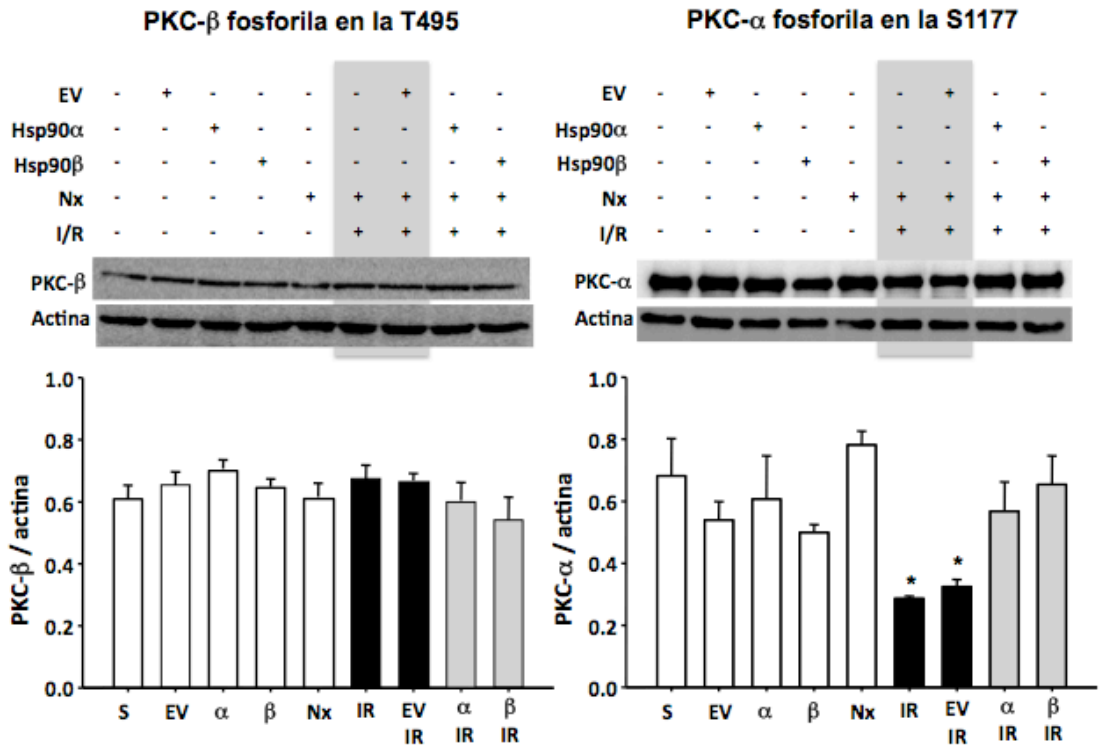

Figura 29. Efecto de la isquemia/reperfusión y de la transfección de Hsp90α ó de Hsp90β sobre la expresión de PKC-α y PKC-β. n = 5 ratas por grupo. *p<0.05 vs. S.

Para evaluar otro posible mecanismo de daño renal y de la reno-protección conferida por la sobre-expresión de las isoformas de Hsp90, evaluamos los niveles de la cinasa Akt y su estado se fosforilación activante (S473) debido a que previamente se ha reportado que esta cinasa se activa después de la I/R [125] y puede fosforilar a los factores de transcripción FOXO1a y FOXO3, responsables de inducir un arresto en el ciclo celular que también se conoce como un mecanismo responsable de iniciar la progresión a ERC después de un episodio de lesión renal aguda. Como podemos apreciar en la figura 30, la I/R indujo un incremento en la

fosforilación de Akt, que se previno con la transfección de ambas isoformas de Hsp90.

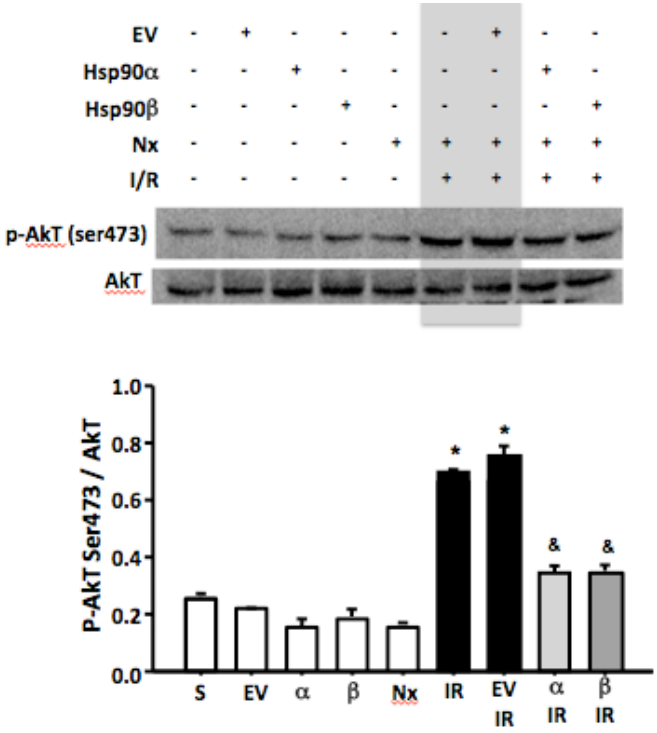

Figura 30. Efecto de la I/R y de la transfección de Hsp90α ó Hsp90β sobre la fosforilación de Akt. n = 5 ratas por grupo. *p<0.05 vs. S.

En resumen, en esta segunda parte de mi proyecto doctoral encontramos que ambas isoformas tienen el mismo efecto renoprotector al ser transfectadas 48 h previo a la inducción de la isquemia renal. El efecto renoprotector se asoció con la preservación en la síntesis de óxido nítrico y del estado de fosforilación activante de la sintasa de óxido nítrico endotelial. Además demostramos que la técnica de transfección intra-renal es eficiente para que el material genético alcance a la vasculatura y al epitelio tubular.

RESULTADOS DEL PROTOCOLO III: La prevención del daño inducido por un evento de LRA evita la progresión a ERC

A pesar de la gran importancia que tiene la LRA como factor de riesgo para desarrollar ERC, poco se ha estudiado sobre los mecanismos responsables, en parte por la ausencia de un modelo experimental, lo que además permitirá estudiar estrategias farmacológicas para reducir o prevenir la ERC inducida por un episodio de LRA. Por lo tanto, la tercera parte de mi tesis doctoral se diseñó para: 1) Desarrollar un modelo de ERC inducido por un episodio de LRA, 2) Estudiar los mecanismos por los cuales un episodio de LRA pueden llevar al desarrollo de la ERC y 3) y evaluar si el antagonismo de los RM antes de inducir isquemia puede prevenir el desarrollo de la ERC provocada por un episodio de LRA.

Previamente mostramos que después de 24 h de isquemia renal bilateral, las ratas desarrollan disfunción renal y daño tubular. La figura 31 muestra que la disfunción renal inducida por la isquemia renal fue prácticamente resuelta 10 días después, un comportamiento similar ocurre con los pacientes que tuvieron un episodio de LRA. Como era de esperarse, los animales sometidos a isquemia presentaron una elevación de la proteinuria después de 24 h y fue disminuyendo progresivamente hasta alcanzar valores normales después de 6 días de reperfusión (Figura 31A). En cambio, las ratas pre-tratadas con espironolactona antes de inducir la isquemia presentaron una proteinuria 50% menor a las 24 h, alcanzándose valores normales más rápidamente que el grupo con isquemia sin tratamiento. Aunado a esto, después de 10 días de inducir la isquemia, los animales recuperaron la función renal, como se evidenció por la normalización del flujo sanguíneo renal, la creatinina sérica y la depuración de creatinina (Figuras 31 B-D). A pesar de la mejoría en la función renal, los niveles de RNAm de interleucina 6 (IL-6) y la

fosforilación de la proteína Smad-3 permanecieron significativamente elevados con respecto al grupo con cirugía falsa. Efecto que no fue observado en los tejidos de las ratas pre-tratadas con espironolactona (Figures 31 E-F). ***Estos resultados sugieren que a pesar de que, la disfunción renal se recuperó, las vías de procesos inflamatorios y pro-fibróticos permanecieron activadas, pudiendo contribuir al desarrollo de la ERC, situación que fue prevenida por el pre-tratamiento con espironolactona*.**

El daño por I/R conduce al desarrollo progresivo de disfunción renal que puede ser prevenido con el pre-tratamiento con espironolactona

En una segunda serie de experimentos, las ratas se estudiaron 270 días después de inducir la isquemia. Observamos que dentro de los primeros diez días, hubo una mortalidad considerable (57%)en el grupo sometido a isquemia (A-a-C) , en cambio la mortalidad fue significativamente menor cuando los animales se pre-trataron con espironolactona (A-a-C+Sp) (15%). Después de estos primeros diez días, ninguna rata murió durante el resto del estudio (Figura 32A).

Cada 30 días se evaluó la excreción urinaria de proteínas. Los animales que sobrevivieron al insulto isquémico desarrollaron un aumento progresivo en la proteinuria de 20.2 ± 1.5 a los 30 días hasta 164.8 ± 11.3 mg/24 h a los 270 días. Esta alteración no se observó en el grupo A-a-C+Sp (9.2 ± 1.0 a los 30-días y 27.1 ± 2.0 mg/24 h a los 270-días) (Figura 32B). Después de 9 meses de haber inducido la isquemia renal bilateral, el grupo A-a-C desarrolló disfunción renal que se caracterizó por una reducción significativa del flujo sanguíneo renal (FSR) y de la depuración de creatinina (Figuras 32C-D). Interesantemente, el grupo A-a-C+Sp no desarrolló disfunción renal. La presión arterial al final del estudio fue similar en todos los grupos

(Figura 32E). *Por lo tanto, el daño renal observado en las ratas que desarrollaron ERC no fue debido a elevación de la presión sanguínea.*

De acuerdo con nuestras observaciones previas, en el grupo A-a-C, los niveles de la molécula de daño renal Kim-1 fueron significativamente mayores que el grupo control y el grupo A-a-C+Sp (Figura 32F).

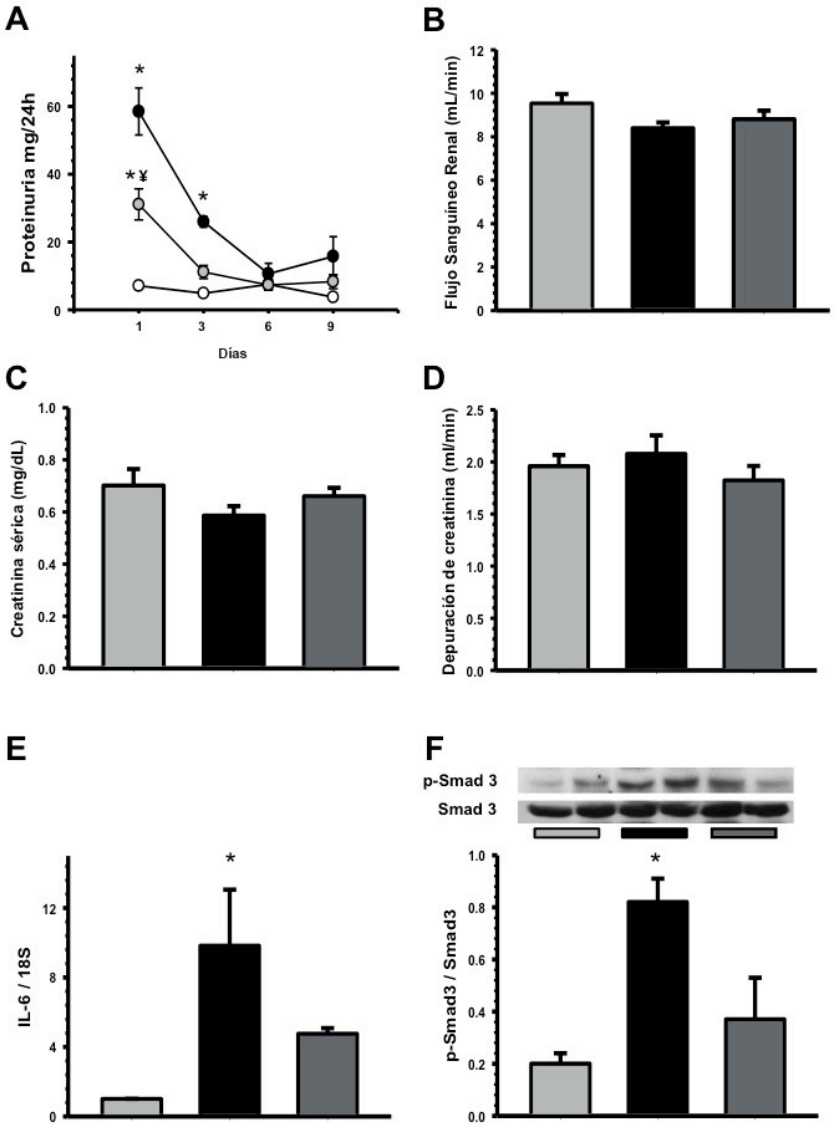

Figura 31. La disfunción renal inducida por isquemia fue completamente resuelta después de 10 días de reperfusión, pero las citocinas pro-inflamatorias y pro-fibróticas permanecieron elevadas. A) Excreción urinaria de proteínas después de 1, 3, 6 y 9 días de reperfusión en las ratas operadas en forma falsa (círculo blanco o barras gris claro), grupo sometido a isquemia renal bilateral (círculo negro ó barras negras), y ratas pre-tratadas con espironolactona 3 días antes de inducir la isquemia (círculo gris oscuro o barras gris oscuro). Las ratas fueron anestesiadas y posteriormente sacrificadas después de 10 días de reperfusión y se determine la función renal. B) Flujo sanguíneo renal, C) creatinina sérica y D) depuración de creatinina. E) Niveles de RNAm de IL-6 F) Niveles de proteína y de fosforilación de Smad-3. n=6 ratas por grupo. *p<0.05 vs. el grupo sham y ¥p<0.05 vs. el grupo sometido a isquemia bilateral.

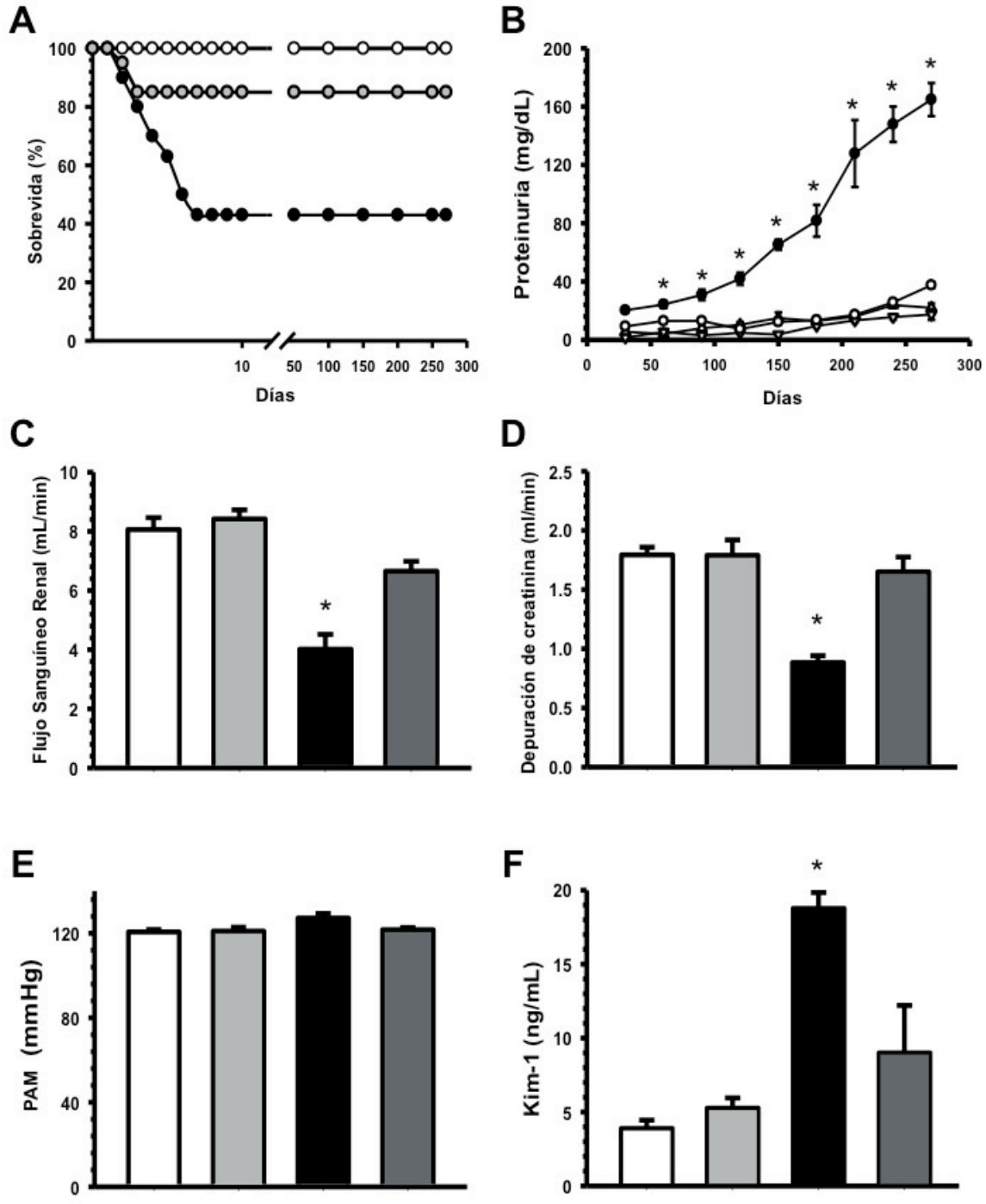

Figura 32. La lesión renal aguda (LRA) propicia el desarrollo de ERC, efecto que puede ser prevenido con el pre-tratamiento con espironolactona. Se incluyeron cuatro grupos: cirugía falsa (S), n=9; ratas que recibieron espironolactona (20 mg/kg/día) tres días antes de la cirugía falsa, n=9 (Sp); ratas sometidas a isquemia renal bilateral, n=28 (A-a-C); y ratas que recibieron espironolactona tres días antes de la isquemia bilateral, n=13 (A-a-C+Sp). A) El Porcentaje de sobrevida para el grupo A-a-C (círculo negro) fue del 43%, comparado con el 85 % en el grupo A-a-C+Sp (círculo gris) y el 100 % en el grupo S (círculo blanco). B) Excreción urinaria de proteínas que fue medida cada 30 días a lo largo del estudio en los grupos: S (o), Sp (•), A-a-C (▼), and A-a-C+Sp (Δ). Al final del periodo experimental se determinó: C) flujo sanguíneo renal, D) depuración de creatinina, E) la presión arterial media, y F) los niveles urinarios de Kim-1 en las ratas con cirugía falsa (barras blancas), Sp (barras gris claro), A-a-C (barras negras) y A-a-C+Sp (barras gris oscuro). *p<0.05 vs. los grupos S y Sp.

El insulto isquémico condujo al desarrollo de daño estructural severo

Los hallazgos histopatológicos observados en las laminillas de los cortes histológicos teñidos con PAS de los riñones del grupo A-a-C después de 270 días mostraron serias alteraciones estructurales que se caracterizaron por hipertrofia y esclerosis glomerular, así como dilatación tubular severa y formación de cilindros como se puede apreciar en las figuras 33A y 33B. En cambio, en el grupo A-a-C+Sp, estas lesiones fueron prácticamente ausentes (Figuras 33C-D). Estos hallazgos fueron confirmados cuando se cuantificó el porcentaje de túbulos dilatados y de glomeruloesclerosis. Como muestra la figura 33E, la dilatación tubular estuvo presente en el 42.3 ± 5.0% de los túbulos, mientras que en el grupo A-a-C+Sp el porcentaje fue significativamente menor (13.1 ± 2.7%). De forma similar, el grupo A-a-C presentó un mayor porcentaje de glomeruloesclerosis (10.0±4.4%) que los grupos control y A-a-C+Sp (0 and 0.4 ± 0.4%, respectivamente).

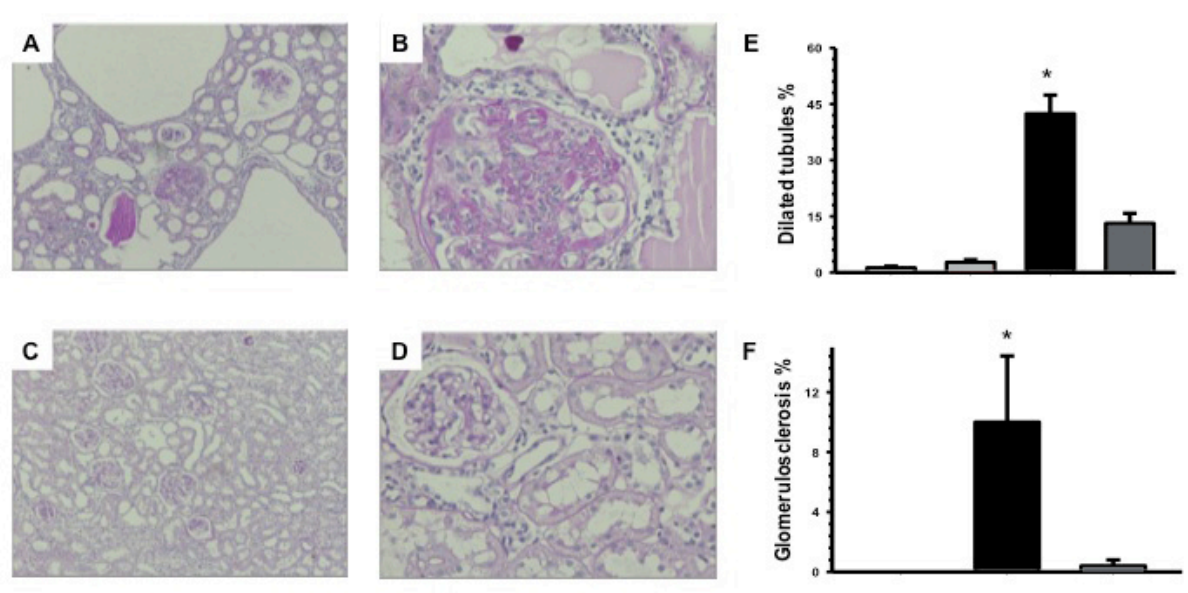

Figura 33. Un episodio de LRA ocasiona el desarrollo de daño estructural severo, que es completamente prevenido con espironolactona. Imágenes representativas de cortes histológicos de riñón teñidas con PAS de una rata del grupo A-a-C se muestran en el panel A (magnificación x100) y B (magnificación x400), mientras que los paneles C (magnificación x100) y D (magnificación 400x) muestran las imágenes de una rata del grupo A-a-C+Sp. E) Porcentaje de túbulos dilatados, F) Porcentaje de glomerulosclerosis porcentaje en las ratas con cirugía falsa (barras blancas), Sp (barras gris claro), A-a-C (barras negras) y A-a-C+Sp (barras gris oscuro). n=6 ratas por grupo. *p<0.05 vs. los grupos S y Sp.

Con el fin de evaluar cuantitativamente la hipertrofia glomerular, se midieron los diámetros glomerulares de al menos 100 glomérulos de cada rata y se distribuyeron según su diámetro. La figura 34A muestra la distribución de los diámetros glomerulares para el grupo control (Sham) en donde se aprecia una distribución en forma Gausiana como previamente hemos reportado [116]. En donde la mayor parte de los glomérulos tenían un diámetro entre 101 y 125 μm (38.3%) y solo una menor proporción se encontró entre 76 y100 μm (19.5%) y entre 126 y150 μm (27.5%). En cambio, en los animales que desarrollaron ERC se observó una mayor proporción de glomérulos con diámetros superiores a 125 micras, reflejando la presencia de hipertrofia glomerular. El 43.3% de los glomérulos tuvieron un diámetro mayor que 151 μm y una menor proporción se observó en los intervalos de 101-125 μm (20.4%), 76-100 μm (8.3%) y de 50-75 μm (0%). Todas estas diferencias fueron estadísticamente diferentes de acuerdo con el análisis de contingencia, como se detalla en la figura 34B. La distribución de los diámetros glomerulares del grupo A-a-C+Sp fue similar al grupo control (Figura 34C), indicando que en este grupo, la hipertrofia glomerular fue prácticamente ausente. De acuerdo con estos resultados, observamos que el peso renal en el grupo A-a-C fue significativamente mayor (2.5±0.2 g) que en los grupos S y Sp (1.6±0.1 and 1.6±0.1 g); este aumento no se observó en el grupo A-a-C+Sp (1.5±0.1 g). La microscopía electrónica de los riñones de los animales que desarrollaron ERC reveló alteraciones ultra-estructurales como fusión y desprendimiento de los procesos podocitarios (Figura 34E). Estas alteraciones fueron raramente observadas en el grupo A-a-C+Sp (Figura 34F).

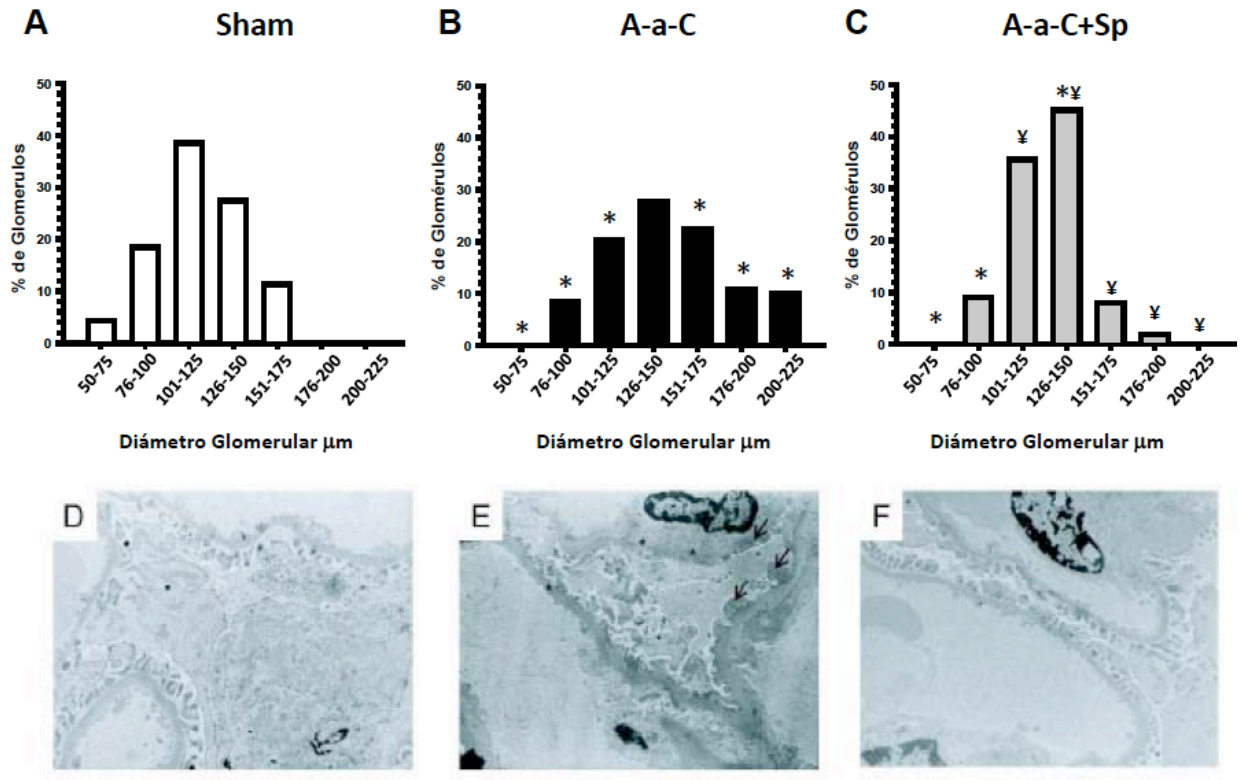

Figura 34. Las ratas que desarrollaron ERC presentaron hipertrofia glomerular y lesión en la ultra-estructura. La distribución del diámetro glomerular es representada en barras blancas para el grupo control (A), en barras negras para el grupo A-a-C (B) y en barras grises para el grupo A-a-C+Sp (C). Microfotografías que muestran la microscopía electrónica de: D) un corte de riñón de una rata del grupo control, E) para el grupo A-a-C and F) para el grupo A-a-C+Sp. Las flechas negras indican el proceso de fusión de podocitos y los asteriscos, el desprendimiento de podocitos Magnificación original: x6300. *p<0.05 vs. el grupo S y ¥p<0.05 vs. el grupo A-to-C.

Para evaluar la fibrosis túbulo-intersticial, los cortes histológicos de los grupos estudiados ahora se tiñeron con rojo de sirio. Como se aprecia en las figuras 35A y 35B, se encontró una área extensiva afectada por fibrosis en el grupo A-a-C y en mucho menor grado se observó en el grupo A-a-C+Sp (Figuras 35C-D). Estas observaciones se confirmaron con el análisis morfométrico que se representa en la figura 35E. El grupo A-a-C presentó un 44.8 ± 16.0% del área túbulo-intersticial afectada por fibrosis en comparación un 18.7 ± 4.5% en el grupo A-a-C+Sp. ***Estos resultados muestran que la ERC inducida por isquemia produjo daño glomerular y tubular y que el empleo de espironolactona no solo previno la disfunción renal, sino también el daño glomerular y tubular.***

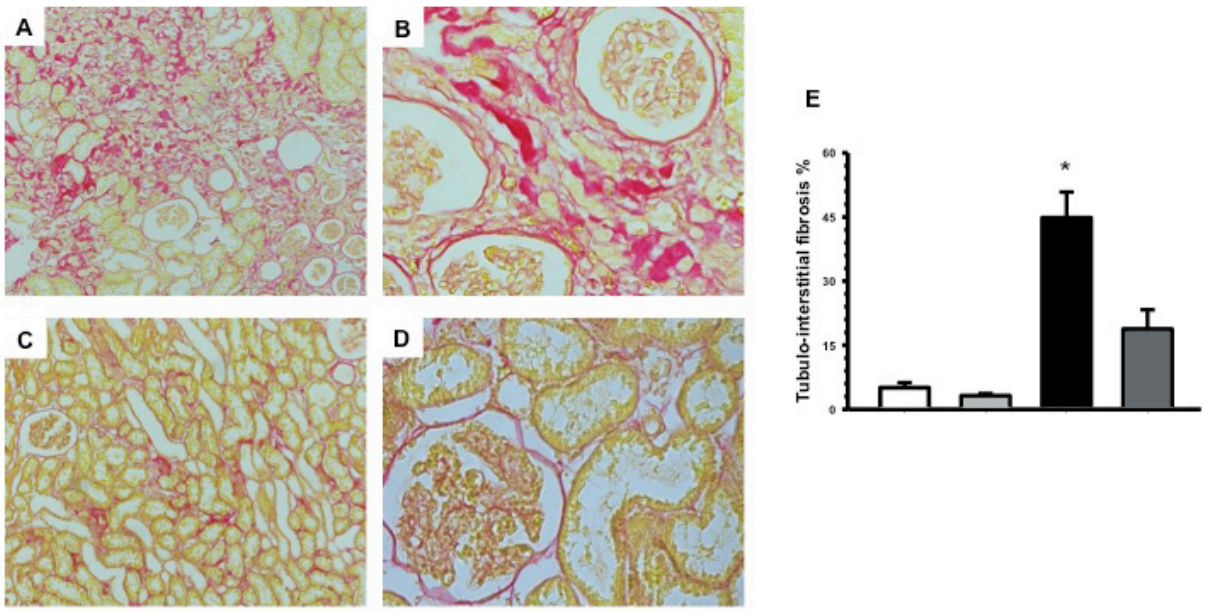

Figura 35. La fibrosis túbulo-intersticial observado en el grupo que desarrollo ERC fue prevenida por el pre-tratamiento con espironolactona. Imágenes representativas de la microscopía de luz de cortes histológicos de riñones teñidos con rojo de sirio que muestran la presencia de fibrosis en el grupo A-a-C y que es representado en A (magnificación x100) y en B (magnificación x400), y las microfotografías del grupo A-a-C+Sp group son representadas en (magnificación x100) y en D (magnificación x400). E) Análisis morfométrico del porcentaje de fibrosis tubulo-intersticial en los cuatro grupos estudiados después de 270 días de reperfusión. Sham (barra blanca), Sp (barra gris claro), A-a-C (barra negra) y A-a-C+Sp (barra gris oscuro) *p<0.05 vs. los grupos S y Sp.

La dilatación tubular fue en parte mediado por un aumento en la proliferación celular

Con el fin de evaluar si la dilatación tubular observada en los animales que desarrollaron ERC se relacionaba con proliferación tubular, se analizó la inmunotinción del antígeno nuclear de células en proliferación (PCNA). El grupo A-a-C mostró una considerable proliferación celular que se evidenció por el número de núcleos positivos a PCNA en el epitelio tubular, efecto que casi estuvo ausente en el grupo A-a-C+Sp (Figuras 36A-36C). Estos hallazgos fueron cuantificados mediante la obtención del porcentaje de células tubulares positivas para PCNA (Figura 36D). Además observamos una correlación significativa entre el porcentaje de túbulos dilatados y el porcentaje de células positivas a PCNA (Figura 30E, r^2=0.87**).** ***Estos***

resultados sugieren que la proliferación celular puede ser responsable en parte de la dilatación tubular que se aprecia en el grupo que desarrolló ERC.

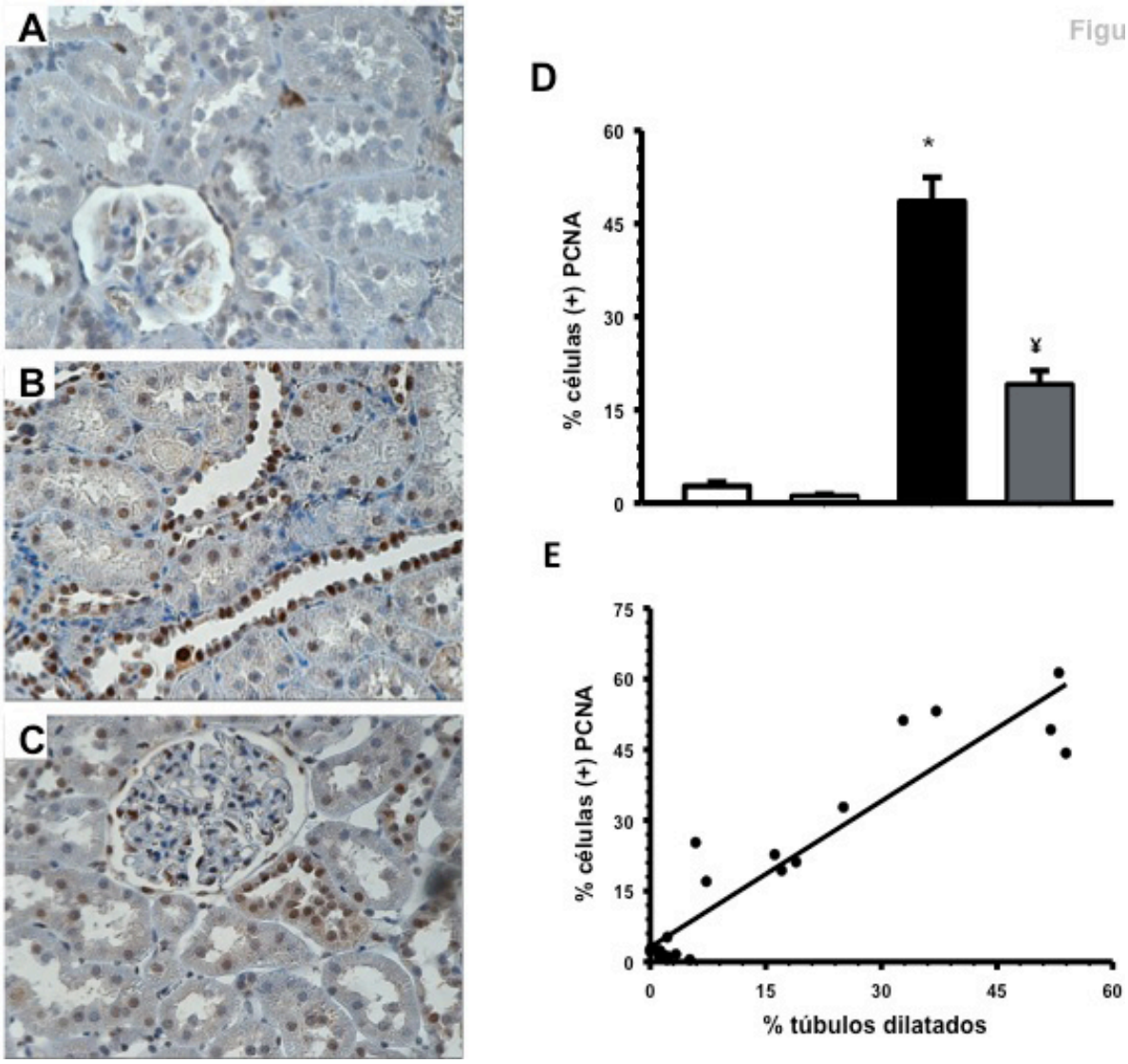

Figura 36. Proliferación del epitelio tubular determinada por la inmunotinción de PCNA. A) Imagen representativa del grupo S, B) A-a-C and C) A-a-C+Sp. D) Porcentaje de células positivas de PCNA para los grupos de cirugía falsa (barras blancas), Sp (barras gris claro), A-a-C (barras negras) y A-a-C+Sp (barras gris oscuro). *p<0.05 vs. los grupos S y Sp. E) Correlación entre el porcentaje de células positivas para PCNA y el porcentaje de túbulos dilatados (r2 = 0.87). *p<0.05 vs. los grupos S y Sp.

La fibrosis túbulo-intersticial es mediada por la activación de la vía de TGF-β

La enfermedad renal crónica se ha atribuido a la activación de la vía de señalización de la citiocina pro-fibrótica TGFβ, por lo que en este estudio evaluamos los niveles de proteína y la actividad de TGFβ a través de medir los niveles de fosforilación de Smad3 y de sus genes blanco de la señalización intracelular de

TGFβ, como la fibronectina y colágena tipo I. En el grupo A-a-C se observó un aumento significativo de dos veces en los niveles de RNAm de TGF-β. Este incremento no se observó en el grupo A-a-C+Sp (Figura 37A). La activación de la vía de TGF-β en el grupo A-a-C fue monitoreada a través del aumento en los niveles de proteína de fibronectina, colágena I, y α-SMA, así como en el aumento en la fosforilación de Smad-3 (Figuras 37B a la 37E). El incremento en la activación de la vía de TGF-β fue completamente prevenida con el pre-tratamiento con espironolactona.

Debido a que recientemente se reportó que la fosforilación de Smad2 puede actuar como un mediador anti-fibrótico [126], también se evaluó el estado de fosforilación de Smad2 y encontramos que en el grupo A-a-C+Sp, el cual presentó menor fibrosis túbulo-intersticial, también presenta una elevación significativa en la fosforilación de Smad2 (Figura 37F).

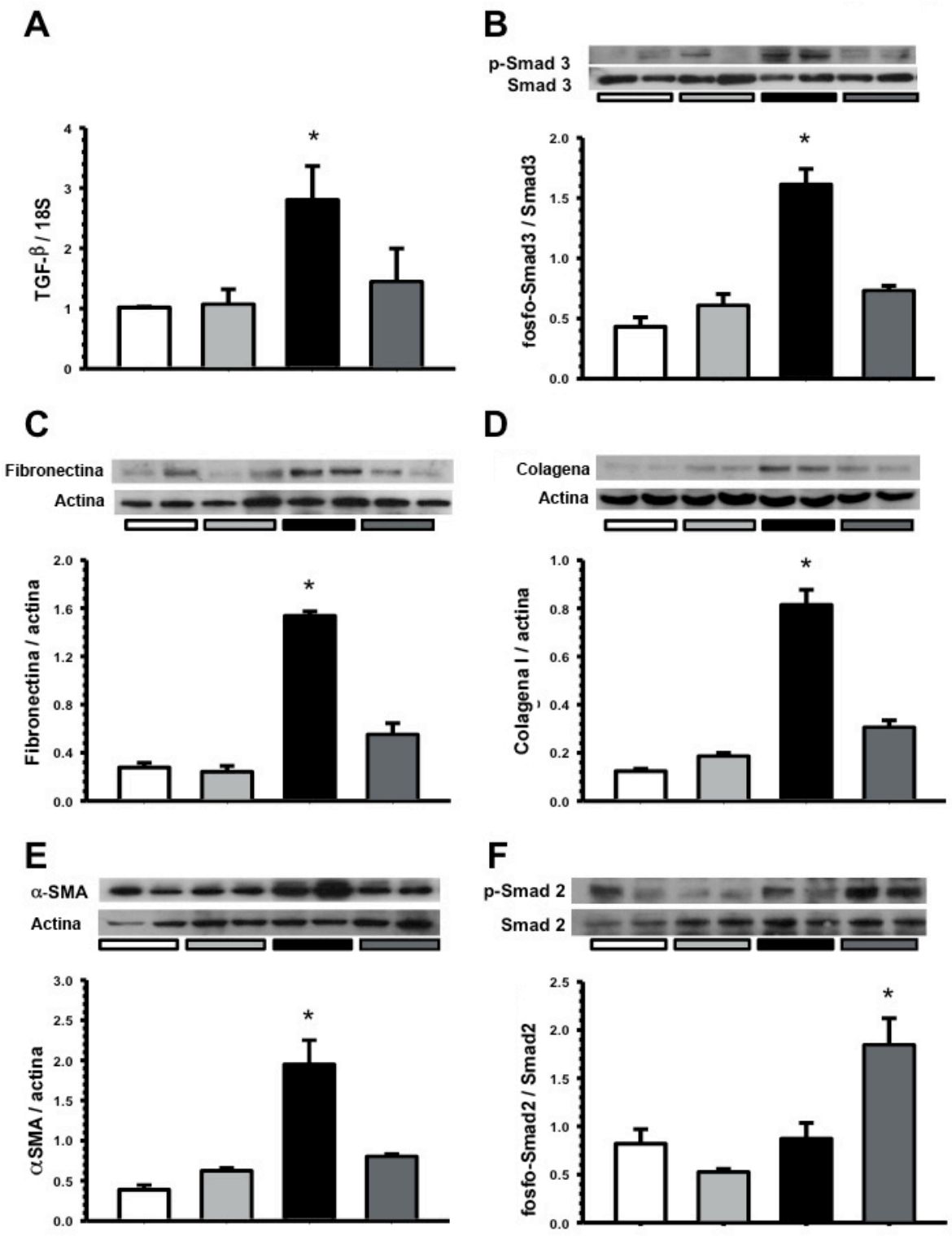

Figura 37. La fibrosis renal en el grupo que desarrolló ERC se asoció con activación de la vía de señalización de TGF-β, efecto que no se observe en el grupo que recibió espironolactona A) Niveles de RNAm de TGF-b. B) Niveles de proteína y fosforilación de Smad3, C) fibronectina D), colágena tipo I E) a-SMA, y F) fosforilación de Smad2 (F) para los grupos: en las ratas con cirugía falsa (barras blancas), Sp (barras gris claro), A-a-C (barras negras) y A-a-C+Sp (barras gris oscuro). n=6 ratas por grupo. *p<0.05 vs. los grupos S y Sp.

El daño renal crónico inducido por un insulto isquémico es también mediado por un incremento en el estrés oxidante

La excreción urinaria de H_2O_2 en el grupo A-a-C fue significativamente mayor que en los grupos S y Sp (64.1±7.5 vs. 10.4±1.1 y 5.9±1.0 nmol/24-h) (Figura 38A). Sin embargo, esta elevación fue abatida en el grupo A-a-C+Sp (14.8±2.5 nmol/24-h). Así mismo, la actividad de la catalasa fue significativamente menor en el grupo A-a-C (Figura 38B), efecto que no fue observado en el grupo A-a-C+Sp. No se observaron diferencias en la actividad de la peroxidasa de glutatión (Gpx) en los grupos estudiados (Figura 38C). *Estos resultados muestran que el desarrollo de ERC se asocia con un incremento en el estrés oxidante y que esto no se observa en los animales que recibieron espironolactona antes de inducir la isquemia.*

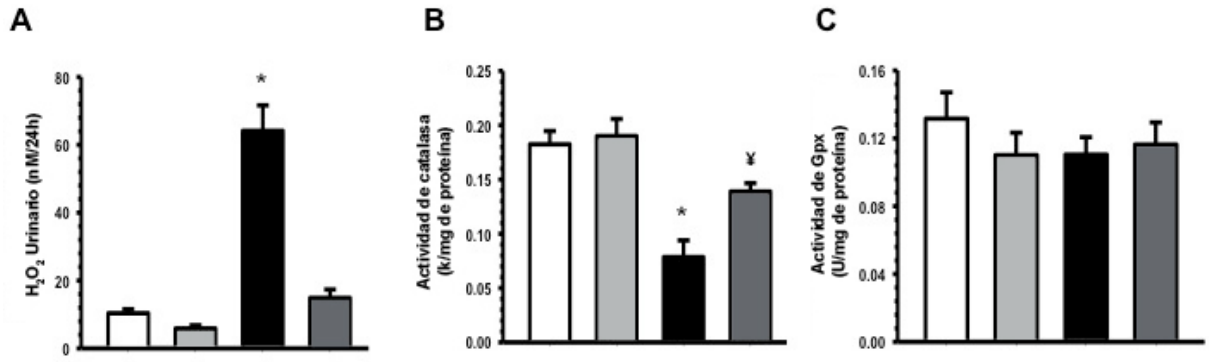

Figura 38. Contribución del estrés oxidativo en el desarrollo de ERC y su prevención con el uso de espironolactona. A) Excreción urinaria de H_2O_2 después de 270 días de reperfusión. B) Actividad de catalasa C) Actividad de la peroxidase de glutatión en las ratas con cirugía falsa (barras blancas), Sp (barras gris claro), A-a-C (barras negras) y A-a-C+Sp (barras gris oscuro). n=6 ratas por grupo. *p<0.05 vs. los grupos S y Sp, ¥p<0.05 vs. el grupo A-a-C.

La respuesta inflamatoria está involucrada en el desarrollo de ERC inducida por la isquemia

Los niveles de RNAm y de proteínas de TNF-α, MCP-1 e IL-6 fueron analizados por RT-PCR en tiempo real y por un análisis de ELISA, respectivamente. Como se muestra en la figura 39, los niveles de RNAm de estas citocinas fueron significativamente mayores en el grupo A-a-C por 1.6 veces para TNF-α y 13 veces

para MCP-1 e IL-6, considerando como niveles basales los de los dos grupos controles. En forma interesante, el grupo A-a-C+Sp mostró valores similares al grupo control. Por lo tanto los hallazgos a nivel de RNAm fueron corroborados a nivel de proteína mediante ELISA y los resultados fueron muy similares a los observados por RNAm.

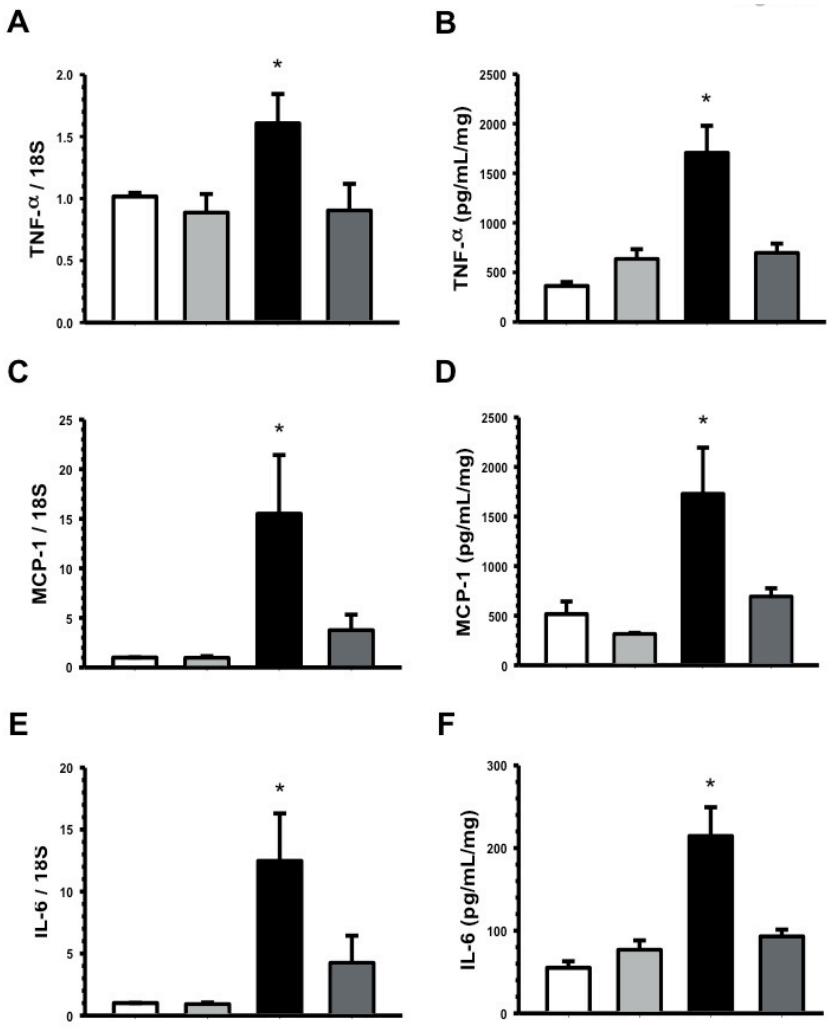

Figura 39. Contribución de la respuesta inflamatoria en el desarrollo de ERC. Niveles de RNAm: A) de TNF-a, C) MCP-1, y E) IL-6 para las ratas con cirugía falsa (barras blancas), Sp (barras gris claro), A-a-C (barras negras) y A-a-C+Sp (barras gris oscuro). Niveles de proteína determinados por ELISA: B) TNFα, D) MCP-1 y F) IL-6 . n=6 ratas por grupo. *p<0.05 vs. los grupos S y Sp.

La ERC inducida por LRA también se puede prevenir por la administración de espironolactona después que el insulto isquémico ha ocurrido

Debido a que la lesión renal aguda se presenta de manera inesperada, es necesario conocer si la administración de espironolactona post-isquemia puede

prevenir el desarrollo de enfermedad renal crónica. Para ello incluimos nuevos grupos de ratas que tuvieron un seguimiento de 90 días. Los grupos fueron 1) sham, 2) I/R 45 min, 3) I/R 45 min y Sp 20 mg inmediatamente después de la I/R (Sp0-20), 4) I/R 45 min y Sp 20 mg 1.5 horas después de la I/R (Sp1.5-20), 5) I/R 45 min y Sp 20 mg 3 horas después de la I/R, 6) I/R 45 min y Sp 80 mg inmediatamente después de la I/R (Sp0-80) y 7) I/R 45 min y Sp 80 mg con Sp 1.5 horas después de la I/R (Sp1.5-80).

Como se observa en la figura 40A, la administración de la dosis baja de Sp después de la I/R no previno la elevación en la excreción urinaria de proteínas a las 24 h de reperfusión, sin embargo, a largo plazo se observó un efecto protector respecto al desarrollo de proteinuria en todos los grupos, excepto en el de Sp3 a los 90 días. Con la administración de la dosis alta de Sp (80 mg) se redujo parcialmente la proteinuria a las 24 h de reperfusión y se previno totalmente el desarrollo de proteinuria a lo largo de los 90 días (Figura 40B).

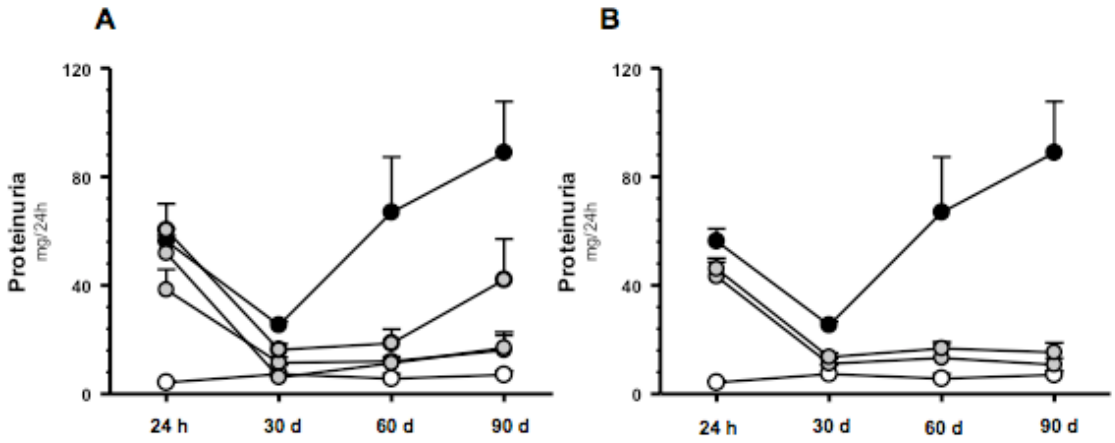

Figura 40. Excreción urinaria de proteínas en: sham (círculo blanco), I/R (circulo negro) y grupos tratados con espironolactona (circulo gris) A) dosis de 20 mg/kg y B) dosis de 80 mg/kg.

Respecto a los parámetros de función renal, se observó que a los 90 días de seguimiento los animales sometidos a isquemia sin tratamiento presentaron valores

menores de flujo sanguíneo renal y de depuración de creatinina, sin embargo, las diferencias no fueron estadísticamente significativas. Esta tendencia no se observó en los animales que fueron tratados con la dosis baja o alta de espironolactona (Figura 41).

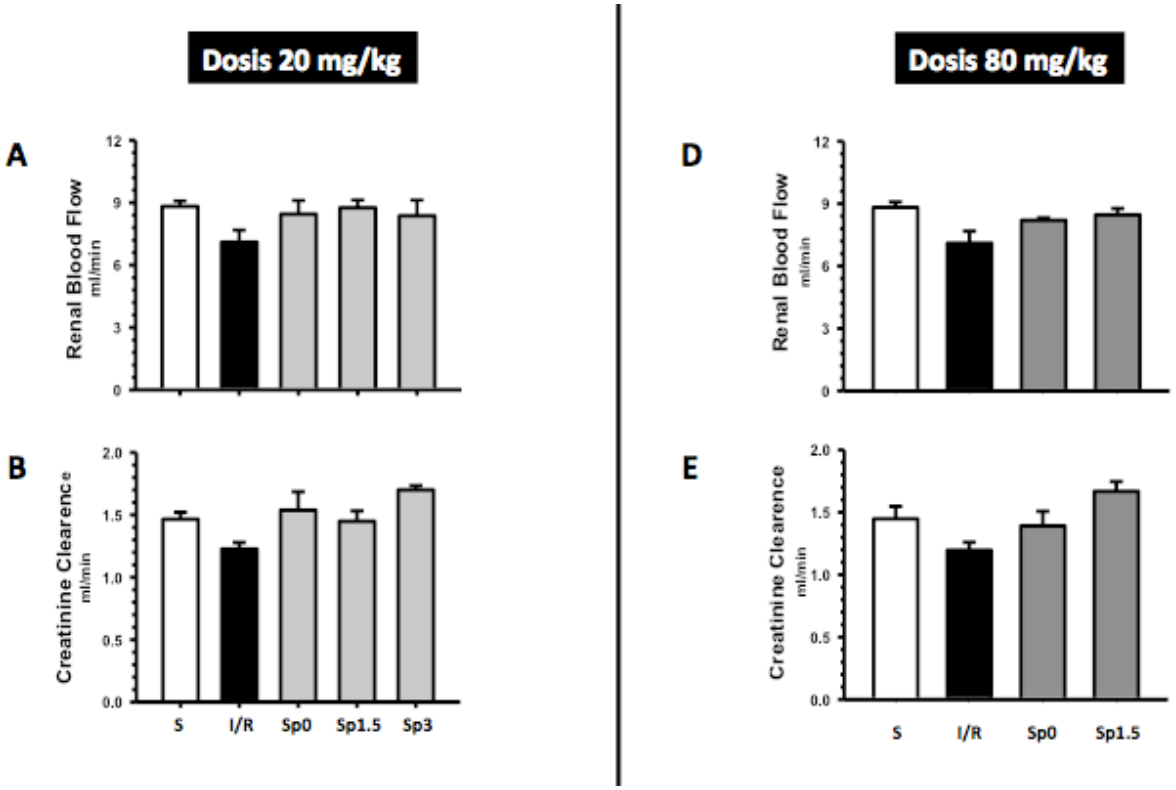

Figura 41. Flujo sanguíneo renal y depuración de creatinina en ratas sham (blanco), I/R (negro) y tratadas con espironolactona (gris).

También determinamos la presencia de marcadores moleculares de fibrosis e inflamación. Estos marcadores mostraron evidencia de la protección conferida por espironolactona. La sobre-regulación de los niveles de RNAm de TGFβ se previno o se redujo con el tratamiento con la dosis baja o alta de espironolactona cuando se administró a las 0 o 1.5 h después de la isquemia (Figura 42A y 42E). Sin embargo, los niveles de fosfo-Smad 3 siguieron elevados en las ratas tratadas con la dosis baja, pero no con la dosis alta de espironolactona (Figura 42B y 42F). El efecto

renoprotector de la espironolactona también se asoció con la prevención de la sobre-regulación de α-SMA y MCP-1 (Figura 42C y 42H).

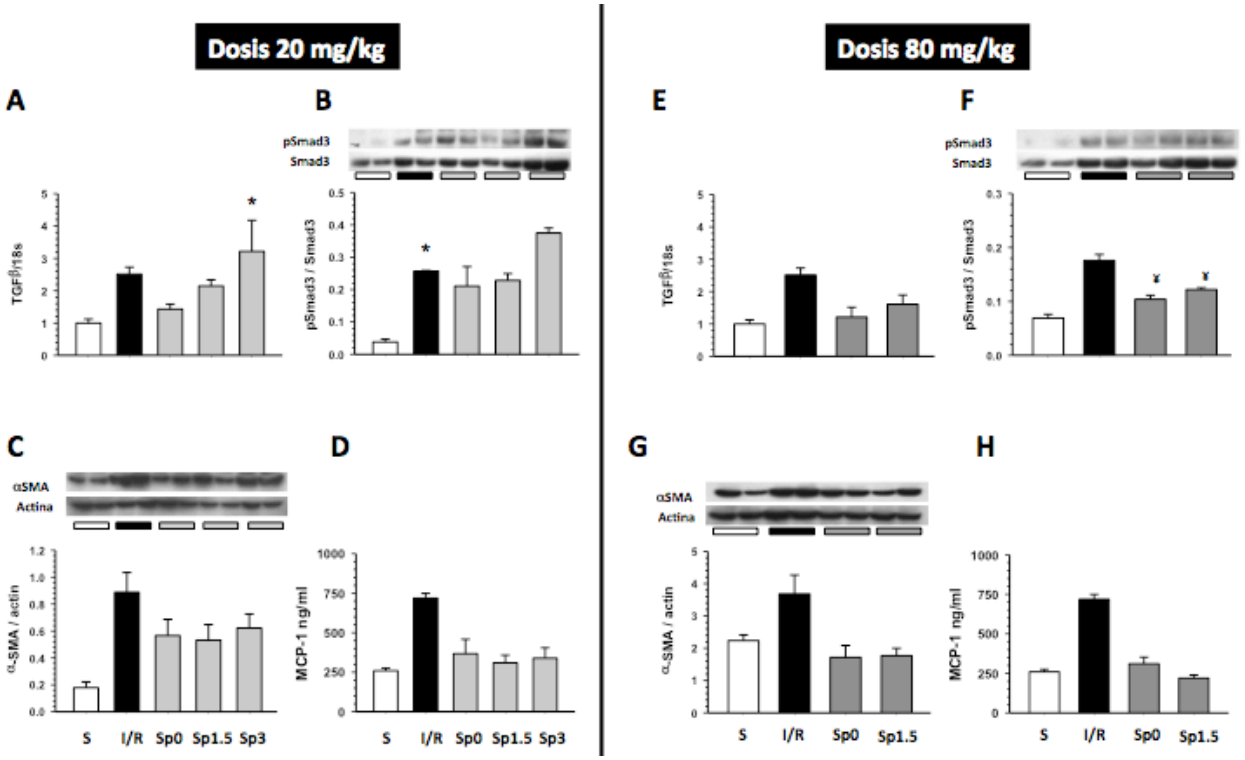

Figura 42. Niveles de RNAm de TGF-β, de proteína de fosfo-Smad3, de alpha-SMA y de MCP-1 en ratas sham (blanco), I/R (negro) y tratadas con espironolactona (gris).

En resumen, caracterizamos un modelo experimental de ERC inducida por un periodo de LRA en la rata. Diversos mecanismos fueron los responsables del desarrollo de ERC, entre ellos se encuentran: una mayor proliferación celular en los túbulos, la activación de la vía de TGF-β, el desarrollo de fibrosis túbulo-intersticial, un mayor estrés oxidante y una mayor respuesta inflamatoria. Además mostramos que el prevenir la LRA con espironolactona previene el desarrollo de ERC. Finalmente también se demostró que la administración de espironolactona después del insulto isquémico puede también prevenir el desarrollo de ERC.

V. D I S C U S I Ó N

Y

C O N C L U S I O N E S

La lesión renal aguda es un síndrome cuya frecuencia en la población es cada vez más elevada y que además presenta consecuencias graves como el desarrollo de enfermedad renal crónica o la pérdida total de la función renal, condición que solo es compatible con la vida, si los pacientes reciben terapia de reemplazo renal (diálisis o hemodiálisis) o bien un trasplante renal. A pesar de los grandes avances en la medicina moderna, la tasa de mortalidad de la LRA no ha sido mejorada en las últimas cuatro décadas debido al poco conocimiento de los mecanismos involucrados durante la patogénesis de la LRA, la falta de un marcador temprano que nos permita establecer un diagnóstico oportuno y a la falta de terapias farmacológicas eficientes. Es por ello que resulta imperativo estudiar a la LRA desde tres perspectivas: 1) comprender a detalle los mecanismos moleculares involucrados, 2) caracterizar un biomarcador de diagnóstico oportuno y 3) encontrar maniobras farmacológicas que permitan mejorar el pronóstico del paciente y evitar el desarrollo de consecuencias graves como la ERC. El presente trabajo abordó la LRA desde los tres puntos de vista anteriormente mencionados.

En este estudio mostramos que la sobre-expresión de Hsp90α o de Hsp90β protege del daño renal inducido por I/R a través de evitar la caída del FSR. El efecto reno-protector fue mediado a través de la activación de la sintasa de óxido nítrico endotelial y por lo tanto del restablecimiento de la síntesis de óxido nítrico. Además, encontramos que la cuantificación de los niveles urinarios de Hsp72 es un biomarcador confiable para establecer un diagnóstico temprano de la LRA. Este nuevo biomarcador tuvo varias características, entre ellas ser un método de diagnóstico temprano y suficientemente sensible para estratificar diferentes grados de daño renal y de recuperación, así como para monitorear la efectividad de una maniobra reno-protectora en un modelo de daño renal por I/R. Además, los hallazgos experimentales fueron corroborados en humanos diagnosticados con LRA.

El hecho de que Hsp72 sea un biomarcador capaz de estratificar el grado de daño renal que sufre cada paciente permitirá encontrar cuáles de ellos se encuentran en mayor riesgo de desarrollar ERC a largo plazo y poder proporcionarles un adecuado seguimiento. Adicionalmente, desarrollamos un modelo de ERC inducida por un periodo de LRA, el cual nos permitió demostrar que la espironolactona administrada de manera profiláctica o después de la I/R es capaz de prevenir o disminuir el desarrollo de ERC.

En la práctica clínica, es bien conocido que la disminución del flujo sanguíneo renal es determinante en la iniciación y ampliación de la fisiopatología de la insuficiencia renal aguda [110]. Un evento asociado a esta fisiopatología es el hecho de que el tono vascular se encuentra afectado, en parte, por una reducción de NO derivado de la eNOS [21]. En efecto, la disminución de la función de eNOS es una de las características de la disfunción endotelial asociada con insuficiencia renal aguda. En este sentido se ha mostrado que el aumento de la actividad de la eNOS inducida por pre-acondicionamiento isquémico protege a los riñones de I/R [71].

Los mecanismos sobre cómo Hsp90 interactúa con la eNOS para modular su actividad enzimática y el tono vascular siguen siendo actualmente motivo de estudio. No obstante, es bien conocido que Hsp90 tiene un efecto positivo sobre el estado conformacional de eNOS que favorece la producción de NO por eNOS, mientras que su ausencia permite que la enzima adopte una conformación diferente, lo que favorece la generación del anión superóxido [64]. En este sentido, la capacidad de eNOS para generar tanto NO como, el anión superóxido, le permite modular una amplia gama de actividades celulares [127]. Los estudios reportados actualmente sobre el papel fisiológico de Hsp90 son muy escasos y menos aún se conoce el papel específico que tienen Hsp90α y Hsp90β. Como una primera aproximación a este respecto, estudios de nuestro laboratorio sugieren que Hsp90 está implicada en

el mantenimiento de la función renal. En un estudio previo observamos que la inhibición de Hsp90 produjo vasoconstricción renal y una disminución de la filtración glomerular, lo que se asoció con una reducción en la producción de NO. La menor generación de NO se debió en parte por un aumento en la fosforilación inactivante de eNOS y por una reducción en la forma dimérica de eNOS [76]. Lo anterior sugiere que Hsp90 regula la producción de NO mediada por eNOS en el endotelio de los capilares glomerulares y de esta forma regula el tono vascular renal y la filtración glomerular. Sin embargo, se desconoce cual es la participación de Hsp90α o de Hsp90β en el mantenimiento del flujo sanguíneo renal y por lo tanto de la función renal. Como un primer acercamiento para conocer el papel que juega cada isoforma de Hsp90 en la regulación de la eNOS, en un estudio previo de nuestro laboratorio [77] se transfectó Hsp90α o Hsp90β en células epiteliales de riñón humano (HEK-293). Se observó que Hsp90α indujo un incremento en la producción de NO y en la fosforilación activante de Ser1177 en eNOS. Por el contrario Hsp90β produjo una disminución en la síntesis de NO y un incremento en la fosforilación inactivante de eNOS; sin embargo se desconoce si este efecto también se puede observar “in vivo” y cuál sería su repercusión sobre la función renal normal y frente a un fenómeno de I/R. Debido a que los animales deficientes en Hsp90 (Knockout) no sobreviven, decidimos evaluar el efecto de la sobre-expresión de Hsp90α y Hsp90β específicamente en los riñones. En esta parte del proyecto, no realizamos la transfección bilateral debido a que técnicamente es muy complicado transfectar el riñón derecho. En un inicio decidimos realizar isquemia bilateral y transfectar únicamente el riñón izquierdo. En este modelo observamos que el riñón transfectado tenía una mejor perfusión renal, pero esto no se reflejaba en la función renal total, ni en la proteinuria, debido a la contribución del daño renal del riñón no protegido con

la transfección (riñón derecho). Por esta razón decidimos utilizar otro modelo en donde solo se indujo isquemia en el riñón izquierdo que había sido previamente transfectado. Aunque si observamos nuevamente un restablecimiento del flujo sanguíneo con la transfección de las dos isoformas citosólicas de Hsp90, este modelo tampoco fue útil ya que el riñón derecho con una fisiología normal enmascaró lo que estaba sucediendo en el riñón izquierdo gracias a que compensó la función renal. Esto nos llevó a proponer un tercer modelo en donde efectuamos uninefrectomía del riñón derecho y transfectamos el riñón izquierdo para después inducir isquemia unilateral. Este modelo fue el mejor para poder distinguir lo que ocurría con la sobre-expresión de Hsp90α o de Hsp90β. De manera sorprendente encontramos que ambas isoformas fueron capaces de proteger al riñón frente a un fenómeno de isquemia/reperfusión renal. De forma tal, que los animales transfectadas con cualquiera de las dos isoformas de Hsp90 no presentaban disminución del FSR ni elevación de la creatinina sérica. En estos animales uninefrectomizados y sometidos a isquemia renal durante 30 min y reperfusión de 24 h, observamos una reducción significativa en la excreción urinaria de NO_2/NO_3. De forma interesante, la sobre-expresión de Hsp90α o de Hsp90β fue capaz de prevenir la caída del flujo sanguíneo renal y la reducción en la generación de NO. Esto por lo tanto, favoreció una eficiente generación de NO, lo que a su vez previno la caída del FSR posterior a la isquemia y que se observa después de 24 h, siendo este efecto uno de los mecanismos renoprotectores que confirió la sobre-expresión de ambas isoformas ante el daño inducido por la I/R. Además, en los animales uninefrectomizados y en los que se les transfectó Hsp90α o Hsp90β y que fueron posteriormente sometidos a I/R, exhibieron niveles de proteinuria y de Hsp72 similares a los del grupo operado en forma falsa, lo que indica que estos grupos no presentaron el daño tubular inducido por la isquemia. Este hecho fue corroborado

mediante el análisis histológico. El estudio de inmunoprecipitación reveló que la transfección de Hsp90α o de Hsp90β indujo una mayor interacción entre Hsp90 y eNOS, promoviendo que eNOS se fosforilara en el residuo activante de Ser-1177, como se ha descrito también por otros grupos [67]. Es importante mencionar que se ha reportado que este residuo puede ser fosforilado por la cinasa PKC-α y por la cinasa AKT [128]. Interesantemente, en este estudio encontramos que el grupo sometido a I/R presentó una menor expresión de PKC-α, lo que también puede explicar en parte la menor fosforilación en la Ser-1177 de eNOS y la consecuente menor producción de NO en estos animales. En cambio la sobre-expresión de Hsp90α o de Hsp90β restableció los niveles de proteína de esta cinasa y esto a su vez se asoció con el restablecimiento de la fosforilación en la Ser-1177 de eNOS. Estos hallazgos concuerdan con estudios previos que han demostrado que Hsp90 participa en mantener la estabilidad de PKC-α [129]. Respecto a la cinasa Akt encontramos que en las ratas sometidas a I/R sin transfección de Hsp90, la fosforilación de esta cinasa se encontraba incrementada en el tejido renal, efecto que pudo ser prevenido con la transfección de ambas isoformas de Hsp90. Esto es importante ya que se ha reportado que Akt es capaz de fosforilar al factor de transcripción FOXO3a el cual a su vez induce arresto en el ciclo celular y propicia el desarrollo de fibrosis después de la I/R [130]. En cambio, el residuo inactivante de eNOS, la Tre495, aumentó su fosforilación durante la isquemia y ésta se previno parcialmente con la transfección de Hsp90.

En resumen, en esta parte de este trabajo mostramos por primera vez que la sobre-expresión de Hsp90α o de Hsp90β protege contra el daño renal inducido por un fenómeno de isquemia/reperfusión. Observamos que la interacción Hsp90-eNOS se disminuye durante la I/R, efecto que se acompaña de una disminución en la

producción de NO y con cambios en la fosforilación de la Ser1177 y Tre495 de eNOS. La transfección de Hsp90α o de Hsp90β promovió un incremento en la interacción Hsp90-eNOS, lo que se asoció con el mantenimiento del estado de fosforilación de eNOS. A este respecto se ha mostrado que el acoplamiento entre Hsp90 y eNOS promueve un incremento en la fosforilación de la Ser1177 y que la fosforilación de la Tre495 resulta de la pérdida en la interacción de Hsp90 y eNOS. Por lo tanto es posible que durante la I/R, Hsp90 se encuentra mayormente ocupada en restablecer la homeostasis celular y en consecuencia se pierde la interacción Hsp90-eNOS y disminuye la generación de NO. En cambio en los riñones transfectados con Hsp90α o Hsp90β se promovió una mayor interacción Hsp90-eNOS y por lo tanto la producción de NO se reestableció, protegiendo así a los riñon es contra el daño por I/R.

Como se comentó previamente, una de las dificultades por las que la LRA puede tener complicaciones graves es por falta de un biomarcador sensible y temprano para el diagnóstico oportuno de esta enfermedad [131]. Ya que se ha mostrado que la intervención oportuna del paciente puede mejorar drásticamente el pronóstico esperado [132]. Previamente se reportó la expresión de Hsp72 puede ser altamente inducida por un proceso isquémico o bien por el uso de agentes nefrotóxicos [133] [134] [135]. Además es bien conocido que después de un fenómeno isquémico se propicia el desprendimiento de células viables y no viables, así como muerte de células del epitelio tubular, lo que genera que estas células drenen por el espacio tubular y aparezcan en la orina [136]. Además de que se ha descrito que el desprendimiento y muerte celular del epitelio tubular es proporcional a la severidad del daño. Considerando lo anterior, consideramos que la detección de Hsp72 en la orina podía ser útil para estratificar la extensión del daño renal inducido por un fenómeno de I/R. De hecho encontramos que después de 24 horas de

reperfusión, la expresión de Hsp72 en el tejido renal se incrementa de manera proporcional al periodo de isquemia inducido y lo hace desde un periodo de isquemia leve por 10 min. El mismo patrón de comportamiento de Hsp72 se observó en la orina de estos animales tanto a nivel de RNAm como de la proteína, lo que además correlacionó significativamente con el grado de daño tubular cuantificado por morfometría. La siguiente característica que nuestro biomarcador debería cumplir era que su inducción ocurriera de forma temprana. Para ello se determinaron los niveles de Hsp72 en orina de ratas sometidas a 30 min de isquemia con diferentes periodos de reperfusión. Encontramos que desde las 3 h después de la isquemia se puede encontrar esta proteína en la orina de los animales y que además su concentración disminuyó después de 72 horas de la isquemia, lo cual, correlacionó con la regeneración tubular que ocurre posterior a un fenómeno de isquemia. Estos hallazgos sugieren que esta proteína no solo puede ser utilizada como marcador de daño renal para detectar LRA, sino que también puede reflejar la recuperación y regeneración del epitelio tubular. Además Hsp72 fue capaz de monitorear la eficacia de una maniobra reno-protectora como lo es la espironolactona.

En este trabajo se comparó la cinética de Hsp72 con la de Kim-1, NGAL e IL-18. Kim-1 fue capaz de diferenciar entre el daño leve de uno moderado, pero no fue capaz de estratificar un daño renal severo, además su inducción fue tardía ya que se elevó significativamente hasta las 9 h después de la isquemia. Respecto a NGAL, este biomarcador no fue capaz de reflejar el progreso del daño tubular que ocurre durante la reperfusión. Finalmente, IL-18 fue un biomarcador menos temprano que Hsp72, pues su elevación ocurrió hasta 6 h después de la I/R.

En la práctica clínica, a pesar de las limitaciones que tiene la creatinina sérica, el diagnóstico de LRA continúa basándose en la elevación de este producto de

desecho. El diagnóstico de LRA se basa entonces, en los criterios de RIFLE o de AKIN [7]. Sin embargo, la creatinina sérica no es un marcador sensible del daño renal ya que se eleva cuando una gran parte del tejido renal se encuentra afectado o hasta 48 h después del insulto [8]. Por lo que, en este estudió evaluamos la sensibilidad de Hsp72 para establecer un diagnóstico oportuno de LRA en humanos. Encontramos que los niveles urinarios de Hsp72 son muy bajos en sujetos sanos, en contraste con los pacientes que fueron diagnosticados con LRA (por la elevación de la creatinina sérica), en los que se observó un incremento significativo de Hsp72 en la orina de estos sujetos. También evaluamos si Hsp72 era un marcador temprano de LRA en pacientes críticamente enfermos que se encontraban en la terapia intensiva del Instituto Nacional de Ciencias Médicas y Nutrición Salvador Zubirán, que fueron incluidos por presentar al menos dos fallas orgánicas. Al momento de la inclusión de los pacientes no sabíamos cuáles de ellos desarrollarían LRA, sino esto se supo hasta que se diagnosticó por la elevación de la creatinina sérica. Lo que encontramos fue que Hsp72 se incrementó en la orina de los pacientes que habían desarrollado LRA hasta con 48 horas de anticipación a la elevación de la creatinina sérica. En conjunto estos datos sugieren que la detección urinaria de Hsp72 es un biomarcador promisorio en un contexto clínico. Sin embargo, se requieren más estudios clínicos que incluyan un mayor número de pacientes para validar su uso como un biomarcador oportuno de LRA.

Finalmente, en este estudio caracterizamos un modelo de ERC inducida por un episodio de LRA. En este modelo indujimos isquemia renal bilateral de 45 min y los animales dejaron evolucionar por 10 o 270 días. Después de 10 días de haber inducido la isquemia observamos que los animales se habían recuperado completamente a nivel funcional sin embargo, la activación de vías pro-inflamatorias y pro-fibróticas permanecieron activadas. Durante el seguimiento de 9 meses

posteriores se encontró un incremento progresivo de excreción urinaria de proteínas, característica de la ERC. Así que consideramos que este modelo semeja lo que ocurre en la práctica clínica, en los pacientes que sobreviven a un episodio de LRA y recuperan su función renal y que están en inminente riesgo de desarrollar ERC. También observamos que la administración de espironolactona antes o después de la isquemia previno o disminuyó la severidad de la ERC. El mecanismo involucrado en la reno-protección conferida por espironolactona no ha sido claramente elucidado. Sin embargo, estudios reciente proponen a la aldosterona como un orquestador del daño renal tanto agudo como crónico [137] [138]. De forma tal que se ha evidenciado que la unión de la aldosterona a los receptores a mineralocorticoides (RM) localizados en la vasculatura es capaz de influenciar el tono vascular [139]. Esto ha sido más claramente mostrado en los ratones que sobre-expresan el RM en el endotelio, lo que provoca que el tono vascular sea alterado [119]. Además, se ha reportado que los ratones deficientes de RM exclusivamente en las células del músculo liso vascular presentan menor presión arterial con el envejecimiento, que los ratones controles [120]. En este sentido, estudios previos de nuestro laboratorio muestran que el bloqueo de los RM previene la hipo-perfusión renal característica del modelo de I/R, sugiriendo que la aldosterona tiene un papel esencial en mediar la disfunción renal. Es posible que el endotelio y el flujo sanguíneo renal en las ratas tratadas con espironolactona se hayan afectado mínimamente como consecuencia de la I/R y por lo tanto se pudieran prevenir las alteraciones micro-vasculares y el círculo vicioso de hipoxia crónica que finalmente desencadenaría el desarrollo de ERC. En este sentido la severidad de la LRA fue menor probablemente debido al bloqueo de la activación de los RM con espironolactona impidió el efecto vasoconstrictor que la aldosterona media a través de los RM, manteniendo así un FSR normal, lo que previno el daño

celular en el túbulo proximal. Además el hecho de que la espironolactona también previno el desarrollo de ERC aún después de inducir la I/R sugiere que la espironolactona impidió la activación de vías pro-inflamatorias y pro-fibróticas después de la I/R con lo que se evitó el desarrollo de ERC.

En conjunto los resultados del presente trabajo son la base para estudios de investigación traslacional donde se evaluará el poder diagnóstico de Hsp72 para la detección de la LRA. Además estos resultados sugieren que el tratamiento de los pacientes con espironolactona antes o después de un episodio de LRA puede ayudar a prevenir el desarrollo de ERC. Por lo tanto este trabajo contribuye de manera importante al entendimiento de los mecanismos involucrados en la LRA, a resolver la problemática de establecer un diagnóstico oportuno de LRA y a la prevención de la ERC inducida por un episodio de LRA.

VI. B I B L I O G R A F Í A

1. Hall JE, Guyton AC: *Pocket companion to Guyton & Hall textbook of medical physiology.* 11th ed ed. Edinburgh, Scotland, Elsevier Saunders, 2006

2. Drucker-Colin RR: *Fisiología médica.* México, Manual Moderno, 2005

3. Friedewald JJ, Rabb H: Inflammatory cells in ischemic acute renal failure. *Kidney Int* 66:486-491, 2004

4. Bonventre JV, Yang L: Cellular pathophysiology of ischemic acute kidney injury. *J Clin Invest* 121:4210-4221, 2011

5. Wu I, Parikh CR: Screening for kidney diseases: older measures versus novel biomarkers. *Clin J Am Soc Nephrol* 3:1895-1901, 2008

6. Kelly KJ: Acute renal failure: much more than a kidney disease. *Semin Nephrol* 26:105-113, 2006

7. Bagshaw SM: Acute kidney injury: diagnosis and classification of AKI: AKIN or RIFLE? *Nat Rev Nephrol* 6:71-73, 2010

8. Mehta RL, Chertow GM: Acute renal failure definitions and classification: time for change? *J Am Soc Nephrol* 14:2178-2187, 2003

9. Coca SG, Parikh CR: Urinary biomarkers for acute kidney injury: perspectives on translation. *Clin J Am Soc Nephrol* 3:481-490, 2008

10. Yamamoto T, Noiri E, Ono Y *et al.*: Renal L-type fatty acid--binding protein in acute ischemic injury. *J Am Soc Nephrol* 18:2894-2902, 2007

11. Cerda J, Lameire N, Eggers P *et al.*: Epidemiology of acute kidney injury. *Clin J Am Soc Nephrol* 3:881-886, 2008

12. Mosier MJ, Pham TN, Klein MB *et al.*: Early acute kidney injury predicts progressive renal dysfunction and higher mortality in severely burned adults. *J Burn Care Res* 31:83-92, 2010

13. Block CA, Schoolwerth AC: Acute renal failure: outcomes and risk of chronic kidney disease. *Minerva Urol Nefrol* 59:327-335, 2007

14. Venkatachalam MA, Griffin KA, Lan R *et al.*: Acute kidney injury: a springboard for progression in chronic kidney disease. *Am J Physiol Renal Physiol*, 2010

15. Bucaloiu ID, Kirchner HL, Norfolk ER *et al.*: Increased risk of death and de novo chronic kidney disease following reversible acute kidney injury. *Kidney Int* 81:477-485, 2012

16. Chawla LS, Amdur RL, Amodeo S *et al.*: The severity of acute kidney injury predicts progression to chronic kidney disease. *Kidney Int* 79:1361-1369, 2011

17. Conger JD, Kim GE, Robinette JB: Effects of ANG II, ETA, and TxA2 receptor antagonists on cyclosporin A renal vasoconstriction. *Am J Physiol* 267:F443-F449, 1994

18. Brooks DP: Role of endothelin in renal function and dysfunction. *Clin Exp Pharmacol Physiol* 23:345-348, 1996

19. Kurata H, Takaoka M, Kubo Y *et al.*: Protective effect of nitric oxide on ischemia/reperfusion-induced renal injury and endothelin-1 overproduction. *Eur J Pharmacol* 517:232-239, 2005

20. Tuladhar SM, Puntmann VO, Soni M *et al.*: Rapid detection of acute kidney injury by plasma and urinary neutrophil gelatinase-associated lipocalin after cardiopulmonary bypass. *J Cardiovasc Pharmacol* 53:261-266, 2009

21. Kwon O, Hong SM, Ramesh G: Diminished NO generation by injured endothelium and loss of macula densa nNOS may contribute to sustained acute kidney injury after ischemia-reperfusion. *Am J Physiol Renal Physiol* 296:F25-F33, 2009

22. Basile DP: The endothelial cell in ischemic acute kidney injury: implications for acute and chronic function. *Kidney Int* 72:151-156, 2007

23. Basile DP: Rarefaction of peritubular capillaries following ischemic acute renal failure: a potential factor predisposing to progressive nephropathy. *Curr Opin Nephrol Hypertens* 13:1-7, 2004

24. Bonventre JV, Zuk A: Ischemic acute renal failure: an inflammatory disease? *Kidney Int* 66:480-485, 2004

25. Awad AS, Rouse M, Huang L *et al.*: Compartmentalization of neutrophils in the kidney and lung following acute ischemic kidney injury. *Kidney Int* 75:689-698, 2009

26. Jang HR, Rabb H: The innate immune response in ischemic acute kidney injury. *Clin Immunol* 130:41-50, 2009

27. Zhang MZ, Yao B, Yang S *et al.*: CSF-1 signaling mediates recovery from acute kidney injury. *J Clin Invest* 122:4519-4532, 2012

28. Bonventre JV: Pathogenetic and regenerative mechanisms in acute tubular necrosis. *Kidney Blood Press Res* 21:226-229, 1998

29. Heyman SN, Rosenberger C, Rosen S: Experimental ischemia-reperfusion: biases and myths-the proximal vs. distal hypoxic tubular injury debate revisited. *Kidney Int* 77:9-16, 2010

30. Sutton TA, Molitoris BA: Mechanisms of cellular injury in ischemic acute renal failure. *Semin Nephrol* 18:490-497, 1998

31. Molitoris BA, Dahl R, Geerdes A: Cytoskeleton disruption and apical redistribution of proximal tubule Na(+)-K(+)-ATPase during ischemia. *Am J Physiol* 263:F488-F495, 1992

32. Gailit J, Colflesh D, Rabiner I *et al.*: Redistribution and dysfunction of integrins in cultured renal epithelial cells exposed to oxidative stress. *Am J Physiol* 264:F149-F157, 1993

33. Zuk A, Bonventre JV, Brown D, Matlin KS: Polarity, integrin, and extracellular matrix dynamics in the postischemic rat kidney. *Am J Physiol* 275:C711-C731, 1998

34. Bush KT, Keller SH, Nigam SK: Genesis and reversal of the ischemic phenotype in epithelial cells. *J Clin Invest* 106:621-626, 2000

35. Brown D, Lee R, Bonventre JV: Redistribution of villin to proximal tubule basolateral membranes after ischemia and reperfusion. *Am J Physiol* 273:F1003-F1012, 1997

36. Wei Q, Hill WD, Su Y *et al.*: Heme oxygenase-1 induction contributes to renoprotection by G-CSF during rhabdomyolysis-associated acute kidney injury. *Am J Physiol Renal Physiol* 301:F162-F170, 2011

37. Nath KA: Heme oxygenase-1: a provenance for cytoprotective pathways in the kidney and other tissues. *Kidney Int* 70:432-443, 2006

38. Wang Z, Gall JM, Bonegio RG *et al.*: Induction of heat shock protein 70 inhibits ischemic renal injury. *Kidney Int* 79:861-870, 2011

39. Ritossa FA: New puffing pattern induced by temperature shoch and DNP in Drosophila. *Experientia* 18:571-573, 1962

40. Borkan SC, Gullans SR: Molecular chaperones in the kidney. *Annu Rev Physiol* 64:503-527, 2002

41. Benjamin IJ, McMillan DR: Stress (heat shock) proteins: molecular chaperones in cardiovascular biology and disease. *Circ Res* 83:117-132, 1998

42. Jaattela M: Heat shock proteins as cellular lifeguards. *Ann Med* 31:261-271, 1999

43. Sreedhar AS, Kalmar E, Csermely P, Shen YF: Hsp90 isoforms: functions, expression and clinical importance. *FEBS Lett* 562:11-15, 2004

44. Moore SK, Kozak C, Robinson EA *et al.*: Murine 86- and 84-kDa heat shock proteins, cDNA sequences, chromosome assignments, and evolutionary origins. *J Biol Chem* 264:5343-5351, 1989

45. Rebbe NF, Ware J, Bertina RM *et al.*: Nucleotide sequence of a cDNA for a member of the human 90-kDa heat- shock protein family. *Gene* 53:235-245, 1987

46. Ullrich SJ, Moore SK, Appella E: Transcriptional and translational analysis of the murine 84- and 86-kDa heat shock proteins. *J Biol Chem* 264:6810-6816, 1989

47. Zhang SL, Yu J, Cheng XK *et al.*: Regulation of human hsp90alpha gene expression. *FEBS Lett* 444:130-135, 1999

48. Bharadwaj S, Ali A, Ovsenek N: Multiple components of the HSP90 chaperone complex function in regulation of heat shock factor 1 In vivo. *Mol Cell Biol* 19:8033-8041, 1999

49. Morimoto RI: Regulation of the heat shock transcriptional response: cross talk between a family of heat shock factors, molecular chaperones, and negative regulators. *Genes Dev* 12:3788-3796, 1998

50. Hessling M, Richter K, Buchner J: Dissection of the ATP-induced conformational cycle of the molecular chaperone Hsp90. *Nat Struct Mol Biol* 16:287-293, 2009

51. Tsutsumi S, Mollapour M, Graf C *et al.*: Hsp90 charged-linker truncation reverses the functional consequences of weakened hydrophobic contacts in the N domain. *Nat Struct Mol Biol* 16:1141-1147, 2009

52. Hainzl O, Lapina MC, Buchner J, Richter K: The charged linker region is an important regulator of Hsp90 function. *J Biol Chem* 284:22559-22567, 2009

53. Prodromou C, Roe SM, O'Brien R *et al.*: Identification and structural characterization of the ATP/ADP-binding site in the Hsp90 molecular chaperone. *Cell* 90:65-75, 1997

54. Mollapour M, Tsutsumi S, Truman AW *et al.*: Threonine 22 phosphorylation attenuates Hsp90 interaction with cochaperones and affects its chaperone activity. *Mol Cell* 41:672-681, 2011

55. Cortes-Gonzalez CC, Ramirez-Gonzalez V, Ariza AC, Bobadilla NA: [Functional significance of heat shock protein 90]. *Rev Invest Clin* 60:311-320, 2008

56. Garcia-Cardena G, Fan R, Shah V *et al.*: Dynamic activation of endothelial nitric oxide synthase by Hsp90. *Nature* 392:821-824, 1998

57. Bender AT, Silverstein AM, Demady DR *et al.*: Neuronal nitric-oxide synthase is regulated by the Hsp90-based chaperone system in vivo. *J Biol Chem* 274:1472-1478, 1999

58. Yoshida M, Xia Y: Heat shock protein 90 as an endogenous protein enhancer of inducible nitric-oxide synthase. *J Biol Chem* 278:36953-36958, 2003

59. Brouet A, Sonveaux P, Dessy C *et al.*: Hsp90 ensures the transition from the early Ca2+-dependent to the late phosphorylation-dependent activation of the endothelial nitric-oxide synthase in vascular endothelial growth factor-exposed endothelial cells. *J Biol Chem* 276:32663-32669, 2001

60. Sun J, Liao JK: Induction of angiogenesis by heat shock protein 90 mediated by protein kinase Akt and endothelial nitric oxide synthase. *Arterioscler Thromb Vasc Biol* 24:2238-2244, 2004

61. Sessa WC: eNOS at a glance. *J Cell Sci* 117:2427-2429, 2004

62. Fleming I, Busse R: Signal transduction of eNOS activation. *Cardiovasc Res* 43:532-541, 1999

63. Xu H, Shi Y, Wang J *et al.*: A Heat Shock Protein 90 Binding Domain in Endothelial Nitric-oxide Synthase Influences Enzyme Function. *J Biol Chem* 282:37567-37574, 2007

64. Pritchard KA, Jr., Ackerman AW, Gross ER *et al.*: Heat shock protein 90 mediates the balance of nitric oxide and superoxide anion from endothelial nitric-oxide synthase. *J Biol Chem* 276:17621-17624, 2001

65. Fleming I, Fisslthaler B, Dimmeler S *et al.*: Phosphorylation of Thr(495) regulates Ca(2+)/calmodulin-dependent endothelial nitric oxide synthase activity. *Circ Res* 88:E68-E75, 2001

66. Lin MI, Fulton D, Babbitt R *et al.*: Phosphorylation of threonine 497 in endothelial nitric-oxide synthase coordinates the coupling of L-arginine metabolism to efficient nitric oxide production. *J Biol Chem* 278:44719-44726, 2003

67. Takahashi S, Mendelsohn ME: Synergistic activation of endothelial nitric-oxide synthase (eNOS) by HSP90 and Akt: calcium-independent eNOS activation involves formation of an HSP90-Akt-CaM-bound eNOS complex. *J Biol Chem* 278:30821-30827, 2003

68. Fleming I: Molecular mechanisms underlying the activation of eNOS. *Pflugers Arch* 459:793-806, 2010

69. Yang D, Xie P, Liu Z: Ischemia/reperfusion-induced MKP-3 impairs endothelial NO formation via inactivation of ERK1/2 pathway. *PLoS ONE* 7:e42076, 2012

70. An J, Du J, Wei N *et al.*: Role of tetrahydrobiopterin in resistance to myocardial ischemia in Brown Norway and Dahl S rats. *Am J Physiol Heart Circ Physiol* 297:H1783-H1791, 2009

71. Mahfoudh-Boussaid A, Zaouali MA, Hadj-Ayed K *et al.*: Ischemic preconditioning reduces endoplasmic reticulum stress and upregulates hypoxia inducible factor-1alpha in ischemic kidney: the role of nitric oxide. *J Biomed Sci* 19:7, 2012

72. Roviezzo F, Cuzzocrea S, Di LA *et al.*: Protective role of PI3-kinase-Akt-eNOS signalling pathway in intestinal injury associated with splanchnic artery occlusion shock. *Br J Pharmacol* 151:377-383, 2007

73. Harrison EM, Sharpe E, Bellamy CO *et al.*: Heat shock protein 90-binding agents protect renal cells from oxidative stress and reduce kidney ischemia-reperfusion injury. *Am J Physiol Renal Physiol* 295:F397-F405, 2008

74. Noh H, Kim HJ, Yu MR *et al.*: Heat shock protein 90 inhibitor attenuates renal fibrosis through degradation of transforming growth factor-beta type II receptor. *Lab Invest* 92:1583-1596, 2012

75. Ramirez V, Uribe N, Garcia-Torres R *et al.*: Upregulation and intrarenal redistribution of heat shock proteins 90alpha and 90beta by low-sodium diet in the rat. *Cell Stress Chaperones* 9:198-206, 2004

76. Ramirez V, Mejia-Vilet JM, Hernandez D *et al.*: Radicicol, a heat shock protein 90 inhibitor, reduces glomerular filtration rate. *Am J Physiol Renal Physiol* 295:F1044-F1051, 2008

77. Cortes-Gonzalez C, Barrera-Chimal J, Ibarra-Sanchez M *et al.*: Opposite effect of Hsp90alpha and Hsp90beta on eNOS ability to produce nitric oxide or superoxide anion in human embryonic kidney cells. *Cell Physiol Biochem* 26:657-668, 2010

78. Chen SW, Kim M, Kim M *et al.*: Mice that overexpress human heat shock protein 27 have increased renal injury following ischemia reperfusion. *Kidney Int* 75:499-510, 2009

79. Herrera J, Rodriguez-Iturbe B: Stimulation of tubular secretion of creatinine in health and in conditions associated with reduced nephron mass. Evidence for a tubular functional reserve. *Nephrol Dial Transplant* 13:623-629, 1998

80. Ronco C, Grammaticopoulos S, Rosner M *et al.*: Oliguria, creatinine and other biomarkers of acute kidney injury. *Contrib Nephrol* 164:118-127, 2010

81. Siew ED, Ware LB, Ikizler TA: Biological markers of acute kidney injury. *J Am Soc Nephrol* 22:810-820, 2011

82. Cowland JB, Borregaard N: Molecular characterization and pattern of tissue expression of the gene for neutrophil gelatinase-associated lipocalin from humans. *Genomics* 45:17-23, 1997

83. Flower DR, North AC, Sansom CE: The lipocalin protein family: structural and sequence overview. *Biochim Biophys Acta* 1482:9-24, 2000

84. Mishra J, Dent C, Tarabishi R *et al.*: Neutrophil gelatinase-associated lipocalin (NGAL) as a biomarker for acute renal injury after cardiac surgery. *Lancet* 365:1231-1238, 2005

85. Parikh CR, Devarajan P, Zappitelli M *et al.*: Postoperative biomarkers predict acute kidney injury and poor outcomes after adult cardiac surgery. *J Am Soc Nephrol* 22:1748-1757, 2011

86. Soni SS, Cruz D, Bobek I *et al.*: NGAL: a biomarker of acute kidney injury and other systemic conditions. *Int Urol Nephrol* 42:141-150, 2010

87. Alpizar-Alpizar W, Laerum OD, Illemann M *et al.*: Neutrophil gelatinase-associated lipocalin (NGAL/Lcn2) is upregulated in gastric mucosa infected with Helicobacter pylori. *Virchows Arch* 455:225-233, 2009

88. Ichimura T, Bonventre JV, Bailly V *et al.*: Kidney injury molecule-1 (KIM-1), a putative epithelial cell adhesion molecule containing a novel immunoglobulin domain, is up-regulated in renal cells after injury. *J Biol Chem* 273:4135-4142, 1998

89. Ichimura T, Asseldonk EJ, Humphreys BD *et al.*: Kidney injury molecule-1 is a phosphatidylserine receptor that confers a phagocytic phenotype on epithelial cells. *J Clin Invest* 118:1657-1668, 2008

90. Vaidya VS, Ramirez V, Ichimura T *et al.*: Urinary kidney injury molecule-1: a sensitive quantitative biomarker for early detection of kidney tubular injury. *Am J Physiol Renal Physiol* 290:F517-F529, 2006

91. Zhang Z, Humphreys BD, Bonventre JV: Shedding of the Urinary Biomarker Kidney Injury Molecule-1 (KIM-1) Is Regulated by MAP Kinases and Juxtamembrane Region. *J Am Soc Nephrol* 18:2704-2714, 2007

92. Han WK, Bailly V, Abichandani R *et al.*: Kidney Injury Molecule-1 (KIM-1): a novel biomarker for human renal proximal tubule injury. *Kidney Int* 62:237-244, 2002

93. Liangos O, Perianayagam MC, Vaidya VS *et al.*: Urinary N-acetyl-beta-(D)-glucosaminidase activity and kidney injury molecule-1 level are associated with adverse outcomes in acute renal failure. *J Am Soc Nephrol* 18:904-912, 2007

94. Han WK, Waikar SS, Johnson A *et al.*: Urinary biomarkers in the early diagnosis of acute kidney injury. *Kidney Int* 73:863-869, 2008

95. Melnikov VY, Ecder T, Fantuzzi G *et al.*: Impaired IL-18 processing protects caspase-1-deficient mice from ischemic acute renal failure. *J Clin Invest* 107:1145-1152, 2001

96. Fantuzzi G, Puren AJ, Harding MW *et al.*: Interleukin-18 regulation of interferon gamma production and cell proliferation as shown in interleukin-1beta-converting enzyme (caspase-1)-deficient mice. *Blood* 91:2118-2125, 1998

97. Parikh CR, Abraham E, Ancukiewicz M, Edelstein CL: Urine IL-18 is an early diagnostic marker for acute kidney injury and predicts mortality in the intensive care unit. *J Am Soc Nephrol* 16:3046-3052, 2005

98. Torregrosa I, Montoliu C, Urios A *et al.*: Early biomarkers of acute kidney failure after heart angiography or heart surgery in patients with acute coronary syndrome or acute heart failure. *Nefrologia* 32:44-52, 2012

99. Herget-Rosenthal S, Marggraf G, Husing J *et al.*: Early detection of acute renal failure by serum cystatin C. *Kidney Int* 66:1115-1122, 2004

100. Zhang Z, Lu B, Sheng X, Jin N: Cystatin C in prediction of acute kidney injury: a systemic review and meta-analysis. *Am J Kidney Dis* 58:356-365, 2011

101. Bazzi C, Petrini C, Rizza V *et al.*: A modern approach to selectivity of proteinuria and tubulointerstitial damage in nephrotic syndrome. *Kidney Int* 58:1732-1741, 2000

102. Katagiri D, Doi K, Honda K *et al.*: Combination of two urinary biomarkers predicts acute kidney injury after adult cardiac surgery. *Ann Thorac Surg* 93:577-583, 2012

103. Erdener D, Aksu K, Bicer I *et al.*: Urinary N-acetyl-beta-D-glucosaminidase (NAG) in lupus nephritis and rheumatoid arthritis. *J Clin Lab Anal* 19:172-176, 2005

104. Veerkamp JH, Peeters RA, Maatman RG: Structural and functional features of different types of cytoplasmic fatty acid-binding proteins. *Biochim Biophys Acta* 1081:1-24, 1991

105. Maatman RG, van de Westerlo EM, van Kuppevelt TH, Veerkamp JH: Molecular identification of the liver- and the heart-type fatty acid-binding proteins in human and rat kidney. Use of the reverse transcriptase polymerase chain reaction. *Biochem J* 288 (Pt 1):285-290, 1992

106. Negishi K, Noiri E, Doi K *et al.*: Monitoring of urinary L-type fatty acid-binding protein predicts histological severity of acute kidney injury. *Am J Pathol* 174:1154-1159, 2009

107. Zhang PL, Lun M, Schworer CM *et al.*: Heat shock protein expression is highly sensitive to ischemia-reperfusion injury in rat kidneys. *Ann Clin Lab Sci* 38:57-64, 2008

108. Basile DP, Friedrich JL, Spahic J *et al.*: Impaired endothelial proliferation and mesenchymal transition contribute to vascular rarefaction following acute kidney injury. *Am J Physiol Renal Physiol* 300:F721-F733, 2011

109. Basile DP, Donohoe D, Roethe K, Osborn JL: Renal ischemic injury results in permanent damage to peritubular capillaries and influences long-term function. *Am J Physiol Renal Physiol* 281:F887-F899, 2001

110. Conger JD, Robinette JB, Hammond WS: Differences in vascular reactivity in models of ischemic acute renal failure. *Kidney Int* 39:1087-1097, 1991

111. Yang L, Besschetnova TY, Brooks CR *et al.*: Epithelial cell cycle arrest in G2/M mediates kidney fibrosis after injury. *Nat Med* 16:535-43, 1p, 2010

112. Bechtel W, McGoohan S, Zeisberg EM *et al.*: Methylation determines fibroblast activation and fibrogenesis in the kidney. *Nat Med* 16:544-550, 2010

113. Mejia-Vilet JM, Ramirez V, Cruz C *et al.*: Renal ischemia-reperfusion injury is prevented by the mineralocorticoid receptor blocker spironolactone. *Am J Physiol Renal Physiol* 293:F78-F86, 2007

114. Ramirez V, Trujillo J, Valdes R *et al.*: Adrenalectomy prevents renal ischemia-reperfusion injury. *Am J Physiol Renal Physiol* 297:F932-F942, 2009

115. Feria I, Pichardo I, Juarez P *et al.*: Therapeutic benefit of spironolactone in experimental chronic cyclosporine A nephrotoxicity. *Kidney Int* 63:43-52, 2003

116. Perez-Rojas J, Blanco JA, Cruz C *et al.*: Mineralocorticoid receptor blockade confers renoprotection in preexisting chronic cyclosporine nephrotoxicity. *Am J Physiol Renal Physiol* 292:F131-F139, 2007

117. Sánchez-Pozos K., Barrera-Chimal J., Garzón-Muvdi J., Pérez-Villalva R., Rodríguez-Romo R, Cruz C., Gamba G., and Bobadilla N.A. Recovery from ischemic acute kidney injury by spironolactone administration. Nephrol.Dial.Transplant. 2012.

118. Perez-Rojas JM, Derive S, Blanco JA *et al.*: Renocortical mRNA expression of vasoactive factors during spironolactone protective effect in chronic cyclosporine nephrotoxicity. *Am J Physiol Renal Physiol* 289:F1020-F1030, 2005

119. Nguyen Dinh CA, Griol-Charhbili V, Loufrani L *et al.*: The endothelial mineralocorticoid receptor regulates vasoconstrictor tone and blood pressure. *FASEB J* 24:2454-2463, 2010

120. McCurley A, Pires PW, Bender SB *et al.*: Direct regulation of blood pressure by smooth muscle cell mineralocorticoid receptors. *Nat Med* 18:1429-1433, 2012

121. Livak KJ, Schmittgen TD: Analysis of relative gene expression data using real-time quantitative PCR and the 2(-Delta Delta C(T)) Method. *Methods* 25:402-408, 2001

122. Aebi HE: Catalase, in *Methods of enzymatic analysis* 1982, pp 273-286

123. Lawrence RA, Burk RF: Glutathione peroxidase activity in selenium-deficient rat liver. *Biochem Biophys Res Commun* 71:952-958, 1976

124. Lowry OH, ROSEBROUGH NJ, FARR AL, RANDALL RJ: Protein measurement with the Folin phenol reagent. *J Biol Chem* 193:265-275, 1951

125. Andreucci M, Michael A, Kramers C *et al.*: Renal ischemia/reperfusion and ATP depletion/repletion in LLC-PK(1) cells result in phosphorylation of FKHR and FKHRL1. *Kidney Int* 64:1189-1198, 2003

126. Meng XM, Huang XR, Chung AC *et al.*: Smad2 protects against TGF-beta/Smad3-mediated renal fibrosis. *J Am Soc Nephrol* 21:1477-1487, 2010

127. Sessa WC: Regulation of endothelial derived nitric oxide in health and disease. *Mem Inst Oswaldo Cruz* 100 Suppl 1:15-18, 2005

128. Partovian C, Zhuang Z, Moodie K *et al.*: PKCalpha activates eNOS and increases arterial blood flow in vivo. *Circ Res* 97:482-487, 2005

129. Gould CM, Kannan N, Taylor SS, Newton AC: The chaperones Hsp90 and Cdc37 mediate the maturation and stabilization of protein kinase C through a conserved PXXP motif in the C-terminal tail. *J Biol Chem* 284:4921-4935, 2009

130. Nemoto S, Finkel T: Redox regulation of forkhead proteins through a p66shc-dependent signaling pathway. *Science* 295:2450-2452, 2002

131. Coca SG, Yalavarthy R, Concato J, Parikh CR: Biomarkers for the diagnosis and risk stratification of acute kidney injury: a systematic review. *Kidney Int* 73:1008-1016, 2008

132. McIlroy DR, Wagener G, Lee HT: Neutrophil Gelatinase-Associated Lipocalin and acute kidney injury after cardiac surgery: the effect of baseline renal function on diagnostic performance. *Clin J Am Soc Nephrol* 5:211-219, 2010

133. Hernadez-Pando R, Pedraza-Chaverri J, Orozco-Estevez H *et al.*: Histological and subcellular distribution of 65 and 70 kD heat shock proteins in experimental nephrotoxic injury. *Exp Toxicol Pathol* 47:501-508, 1995

134. Kelly KJ: Stress response proteins and renal ischemia. *Minerva Urol Nefrol* 54:81-91, 2002

135. Kelly KJ, Baird NR, Greene AL: Induction of stress response proteins and experimental renal ischemia/reperfusion. *Kidney Int* 59:1798-1802, 2001

136. Lamchiagdhase P, Preechaborisutkul K, Lomsomboon P *et al.*: Urine sediment examination: a comparison between the manual method and the iQ200 automated urine microscopy analyzer. *Clin Chim Acta* 358:167-174, 2005

137. Bobadilla NA, Gamba G: New insights into the pathophysiology of cyclosporine nephrotoxicity: a role of aldosterone. *Am J Physiol Renal Physiol* 293:F2-F9, 2007

138. Shavit L, Lifschitz MD, Epstein M: Aldosterone blockade and the mineralocorticoid receptor in the management of chronic kidney disease: current concepts and emerging treatment paradigms. *Kidney Int* 81:955-968, 2012

139. McCurley A, Jaffe IZ: Mineralocorticoid receptors in vascular function and disease. *Mol Cell Endocrinol* 350:256-265, 2012

VII. ARTÍCULOS PUBLICADOS

EMBO Molecular Medicine

Hsp72 is an early and sensitive biomarker to detect acute kidney injury

*Jonatan Barrera-Chimal[1,2], Rosalba Pérez-Villalva[1,2], Cesar Cortés-González[1,2], Marcos Ojeda-Cervantes[2], Gerardo Gamba[1,2,3], Luis E. Morales-Buenrostro[2], Norma A. Bobadilla[1,2]**

Keywords: early biomarker; stratifying biomarker; spironolactone renoprotection; patients with AKI

DOI 10.1002/emmm.201000105

Received May 17, 2010
Revised November 01, 2010
Accepted November 08, 2010

This study was designed to assess whether heat shock protein Hsp72 is an early and sensitive biomarker of acute kidney injury (AKI) as well as to monitor a renoprotective strategy. Seventy-two Wistar rats were divided into six groups: sham-operated and rats subjected to 10, 20, 30, 45 and 60 min of bilateral ischemia (I) and 24 h of reperfusion (R). Different times of reperfusion (3, 6, 9, 12, 18, 24, 48, 72, 96 and 120 h) were also evaluated in 30 other rats subjected to 30 min of ischemia. Hsp72 messenger RNA (mRNA) and protein levels were determined in both kidney and urine. Hsp72-specificity as a biomarker to assess the success of a renoprotective intervention was evaluated in rats treated with different doses of spironolactone before I/R. Renal Hsp72 mRNA and protein, as well as urinary Hsp72 levels, gradually increased relative to the extent of renal injury induced by different periods of ischemia quantified by histomorphometry as a benchmark of kidney damage. Urinary Hsp72 increased significantly after 3 h and continued rising until 18 h, followed by restoration after 120 h of reperfusion in accord with histopathological findings. Spironolactone renoprotection was associated with normalization of urinary Hsp72 levels. Accordingly, urinary Hsp72 was significantly increased in patients with clinical AKI before serum creatinine elevation. Our results show that urinary Hsp72 is a useful biomarker for early detection and stratification of AKI. In addition, urinary Hsp72 levels are sensitive enough to monitor therapeutic interventions and the degree of tubular recovery following an I/R insult.

INTRODUCTION

Ischemia/reperfusion (I/R) and nephrotoxic injuries are the major causes of acute kidney injury (AKI) in native and transplanted kidneys (Friedewald & Rabb, 2004). AKI occurs in about 5% of hospitalized patients and up to 40–60% of intensive care unit (ICU) patients (Kelly, 2006). Despite technical improvements in clinical care and the development of preventive strategies, the prevalence of AKI has risen significantly in the last 15 years due to population aging and the rising pandemics of obesity, diabetes and hypertension (Liano & Pascual, 1996; Waikar et al, 2006). Despite efforts and advances in the development of new therapeutics, the mortality rate of AKI remains between 40 and 80% and has not been reduced in the last four decades, mainly because current tools used for the early detection of AKI are not adequately sensitive or specific (Wu & Parikh, 2008). In current clinical practice, AKI is typically diagnosed by a rise in serum creatinine (SCr). Indeed, acute kidney injury network (AKIN) and risk injury failure lost end stage renal disease (RIFLE) classifications for the detection of AKI are based on elevation of SCr (Bagshaw, 2010; Lopes et al, 2008; Wu & Parikh, 2008). It is generally accepted, however, that SCr is an unreliable and delayed marker of kidney injury. Substantial injury to the kidney may occur without affecting glomerular filtration; for

(1) Molecular Physiology Unit, Instituto de Investigaciones Biomédicas, Universidad Nacional Autónoma de México, Mexico City, Mexico.
(2) Department of Nephrology, Instituto Nacional de Ciencias Médicas y Nutrición Salvador Zubirán, Tlalpan, Mexico.
(3) Department of Nephrology, Instituto Nacional de Cardiología Ignacio Chávez, Mexico City, Mexico.
***Corresponding author:** Tel: +5255 5485 2676; Fax: +5255 5655 0382; E-mail: nab@biomedicas.unam.mx

example, extensive kidney mass reduction may occur without changes in SCr levels, and urinary obstruction caused by post-renal factors may be associated with an elevation in SCr without renal tubular injury (Coca & Parikh, 2008). Moreover, it has been demonstrated that SCr rises too late to facilitate early diagnosis of AKI; creatinine elevation is detected after 48 h of ischemic insult (Parikh et al, 2006).

It is known that early initiation of treatment substantially improves the prognosis for patients with AKI. Therefore, the development of novel, sensitive renal biomarkers is crucial for the identification of new therapeutic strategies for AKI; such biomarkers will facilitate early treatment and monitoring of the disease course (Yamamoto et al, 2007). Ideally, a sensitive biomarker for AKI should comprise the following characteristics: easy detection, non-invasive and capable of detecting AKI early in the clinical course. Because acute tubular necrosis (ATN), which is characterized by loss of brush border and polarity in the tubular epithelium with necrosis and apoptosis as well as cell tubular detachment (Devarajan, 2006; Liu & Brakeman, 2008; Price et al, 2009), is a common feature of most AKI, a good biomarker should also possess the ability to predict the extent of tubular injury. The detection of the extent of insult would identify those patients with severe tubular damage and who could be at risk for developing end stage chronic kidney disease. Consequently, a good biomarker could also be used to identify patients that will require subsequent follow-up to decrease or slow the progression of chronic renal failure. In addition to early diagnosis and prognosis, it would also be desirable to identify biomarkers capable of discerning AKI subtypes, identifying etiologies, predicting clinical outcomes, allowing for risk stratification and monitoring the response to interventions (Coca & Parikh, 2008).

It is well known that, during AKI, several mechanisms are activated to compensate for the resultant cell injury; one of these compensatory mechanisms is the up-regulation of heat shock proteins (Hsp) (Csermely et al, 2007; Ritossa, 1962), which help to restore cell homeostasis. These proteins, which have molecular weights ranging from 10 to 150 kDa (Lindquist & Craig, 1988), are encoded by different genes. The Hsp70 subfamily is composed of four isoforms: Hsc70, the inducible isoform Hsp72, mHsp75 and Grp78. Hsp72 is expressed in response to cell stress, and its induction can be as great as 15% of the total cell protein (Fan et al, 2003). Several studies have shown that Hsp72 is up-regulated in damaged tubules after ischemic and toxic kidney injury (Hernadez-Pando et al, 1995; Kelly, 2002; Kelly et al, 2001; Molinas et al, 2010; Mueller et al, 2003; Turman & Rosenfeld, 1999; Zhipeng et al, 2006). Given that Hsp72 is induced in renal tubules during AKI and that proximal tubular detachment is projected to the urinary space, we reasoned that the urinary Hsp72 level could serve as an early biomarker to detect, monitor and/or stratify AKI. The performance of Hsp72 as a sensitive biomarker to detect different degrees of renal injury and recovery was corroborated by using histopathological analysis as a benchmark of kidney damage. Here, we provide evidence that Hsp72 is an early and sensitive biomarker of AKI in both rats subjected to I/R and in humans with clinical AKI.

RESULTS

Different degrees of renal injury were induced in five groups of rats that underwent various periods of bilateral renal ischemia (10 to 60 min); all rats were studied after 24 h of reperfusion. Figure 1 shows the renal function parameters in the six groups studied together with the quantification of two classic tubular injury markers. Although increases in SCr were only significant after 30 min of bilateral ischemia (Fig 1A), all rats that underwent I/R exhibited renal dysfunction characterized by gradual reduction in creatinine clearance (Fig 1B) and renal plasma flow (Fig 1C). These alterations were not associated with changes in mean arterial pressure (MAP) (Fig 1D). As expected, the worst renal dysfunction was observed in the animals subjected to 60 min of bilateral ischemia. Tubular injury induced by different periods of ischemia was assessed by the elevation of urinary *N*-acetyl-β-D-glucosaminidase (NAG) and proteinuria. Statistical differences in NAG were seen only after 30 min of ischemia, suggesting that NAG is not adequately sensitive to detect slight or mild renal injury.

Tubular injury was also detected by light microscopy, the gold standard in evaluating acute renal injury. The left panels of Fig 2 show representative images of kidney sections from rats subjected to different periods of ischemia, and the right panels show quantified cast numbers and the percentage of injured tubular area quantified by morphometry. Tubular histopathology induced by I/R was characterized by brush border loss, lumen dilatation or collapse and cellular detachment from tubular basement membranes (Fig 2A–F). Thus, a proportional increase in tubular injury correlates to a longer period of induced renal ischemia. After 24 h of reperfusion, the smallest degree of tubular injury was observed in rats that underwent 10 min of bilateral ischemia, and the worst injury was observed in rats subjected to 60 min of ischemia (Fig 2 G–H). Therefore, progressive increases in tubular damage are proportional to the ischemia period provoked.

I/R induced renal Hsp72 up-regulation

To evaluate if Hsp72 is proportionally induced with different degrees of ischemic injury, messenger RNA (mRNA) and protein levels were detected in the renal cortex from rats subjected to different periods of ischemia. As shown in Fig 3A, after 24 h of reperfusion, Hsp72 mRNA levels were significantly and progressively increased following 10 min of bilateral ischemia. These findings were reflected at protein level, as is shown in Fig 3B. Renal injury induced by different periods of renal ischemia was associated with a gradual and significant increase in Hsp72 expression, compared with almost undetectable levels in sham-operated rats. The greatest expression of Hsp72 was observed in the group with severe tubular injury, around 30-fold greater compared to control levels. These results show that Hsp72 is gradually increased relative to the intensity of induced renal injury.

Urinary Hsp72 levels as a biomarker of AKI

Consequently, we addressed whether Hsp72 could be detected in the urine of animals that suffered from AKI. First, Hsp72

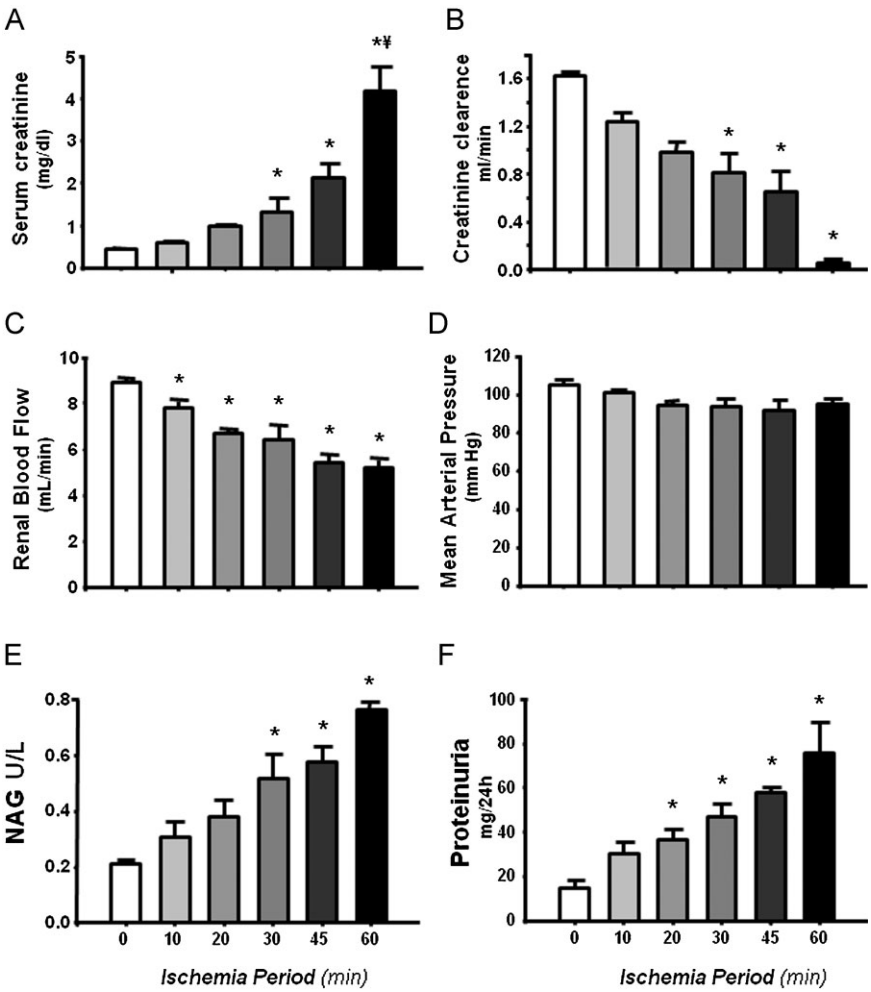

Figure 1. Renal functional parameters in rats underwent which different periods of bilateral renal ischemia (10, 20, 30, 45, and 60 min) and 24 h of reperfusion compared to sham-operated rats (white bars).

A. Serum creatinine levels.
B. Creatinine clearance.
C. Renal blood flow.
D. Mean arterial pressure.
E. Urinary NAG excretion.
F. Protein excretion.

$n = 6$, $^{*}p < 0.05$ *versus* sham-operated rats and $^{¥}p < 0.05$ *versus* 45 min I/R group.

mRNA levels were analyzed in collected urine samples of the different groups studied. As shown in Fig 4A, Hsp72 mRNA levels were increased following 10 min of ischemia compared to the control group, and the incremental increase in Hsp72 was progressively enhanced relative to the duration of ischemia. When these values were compared to the number of casts, a significant correlation was found ($r^2 = 0.72$ and $p < 0.0001$, data not shown). Similar results were observed when Hsp72 mRNA levels and tubular affected area were correlated, as is shown in Fig 4B ($r^2 = 0.82$ and $p < 0.0001$).

Urinary protein levels of Hsp72 were assessed by two immunoassays: enzyme-linked immunosorbent assay (ELISA) and Western blot analysis. The urinary determination of Hsp72 by ELISA is shown in Fig 4C and revealed that this protein can be detected in urine samples and that it is an excellent marker of acute renal injury as it is capable of differentiating scant (since 10 min), moderate (20 and 30 min) and severe renal injury (45 and 60 min of ischemia). Thus, Hsp72 correlates with the extent of renal injury induced by different periods of ischemia. The amount of Hsp72 detected was the greatest in the group that underwent 60 min of ischemia; it increased by 23-fold compared to the control group. As demonstrated in Fig 4D, the progressive urinary elevation of Hsp72 correlated with the intensity of renal injury, as measured by tubular injured area, $r^2 = 0.62$ ($p < 0.0001$). Similar results, but with a greater sensitivity, were observed when urinary Hsp72 protein levels were detected by Western blot. The upper panel of Fig 4E shows Western blots of the urine from four different rats from each group studied. Hsp72 was undetectable in the urine of sham-operated rats; in contrast, Hsp72 was progressively increased in the urine from rats that suffered increasing periods of ischemia. As shown in Fig 4E, Hsp72 protein levels, assessed by Western blot, were significantly enhanced after 10 min of ischemia and increased in animals subjected to longer ischemia periods. However, the sensitivity to detect different degrees of renal damage was greater with Western blot analysis than with ELISA. Urinary Hsp72 was 40-fold increased in the group subjected to 10 min of ischemia and 535-fold in the group with severe renal damage (60 min of ischemia) compared to sham-operated rats. As shown in Fig 4F, stronger correlations were found between the amount of Hsp72 in the urine and the % affected tubular area, $r^2 = 0.89$ ($p < 0.0001$). These findings show that Hsp72 is found in the urine of ischemic rats and its urinary detection is adequately sensitive to assess the extent of tubular injury.

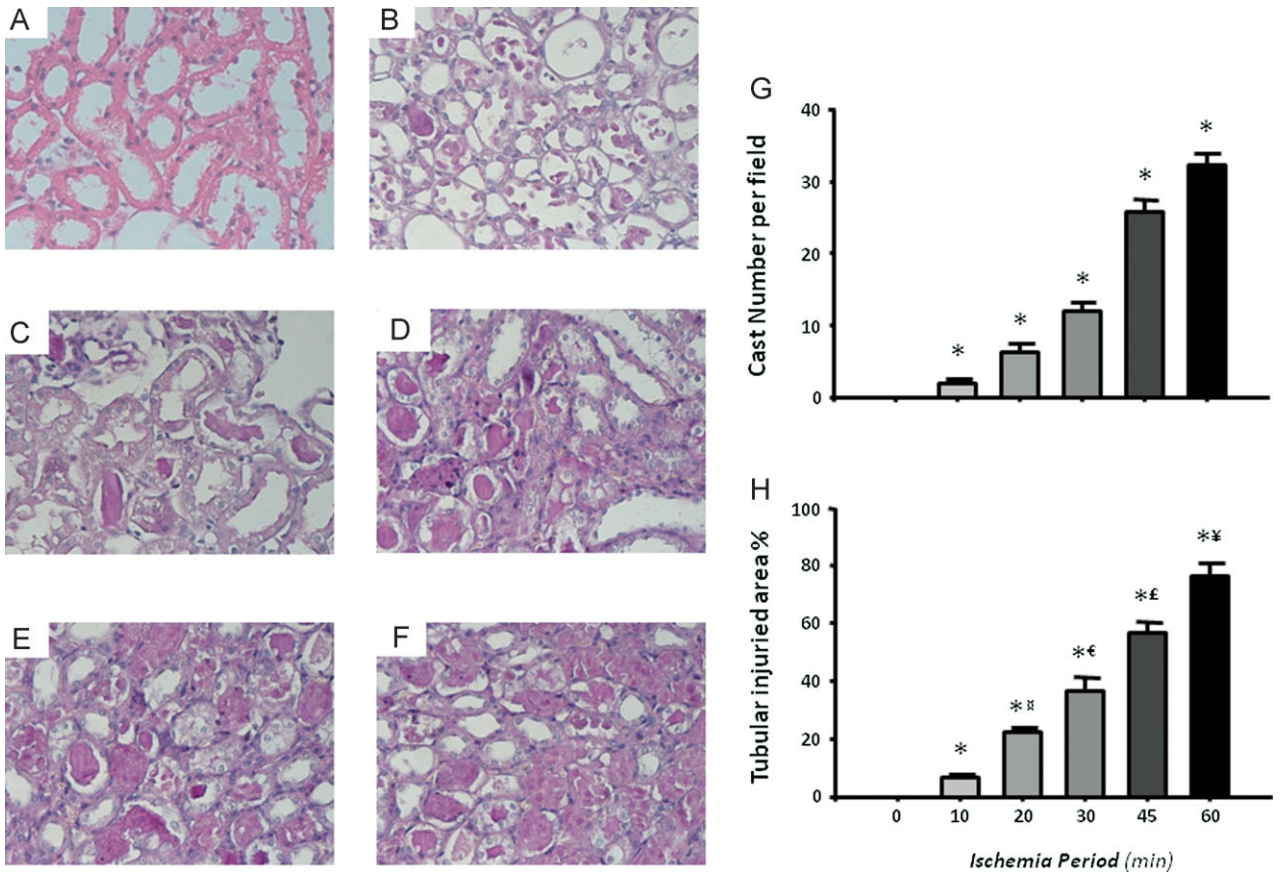

Figure 2. Representative images and morphometry of subcortical histopathological lesions induced by different periods of ischemia and 24 h of reperfusion.

A. Sham-operated rats.
B. 10 min.
C. 20 min.
D. 30 min.
E. 45 min.
F. 60 min.
G. Mean cast number per field.
H. Percentage of tubular affected area.

$^{*}p < 0.05$ *versus* sham-operated rats, $^{¤}p < 0.05$ *versus* 10 min, $^{€}p < 0.05$ *versus* 20 min, $^{£}p < 0.05$ *versus* 30 min and $^{¥}p < 0.05$ *versus* 45 min of ischemia group.

Urinary Hsp72 as an early biomarker of AKI

To evaluate if Hsp72 could be utilized as an early biomarker of AKI and if it is adequately sensitive to detect tubular recovery after an ischemic insult, urinary Hsp72 concentrations were assessed in animals subjected to 30 min of bilateral ischemia followed by 3–120 h of reperfusion. Figure 5 shows representative microphotographs from kidneys after reperfusion periods of 3, 6, 9, 12, 18, 24, 48, 72 and 120 h (Fig 5A–J). In the right panels, quantification of injured areas and casts number per field are shown. As the morphometric analysis shows in Fig 5K, there was a progressive increment in tubular injury, reaching the maximal degree after 18 h of reperfusion, at which point more than 50% of the tubular area was damaged. After this point, there was progressive tubular recovery until 120 h of reperfusion, at which point only 12% of tubular area was injured. The same pattern was observed when casts number were quantified, as depicted in Fig 5L.

In Fig 6A (urinary detection of Hsp72 by ELISA), a significant elevation was detected from 3 h after reperfusion. Similarly to histological injury, the greatest urinary Hsp72 was found after 18 h and return to basal values after 96 h of reperfusión. Again a significant correlation between urinary Hsp72 and % of tubular injured area was observed, $r^2 = 0.65$ ($p < 0.0001$). Insets in the top of Fig 6C show Western blots from three rats of each group; densitometric analysis is shown below. Urinary Hsp72 was almost undetectable in sham-operated rats; in contrast, there was a significant increase in Hsp72 in groups subjected to renal ischemia followed by 3 h of reperfusion and a progressive increase in the amount of Hsp72 detected in the urine was observed relative to the reperfusion period, peaking at 18 h of reperfusion with a

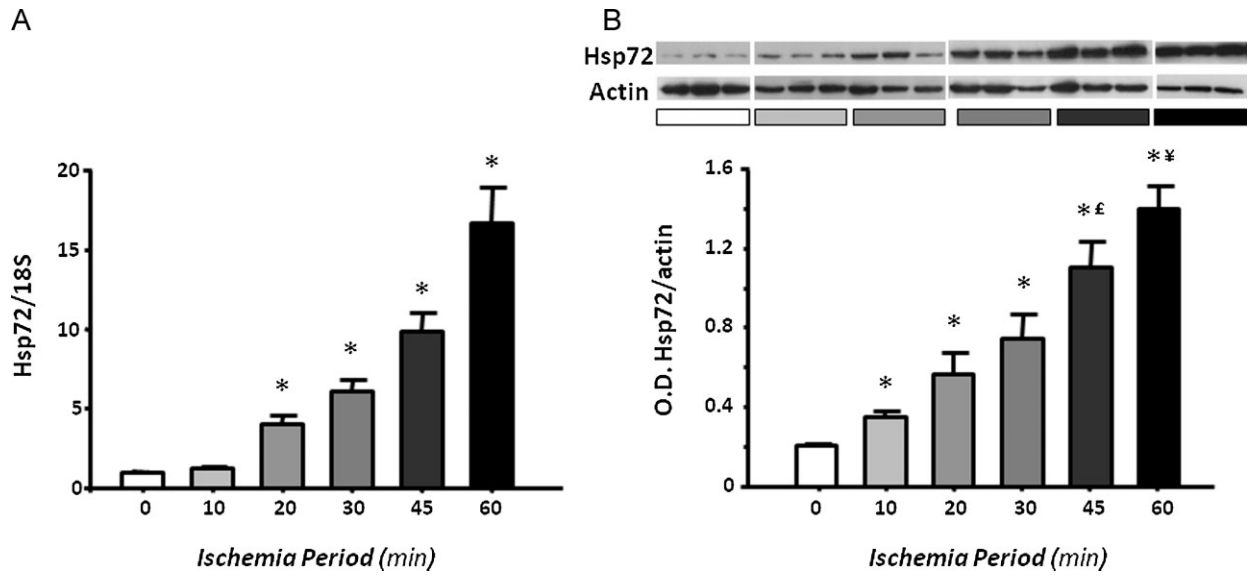

Figure 3. Renal Hsp72 expression in rats subjected to different periods of ischemia.

A. Total RNA was individually extracted from the renal cortex of all studied groups ($n = 5$) and Hsp72 mRNA levels were determined by real time RT-PCR.

B. Renal cortex proteins were individually extracted from three rats of each group, and Hsp72 protein levels were assessed by western blot. Upper inset shows a representative image of the autoradiography of the membrane and the lower graph depicts densitometric analyses of the ratio of Hsp72 to β-actin. $^{*}p < 0.05$ *versus* sham-operated rats, $^{£}p < 0.05$ *versus* 30 min and $^{¥}p < 0.05$ *versus* 45 min of ischemia group.

subsequent decrease in excretion of this protein. Intriguingly, there was a significant correlation between urinary Hsp72 and the % area of tubular injury, $r^2 = 0.55$ ($p < 0.0001$) as depicted in Fig 6D. A better correlation was found between Hsp72 and cast formation, $r^2 = 0.73$ ($p < 0.0001$, data not shown). These results demonstrate that Hsp72 is an early biomarker to detect AKI and suggest that the amount of Hsp72 detected in the urine might reveal the state of tubular injury and recovery.

Kim-1, NGAL, IL-18 as biomarkers for stratifying and early detecting AKI

The performance of the kidney injury molecule 1 (Kim-1), neutrophil gelatinase-associated lipocalin (NGAL) and Interleukin 18 (IL-18) for stratification and early detection of AKI was also investigated to compare it with performance of Hsp72. As shown in figure Fig 7A, urinary Kim-1 levels significantly increased after 20 min of ischemia, and these values reached the maximum increment at 30 min; thus Kim-1 was unable to differentiate greater renal injury induced by 45 and 60 min of ischemia. As a result, a lower correlation between percent of tubular injured area and Kim-1 levels was found ($r^2 = 0.46$). NGAL levels progressively increased with the extent of renal injury induced by different periods of ischemia, $r^2 = 0.61$ ($p < 0.001$) as shown in Fig 7B. However, statistical differences between different periods of ischemia were not found. Thus, NGAL was not as good a biomarker as Hsp72 to predict different degrees of renal damage. Similarly to Hsp72 and NGAL, IL-18 increased proportionally to the renal injury induced from 20 min of ischemia ($r^2 = 0.59$, $p < 0.001$), as depicted in Fig 7C.

The usefulness of these biomarkers for early diagnosis of AKI was also assessed. Figure 7D shows the urinary Kim-1 values from rats exposed to different periods of reperfusion. A significant elevation of Kim-1 was observed after 9 h of reperfusion, reaching the maximal value after 48 h. As a result, a low correlation between tubular affected area and urinary Kim-1 levels ($r^2 = 0.27$) was found. In the case of urinary NGAL, a significant elevation was found after 3 h of reperfusion; however, NGAL levels reached the maximum peak at 6 h and did not reflect the greater renal injury that is observed after 18 h. As a result, a lower correlation between urinary NGAL levels and tubular affected area was observed, $r^2 = 0.48$ *versus* $r^2 = 0.65$ observed with Hsp72. When IL-18 was assessed, a significant increase was observed after 6 h and levels remained elevated after 24 h of reperfusion. As a result, the correlation between tubular affected area and urinary IL-18 was $r^2 = 0.51$, $p < 0.001$ (Fig 7F), which was similar to NGAL ($r^2 = 0.48$), but lower than Hsp72 ($r^2 = 0.65$).

Urinary Hsp72 levels as a monitor of a renoprotective intervention in AKI

Because we previously reported that aldosterone blockade is a helpful treatment to prevent renal injury induced by I/R (Mejia-Vilet et al, 2007; Ramirez et al, 2009), we assessed if this renoprotective effect could be reflected by the prevention of Hsp72 elevation. Figure 8A and B shows the SCr and creatinine clearance in two groups of rats subjected to ischemia and 24 h of reperfusion without treatment (I/R) and pre-treated with spironolactone 3 days before I/R (I/R + Sp). Spironolactone administration prevented renal dysfunction. This renoprotective effect was associated with a significant reduction in urinary Hsp72 levels detected by ELISA and Western blot, as shown in Fig 8C and D, respectively. In order to evaluate if Hsp72 might allow to monitor different degrees of renoprotection in the

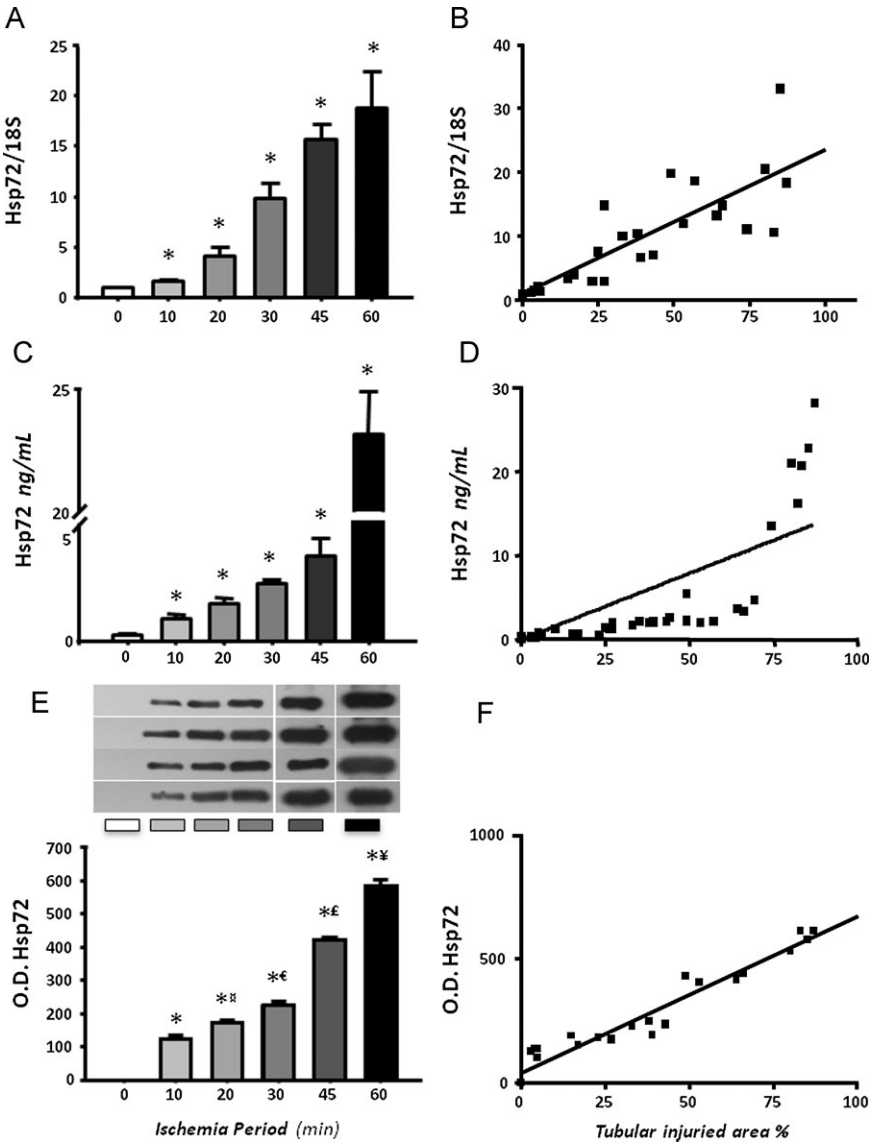

Figure 4. Urinary Hsp72 mRNA and protein levels from rats subjected to different periods of ischemia.

A. Total RNA was individually extracted from the urine of six rats per group and Hsp72 mRNA levels were determined by real time RT-PCR.

B. Relationship between mRNA levels and tubular affected area.

C. Urinary Hsp72 levels assessed by ELISA.

D. Relationship between urinary Hsp72 levels and the % of tubular affected area.

E. Urinary Hsp72 levels assessed by WB analysis from four rats of each group.

F. Relationship between urinary Hsp72 levels detected by WB and tubular injured area. $^{*}p < 0.05$ *versus* sham-operated rats, $^{¤}p < 0.05$ *versus* 10 min, $^{€}p < 0.05$ *versus* 20 min, $^{£}p < 0.05$ *versus* 30 min and $^{¥}p < 0.05$ *versus* 45 min of ischemia group.

absence of creatinine elevation, different groups with I/R were pre-treated with lower doses of spironolactone. As is shown in Fig 8E, rats pre-treated with spironolactone at 10 and 5 mg/kg exhibited normal values of SCr that contrast with the 2.5 mg/kg dose, in which the values were similar to untreated I/R group. Interestingly, urinary Hsp72 levels were significantly increased from 10 mg/kg of spironolactone and progressively enhanced when the lower doses of were administrated, as is depicted in Fig 8F. These findings suggest that the lower the dose of spironolactone, the lower the renoprotection. This can be efficiently detected by urinary Hsp72.

Urinary Hsp72 levels in healthy kidney donors and patients with AKI

To determine whether Hsp72 is a sensitive biomarker to detect AKI in humans, the levels of this protein were assessed by Western blot in the urine of normal subjects and compared to those patients who developed AKI in the ICU of our institution. AKI was defined as an increase in SCr by at least 0.3 mg/dL, or urine output $\leq$0.5 ml/kg/h over 6 h. The Supplementary Table 1 shows general characteristics and renal function of five healthy kidney donors and nine patients with septic AKI. AKI patients included five females and four males aged between 24 and 84 years. At admission to the ICU, all patients exhibited normal creatinine levels; however, increases in SCr from 0.55 ± 0.05 to 2.30 ± 0.52 mg/dl were subsequently observed ($p = 0.004$). Urinary Hsp72 levels are depicted in Fig 9A. In the urine of healthy kidney donors, Hsp72 was almost undetectable (3.4 ± 0.7 arbitrary units), whereas urinary Hsp72 levels significantly increased by 17.3-fold in patients with clinical AKI (58.3 ± 8.5 arbitrary units). These results were confirmed by ELISA. The basal levels of urinary Hsp72 from healthy living donors were 0.22 ± 0.07, contrasting with the values in patients diagnosed with AKI of 4.90 ± 1.5 ng/ml (22-fold increase). Of

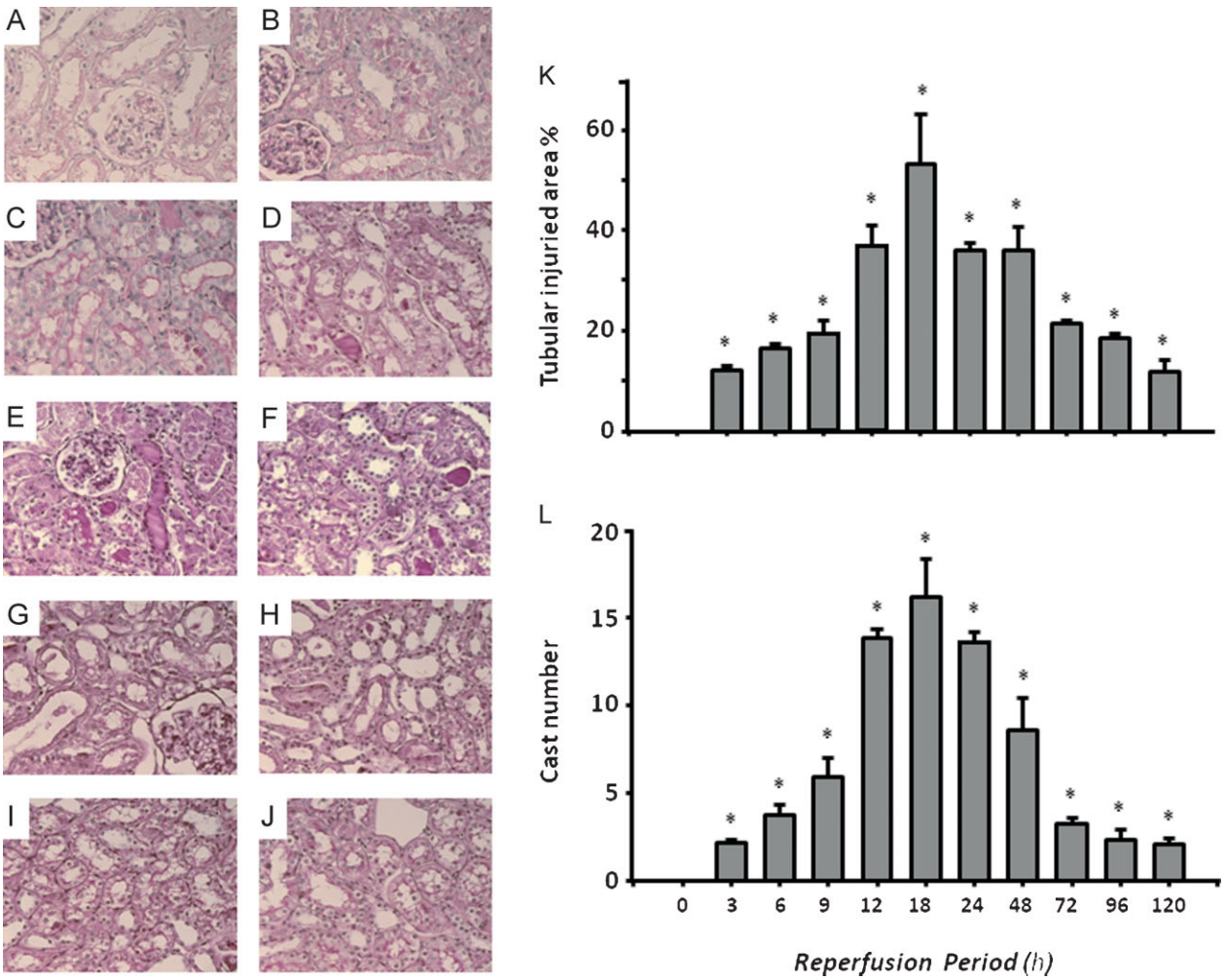

Figure 5. Representative images and morphometry of subcortical histopathological lesions induced by 30 min of ischemia and different periods of reperfusion.

A. 3 h, **B**. 6 h, **C**. 9 h, **D**. 12 h, **E**. 18 h, **F**. 24 h, **G**. 48 h, **H**. 72 h, **I**. 96 h and **J**. 120 h of reperfusion.

K. Morphometric quantification of affected tubular area.

L. Mean cast number per field $^{*}p < 0.05$ *versus* sham-operated rats.

note, two patients diagnosed with AKI died during hospitalization; these patients exhibited greater urinary values of Hsp72 as assessed by either Western blot or ELISA.

To identify if Hsp72 is an early biomarker to detect AKI in humans, daily urine samples were collected from patients who were admitted to the ICU exhibited and respiratory failure (mechanical ventilation) complicated with other organ failure. These patients had normal renal function at the admission. Five patients that developed AKI and five patients with no evidence of clinical AKI were included. Urine samples taken every day were analyzed to investigate if an elevation of Hsp72 could be detected before AKI criteria was fulfilled. Figure 9C and 9D show the mean daily serum creatinine and urine output from patients with or without AKI. Day 0 means the day at which AKI was diagnosed based on AKI criteria. Figure 9E depicts Western blots showing the daily urinary Hsp72 levels from the patients diagnosed with AKI, compared with the Western blots from patients without AKI (Fig 9F). The basal levels of Hsp72 were minimal in patients without AKI and three days before AKI was diagnosed in AKI patients. In agreement with our experimental studies, one or two days before AKI diagnosis, there was a significant increase in urinary Hsp72 levels, suggesting that, indeed, Hsp72 can be an early marker of AKI in humans.

DISCUSSION

In this study, we found that urinary Hsp72 is a reliable biomarker for the early detection of AKI. This novel biomarker was adequately sensitive for stratifying different degrees of tubular injury and recovery, as well as for monitoring a renoprotective intervention in an experimental rat model of AKI.

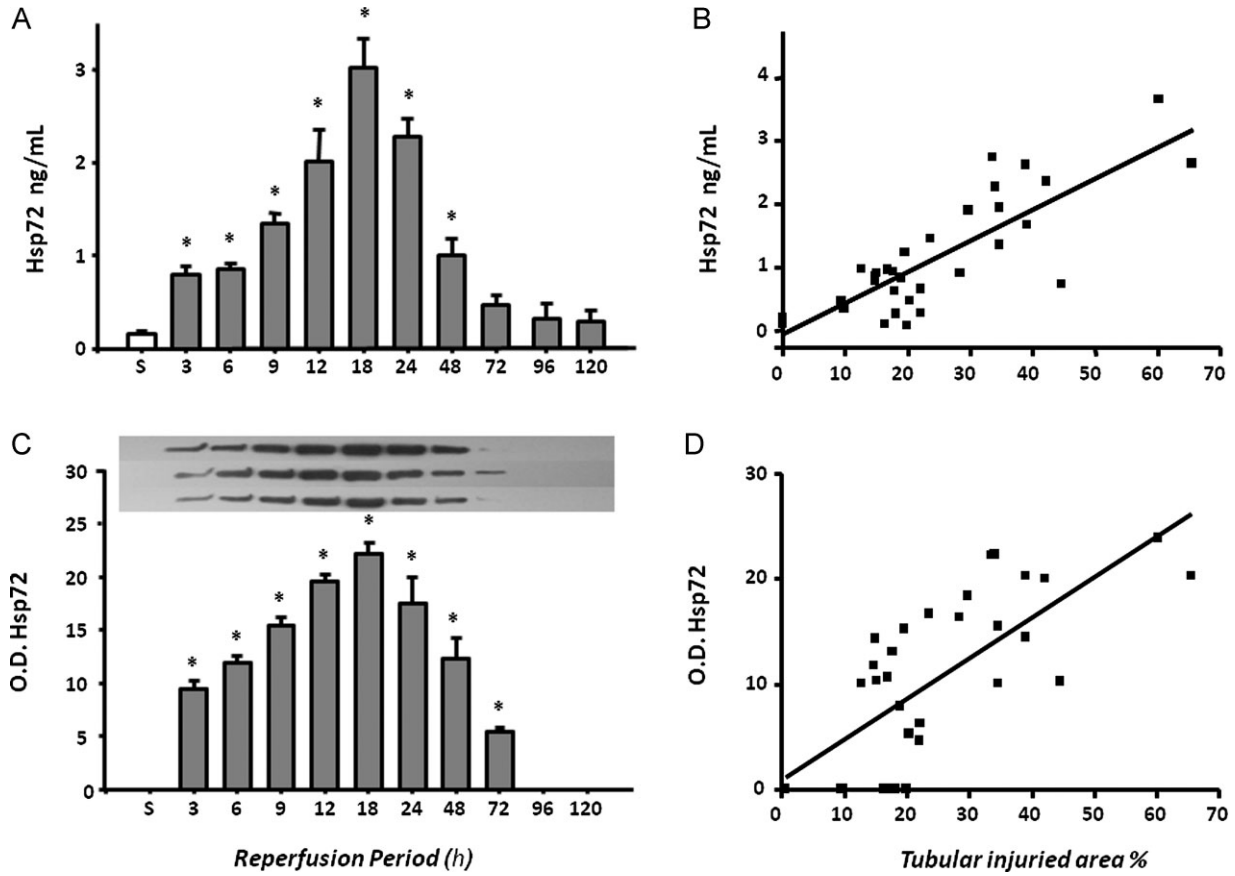

Figure 6. Urinary Hsp72 levels in rats which underwent to 30 min of ischemia with different periods of reperfusion.

A. Urinary Hsp72 levels assessed by ELISA.

B. Relationship between urinary Hsp72 and % of tubular damaged area.

C. Urinary Hp72 protein levels determined by Western blot.

D. Relationship between Hsp72 and % of tubular injured area.

$n = 3$ per period of reperfusion, $^{*}p < 0.05$ *versus* sham operated rats.

In addition, these experimental findings were corroborated in humans who suffered from AKI. Thus, a significant increase in urinary Hsp72 was observed in patients diagnosed with AKI even 48 h before SCr elevation occurred, revealing that this Hsp is a promising biomarker for both early detection and stratification of AKI.

Because Hsp72 expression could increase during stress conditions to as much as 15% of total cellular proteins (Fan et al, 2003) and tubular detachment is proportional to the extent of renal injury, we reasoned that urinary Hsp72 levels could be used to stratify renal injury induced by ischemic insult. First, we observed that, after 24 h of reperfusion, kidney Hsp72 expression was proportionally increased in response to the ischemic insult provoked by different periods of ischemia. Thus, Hsp72 increased significantly following slight injury induced by 10 min of ischemia and increased progressively more with mild to severe ischemia, suggesting that the induction of this protein in the kidney is proportional to the degree of the resulting damage. Furthermore, the same pattern was found in the urine of these animals when Hsp72 was detected both at mRNA and at protein levels. Significant increase in urinary Hsp72 was observed in rats that underwent 10 min of ischemia and greater amounts were found in rats following 60 min of ischemia. In contrast, increase in SCr, NAG and urinary protein excretion reached significance after 30 min of ischemia.

In this study, we performed a blindly morphometric quantification of the tubular affected area and the casts number per field. Thus, when the amount of Hsp72 was interrelated with the tubular injured area affected by different periods of ischemia, a significant correlation was found at mRNA and protein levels. These data show that Hsp72 seems to be a sensitive biomarker to stratify the extent of the renal insult.

To investigate if urinary Hsp72 levels could detect early stages of AKI, different groups of rats were subjected to renal ischemia of 30 min and were studied at different periods of reperfusion. Histopathologic analysis showed that the greatest tubular injury was found after 18 h of reperfusion, and the extent was progressively reduced with longer periods of reperfusion due to

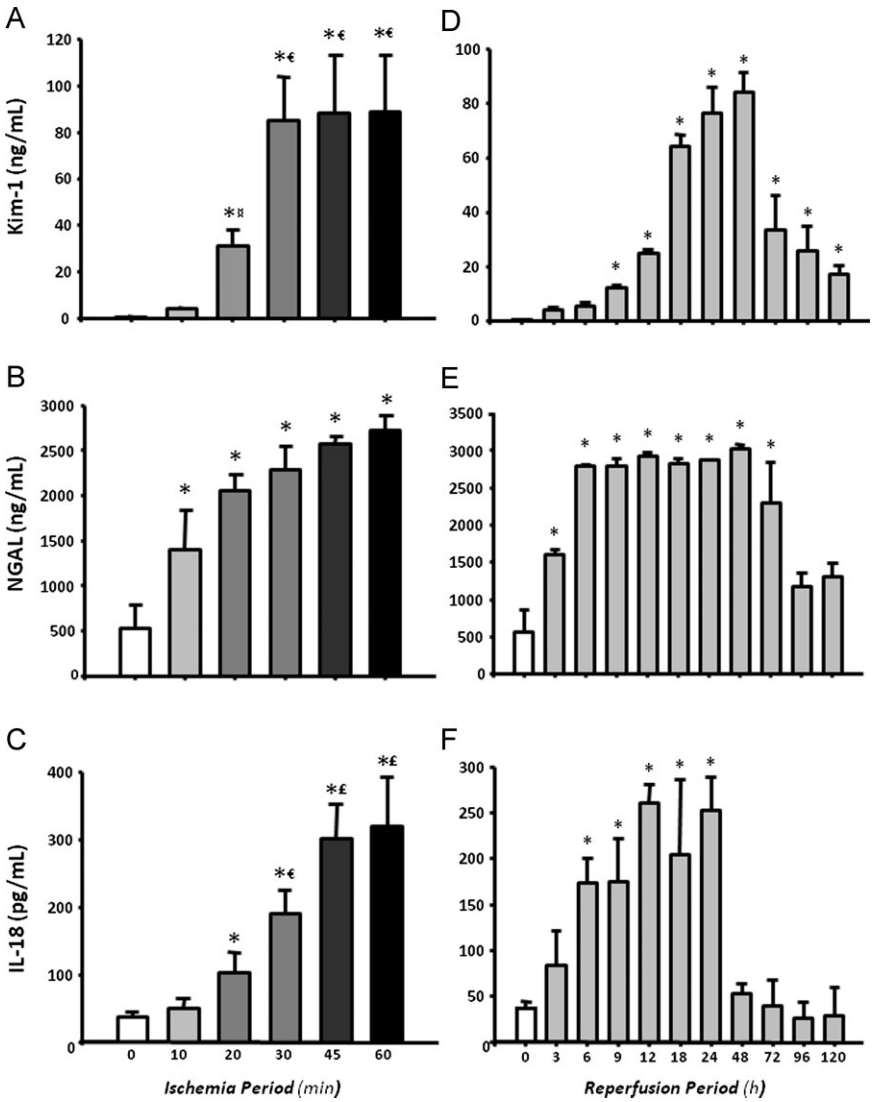

Figure 7. Urinary levels of Kim-1, NGAL and IL-18 in rats which underwent different periods of ischemia and reperfusion ($n = 6$).

A, B, C. Urinary levels of Kim-1, NGAL, and IL-18 in different degrees of renal injury induced by increasing periods of ischemia (10, 20, 30, 45 and 60 min), respectively.

D, E, F. Urinary concentrations of Kim-1, NGAL and IL-18 after several times of reperfusion (3, 6, 9, 12, 18, 24, 48, 72, 96 and 120 h), respectively.

$^{¤}p < 0.05$ *versus* 10 min, $^{€}p < 0.05$ *versus* 20-min, $^{£}p < 0.05$ *versus* 30 min and $^{¥}p < 0.05$ *versus* 45 min of ischemia group.

the concomitant tubular recovery observed after 72 h. Interestingly, the amount of urinary Hsp72 detected also reflected the extent of tubular epithelium injury during different periods of reperfusion and the regeneration of tubular epithelium. Urinary Hsp72 increased significantly after 3 h and continually rose until 18 h of reperfusion. After this time, a progressive reduction was detected until 120 h of reperfusion, at which point Hsp72 returned to basal levels. The pattern of urinary Hsp72 expression observed with different periods of reperfusion significantly correlated with the tubular injury quantified by morphometry. This finding suggests that this protein was not only able to detect early AKI but that it could also reflect the tubular recovery processes that occur after the epithelium is exposed following ischemic/reperfusion insult.

Recently, a sequence of studies which evaluated seven different biomarkers of glomerular or tubular injury induced by different nephrotoxic drugs in the rat was reported. These biomarkers included urinary total protein, cystatin C, α2-microglobulin, Kim-1, urinary trefoil factor 3 (TFF3), clusterin (CLU) and albumin urinary excretion. Renal histopathology was used as the benchmark or gold standard to define renal injury (Dieterle et al, 2010a; Vaidya et al, 2010; Yu et al, 2010). As was discussed by the FDA-EMEA and Predictive Safety Testing Consortium, in these rat toxicology studies, Kim-1, CLU, urinary albumin excretion and TFF3 were helpful to diagnose drug-induced acute kidney tubular injury in the rat and were superior to the traditional markers such as SCr and blood urea nitrogen (BUN), whereas urinary total protein, cystatin C, and α2-microglobulin were useful to identify acute drug-induced glomerular damage or impairment of kidney tubular reabsorption (Dieterle et al, 2010b). This consortium emphasized, however, that these findings must wait validation in order to be employed for clinical practice. The renal injury induced by I/R, as the most common cause of AKI in ICUs and during cardiovascular surgery, was not addressed in most of these studies (Dieterle et al, 2010; Vaidya et al, 2010; Yu et al, 2010).

Regarding AKI induced by renal ischemia in animals and humans, several urinary biomarkers have been identified over

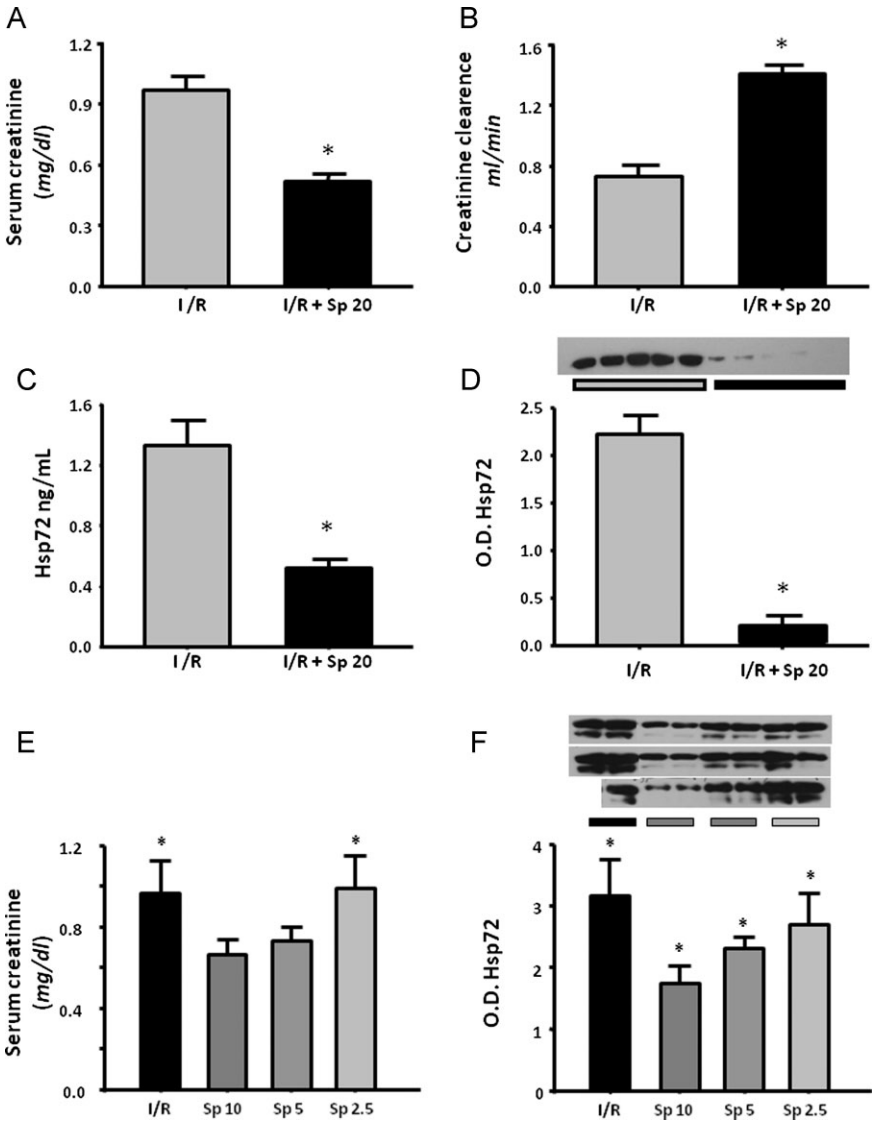

Figure 8. Urinary Hsp72 as a biomarker of renoprotection conferred by spironolactone in I/R rats ($n = 5$).

A. Serum creatinine in I/R group without treatment (gray bar) and rats pre-treated with spironolactone (black bar),

B. Creatinine clearance,

C. Urinary Hsp72 assessed by ELISA and

D. By WB analysis, the inset shows the individual analysis from five individual urines.

E. Serum creatinine in I/R group and in rats pre-treated with lower doses of spironolactone (10, 5 and 2.5 mg/kg) and

F. WB analysis of Hsp72 in rats pre-treated with lower doses of spironolactone, the superior inset shows the individual Hsp72 level from five different animals. $^{*}p < 0.05$ *versus* I/R group.

the past few years. These biomarkers include the following: NAG (Tsutsumi & Neckers, 2007), neutrophil gelatinase associated lipocalin (NGAL) (McIlroy et al, 2010; Mishra et al, 2003, 2005), Kim-1 (Han et al, 2009; Vaidya et al, 2006, 2009), cystatin C (Nejat et al, 2010; Uchida & Gotoh, 2002), interleukin-18 (IL-18) (Melnikov et al, 2001; Parikh et al, 2005, 2006), hepatocyte growth factor (HGF) (Taman et al, 1997) and liver fatty acid binding protein (L-FABP) (Ferguson et al, 2010; Negishi et al, 2009; Yamamoto et al, 2007). In humans with AKI induced by an ischemic insult, NGAL, NAG and IL-18 have shown to be early biomarkers (Han et al, 2009; Parikh et al, 2006; Wagener et al, 2006), whereas Kim-1 elevation is seen several hours after AKI has occurred and remains elevated along the time (Han et al, 2009). In addition, it is still unknown if these biomarkers individually possess the features that an ideal biomarker should have, such as the ability to detect AKI early in the disease course, to stratify different degrees of renal injury, to identify tubular recovery, to predict patients at risk of developing end stage renal disease (ESRD) and those at increased risk of death. In fact, it has been proposed that a panel of biomarkers might be a powerful tool to diagnose AKI before SCr elevation occurs; however, this strategy represents greater effort and cost (Han et al, 2009; Liangos et al, 2007; Vaidya et al, 2008). In this study, we compared the performance of Kim-1, NGAL and IL-18 for stratifying and early detecting AKI compared to Hsp72. As was shown before (Han et al, 2009), although Kim-1 differentiated low and moderate renal injury, it was unable to stratify severe renal injury degrees (Fig 7A). This is supported by the low correlation between tubular affected area and urinary Kim-1 levels ($r^2 = 0.27$). In addition, Kim-1 did not perform well as an early biomarker, since a significant elevation of Kim-1 was observed only after 9 h of reperfusion. With respect to NGAL, this biomarker increased progressively with the extent of renal injury induced by different periods of ischemia, but statistical differences between different periods of ischemia were not found. Although NGAL was an early

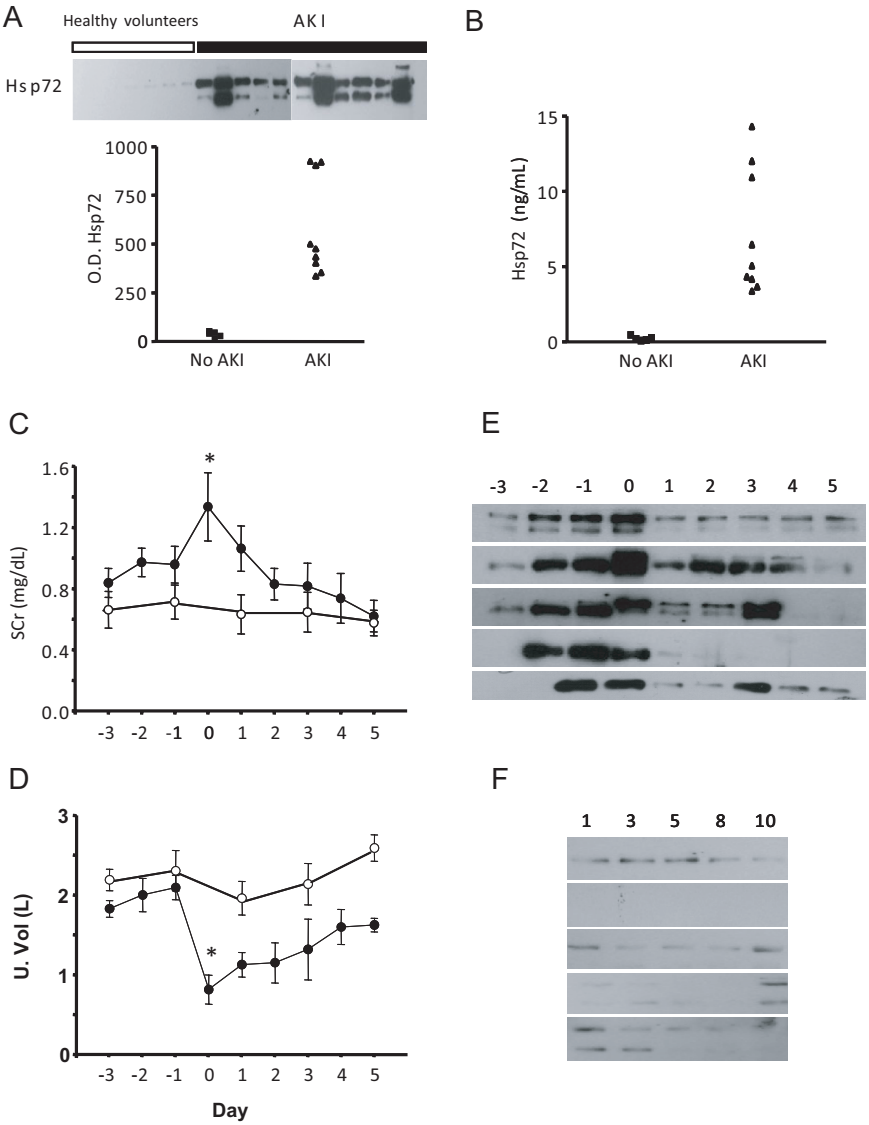

Figure 9. Urinary Hsp72 levels as a biomarker of AKI in humans.

A, B. Hsp72 levels assessed by Western blot and ELISA, respectively, in five healthy kidney donors (■) and nine patients that were diagnosed with AKI (▲).

C. Serum creatinine from five patients with no evidence of AKI (○) or in five patients with AKI diagnosed with AKIN criteria (●).

D. Urine output from five patients with no evidence of AKI (○) or in five patients with AKI diagnosed with AKIN criteria (●).

E. Daily urinary Hsp72 levels from patients with diagnosed AKI.

F. Daily urinary Hsp72 levels in patients without AKI.

The samples were collected during three days before and 5 days after AKI was diagnosed. $^{*}p < 0.05$ *versus* 3 days before AKI.

biomarker as Hsp72, it reached the maximum peak at 6 h and thus did not reflect the greater renal injury that is observed after 18 h of reperfusion. In the case of IL-18, it showed a similar pattern to Hsp72 for stratifying renal injury induced by different periods of ischemia; however, it was unable to detect slight renal injury induced by 10 min of ischemia. In addition, IL-18 was not useful for early AKI detection.

It has been reported that a sensitive biomarker must sense if a therapeutic strategy could reduce AKI (Yamamoto et al, 2007). In this regard, we have previously shown that mineralocorticoid receptor blockade is an effective intervention to prevent renal injury induced by I/R (Mejia-Vilet et al, 2007; Ramirez et al, 2009). Therefore, in this study, we pre-treated rats with spironolactone 3 days before induction of ischemia. Then, renal function and urinary Hsp72 were detected. In untreated rats, renal function was significantly reduced, and a significant rise in urinary Hsp72 was observed. The renoprotection conferred by spironolactone was associated with the prevention of this Hsp72 increase, and this effect was consistent with the preservation of tubular architecture, as we previously reported (Mejia-Vilet et al, 2007; Ramirez et al, 2009). In this study, we also evaluated urinary Hsp72 performance for monitoring different degrees of renoprotection. For this purpose, rats subjected to I/R were pre-treated with different doses of spironolactone. The lower dose employed (2.5 mg/kg) was not able to protect the kidneys from ischemic injury, as demonstrated by a similar increase in SCr in rats treated with this dose as compared to those untreated (Fig 8E). In contrast, some degree of protection was observed with administration of 5 or 10 mg/kg. Consistent with urinary Hsp72 being a good biomarker, the lower the renoprotection, the higher the Hsp72 amount in urine. These data suggest that urinary Hsp72 is a helpful tool for monitoring the effectiveness of a pharmacological intervention to prevent ischemic insult.

Acute kidney injury remains a common syndrome in hospitalized patients and has consistently been associated

with increased morbidity and mortality. However, advances in reducing this complication have long been hindered by the lack of early and sensitive biomarkers. In spite of creatinine limitations, current AKIN and RIFLE classifications for diagnosing AKI are based on the elevation of SCr or urine output reduction. In this study, we included patients that developed AKI and were diagnosed by the AKIN classification. Once the diagnosis was made, a urine sample was taken to evaluate urinary Hsp72 levels to compare with healthy living donors. To determine Hsp72 concentration, the urine sample was analyzed by Western blot analysis and ELISA. Hsp72 levels were almost undetectable in healthy subjects; in contrast, patients with clinical AKI exhibited an abrupt increase in this protein. The variability in the AKI patients observed might result from different degrees and extension of the renal injury. In this regard, two of three patients that exhibited high urinary Hsp72 died during their hospitalization, suggesting that this protein could also serve as a biomarker of AKI-associated death. However, more studies are necessary to evaluate this issue.

To evaluate the potential of urinary Hsp72 as an early biomarker in humans, daily urine samples from ten patients with normal renal function at the admission to ICU in severe conditions (mechanical ventilation and other organ failure) were included. In accord with our experimental data, an increase in urinary Hsp72 was found even two days before AKI criteria were fulfilled (SCr elevation or urine output reduction), suggesting that urinary Hsp72 could be a promising early biomarker of AKI in humans. Most of the biomarkers studies include patients that are expected to develop AKI, such as after cardiovascular surgery or organ transplantation (Han et al, 2009; McIlroy et al, 2010; Mishra et al, 2005; Parikh et al, 2006; Yamamoto et al, 2007), however, in the daily clinical setting, we cannot predict which patients will develop AKI. In this study, urinary Hsp72 had the potential to predict AKI 48 h before AKIN criteria were fulfilled. Further clinical studies will be required to validate its use in multiple cohort studies. In this regard, it has been reported that there are five critical phases in a biomarker development that include: (1) experimental studies that identify proteins that are up-regulated in AKI mice and rat models, (2) development of clinical assays to detect the biomarker in samples from patients with clinical AKI that should be obtained non-invasively, (3) evaluation of the biomarker's ability to detect preclinical disease prior to clinical diagnosis, and (4) phase IV and V studies that involve large-scale biomarker validation (Coca & Parikh, 2008).

In summary, in an experimental model of AKI, our results revealed that Hsp72 possesses most of the specific characteristics of an ideal sensitive biomarker. Hsp72 is an early, non-invasive and easily detected biomarker that can be used to stratify renal injury that correlates with tubular injury and recovery. It also seems to be a tool to monitor the effectiveness of a pharmacological intervention. In addition, the preliminary data that we found in humans support the notion that Hsp72 could be an early predictor of AKI in the clinical setting. Taken together, these results suggest that urinary Hsp72 detection is a promising and sensitive biomarker in a clinical translational context.

MATERIALS AND METHODS

All experiments involving animals were conducted in accordance with the *Guide for the Care and Use of Laboratory Animals* (National Academy Press, Washington, DC, 1996) and were approved by the Animal Care and Use Committee of our Institution. One hundred and five male Wistar rats, weighing 270–300 g, were included in this study and divided into two different experimental protocols. In the first protocol, seventy-two rats were randomly divided into six groups: sham-operated (sham) or subjected to bilateral ischemia of 10, 20, 30, 45 or 60 min. All of these groups were studied after 24 h of reperfusion. One half of each group was used only for the determination of urinary Hsp72 mRNA levels, as is described below. In the second protocol, thirty rats were subjected to 30 min of bilateral ischemia and divided in ten different groups, which differed by reperfusion time: 3, 6, 9, 12, 18, 24, 48, 72, 96 and 120 h. A sham-operated group was also included in this protocol.

Kidney I/R injury animal model

Rats were anesthetized with an intraperitoneal injection of sodium pentobarbital (30 mg/kg), placed on a heating pad to maintain core body temperature at 37°C and monitored with a rectal thermometer. A midline abdominal incision was made, and both kidneys were exposed. Renal pedicles were isolated, and bilateral ischemia was induced by non-traumatic clamps over the pedicles for different times, as we previously described (Mejia-Vilet et al, 2007; Ramirez et al, 2009). Ischemia was verified visually by change in kidney colour. Reperfusion was achieved by release of the clips and confirmed by return of oxygenated blood to the kidney. After reperfusion, the incision was closed in two layers with 3–0 sutures. Sham-operated rats underwent anesthesia, laparotomy and renal pedicle dissection only.

Functional studies

Rats were placed in metabolic cages at 22°C with a 12:12 h light–dark cycle and allowed free access to water. Individual urine samples were collected from all studied rats. For urine ribonucleic acid (RNA) isolation, metabolic cages were previously cleaned with RNAse ZAP (Ambion) and 300 μL of RNAlater (Ambion) added to the urine recipient. In both cases, urine samples were aliquoted and quickly frozen at 80°C until biomarker analysis.

After the reperfusion period, rats were anesthetized with an intraperitoneal injection of sodium pentobarbital (30 mg/kg) and placed on a homoeothermic table. The trachea and femoral arteries were catheterized with polyethylene tubing (PE-240 and PE-50). The rats were maintained under euvolemic conditions by infusing 10 ml of rat plasma per kg of body weight during surgery. MAP was monitored with a pressure transducer (model p23 db, Gould) and recorded on a polygraph (Grass Instruments, Quincy, MA). An ultrasound transit-time flow probe was placed around the left artery and filled with ultrasonic coupling gel (HR Lubricating Jelly, Carter-Wallace, New York, NY) to record renal blood flow. Blood samples were taken at the end of the study. Serum and creatinine concentrations were measured with an autoanalyzer (Technicon RA-1000, Bayer, Tarrytown, NY), and renal creatinine clearance was calculated by the standard formula $C = (U \times V)/P$, where U is the concentration in urine, V is the urine flow rate and P is the serum concentration. Urinary protein excretion was measured by a trichloroacetic acid (TCA) turbidimetric method, and NAG was measured spectrophotometrically.

The paper explained

PROBLEM:

Acute kidney injury is a common and serious complication in critically ill patients, especially in the ICU in both native and transplanted kidneys and may also be associated with long-term chronic kidney disease development. AKI may occur in about 5% of hospitalized patients and up to 40–60% patients in ICU. In addition, over the last decade the incidence of AKI has increased mainly due to population aging and the rising pandemics of obesity, diabetes and hypertension. Despite efforts and advances in new therapeutics, the mortality rate of AKI remains between 40 and 80% and has not been reduced in the last four decades, mainly because current tools used for early AKI detection are not adequately sensitive or specific. Therefore, novel renal early biomarkers indicating tubular injury extent are needed.

RESULTS:

In an experimental model of AKI, we found that Hsp72 possess most of the specific characteristics of an ideal biomarker should have such as: non-invasive, easily detected, to be able to early detect AKI, to stratify renal injury that correlates with tubular injury and recovery, and to be a tool to monitor the effectiveness of a pharmacological intervention. In addition, urinary Hsp72 levels performance to detect and stratify renal injury induced by different periods of ischemia was better than urinary NGAL, Kim-1 and IL-18. Our preliminary data in humans support the notion that Hsp72 could be an early predictor of AKI in the clinical setting.

IMPACT:

Hsp72 may be a useful tool to early AKI diagnose in patients admitted to ICU or with high risk of developing renal injury such as those patients undergoing cardiac surgery, renal transplant or under nephrotoxic treatment. The opportune AKI diagnosis would permit the clinician to make an adequate pharmacologic intervention to improve patient survival and to avoid end stage renal disease development.

Histopathologic studies

At the end of the experiment, the right kidney was removed and quickly frozen for molecular studies, and the left kidney was perfused through the femoral catheter with phosphate buffered saline (PBS). Following blanching of the kidney, the perfusate was replaced by a freshly prepared 4% formalin buffer, and perfusion was continued until fixation was completed. After appropriate dehydration, kidney slices were embedded in paraffin, sectioned at 4 μm and stained via a periodic acid-Schiff (PAS) technique. Ten subcortical and juxtamedullary fields were randomly recorded from each kidney slide using a digital camera incorporated in a Nikon Light microscope. In each microphotograph, tubular cast per field were counted, and the results were expressed as the average of fields observed. The affected tubular area was analyzed blindly. Tubular damage was characterized by a loss of brush border, lumen dilatation or collapse and detachment from basement membrane. Digital microphotographs were recorded for each rat to assess, by morphometric analysis, the total tubular area (excluding luminal, interstitial and glomerular areas) and damaged tubular area, delimited by using eclipse net software (magnification 400×). The damaged tubular area was expressed as a proportion of the affected tubular area and total tubular area.

Hsp72 mRNA levels

Each renal cortex was isolated and snap frozen in liquid nitrogen. Total RNA was isolated with the TRIzol method (Invitrogen) and checked for integrity by 1% agarose gel electrophoresis. To avoid DNA contamination, all total RNA samples were treated with DNAse (DNAase I, Invitrogen). For urine RNA isolation, 24 h urine-collection from each rat was centrifuged at 3000 rpm for 30 min at 4°C. The sediment was resuspended in 1 ml of PBS; afterward, it was centrifuged at 13,000 rpm for 3 min and processed by the TrIzol method for RNA isolation. Reverse transcription (RT) was carried out with 1 μg of total RNA and 200 U of Moloney murine leukemia virus reverse transcriptase (Invitrogen). The mRNA levels of Hsp72 were quantified by real-time PCR on an ABI Prism 7300 Sequence Detection System (TaqMan, ABI, Foster City, CA). Primer and probe for Hsp72 were ordered as a kit: Rn00583013_s1 (Assay-on-Demand, ABI). As an endogenous control, eukaryotic 18S rRNA (predesigned assay reagent Applied by ABI, external run) was used. Relative quantification of Hsp72 gene expression was performed with the comparative threshold cycle (Ct) method (Livak & Schmittgen, 2001).

Kidney and urinary Hsp72 protein levels

Hsp72 detected by Western blot

Total renal proteins were isolated from six cortexes from each group and homogenized separately in lysis buffer (50 mM HEPES pH 7.4, 250 mM NaCl, 5 mM EDTA, 0.1% NP-40 and complete protease inhibitor (Roche)). Protein samples containing 20 μg of total protein were resolved by 8.5% sodium polyacrylamide gel electrophoresis (SDS–PAGE) electrophoresis and electroblotted onto polyvinylidinediuoride membranes (Amersham). For urinary Hsp72 detection by western blot, urine was diluted 1:100 in 0.9% saline solution, and 10 μL of each dilution was loaded and resolved by 8.5% SDS–PAGE electrophoresis and electroblotted, as previously described. Membranes were then blocked with 5% blotting-grade non-fat dry milk. Membranes were then incubated in 0.1% blotting-grade non-fat dry milk with their respective antibodies. For detection of Hsp72 in the renal cortex, the lower parts of the membranes were incubated with goat anti-actin antibody (1:5000 dilution) overnight at 4°C. (Santa Cruz Biotechnology, Santa Barbara CA). Upper membranes were

incubated with monoclonal anti-Hsp72 antibody. Afterward, membranes for Hsp72 were incubated with a secondary antibody, HRP-conjugated goat anti-mouse IgG (1:500, Santa Cruz Biotechnology). Actin detection was performed using donkey anti-goat IgG-HRP (1:5000, Santa Cruz Biotechnology). Proteins were detected with an enhanced chemiluminescence kit (Amersham) and autoradiography, following the manufacturer's recommendations. The bands were scanned for densitometric analysis.

Hsp72 detected by ELISA

Urine Hsp72 was analyzed using a commercially available high-sensitivity ELISA (Assay Designs EKS-715, MI, USA). Briey, samples and standards were added to wells coated with a mouse monoclonal antibody. Hsp72 was captured by the antibody and then detected by adding a rabbit polyclonal detection antibody. Both antibodies are specic for inducible Hsp72 and do not react with other members of the HSP70 family. A horseradish peroxidase conjugate bound to the detection antibody and colour development was accomplished by the addition of tetramethylbenzidine substrate and stopped with an acid stop solution. The optical density of samples was read at 450 nm by a plate reader and was overlapped with the standard curve generated from known concentrations of recombinant Hsp72 that ranged from 0.1 to 12.5 ng/ml.

Urinary Hsp72 levels as a monitor of a renoprotective intervention in AKI

Because we previously found that aldosterone antagonism with spironolactone at 20 mg/kg prevented renal injury induced by I/R, urinary Hsp72 levels as a monitor of a renoprotective intervention in AKI was assessed. Twenty-five Wistar rats, weighing 270–300 g, were divided in five groups: rats subjected to 30 min of ischemia and 24 h of reperfusion and rats that received spironolactone at different doses (20, 10, 5 or 2.5 mg/kg, by gastric gavage) 3 days before I/R was induced. After ischemia, urine was collected in metabolic cages, and blood samples were taken.

NGAL, Kim-1 and IL-18 detected by ELISA

Urine NGAL, Kim-1 and IL-18 levels were analyzed using commercially available ELISA kits: rat NGAL ELISA kit (Innovative Research IRNGALKT), rat Kim-1 ELISA kit (CosmoBIO Co CSB-E08808r) and rat IL-18 ELISA Kit (Invitrogen KRC2341). All procedures were performed accordingly manufacturer's instructions.

Evaluation of urinary Hsp72 in healthy kidney donors and patients with AKI

Urine samples from five healthy living-kidney donors (controls) and nine patients with septic AKI from the ICU were tested. AKI was defined as a 30% or greater increase in SCr from baseline according to the AKIN criteria (Mehta et al, 2007). In healthy donors, urine samples were collected from the first morning voids one day previous to nephrectomy (previously signed consent). All patients with sepsis in the ICU were followed every day, and, when the AKI criteria were fulfiled, a fresh urine sample was taken after draining the urine collection bag. Moreover, daily fresh urine samples were collected from patients in the ICU that exhibited respiratory failure with mechanical ventilation and together with other organ failure. These patients had normal renal function at the admission. From these patients, we analyzed, five patients that developed AKI and five that did not. In the urine samples Hsp72 levels were assessed in order to test if this biomarker could predict AKI criteria was fulfil (SCr elevation or urine output reduction). All urine samples were frozen and stored at 80°C until Hsp72 levels were evaluated. The human subjects included in these study form part of two ongoing clinical studies, which are in accordance with national and international guidelines and regulations and were approved by our institutional ethical review board. All subjects or designed surrogate (when ICU patients could not sign) signed the informed consent form.

Statistical analysis

Results are presented as means ± SE. Significance of the differences between groups was tested by ANOVA using Bonferroni's correction for multiple comparisons. All comparisons passed the normality test. Statistical significance was defined as p-value <0.05.

Author Contributions

JBC, LEM and NAB: Conceived and designed the experiments. JBC, RPV, CCG and MOC: performed the experiments. JBC, GG, LEMB and NAB: analyzed the data. GG and NAB: contributed reagents or analysis tools. JBC, GG and NAB: wrote the paper.

Acknowledgements

We are grateful to the members of the Molecular Physiology Unit for their suggestions and to Dr. Octavio Villanueva for his help with animal care, as well as to Martha Carrrasco for her technical assistance. The results presented in this paper have not been published previously neither in whole nor in abstract. This project was supported by grants from the Mexican Council of Science and Technology (CONACyT) 101030 and 112780 to NAB, by a grant from the National University of Mexico IN200909-3 to NAB and by a grant from Fundación Miguel Aleman AC to NAB. JBC is a PhD student supported by fellowship grant from CONACyT.

Supporting information is available at EMBO Molecular Medicine online.

The authors declare that they have no conflict of interest.

For more information

Heat Shock 70-kd protein:
http://www.ncbi.nlm.nih.gov/omim/140550
National Kidney Foundation
http://www.kidney.org/

References

Bagshaw SM (2010) Acute kidney injury: diagnosis and classification of AKI: AKIN or RIFLE? Nat Rev Nephrol 6: 71-73

Coca SG, Parikh CR (2008) Urinary biomarkers for acute kidney injury: perspectives on translation. Clin J Am Soc Nephrol 3: 481-490

Csermely P, Soti C, Blatch GL (2007) Chaperones as parts of cellular networks. Adv Exp Med Biol 594: 55-63

Devarajan P (2006) Update on mechanisms of ischemic acute kidney injury. J Am Soc Nephrol 17: 1503-1520

Dieterle F, Perentes E, Cordier A, Roth DR, Verdes P, Grenet O, Pantano S, Moulin P, Wahl D, Mahl, *et al* (2010) Urinary clusterin, cystatin C, beta2-microglobulin and total protein as markers to detect drug-induced kidney injury. Nat Biotechnol 28: 463-469

Dieterle F, Sistare F, Goodsaid F, Papaluca M, Ozer JS, Webb CP, Baer W, Senagore A, Schipper MJ, Vonderscher J, *et al* (2010) Renal biomarker qualification submission: a dialog between the FDA-EMEA and Predictive Safety Testing Consortium. Nat Biotechnol 28: 455-462

Fan CY, Lee S, Cyr DM (2003) Mechanisms for regulation of Hsp70 function by Hsp40 cell stress. Chaperones 8: 309-316

Ferguson MA, Vaidya VS, Waikar SS, Collings FB, Sunderland KE, Gioules CJ, Bonventre JV (2010) Urinary liver-type fatty acid-binding protein predicts adverse outcomes in acute kidney injury. Kidney Int 77: 708-714

Friedewald JJ, Rabb H (2004) Inflammatory cells in ischemic acute renal failure. Kidney Int 66: 486-491

Han WK, Wagener G, Zhu Y, Wang S, Lee HT (2009) Urinary biomarkers in the early detection of acute kidney injury after cardiac surgery. Clin J Am Soc Nephrol 4: 873-882

Hernadez-Pando R, Pedraza-Chaverri J, Orozco-Estevez H, Silva-Serna P, Moreno I, Rondan-Zarate A, Elinos M, Correa-Rotter R, Larriva-Sahd J (1995) Histological and subcellular distribution of 65 and 70 kD heat shock proteins in experimental nephrotoxic injury. Exp Toxicol Pathol 47: 501-508

Kelly KJ (2002) Stress response proteins and renal ischemia. Minerva Urol Nefrol 54: 81-91

Kelly KJ (2006) Acute renal failure: much more than a kidney disease. Semin Nephrol 26: 105-113

Kelly KJ, Baird NR, Greene AL (2001) Induction of stress response proteins and experimental renal ischemia/reperfusion. Kidney Int 59: 1798-1802

Liangos O, Perianayagam MC, Vaidya VS, Han WK, Wald R, Tighiouart H, MacKinnon RW, Li L, Balakrishnan VS, Pereira BJ, *et al* (2007) Urinary N-acetyl-beta-(D)-glucosaminidase activity and kidney injury molecule-1 level are associated with adverse outcomes in acute renal failure. J AmSoc Nephrol 18: 904-912

Liano F, Pascual J (1996) Epidemiology of acute renal failure: a prospective, multicenter, community-based study. Madrid Acute Renal Failure Study Group. Kidney Int 50: 811-818

Lindquist S, Craig EA (1988) The heat-shock proteins. Annu Rev Genet 22: 631-677

Liu KD, Brakeman PR (2008) Renal repair and recovery. Crit Care Med 36: S187-S192

Livak KJ, Schmittgen TD (2001) Analysis of relative gene expression data using real-time quantitative PCR and the 2(-Delta Delta C(T)). Method Methods 25: 402-408

Lopes JA, Fernandes P, Jorge S, Goncalves S, Alvarez A, Costa e S, Franca C, Prata MM (2008) Acute kidney injury in intensive care unit patients: a comparison between the RIFLE and the acute kidney injury network classifications. Crit Care 12: R110

McIlroy DR, Wagener G, Lee HT (2010) Neutrophil gelatinase-associated lipocalin and acute kidney injury after cardiac surgery: the effect of baseline renal function on diagnostic performance. Clin J Am Soc Nephrol 5: 211-219

Mehta RL, Kellum JA, Shah SV, Molitoris BA, Ronco C, Warnock DG, Levin A (2007) Acute kidney injury network: report of an initiative to improve outcomes in acute kidney injury. Crit Care 11: R31

Mejia-Vilet JM, Ramirez V, Cruz C, Uribe N, Gamba G, Bobadilla NA (2007) Renal ischemia-reperfusion injury is prevented by the mineralocorticoid receptor blocker spironolactone. Am J Physiol Renal Physiol 293: F78-F86

Melnikov VY, Ecder T, Fantuzzi G, Siegmund B, Lucia MS, Dinarello CA, Schrier RW, Edelstein CL (2001) Impaired IL-18 processing protects caspase-1-deficient mice from ischemic acute renal failure. J Clin Invest 107: 1145-1152

Mishra J, Ma Q, Prada A, Mitsnefes M, Zahedi K, Yang J, Barasch J, Devarajan P (2003) Identification of neutrophil gelatinase-associated lipocalin as a novel early urinary biomarker for ischemic renal injury. J Am Soc Nephrol 14: 2534-2543

Mishra J, Dent C, Tarabishi R, Mitsnefes MM, Ma Q, Kelly C, Ruff SM, Zahedi K, Shao M, Bean J, *et al* (2005) Neutrophil gelatinase-associated lipocalin (NGAL) as a biomarker for acute renal injury after cardiac surgery. Lancet 365: 1231-1238

Molinas SM, Rosso M, Wayllace NZ, Pagotto MA, Pisani GB, Monasterolo LA, Trumper L (2010) Heat shock protein 70 induction and its urinary excretion in a model of acetaminophen nephrotoxicity. Pediatr Nephrol 25: 1245-1253

Mueller T, Bidmon B, Pichler P, Arbeiter K, Ruffingshofer D, VanWhy SK, Aufricht C (2003) Urinary heat shock protein-72 excretion in clinical and experimental renal ischemia. Pediatr Nephrol 18: 97-99

Negishi K, Noiri E, Doi K, Maeda-Mamiya R, Sugaya T, Portilla D, Fujita T (2009) Monitoring of urinary L-type fatty acid-binding protein predicts histological severity of acute kidney injury. Am J Pathol 174: 1154-1159

Nejat M, Pickering JW, Walker RJ, Endre ZH (2010) Rapid detection of acute kidney injury by plasma cystatin C in the intensive care unit. Nephrol Dial Transplant 25: 3283-3289

Parikh CR, Abraham E, Ancukiewicz M, Edelstein CL (2005) Urine IL-18 is an early diagnostic marker for acute kidney injury and predicts mortality in the intensive care unit. J Am Soc Nephrol 16: 3046-3052

Parikh CR, Mishra J, Thiessen-Philbrook H, Dursun B, Ma Q, Kelly C, Dent C, Devarajan P, Edelstein CL (2006) Urinary IL-18 is an early predictive biomarker of acute kidney injury after cardiac surgery. Kidney Int 70: 199-203

Price PM, Safirstein RL, Megyesi J (2009) The cell cycle and acute kidney injury. Kidney Int 76: 604-613

Ramirez V, Trujillo J, Valdes R, Uribe N, Cruz C, Gamba G, Bobadilla NA (2009) Adrenalectomy prevents renal ischemia-reperfusion injury. Am J Physiol Renal Physiol 297: F932-F942

Ritossa FA (1962) New puffing pattern induced by temperature shoch and DNP in *Drosophila*. Experientia 18: 571-573

Taman M, Liu Y, Tolbert E, Dworkin LD (1997) Increase urinary hepatocyte growth factor excretion in human acute renal failure. Clin Nephrol 48: 241-245

Tsutsumi S, Neckers L (2007) Extracellular heat shock protein 90: a role for a molecular chaperone in cell motility and cancer metastasis. Cancer Sci 98: 1536-1539

Turman MA, Rosenfeld SL (1999) Heat shock protein 70 overexpression protects LLC-PK1 tubular cells from heat shock but not hypoxia. Kidney Int 55: 189-197

Uchida K, Gotoh A (2002) Measurement of cystatin-C and creatinine in urine. Clin Chim Acta 323: 121-128

Vaidya VS, Ramirez V, Ichimura T, Bobadilla NA, Bonventre JV (2006) Urinary kidney injury molecule-1: a sensitive quantitative biomarker for early detection of kidney tubular injury. Am J Physiol Renal Physiol 290: F517-F529

Vaidya VS, Waikar SS, Ferguson MA, Collings FB, Sunderland K, Gioules C, Bradwin G, Matsouaka R, Betensky RA, Curhan GC, *et al* (2008) Urinary biomarkers for sensitive and specific detection of acute kidney injury in humans. Clin Transl Sci 1: 200-208

Vaidya VS, Ford GM, Waikar SS, Wang Y, Clement MB, Ramirez V, Glaab WE, Troth SP, Sistare FD, Prozialeck WC, *et al* (2009) A rapid urine test for early detection of kidney injury. Kidney Int 76: 108-114

Vaidya VS, Ozer JS, Dieterle F, Collings FB, Ramirez V, Troth S, Muniappa N, Thudium D, Gerhold D, Holder DJ, Bobadilla NA, Marrer E, *et al* (2010) Kidney injury molecule-1 outperforms traditional biomarkers of kidney injury in

preclinical biomarker qualification studies. Nat Biotechnol 28: 478-485

Wagener G, Jan M, Kim M, Mori K, Barasch JM, Sladen RN, Lee HT (2006) Association between increases in urinary neutrophil gelatinase-associated lipocalin and acute renal dysfunction after adult cardiac surgery. Anesthesiology 105: 485-491

Waikar SS, Curhan GC, Wald R, McCarthy EP, Chertow GM (2006) Declining mortality in patients with acute renal failure, 1988 to 2002. J Am Soc Nephrol 17: 1143-1150

Wu I, Parikh CR (2008) Screening for kidney diseases: older measures *versus* novel biomarkers. Clin J Am Soc Nephrol 3: 1895-1901

Yamamoto T, Noiri E, Ono Y, Doi K, Negishi K, Kamijo A, Kimura K, Fujita T, Kinukawa T, Taniguchi H, *et al* (2007) Renal L-type fatty acid-binding protein in acute ischemic injury. J Am Soc Nephrol 18: 2894-2902

Yu Y, Jin H, Holder D, Ozer JS, Villarreal S, Shughrue P, Shi S, Figueroa DJ, Clouse H, Su M, *et al* (2010) Urinary biomarkers trefoil factor 3 and albumin enable early detection of kidney tubular injury. Nat Biotechnol 28: 470-477

Zhipeng W, Li L, Qibing M, Linna L, Yuhua R, Rong Z (2006) Increased expression of heat shock protein (HSP)72 in a human proximal tubular cell line (HK-2) with gentamicin-induced injury. J Toxicol Sci 31: 61-70

Spironolactone prevents chronic kidney disease caused by ischemic acute kidney injury

Jonatan Barrera-Chimal[1,2], Rosalba Pérez-Villalva[1,2], Roxana Rodríguez-Romo[1,2], Juan Reyna[1,2], Norma Uribe[3], Gerardo Gamba[1,2] and Norma A. Bobadilla[1,2]

[1]Molecular Physiology Unit, Instituto de Investigaciones Biomédicas, Universidad Nacional Autónoma de México, Mexico City, Mexico; [2]Department of Nephrology, Instituto Nacional de Ciencias Médicas y Nutrición Salvador Zubirán, Mexico City, Mexico and [3]Department of Pathology, Instituto Nacional de Ciencias Médicas y Nutrición Salvador Zubirán, Mexico City, Mexico

Acute kidney injury (AKI) has been recognized as a risk factor for the development of chronic kidney disease (CKD). Aldosterone has a critical role in promoting renal injury induced by ischemia. Here, we evaluated whether spironolactone administered before or after AKI caused by ischemia protects against CKD. In the first set of experiments, Wistar rats underwent a sham operation without or with prior spironolactone treatment, or underwent 45 minutes of bilateral renal ischemia without or with spironolactone treatment before ischemia and assessed over 270 days. The second set of rats received low (20 mg/kg) or high (80 mg/kg) doses of spironolactone at three different times after the sham operation or bilateral renal ischemia and were assessed after 90 days. Untreated animals developed CKD following ischemia-induced AKI as characterized by a progressive increase in proteinuria, renal dysfunction, podocyte injury, glomerular hypertrophy, and focal sclerosis. This was associated with increased oxidative stress, an upregulation of tumor growth factor (TGF)-β, followed by upregulation of the TGF-β downstream effectors phospho-Smad3, collagen I, fibronectin, and proinflammatory cytokines. Treatment with spironolactone either before or after ischemia prevented subsequent CKD by avoiding the activation of fibrotic and inflammatory pathways. Thus, spironolactone may be a promising treatment for the prevention of AKI-induced CKD.

Kidney International (2012) **83,** 93–103; doi:10.1038/ki.2012.352; published online 26 September 2012

KEYWORDS: inflammatory cytokines; mineralocorticoid receptor blockade; oxidative stress; TGF-β pathway; tubular proliferation

Correspondence: *Norma A. Bobadilla, Unidad de Fisiología Molecular, Vasco de Quiroga No. 15, Tlalpan 14000, México City, Mexico. E-mail: nab@biomedicas.unam.mx or norma.bobadillas@quetzal.innsz.mx*

Received 1 January 2012; revised 3 August 2012; accepted 9 August 2012; published online 26 September 2012

Ischemic kidney injury is the primary cause of acute kidney injury (AKI) in hospitalized patients and is associated with high morbidity and mortality rates. In addition, the incidence of AKI has significantly increased in the past 15 years owing to an aging general population and the increased prevalence of obesity, diabetes, and hypertension, which predispose patients to an AKI event.[1–5] AKI occurs in approximately 15% of hospitalized patients and in up to 40–60% of intensive care unit patients.[6,7]

For many years, it was commonly thought that patients surviving episodes of AKI recover their renal function without further consequences. However, recent evidence based on epidemiological observations in patients who suffer from AKI strongly suggests otherwise. AKI has thus been proposed to be a risk factor for developing chronic kidney disease (CKD) and, in particular, for promoting the transition of CKD to end-stage renal disease.[8–11] In support of this hypothesis, the probability of developing CKD or end-stage renal disease over time is proportional to the severity and duration of the AKI event.[8,12,13] Moreover, of great concern is the recent evidence demonstrating that 6.6% of AKI patients who had a complete renal function recovery exhibited a greater risk of death and *de novo* CKD after 2–4 years of follow-up.[12] Until now, however, the progression of AKI to CKD in rats with two intact kidneys, which would allow elucidating the mechanisms causing AKI to progress to CKD, has been rarely explored. Such a model would also be beneficial for identifying pharmacological interventions to prevent injury due to AKI and/or stop the development of CKD and end-stage renal disease.

Several studies involving experimental models have demonstrated that aldosterone has an important role in the physiopathology of renal injury induced by ischemic process, including acute and chronic cyclosporine A nephrotoxicity and ischemia/reperfusion (I/R).[14–21] Accordingly, we have shown that prophylactic spironolactone treatment[16] or adrenal gland removal[17] completely prevents AKI in rats undergoing bilateral renal ischemia. Furthermore, spironolactone administration at different postischemia intervals prevents or reduces functional and structural renal injury,[22] suggesting that aldosterone is a key molecule in mediating ischemic renal

injury and that mineralocorticoid receptor (MR) antagonism, even after ischemia, is a helpful strategy to prevent AKI.

In this study, we characterized a model of CKD induced by a single episode of ischemic AKI and the molecular mechanisms that lead to the development of CKD. Our data reveal that spironolactone administration before or after the ischemic insult is a useful strategy to prevent or reduce the development of CKD.

RESULTS

We have previously shown that, after 24 h of bilateral ischemia, rats develop severe renal dysfunction and tubular injury.[16] Figure 1 shows that renal dysfunction induced by ischemia was completely resolved after 9 days of reperfusion, similar to conditions that often occur in clinical settings. Urinary protein excretion was significantly elevated after 24 h of reperfusion in rats subjected to ischemia and continues to progressively decline until normal values were reached after 6 days of reperfusion (Figure 1a). Proteinuria in spironolactone-pretreated rats was 50% lower than the proteinuria in the untreated group, and normal levels were reached faster. Consequently, the rats undergoing ischemia recovered renal function after 10 days, as demonstrated by normal values of renal blood flow, serum creatinine, and creatinine clearance (Figure 1b–d). Despite the complete improvement in renal function, interleukin (IL)-6 mRNA and phosphorylated Smad3 levels were significantly higher than those in the sham-operated group. Cytokine upregulation was not observed in spironolactone-pretreated rats (Figure 1e–f). These results suggest that although renal function recovered, proinflammatory and profibrotic pathways remained active. These pathways may be able to perpetuate renal injury, which can lead to CKD, a situation that did not occur in spironolactone-pretreated animals.

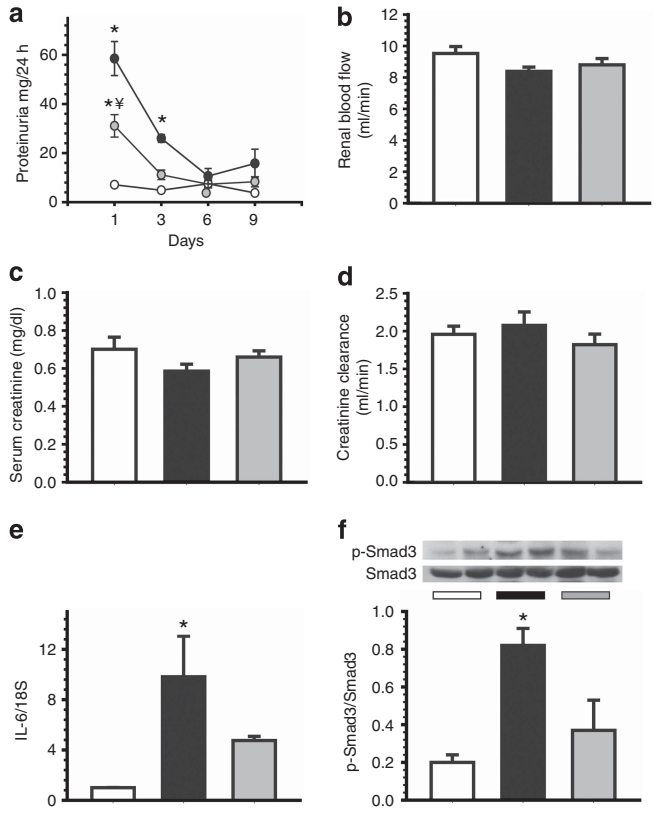

Figure 1 | Renal dysfunction induced by ischemia was completely resolved after 10 days of reperfusion, but proinflammatory and profibrotic cytokines remained enhanced. (**a**) Urinary protein excretion 1, 3, 6, and 9 days after reperfusion, in the sham (o), bilateral renal ischemia (•), and ischemia + Sp pretreatment (•) groups. At 10 days after reperfusion, the rats were killed, and renal function was determined. (**b**) Mean renal blood flow, (**c**) serum creatinine, and (**d**) creatinine clearance. (**e**) Interleukin (IL)-6 mRNA levels were measured in the renal cortex. (**f**) The upper insets show representative autoradiographs from the phosphorylated-Smad3 (p-Smad3) and Smad3 western blot analysis for sham (white bars), bilateral renal ischemia (black bars), and ischemia + Sp pretreatment (gray bars) groups. The lower graphs display the corresponding densitometric analysis. $^{*}P<0.05$ vs. the sham group and $^{¥}P<0.05$ vs. the ischemia group.

Ischemic insult leads to progressive renal dysfunction that can be prevented with spironolactone pretreatment

We assessed whether an AKI episode induced by ischemia leads to CKD. Because we have previously shown that I/R injury is prevented by spironolactone pretreatment or adrenal gland removal,[16,17] we evaluated whether spironolactone pretreatment before ischemia also prevents CKD development. There was considerable mortality in the A-to-C group in the first 10 days after ischemia (57%), and survival was markedly improved by spironolactone pretreatment (15%) (Figure 2a). Proteinuria was assessed every 30 days. The animals that survived the ischemic insult developed a progressive increase in proteinuria, from 20.2 ± 1.5 mg/day at 30 days to 164.8 ± 11.3 mg/day at 270 days. This increase was not observed in the A-to-C + Sp group (9.2 ± 1.0 mg/day at 30 days and 27.1 ± 2.0 mg/day at 270 days) (Figure 2b). Despite the similar body weights of all rats at the beginning of the study, the A-to-C group exhibited a lower average body weight at the end of the study (583 ± 16.3 g) than did the S, Sp, and A-to-C + Sp groups (752 ± 28.3, 729 ± 19.2, and 721 ± 11.8 g, respectively). After 9 months, the A-to-C group developed renal dysfunction that was characterized by a significant reduction in renal blood flow and creatinine clearance (Figure 2c and d). Interestingly, the A-to-C + Sp group failed to develop renal dysfunction. As shown in Figure 2e, at the end of the study, the mean arterial pressure was similar among the groups. Therefore, the renal injury observed in the rats that developed CKD was not due to hypertension. In agreement with these findings, the rats that developed CKD exhibited an increase in the levels of urinary kidney injury molecule-1, an effect that was not observed in the A-to-C + Sp group (Figure 2f).

Ischemic insult leads to severe renal structural injury: prevention by spironolactone pretreatment

Representative light microscopy sections from rat kidneys stained with periodic acid–Schiff are shown in Figure 3a–d.

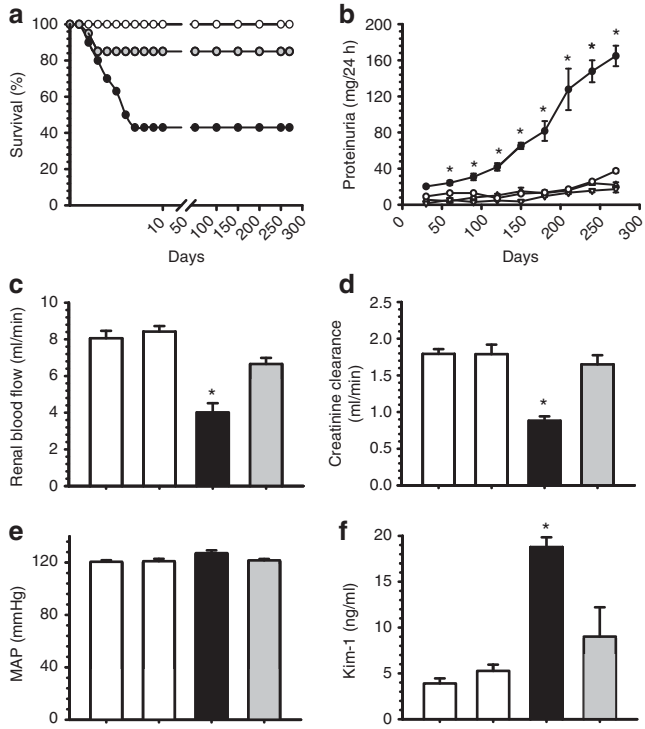

Figure 2 | Acute kidney injury leads to the development of chronic kidney disease (CKD), which can be prevented by spironolactone pretreatment. Four groups were included: sham surgery (S), $n = 9$; rats receiving spironolactone 3 days before sham surgery (20 mg/kg per day), $n = 9$ (Sp); rats undergoing renal bilateral ischemia, $n = 28$ (A-to-C); and rats receiving spironolactone 3 days before bilateral ischemia, $n = 13$ (A-to-C + Sp). (**a**) The survival rate in the A-to-C group (black circles) was 43%, compared with 85% in the A-to-C + Sp group (gray circles) and 100% in the sham and Sp group (overlaid white circles). (**b**) Urinary protein excretion was measured every 30 days during follow-up: sham (▽), Sp (Δ), A-to-C (•), and A-to-C + Sp (o). At the end of the experimental period, (**c**) renal blood flow, (**d**) creatinine clearance, (**e**) mean arterial pressure, and (**f**) urinary kidney injury molecule-1 (Kim-1) levels were determined in the sham (white bars), Sp (white bars), A-to-C (black bars), and A-to-C + Sp groups (gray bars). *$P < 0.05$ vs. the S and Sp groups.

Rats undergoing ischemia exhibited severe structural alterations characterized by glomerular hypertrophy, glomerulosclerosis, cast formation, severe tubular dilation, and tubulointerstitial fibrosis. By contrast, the A-to-C + Sp group exhibited glomerular and tubular architecture similar to that of control rats. These findings were corroborated by quantification of the number of dilated tubules, percentage of glomerulosclerosis, and glomerular diameter size (Figures 3 and 4). Tubular dilation was present in 42.3 ± 5.0% of the total tubules in the A-to-C group, whereas only 13.1 ± 2.7% of the A-to-C + Sp group displayed dilation ($P < 0.01$). Similarly, the A-to-C group exhibited a significantly higher glomerulosclerosis percentage (10.0 ± 4.4%) than the S and A-to-C + Sp groups (0% and 0.4 ± 0.4%, respectively).

The degree of glomerular hypertrophy was evaluated by measuring glomerulus diameter and by generating a distribution of glomerular size. Figure 4a shows the normal diameter distribution of the control group, wherein most of the glomeruli were in the range of 101–125 μm (38.3%), and only a minor proportion was found in the ranges of 76–100 μm (19.5%) and 126–150 μm (27.5%). The histogram for the control group exhibits a typical bell-shaped Gaussian distribution, as we have shown previously.[21] By contrast, in the A-to-C group, the glomerular diameter distribution was shifted to the right, reflecting glomerular hypertrophy. Accordingly, 43.3% of the glomeruli were >151 μm in diameter. In addition, a lower proportion of glomeruli were found in the diameter ranges of 101–125 μm (20.4%), 76–100 μm (8.3%), and 50–75 μm (0%). All of these differences were statistically significant according to contingency analysis, as shown in Figure 4b. The glomerular size distribution of the A-to-C + Sp group was similar to that of the control group, but not to that of the A-to-C group (Figure 4c), indicating that glomerular hypertrophy was nearly absent. In agreement with these findings, renal hypertrophy in the A-to-C group was also evidenced by a significant elevation in the mean kidney weight (2.5 ± 0.2 g) compared with the S and Sp groups (1.6 ± 0.1 and 1.6 ± 0.1 g, respectively); this increase was not observed in the A-to-C + Sp group (1.5 ± 0.1 g).

Transmission electron microscopy of rat kidneys with CKD revealed ultrastructural alterations that included microvillus degeneration and effacement and detachment of podocyte foot processes (Figure 4e). These alterations were rarely observed in the A-to-C + Sp group (Figure 4f). Furthermore, an extensive tubulointerstitial area was affected by fibrosis in the A-to-C group (Figure 5a and b), but a lower extent of fibrosis was observed in the A-to-C + Sp group (Figure 5c and d). These observations were confirmed by the morphometric analysis represented in Figure 5e. The A-to-C group exhibited fibrosis in 44.8 ± 16.0% of the tubulointerstitial area, compared with 18.7 ± 4.5% in the A-to-C + Sp group; this difference was significant.

Tubular dilation is due in part to cellular proliferation

To determine whether the severe tubular dilation observed in the A-to-C group was associated with tubular cell proliferation, immunohistochemical analysis of proliferating cell nuclear antigen (PCNA) was performed. The A-to-C group exhibited considerable tubular cell proliferation as demostrated by the number of PCNA + cells, an effect that was almost absent in the A-to-C + Sp group (Figure 6a–c). These findings were confirmed by calculating the percentage of nuclei that stained positive for PCNA (Figure 6d). The positive cells were primarily located in the dilated tubules, suggesting that enhanced cell proliferation is promoting tubular dilation in the A-to-C group. This assumption is also supported by a significant correlation between the percentage of dilated tubules and the percentage of PCNA + cells (Figure 6e, $r^2 = 0.87$).

Tubulointerstitial fibrosis is mediated by TGF-β pathway activation

The role of the tumor growth factor (TGF)-β pathway in promoting tubulointerstitial fibrosis was also evaluated.

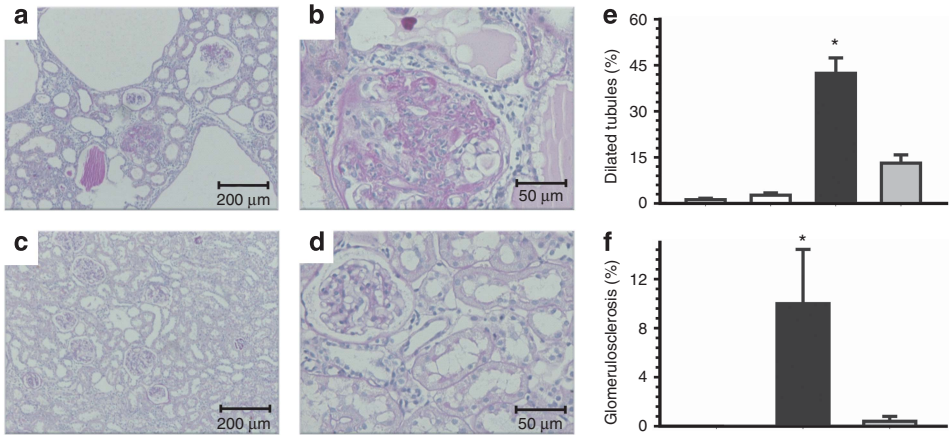

Figure 3 | An acute kidney injury (AKI) episode leads to severe structural damage, which can be prevented by Sp pretreatment. (**a**, **b**) Representative images of periodic acid–Schiff (PAS)-stained sections from the A-to-C group, and (**c**, **d**) sections from the A-to-C + Sp group. (**e**) The percentage of dilated tubules was quantified by counting the number of dilated tubules as a proportion of the total number of tubules. (**f**) Glomerulosclerosis percentage for the sham (white bars), Sp (second set of white bars), A-to-C (black bars), and A-to-C + Sp groups (gray bars). *$P < 0.05$ vs. the S and Sp groups.

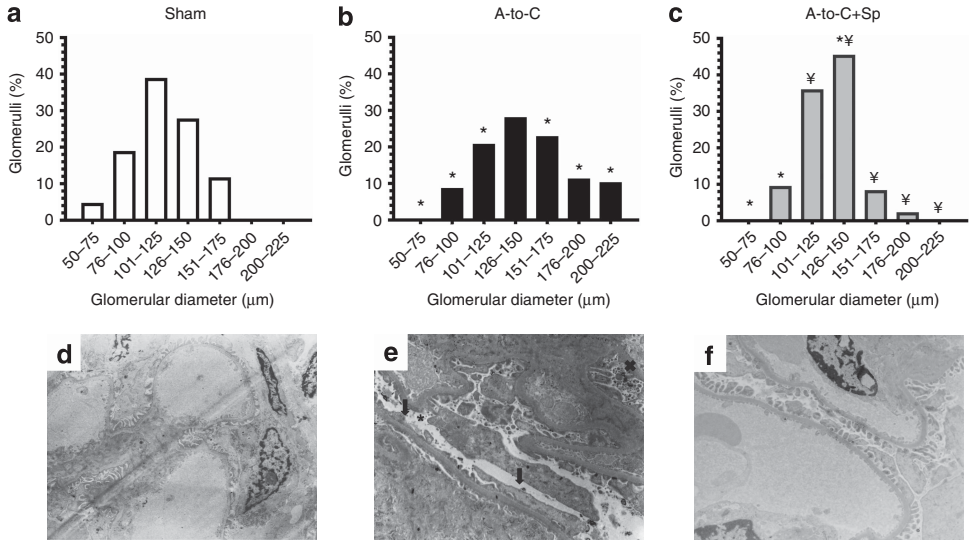

Figure 4 | Glomerular hypertrophy and ultrastructural lesions in rats with chronic kidney disease (CKD). (**a**) The glomerular diameter distribution is represented in white bars for the sham group, (**b**) in black bars for the A-to-C group, and (**c**) in gray bars for the A-to-C + Sp group. Representative transmission electron micrographs are shown in (**d**) the sham group, (**e**) the A-to-C group, and (**f**) the A-to-C + Sp group. Black arrows indicate foot process fusion, and asterisks indicate foot process detachment. Original magnification: ×6,300. *$P < 0.05$ vs. the S group and ¥$P < 0.05$ vs. the A-to-C group.

The A-to-C group exhibited a significant twofold elevation in TGF-β mRNA levels. This increase was not observed in the A-to-C + Sp group (Figure 7a). To assess whether this pathway was efficiently activated, the renal levels of downstream effectors of the TGF-β pathway, including phosphorylated Smad3, fibronectin, collagen I, and α-smooth muscle actin (α-SMA), were measured by western blot analysis as shown in Figure 7b–f. The levels of all of these proteins were significantly elevated in the rats that developed CKD. Intriguingly, the activation of the TGF-β pathway was completely prevented in the A-to-C + Sp group. Recent studies have shown that when Smad2 is phosphorylated, it can act as an antifibrotic modulator of the TGF-β pathway.[23] We found that the A-to-C + Sp group, which exhibited less tubulointerstitial fibrosis, also displayed a significant elevation in phospho-Smad2 levels.

Renal injury induced by an ischemic insult is also mediated by increased oxidative stress

Urinary H_2O_2 excretion in the A-to-C group was significantly elevated compared with the S and Sp groups (64.1 ± 7.5 vs. 10.4 ± 1.1 and 5.9 ± 1.0 nmol/min, respectively) (Figure 8a). However, the elevation in urinary H_2O_2 excretion was abrogated in the A-to-C + Sp group (14.8 ± 2.5 nmol/min). In addition, catalase activity was significantly reduced in the A-to-C group (Figure 8b), and this effect was almost entirely prevented in the

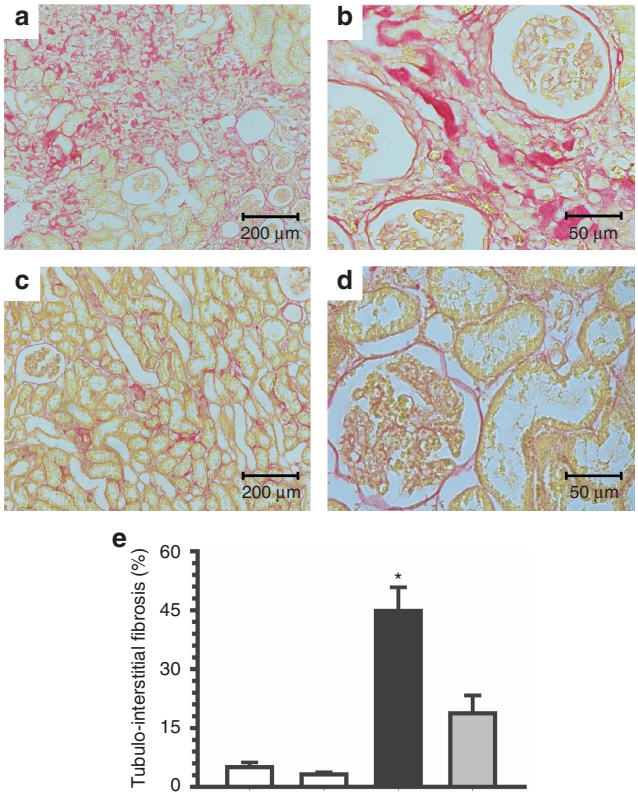

Figure 5 | Tubulointerstitial fibrosis in rats with chronic kidney disease (CKD). (**a**, **b**) Representative light micrographs after Sirius red staining showing the presence of fibrosis (in red) from the A-to-C group, and (**c**, **d**) micrographs from the A-to-C + Sp group. (**e**) The percentage of tubulointerstitial fibrosis in each of the four groups at the end of the 270-day experiment was quantified by morphometric analysis for sham (white bars), Sp (second set of white bars), A-to-C (black bars), and A-to-C + Sp groups (gray bars). $^{*}P < 0.05$ vs. the S and Sp groups.

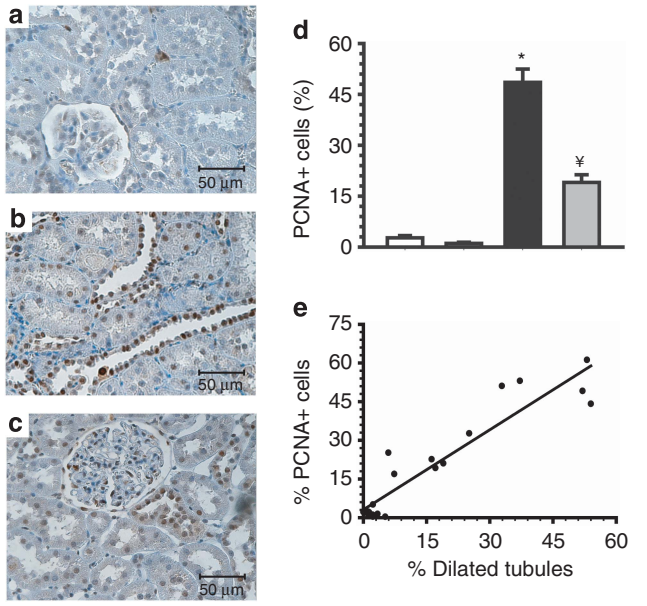

Figure 6 | Tubular cell proliferation as assessed by proliferating cell nuclear antigen (PCNA) immunohistochemistry. To evaluate whether epithelial cells were proliferating and provoking tubule dilation, immunohistochemistry for PCNA was performed in kidney sections from the four groups. (**a**) Representative images from the sham, (**b**) A-to-C, and (**c**) A-to-C + Sp groups. (**d**) The percentage of PCNA + cells in the sham (white bars), Sp (second set of white bars), A-to-C (black bars), and A-to-C + Sp groups (gray bars). (**e**) The correlation between the percentage of PCNA + cells and the percentage of dilated tubules ($r^2 = 0.87$). $^{*}P < 0.05$ vs. the S and Sp groups, and $^{¥}P < 0.05$ vs. the A-to-C group.

A-to-C + Sp group. No differences in glutathione peroxidase activity were observed among the groups (Figure 8c).

Inflammatory cytokine upregulation is involved in ischemia-induced CKD

Tumor necrosis factor alpha (TNF-α), monocyte chemotactic protein-1 (MCP-1), and IL-6 mRNA and protein levels were assessed by real-time reverse transcription–polymerase chain reaction and enzyme-linked immunosorbent assay, respectively. As shown in Figure 9, the mRNA levels of these cytokines were upregulated in the A-to-C group by 1.6-fold for TNF-α and more than 13-fold for MCP-1 and IL-6, compared with the S group. By contrast, the A-to-C + Sp group exhibited mRNA levels similar to the control group. These observations were corroborated at the protein level; a similar pattern was observed in the enzyme-linked immunosorbent assay results.

CKD induced by AKI was also reduced by spironolactone administration after the ischemic insult

Spironolactone administered at 0 or 1.5 h after the ischemic insult prevented the development of proteinuria compared with the untreated A-to-C group either at low or high doses (Figure 10a and d). A low dose of spironolactone administered 3 h after ischemia was unable to prevent, but did significantly reduce, the progressive elevation of proteinuria (Figure 10a). These findings were not associated with significant changes in renal blood flow (Figure 10b and e) or creatinine clearance (Figure 10c and f), probably because 3 months is an early stage of the CKD, often exhibiting proteinuria, without renal dysfunction, as was observed after a longer period of observation after similar ischemia (Figure 2). Despite the lack of significant differences among these groups, spironolactone-treated animals exhibited better renal function than the ischemic group.

At 3 months after inducing bilateral renal ischemia, the untreated A-to-C group, compared with the sham-operated group, exhibited morphological alterations, such as tubular dilation, cast formation, glomerular hypertrophy, and extensive tubulointerstitial fibrosis (Supplementary Figure S1 online). All of these changes were reduced in the animals treated with a low dose of spironolactone (Supplementary Figure S2 online) and were prevented in animals treated with a high dose of spironolactone (Supplementary Figure S3 online). In fact, glomerular hypertrophy (measured as the distribution of glomerular diameters) was prevented in the groups that received a low dose of spironolactone at 0 h

(Figure 11c) or high dose at either 0 or 1.5 h after renal bilateral ischemia (Figure 11f and g, respectively). Although kidney changes were not completely prevented, these renoprotective effects of spironolactone were also observed with a low dose at 1.5 and 3 h after ischemia (Figure 11d and e, respectively). Morphometric analyses demonstrated that, 3 months after inducing ischemia, the untreated rats exhibited fibrotic damage in 33.3% of their tubulointerstitium compared with damage in 3.7% of the tubulointerstitium in the sham-operated rats (Supplementary Figure S1 online). In contrast, a low dose of spironolactone administered either at 0 and 1.5 h post ischemia reduced the tubulointerstitial fibrosis to 14.8% and 15.1%, respectively, and the 3-h administration reduced the fibrosis to a lesser extent, 20.9% (Supplementary Figure S2 online). A high dose of spironolactone at 0 or 1.5 h post ischemia was more effective in reducing the area affected by tubulointerstitial fibrosis to 11.8% and 7.8%, respectively (Supplementary Figure S3 online).

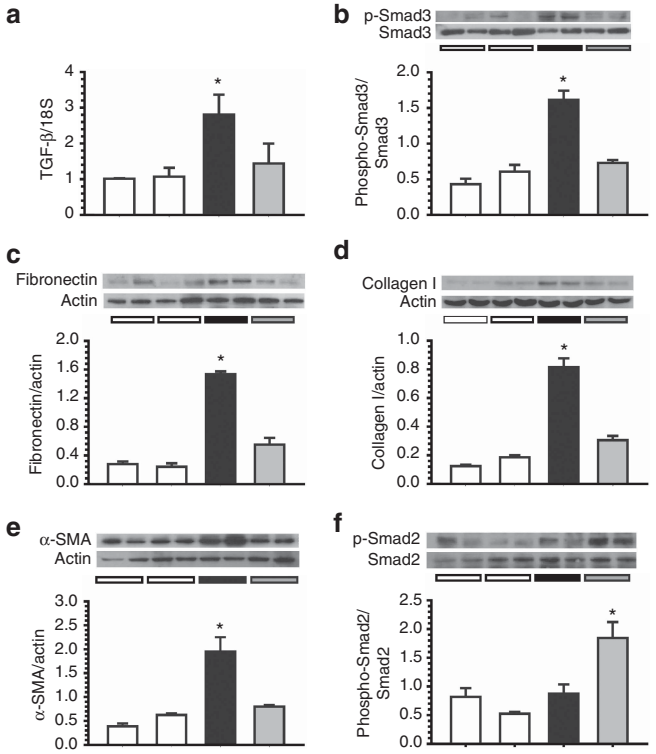

Figure 7 | Association of renal fibrosis with the tumor growth factor (TGF)-β pathway activation. (**a**) TGF-β mRNA levels were quantified by real-time reverse transcription–polymerase chain reaction (RT-PCR). Densitometric analysis of the western blots was performed for (**b**) phospho-Smad3 (p-Smad3), (**c**) fibronectin, (**d**) collagen I, (**e**) α-smooth muscle actin (α-SMA), and (**f**) phospho-Smad2 in the sham (white bars), Sp (second set of white bars), A-to-C (black bars), and A-to-C + Sp groups (gray bars). In each panel, the upper insets depict representative blots of the corresponding proteins. *$P < 0.05$ vs. the S and Sp groups.

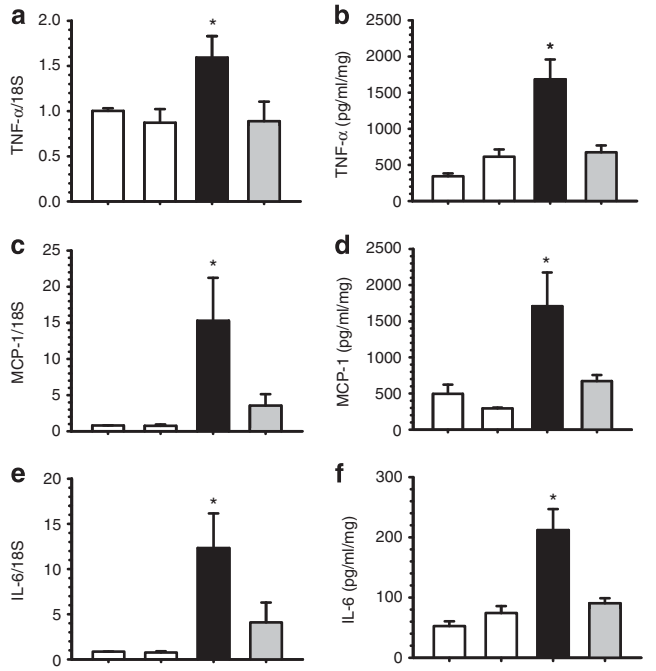

Figure 9 | The contribution of the inflammatory response to chronic kidney disease (CKD) development. (**a**) TNF-α, (**c**) MCP-1, and (**e**) IL-6 mRNA levels measured in total kidney RNA extracted from the sham (white bars), Sp (second set of white bars), A-to-C (black bars), and A-to-C + Sp groups (gray bars). (**b**) TNF-α, (**d**) MCP-1, and (**f**) IL-6 protein levels quantified by enzyme-linked immunosorbent assay (ELISA) in tissue kidney homogenates. *$P < 0.05$ vs. the S and Sp groups.

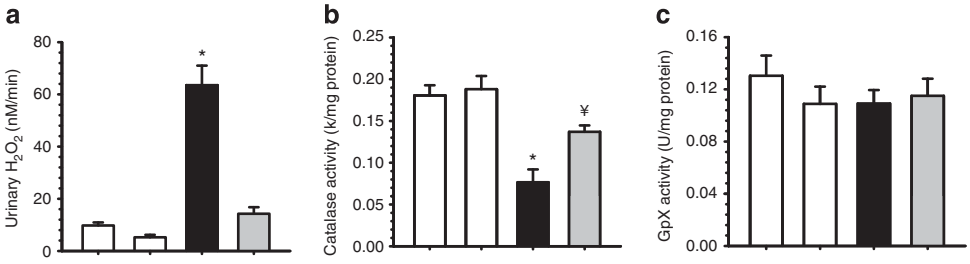

Figure 8 | The contribution of oxidative stress to chronic kidney disease (CKD) development and prevention by spironolactone pretreatment. (**a**) Urinary hydrogen peroxidase (H_2O_2) excretion after 270 days of follow-up. (**b**) Catalase activity and (**c**) glutathione peroxidase (Gpx) activity in the sham (white bars), Sp (second set of white bars), A-to-C (black bars), and A-to-C + Sp groups (gray bars). *$P < 0.05$ vs. the S and Sp groups; ¥$P < 0.05$ vs. the A-to-C group.

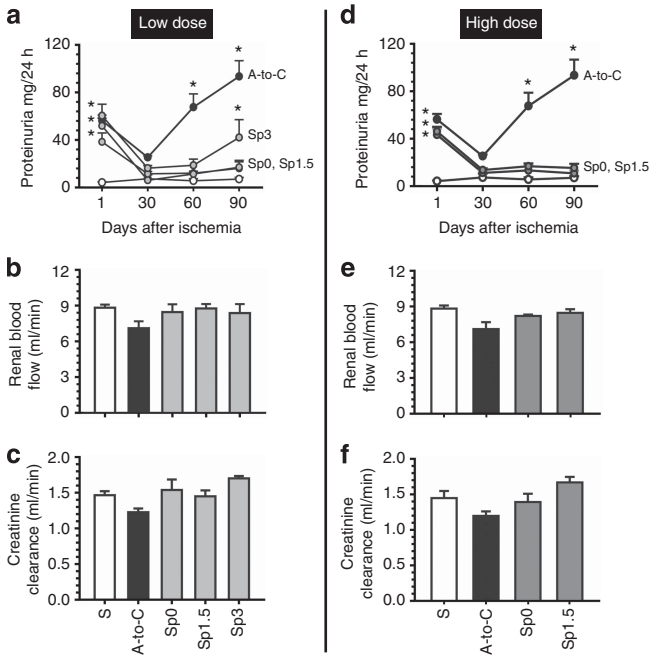

Figure 10 | Spironolactone administration after the ischemic insult prevents the development of proteinuria. (**a**) Urinary protein excretion at 1, 30, 60, and 90 days in sham (white circles), in A-to-C (black circles), and in rats receiving Sp (20 mg/kg) at 0, 1.5, or 3 hours after ischemia (gray circles) or (**d**) treated with a high dose of Sp (80 mg/kg) (dark gray circles) at 0 or 1.5 h after bilateral ischemia. After 90 days of follow-up, (**b**, **e**) renal blood flow and (**c**, **f**) creatinine clearance were determined in the sham group (white bars), A-to-C group (black bars), and the groups receiving a low dose of Sp (gray bars) at 0, 1.5, or 3 h after ischemia or a high dose of Sp (dark gray bars) at 0 or 1.5 h after bilateral ischemia. *$P < 0.05$ vs. sham-operated rats.

Molecular markers of renal fibrosis and inflammation also provided evidence of the protection conferred by spironolactone. The upregulation of TGF-β mRNA levels was prevented or reduced by a low or high dose of spironolactone administered at 0 or 1.5 h after ischemia (Figure 12a and e). However, increased phospho-Smad3 levels remained elevated in rats treated with a low dose, but not with a high dose, of spironolactone (Figure 12b and f). The renoprotective effect of spironolactone was also associated with the prevention of α-SMA and MCP-1 upregulation (Figure 12c–h).

DISCUSSION

In this study, we characterized a rat model of CKD induced by a single episode of AKI. We observed that an episode of AKI was resolved in surviving animals within a period of 10 days. However, although physiological parameters returned to normal values, activation of proinflammatory and profibrotic signals persisted. During the following months, progressive deterioration of renal function and renal structures was observed in rats surviving AKI, leading to the development of CKD. Thus, this model resembles what is currently believed to occur in the clinical setting.[11–13,24–27] Patients who survive an episode of AKI and apparently recover renal function may develop CKD later in life.[8,24] In this study, we observed that spironolactone administration before or after the ischemic insult prevented or significantly diminished the severity of an AKI episode, without signs of proinflammatory or profibrotic activation after 10 days of ischemia. Thus, spironolactone pretreatment resulted in a reduction in rat mortality and in the prevention of CKD. These observations demonstrate the relevance of the prevention of AKI episodes to a reduction in the prevalence of CKD.

CKD development in rats surviving AKI was characterized by a progressive increase in urinary protein excretion, renal dysfunction, glomerular hypertrophy, severe tubular dilation, tubulointerstitial fibrosis, and podocyte injury. Our study supports the hypothesis that an ischemic insult is sufficient to lead to progressive CKD in the rat, despite apparent recovery from the AKI episode. Because it was possible that CKD resulted from irreversible renal artery damage caused by the clamping, a group of rats was studied after 10 days of ischemia, confirming that this was not the case. After 10 days, renal function returned to normal values. Although renal histopathology was not analyzed at this point, we have previously reported that after 3 days of I/R, the tubular epithelium had almost recovered its normal structure.[28,29] However, in this study, we found that profibrotic and inflammatory cytokines remained at high levels despite a return to normal renal function values. In addition, cytokines such as TNF-α and IL-1β, IL-6, IL-12, IL-15, IL-18, and IL-32 are known to be induced as a result of the enhanced leukocyte activation and leukocyte–endothelial adhesion observed after I/R. Moreover, the renal tubular epithelium may generate proinflammatory cytokines such as TNF-α, IL-6, IL-1β, and TGF-β.[30–33] It is important to note that Basile *et al.*[34,35] and Hörbelt *et al.*[36] have demonstrated a persistent reduction in vascular density after I/R that maintains a continuous hypoxic and inflammatory state. Furthermore, Conger *et al.*[37] demonstrated that the postischemic kidney does not properly autoregulate the blood flow. All of these adverse conditions perpetuate continuous cycles of hypoxic damage and inflammation that injure the surrounding tissues and eventually lead to CKD, as has been clearly discussed by Bedfoord *et al.*[38] In agreement with all these findings, we found that, after 9 months, the rats that developed CKD exhibited greater levels of the proinflammatory cytokines compared with the rats that were pretreated with spironolactone. Interestingly, MCP-1 upregulation observed 3 months after ischemia was also prevented when spironolactone was administered after the insult. Our results suggest that the beneficial results of spironolactone in preventing chronic inflammation are a result of its ability to attenuate I/R-induced acute inflammation.

The CKD induced by an AKI episode was characterized by a progressive enhancement in urinary protein excretion and renal dysfunction without changes in mean arterial pressure.

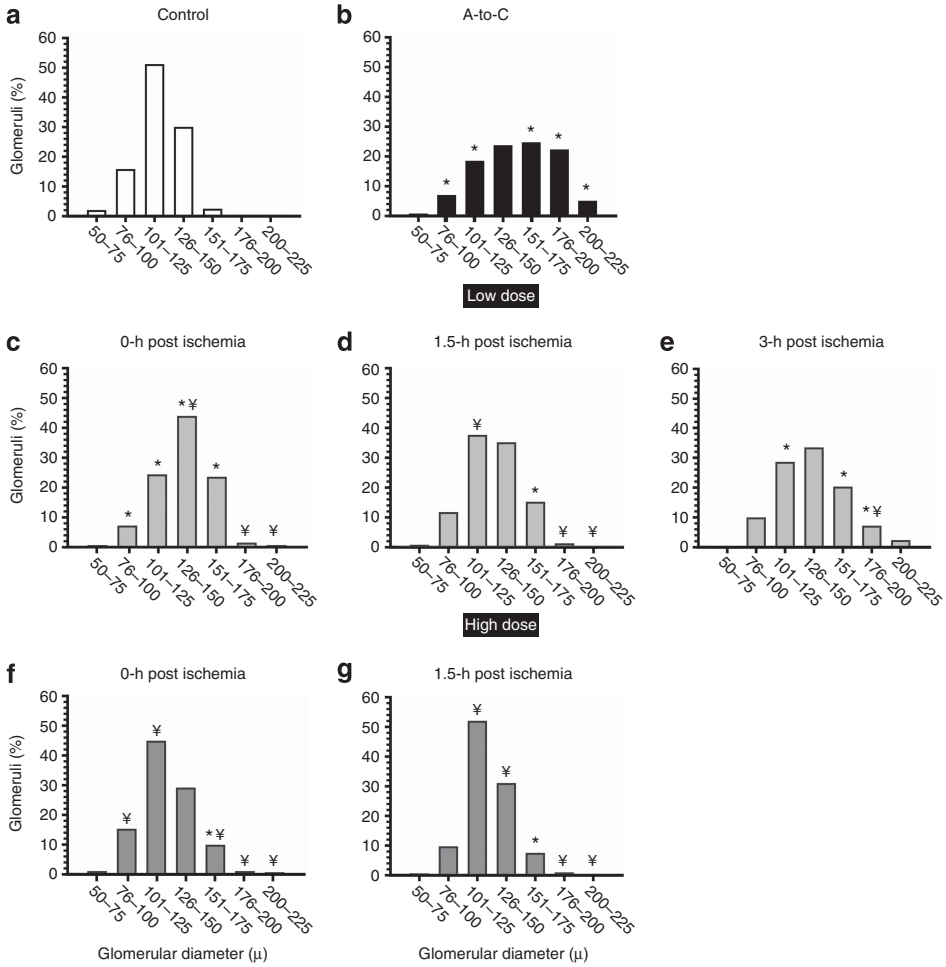

Figure 11 | Glomerular injury is prevented or reduced by spironolactone administration after renal ischemia. Glomerular diameter distribution in sham (white bars), A-to-C (black bars), low spironolactone dose (gray bars), and high spironolactone groups (gray dark bars). *$P<0.05$ vs. the S group and ¥$P<0.05$ vs. the A-to-C group.

These conditions provide us with an experimental model that dissects the detrimental effect of an AKI episode on renal function and structure without changes in blood pressure. Accordingly, the animals that suffered CKD exhibited severe structural injury. Glomerular hypertrophy and glomerulosclerosis were observed 9 months after inducing ischemia. These alterations were also associated with ultrastructural changes. It is plausible that this glomerular injury is a consequence of the endothelial injury and the endothelial-to-mesenchymal transition that occurred after the ischemia.[34,35] Interestingly, in this study, we found that spironolactone administration both before and after renal ischemia prevented the transition of AKI to CKD.

Aldosterone binding to the MR has been suggested to influence endothelial function and vascular tone.[17,19,39,40] Supporting this finding, mice overexpressing MR in the endothelium exhibit altered vascular tone,[40] and aortic wall thickness has been reported in patients with primary hyperaldosteronism.[41] Consistent with this result, aldosterone infusion in mice reduces the expression of glucose-6-phosphate dehydrogenase (G6PDH), a key enzyme in maintaining the balance between nitric oxide and reactive oxygen species production.[42] Therefore, aldosterone has been proposed as a risk factor of vascular injury.[43] The mechanisms involved, however, have not been clearly elucidated. In this regard, we have previously demonstrated that MR antagonism precludes the characteristic hypoperfusion and oxidative stress induced by I/R, suggesting that aldosterone has a pivotal role in mediating renal dysfunction.[16,22] It is possible that the endothelium and the renal plasma flow of spironolactone-treated rats in this study was minimally affected as a consequence of the I/R injury; therefore, the glomerular structure remained unaffected in the long term.

Tubulointerstitial fibrosis is a common feature of CKD progression (for a review, see Rodriguez-Iturbe and Garcia[44]). In fact, severe tubular dilation and an extensive area affected by tubulointerstitial fibrosis were found in the A-to-C group. These results suggest that the tubulointerstitium is more susceptible to the effects of an AKI episode and contributes to the progression and severity of CKD in rats suffering from AKI. Accordingly, the severity of tubular damage reportedly exhibits a more significant correlation

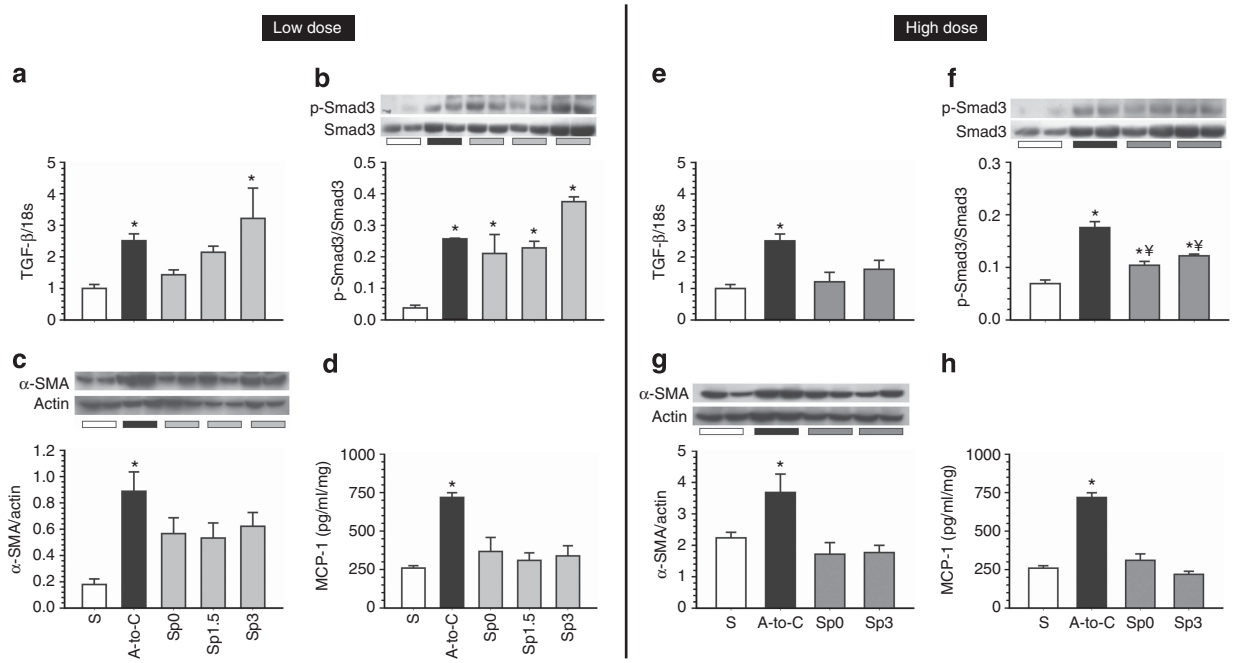

Figure 12 | Tumor growth factor (TGF)-β and inflammation pathways in rats treated with spironolactone after the ischemic insult. (**a**, **e**) TGF-β mRNA levels quantified by real-time reverse transcription–polymerase chain reaction (RT-PCR). Densitometric analysis of the western blots performed for (**b**, **f**) p-Smad3 and (**c**, **g**) α-SMA. (**d**, **h**) MCP-1 protein levels quantified in renal tissue by enzyme-linked immunosorbent assay (ELISA). Sham (white bars), A-to-C (black bars), low Sp dose (gray bars), and high Sp dose (dark gray bars). $^{*}P<0.05$ vs. the S group and $^{¥}P<0.05$ vs. the A-to-C group.

with the reduction in creatinine clearance than with glomerular injury scores.[45,46] These tubular defects were associated with an increase in tubular cell proliferation, as demonstrated by the significant increase in PCNA + staining and by the strong correlation with tubular dilation ($r^2 = 0.87$). In this study, however, the location of PCNA + cells in the epithelium of the dilated tubules strongly suggests that the tubular dilation observed in the A-to-C group was mediated in part by uncontrolled tubular cell proliferation triggered during the regeneration process after the ischemic insult. Although a previous study proposed that the increase in cellular proliferation is a necessary process to regenerate tubular epithelium in a period that typically is completed within 4 weeks after ischemia,[47] recent evidence demonstrated that ischemic, nephrotoxic, and obstructive injuries to the kidney induce a G2/M cell cycle arrest in the proximal tubular epithelial cells, sustaining proliferation indefinitely.[48] In this regard, Wynn[49] has proposed that this cell cycle arrest converts normal epithelial cells to a phenotype that promotes the growth and activation of fibroblasts, turning-on the fibrotic process after an ischemic insult. In addition, TGF-β has been recognized as a key mediator of the genesis of renal fibrosis.[32,50] TGF-β also contributes to the fibrogenesis through inducing epigenetic modifications in fibroblasts in a process that includes the hypermethylation of the gene encoding RASAL1 by the methyltransferase Dnmt1.[51] Accordingly, we found that tubulointerstitial fibrosis developed in the A-to-C group and was associated with increased expression and activation of TGF-β, as evidenced by increases in phospho-Smad3 and its target ECM proteins. Interestingly, activation of the TGF-β signaling pathway was not observed in the animals treated with spironolactone before or after (high dose) ischemia. These data highlight the contribution of TGF-β in mediating renal fibrosis after an ischemic insult. Although Smad2 and Smad3 interact and mediate TGF-β signaling, one recent line of evidence has shown that phospho-Smad2 may act as an antifibrotic effector of the TGF-β pathway.[23] In agreement with those results, the renoprotection conferred by spironolactone was associated with increased levels of phospho-Smad2.

The epithelial-to-mesenchymal transition has been suggested to promote tubulointerstitial fibrosis.[52,53] Under pathological conditions, tubular cells may dedifferentiate into myofibroblasts. TGF-β appears to promote this process by activating the Smad, ILK, and ERK pathways, as observed in tubular cells.[53] To monitor epithelial-to-mesenchymal transition, α-SMA protein levels were measured in the kidney. As expected, the renal fibrosis observed in the A-to-C group was associated with increased α-SMA protein levels. CKD progression has also been linked to an imbalance in free-radical production and antioxidant defense.[44,54] We confirmed that the rats that developed CKD exhibited greater urinary H_2O_2 excretion and a reduction in catalase activity. These changes in α-SMA levels and antioxidant factors were not observed in the A-to-C + Sp group.

In summary, we characterized an experimental model of CKD induced by AKI in the rat. Several mechanisms were responsible for CKD development, including increased

tubular cell proliferation, increased TGF-β pathway activation and oxidative stress, and overexpression of proinflammatory cytokines. By using this model of CKD, we demonstrated that the prevention of AKI with spironolactone completely prevents the progression to CKD. Moreover, we also demonstrate that administering an MR blocker after the ischemic insult also prevented CKD. Our results suggest that the treatment of patients with spironolactone after an AKI episode could be of help in preventing the development of CKD.

MATERIALS AND METHODS

All experiments involving animals were conducted in accordance with the *Guide for the Care and Use of Laboratory Animals* (National Academy Press, Washington, DC, 1996) and were approved by the Animal Care and Use Committee at our Institution.

Protocol 1

In all, 62 male Wistar (weighing 270–300 g) rats were divided into four groups: (1) rats subjected to sham surgery, $n = 9$ (S); (2) rats treated with spironolactone at 20 mg/kg per day by gastric gavage 3 days before sham surgery, $n = 9$ (Sp); (3) rats undergoing bilateral ischemia for 45 min, $n = 28$ (A-to-C); and (4) rats that received spironolactone 3 days before bilateral ischemia, $n = 13$ (A-to-C + Sp). All animals were observed for 9 months. In addition, four rats from the S, A-to-C, and A-to-C + Sp groups were included and observed for 10 days. All animals were kept in a 12:12 h day–night cycle and with free access to water and food.

Protocol 2

Because we recently demonstrated that postischemia MR blockade is beneficial in the prevention of AKI, with the best renoprotection observed in the first 3 h after ischemia,[22] this set of experiments was designed to evaluate whether postischemia spironolactone administration confers protection against the development of CKD. In all, 33 male Wistar (270–315 g) rats were divided into seven groups: sham-operated rats (S); rats subjected to bilateral renal ischemia for 45 min (A–C); and five groups of rats that underwent bilateral renal ischemia for 45 min, but also received one dose of spironolactone at 20 mg/kg by gastric gavage at 0, 1.5, or 3 h after ischemia (A-to-C, 0 h; A-to-C, 1.5 h; and A-to-C, 3 h, respectively), or that received a higher dose of spironolactone (80 mg/kg) at 0 or 1.5 h after ischemia (A-to-C 80, 0 h and A-to-C 80, 1.5 h). These animals were followed up for 3 months.

All other methods are described in the Supplementary Materials online.

Statistical analysis

The results are presented as the mean ± s.e. The significance of the differences between the groups was assessed by analysis of variance (ANOVA) using the Bonferroni correction for multiple comparisons. All of the comparisons passed the normality test. The differences in the ranks of glomerular diameters among the groups were evaluated by contingency analysis, and the differences were assessed using the χ^2 test with the Yates correction. Statistical significance was defined as P–value < 0.05.

DISCLOSURE

All the authors declared no competing interests.

ACKNOWLEDGMENTS

We are grateful to the members of the Molecular Physiology Unit for their suggestions and to Dr Octavio Villanueva for his help with animal care. This project was supported by grants from the Mexican Council of Science and Technology (CONACyT) (101030 and 112780 to NAB) and by the National University of Mexico (IN200909-3 and IN203412-3 to NAB). JBC and RRR are graduate students in the Biomedical Science Ph.D. Program at Universidad Nacional Autónoma de México and were supported by a scholarship from CONACyT-Mexico.

Disclaimer

The results presented in this paper have not been published previously in whole or in part, except as an abstract presented at the Annual Meeting and Scientific Exposition 2011 of the American Society of Nephrology (Philadelphia, PA).

SUPPLEMENTARY MATERIAL

Figure S1. Renal injury observed 90 days after inducing ischemia.
Figure S2. Glomerular and tubular injury is reduced by a low dose of spironolactone administrated after ischemia.
Figure S3. Glomerular and tubular injury is prevented by a high dose of spironolactone administrated after ischemia.
Supplementary material is linked to the online version of the paper at http://www.nature.com/ki

REFERENCES

1. Go AS, Parikh CR, Ikizler TA *et al.* The assessment, serial evaluation, and subsequent sequelae of acute kidney injury (ASSESS-AKI) study: design and methods. *BMC Nephrol* 2010; **11**: 22.
2. Friedewald JJ, Rabb H. Inflammatory cells in ischemic acute renal failure. *Kidney Int* 2004; **66**: 486–491.
3. Okusa MD, Chertow GM, Portilla D. The nexus of acute kidney injury, chronic kidney disease, and World Kidney Day 2009. *Clin J Am Soc Nephrol 2009* **4**: 520–522.
4. Liano F, Pascual J. Epidemiology of acute renal failure: a prospective, multicenter, community-based study. Madrid Acute Renal Failure Study Group. *Kidney Int* 1996; **50**: 811–818.
5. Waikar SS, Curhan GC, Wald R *et al.* Declining mortality in patients with acute renal failure, 1988 to 2002. *J Am Soc Nephrol* 2006; **17**: 1143–1150.
6. Kelly KJ. Acute renal failure: much more than a kidney disease. *Semin Nephrol* 2006; **26**: 105–113.
7. Bonventre JV, Yang L. Cellular pathophysiology of ischemic acute kidney injury. *J Clin Invest* 2011; **121**: 4210–4221.
8. Cerda J, Lameire N, Eggers P *et al.* Epidemiology of acute kidney injury. *Clin J Am Soc Nephrol* 2008; **3**: 881–886.
9. Mosier MJ, Pham TN, Klein MB *et al.* Early acute kidney injury predicts progressive renal dysfunction and higher mortality in severely burned adults. *J Burn Care Res* 2010; **31**: 83–92.
10. Block CA, Schoolwerth AC. Acute renal failure: outcomes and risk of chronic kidney disease. *Minerva Urol Nefrol* **59**: 327–335.
11. Venkatachalam MA, Griffin KA, Lan R *et al.* Acute kidney injury: a springboard for progression in chronic kidney disease. *Am J Physiol Renal Physiol* 2010; **298**: F1078–F1094.
12. Bucaloiu ID, Kirchner HL, Norfolk ER *et al.* Increased risk of death and *de novo* chronic kidney disease following reversible acute kidney injury. *Kidney Int* 2012; **81**: 477–485.
13. Chawla LS, Amdur RL, Amodeo S *et al.* The severity of acute kidney injury predicts progression to chronic kidney disease. *Kidney Int* 2011; **79**: 1361–1369.
14. Macunluoglu B, Arikan H, Atakan A *et al.* Effects of spironolactone in an experimental model of chronic cyclosporine nephrotoxicity. *Transplant Proc* 2008; **40**: 273–278.
15. Thomson AW, McAuley FT, Whiting PH *et al.* Angiotensin-converting enzyme inhibition or aldosterone antagonism reduces cyclosporine nephrotoxicity in the rat. *Transplant Proc* 1987; **19**: 1242–1243.
16. Mejia-Vilet JM, Ramirez V, Cruz C *et al.* Renal ischemia–reperfusion injury is prevented by the mineralocorticoid receptor blocker spironolactone. *Am J Physiol Renal Physiol* 2007; **293**: F78–F86.
17. Ramirez V, Trujillo J, Valdes R *et al.* Adrenalectomy prevents renal ischemia–reperfusion injury. *Am J Physiol Renal Physiol* 2009; **297**: F932–F942.

18. Bobadilla NA, Gamba G. New insights into the pathophysiology of cyclosporine nephrotoxicity: a role of aldosterone. *Am J Physiol Renal Physiol* 2007; **293**: F2–F9.
19. Feria I, Pichardo I, Juarez P *et al.* Therapeutic benefit of spironolactone in experimental chronic cyclosporine A nephrotoxicity. *Kidney Int* 2003; **63**: 43–52.
20. Perez-Rojas JM, Derive S, Blanco JA *et al.* Renocortical mRNA expression of vasoactive factors during spironolactone protective effect in chronic cyclosporine nephrotoxicity. *Am J Physiol Renal Physiol* 2005; **289**: F1020–F1030.
21. Perez-Rojas J, Blanco JA, Cruz C *et al.* Mineralocorticoid receptor blockade confers renoprotection in preexisting chronic cyclosporine nephrotoxicity. *Am J Physiol Renal Physiol* 2007; **292**: F131–F139.
22. Sanchez-Pozos K, Barrera-Chimal J, Garzon-Muvdi J *et al.* Recovery from ischemic acute kidney injury by spironolactone administration. *Nephrol Dial Transplant* 2012; **27**: 3160–3169.
23. Meng XM, Huang XR, Chung AC *et al.* Smad2 protects against TGF-beta/Smad3-mediated renal fibrosis. *J Am Soc Nephrol* 2010; **21**: 1477–1487.
24. Ishani A, Xue JL, Himmelfarb J *et al.* Acute kidney injury increases risk of ESRD among elderly. *J Am Soc Nephrol* 2009; **20**: 223–228.
25. Sharfuddin AA, Molitoris BA. Pathophysiology of ischemic acute kidney injury. *Nat Rev Nephrol* 2011; **7**: 189–200.
26. Coca SG, Yusuf B, Shlipak MG *et al.* Long-term risk of mortality and other adverse outcomes after acute kidney injury: a systematic review and meta-analysis. *Am J Kidney Dis* 2009; **53**: 961–973.
27. Thakar CV, Christianson A, Himmelfarb J *et al.* Acute kidney injury episodes and chronic kidney disease risk in diabetes mellitus. *Clin J Am Soc Nephrol* 2011; **6**: 2567–2572.
28. Barrera-Chimal J, Perez-Villalva R, Cortes-Gonzalez C *et al.* Hsp72 is an early and sensitive biomarker to detect acute kidney injury. *EMBO Mol Med* 2011; **3**: 5–20.
29. Vaidya VS, Ozer JS, Dieterle F *et al.* Kidney injury molecule-1 outperforms traditional biomarkers of kidney injury in preclinical biomarker qualification studies. *Nat Biotechnol* 2010; **28**: 478–485.
30. Donnahoo KK, Meng X, Ayala A *et al.* Early kidney TNF-alpha expression mediates neutrophil infiltration and injury after renal ischemia-reperfusion. *Am J Physiol* 1999; **277**: R922–R929.
31. Donnahoo KK, Meldrum DR, Shenkar R *et al.* Early renal ischemia, with or without reperfusion, activates NFkappaB and increases TNF-alpha bioactivity in the kidney. *J Urol* 2000; **163**: 1328–1332.
32. Lopez-Hernandez FJ, Lopez-Novoa JM. Role of TGF-beta in chronic kidney disease: an integration of tubular, glomerular and vascular effects. *Cell Tissue Res* 2012; **347**: 141–154.
33. Stroo I, Stokman G, Teske GJ *et al.* Chemokine expression in renal ischemia/reperfusion injury is most profound during the reparative phase. *Int Immunol* 2010; **22**: 433–442.
34. Basile DP, Friedrich JL, Spahic J *et al.* Impaired endothelial proliferation and mesenchymal transition contribute to vascular rarefaction following acute kidney injury. *Am J Physiol Renal Physiol* 2011; **300**: F721–F733.
35. Basile DP, Donohoe D, Roethe K *et al.* Renal ischemic injury results in permanent damage to peritubular capillaries and influences long-term function. *Am J Physiol Renal Physiol* 2001; **281**: F887–F899.
36. Horbelt M, Lee SY, Mang HE *et al.* Acute and chronic microvascular alterations in a mouse model of ischemic acute kidney injury. *Am J Physiol Renal Physiol* 2007; **293**: F688–F695.
37. Conger JD, Robinette JB, Hammond WS. Differences in vascular reactivity in models of ischemic acute renal failure. *Kidney Int* 1991; **39**: 1087–1097.
38. Bedford M, Farmer C, Levin A *et al.* Acute kidney injury and CKD: chicken or egg? *Am J Kidney Dis* 2012; **59**: 485–491.
39. Griol-Charhbili V, Fassot C, Messaoudi S *et al.* Epidermal growth factor receptor mediates the vascular dysfunction but not the remodeling induced by aldosterone/salt. *Hypertension* 2011; **57**: 238–244.
40. Nguyen Dinh CA, Griol-Charhbili V, Loufrani L *et al.* The endothelial mineralocorticoid receptor regulates vasoconstrictor tone and blood pressure. *FASEB J* 2010; **24**: 2454–2463.
41. Muiesan ML, Rizzoni D, Salvetti M *et al.* Structural changes in small resistance arteries and left ventricular geometry in patients with primary and secondary hypertension. *J Hypertens* 2002; **20**: 1439–1444.
42. Leopold JA, Dam A, Maron BA *et al.* Aldosterone impairs vascular reactivity by decreasing glucose-6-phosphate dehydrogenase activity. *Nat Med* 2007; **13**: 189–197.
43. Schiffrin EL. Effects of aldosterone on the vasculature. *Hypertension* 2006; **47**: 312–318.
44. Rodriguez-Iturbe B, Garcia GG. The role of tubulointerstitial inflammation in the progression of chronic renal failure. *Nephron Clin Pract* 2010; **116**: c81–c88.
45. Risdon RA, Sloper JC, de Wardener HE. Relationship between renal function and histological changes found in renal-biopsy specimens from patients with persistent glomerular nephritis. *Lancet* 1968; **2**: 363–366.
46. Bohle A, Mackensen-Haen S, von GH *et al.* The consequences of tubulo-interstitial changes for renal function in glomerulopathies. A morphometric and cytological analysis. *Pathol Res Pract* 1990; **186**: 135–144.
47. Shimizu A, Masuda Y, Ishizaki M *et al.* Tubular dilatation in the repair process of ischemic tubular necrosis. *Virchows Arch* 1994; **425**: 281–290.
48. Yang L, Besschetnova TY, Brooks CR *et al.* Epithelial cell cycle arrest in G2/M mediates kidney fibrosis after injury. *Nat Med* 2010; **16**: 535–543.
49. Wynn TA. Fibrosis under arrest. *Nat Med* 2010; **16**: 523–525.
50. Schnaper HW, Jandeska S, Runyan CE *et al.* TGF-beta signal transduction in chronic kidney disease. *Front Biosci* 2009; **14**: 2448–2465.
51. Bechtel W, McGoohan S, Zeisberg EM *et al.* Methylation determines fibroblast activation and fibrogenesis in the kidney. *Nat Med* 2010; **16**: 544–550.
52. Li MX, Liu BC. Epithelial to mesenchymal transition in the progression of tubulointerstitial fibrosis. *Chin Med J (Engl)* 2007; **120**: 1925–1930.
53. Garcia-Sanchez O, Lopez-Hernandez FJ, Lopez-Novoa JM. An integrative view on the role of TGF-beta in the progressive tubular deletion associated with chronic kidney disease. *Kidney Int* 2010; **77**: 950–955.
54. Kao MP, Ang DS, Pall A *et al.* Oxidative stress in renal dysfunction: mechanisms, clinical sequelae and therapeutic options. *J Hum Hypertens* 2010; **24**: 1–8.

Biomarkers, 2012; 17(5): 385–393
© 2012 Informa UK, Ltd.
ISSN 1354-750X print/ISSN 1366-5804 online
DOI: 10.3109/1354750X.2012.680070

COMMENTARY

Are recently reported biomarkers helpful for early and accurate diagnosis of acute kidney injury?

Jonatan Barrera-Chimal and Norma A. Bobadilla

Molecular Physiology Unit, Instituto de Investigaciones Biomédicas, Universidad Nacional Autónoma de México, Mexico City, Mexico and Department of Nephrology Instituto Nacional de Ciencias Médicas y Nutrición Salvador Zubirán, Mexico City, Mexico

Abstract

Over the past few years and with the use of innovative genomic and proteomic tools, several molecules that their urinary concentration is modified during acute kidney injury have been identified and proposed as biomarkers. Among the most studied biomarkers are neutrophil gelatinase-associated lipocalin-2, kidney injury molecule-1, interleukin-18, cystatin C, N-acetyl-β-D-glucosaminidase, liver fatty-acid binding protein, and heat shock protein 72. Here, we reviewed and compared the sensitivity and specificity of each biomarker for the appropriate diagnosis of acute kidney injury, as well as its ability to stratify renal injury and to monitor a renoprotective pharmacologic strategy.

Keywords: NGAL, IL-18, Kim-1, Hsp72, cystatin C, NAG, L-FABP

Introduction

The major causes of acute kidney injury (AKI) are ischaemia/reperfusion (I/R) and nephrotoxic injuries (Friedewald & Rabb 2004). Nearly 15% of hospitalized patients are at risk of developing AKI; however, its incidence increases to 40–60% in patients admitted to the intensive care unit (Kelly 2006). During AKI, many alterations occur at the cellular and molecular levels that finally lead to renal dysfunction and structural injury (Sharfuddin & Molitoris 2011). Despite recent advances in the understanding of AKI pathophysiology, the mortality rate remains elevated mainly because of the lack of effective therapies and early detection of AKI (Wu & Parikh 2008). Furthermore, early treatment of AKI might be correlated with a better prognosis; therefore, the identification of successful biomarkers for early diagnosis, would improve the effectiveness of therapeutic strategies (Yamamoto et al. 2007). In addition, it is imperative to find biomarkers that can correctly stratify the extent of renal injury that each patient suffered because patients who undergo renal dysfunction and tubular damage during AKI are at a high risk of developing chronic kidney disease (CKD) (Siew et al. 2012). The identification of these at-risk patients would allow the clinicians to make an appropriate intervention to ameliorate their prognosis and reduce the risk of a requirement for renal replacement therapy or renal transplant.

Conventional biomarkers for detection of AKI

For many decades, the diagnosis of AKI has been based on an elevation of serum creatinine and blood urea nitrogen (BUN) or the presence of oliguria (Mehta & Chertow 2003). These traditional biomarkers, however, have several shortcomings in establishing an early and sensitive diagnosis of AKI (Bagshaw & Gibney 2008). In the case of creatinine, many factors that modify serum creatinine concentration are not linked to renal injury, such as muscular activity, body weight, age, gender, race, and protein intake. In addition, the elevation of serum creatinine usually occurs from 48 to 72 h after the renal injury has occurred; thus, an early diagnosis based on creatinine elevation is unlikely to be feasible (Coca &

Address for Correspondence: Norma A. Bobadilla, PhD, Unidad de Fisiología Molecular, Vasco de Quiroga No. 15, Tlalpan 14000, México City, Mexico. Tel: +5255–5485-2676. Fax: +5255–5655-0382. E-mail: nab@biomedicas.unam.mx; norma.bobadillas@quetzal.innsz.mx

(Received 15 February 2012; revised 21 March 2012; accepted 24 March 2012)

Parikh 2008). Moreover, a large proportion of the renal tissue may be injured before serum creatinine rises, an outcome that is evidenced in the renal transplantation context, where the kidney donor loses 50% of the total kidney mass without changes in serum creatinine (Herrera & Rodriguez-Iturbe 1998). BUN is also an insensitive AKI marker because its concentration may be altered by non-renal factors, such as a high-protein diet, glucocorticoid therapy or trauma. In addition, in a great number of patients, AKI is developed without loss of excretory function; thus, oliguria might underestimate the number of patients with acute tubular damage (Ronco et al. 2010). In this regard, the identification of novel biomarkers of AKI that would allow for the establishment of an early AKI diagnosis is needed. Once a new biomarker is found, its sensitivity as a reliable and early marker of AKI must be assessed in five critical phases: (i) experimental studies identifying the molecules of which expression or concentration is modified during experimental AKI in mice or rat; (ii) the identification of a reliable and reproducible method to quantify the biomarker in urine samples; (iii) clinical assays to detect the proposed biomarker in samples from patients with clinical AKI and evaluations of the biomarker's ability to detect AKI prior to diagnosis with the conventional methods; (iv) large-scale validation to determine the biomarker's properties, such as sensitivity and specificity; and (v) screening the population with the new biomarker throughout disease treatment, disease evolution and improvement of outcomes (Siew et al. 2011).

Novel biomarkers of AKI

Over the past few years, many studies have focused on the development of early and sensitive biomarkers for AKI. With the use of innovative genomic and proteomic tools, several molecules of which their serum or urine concentration is modified during AKI in experimental models and humans have been identified and proposed as biomarkers. From these studies, nearly 20 molecules have been proposed to serve as biomarkers of AKI. Among the most studied and promising biomarkers are neutrophil gelatinase-associated lipocalin-2 (NGAL), kidney injury molecule-1 (Kim-1), interleukin-18 (IL-18), cystatin C, N-acetyl-β-D-glucosaminidase (NAG), liver fatty-acid binding protein (L-FABP), and heat shock protein 72 (Hsp72).

Neutrophil gelatinase-associated lipocalin-2

NGAL is a 25-kDa protein that is covalently bound to gelatinase from neutrophils and is expressed at low levels in several human tissues, including lung, stomach, colon, and epithelial cells located in the proximal tubule (Cowland & Borregaard 1997; Flower et al. 2000). NGAL is one of the fastest up-regulated proteins after an ischaemic insult in the rat (2 h) as is shown in Table 1 (Mishra et al. 2003). Mori et al. (2005) found that the NGAL concentration displayed a significant increase in plasma and urine by 10-fold and 100-fold, respectively, in patients who suffered from AKI in the intensive care unit (ICU) compared with control humans. These findings indeed showed a substantial elevation of NGAL during an AKI episode. There is also an evidence that NGAL is an early AKI biomarker. Mishra et al. (2005) showed, in a population of children with cardiopulmonary bypass who developed AKI, a 10-fold elevation of NGAL in the urine and plasma 2–6 h after the surgery, whereas the elevation of serum creatinine was observed 1–3 days after the surgery. These observations have also been corroborated in adult populations subjected to cardiopulmonary bypass (CBP) (Parikh et al. 2011a;Tuladhar et al. 2009). As shown in Table 2, NGAL has been extensively studied for the early diagnosis of AKI after cardiac surgery, showing a 100% efficiency in diagnosing AKI at 2 h post-surgery (Bennett et al. 2008; Torregrosa et al. 2012; Matsui et al. 2012). Other studies, however, have reported a lower effectiveness (Han et al. 2002; Wagener et al. 2008; Koyner et al. 2010; Parikh et al. 2011b; Parikh, 2011a; Pechman et al. 2009). Wagener et al. (2009) found that urinary NGAL was consistently elevated after cardiac surgery (1, 3, 8, and 24 h). Unfortunately, NGAL was also elevated in non-AKI patients. The poor effectiveness of NGAL in these patients was evidenced by the low area under the curve (AUC), sensitivity, and specificity (0.67, 69, and 65%, respectively) 3 h after surgery. In the transplantation setting, NGAL seems to show a better performance (Nauta et al. 2011; Jochmans et al. 2011). In a cohort of transplanted patients, NGAL predicted delayed graft function (DGF) at a cut-off value of 1000 ng/mg creatinine with 90% sensibility, 83% specificity, and an AUC of 0.9 (Parikh et al. 2006a). Consequently, the ability of NGAL to predict AKI before serum creatinine elevation has been evaluated in ICU patients (Prabhu et al. 2010; Makris et al. 2009). In a study performed by de Geus et al. (2011), urinary NGAL assessed at ICU admission was able to predict the development of severe AKI with similar efficacy as serum creatinine-derived *estimated glomerular filtration rate* (GFR). Moreover, plasma NGAL quantified in patients in the ICU was a good diagnostic tool for AKI development, with an AUC of 0.78 and with a diagnosis window of 48 h before creatinine-based

Table 1. Comparison of biomarkers performance in: early detection of AKI, renal injury stratification, pharmacological intervention monitoring, recovery of kidney injury and prognosis prediction.

Biomarker	Early Detection	Injury Severity	Pharmacological intervention	Recovery	Prognosis
NGAL	✓	✓	N.D.	✓	✓
Kim-1	x	✓	✓	x	✓
IL-18	✓	✓	N.D.	N.D.	✓
Cystatin C	✓/x	N.D.	N.D.	N.D.	✓
NAG	✓	N.D.	N.D.	N.D.	✓
L-FABP	✓	✓	N.D.	✓	✓
Hsp72	✓	✓	✓	✓	N.D.

Hsp, heat shock protein; IL, interleukin; Kim, kidney injury molecule; L-FABP, liver fatty-acid binding protein; NAG, N-acetyl-β-D-glucosaminidase; N.D., not determined; NGAL, neutrophil gelatinase-associated lipocalin-2.

Table 2. Performance comparison among the biomarkers reviewed in different clinical settings by using the area under the curve reported for each biomarker.

Biomarker	Cardiac surgery (adults)	Cardiac surgery (pediatric)	ICU	Kidney transplantation (DGF)	Nephrotoxic (AKI)
NGAL	0.5/0.57/0.6/0.65/0.77/0.88/0.95/0.98	0.71/0.91	0.77/0.82/0.86/0.86/0.97	0.63/0.85/0.9	0.91/0.92
Kim-1	0.68/0.78/0.91	N.D.	0.9/0.95	0.74	N.D.
IL-18	0.61/0.66/0.72	0.72/0.84	0.62/0.73	0.83/0.9	N.D.
Cystatin C	0.5/0.76/0.86	N.D.	0.62/0.7/0.7/0.72/0.8/0.92	0.74/0.83	0.48
NAG	0.62/0.63/0.75	N.D.	0.84	0.75	N.D.
L-FABP	0.72/0.86	0.77/0.81	0.95	N.D.	N.D.
Hsp72	N.D.	N.D.	N.D.	N.D.	N.D.

DGF, delayed graft function; Hsp, heat shock protein; ICU, intensive care unit; IL, interleukin; Kim, kidney injury molecule; L-FABP, liver fatty-acid binding protein; NAG, N-acetyl-β-D-glucosaminidase; N.D., not determined; NGAL, neutrophil gelatinase-associated lipocalin-2.

diagnosis (Cruz et al. 2010). The ability of NGAL to detect AKI induced by cisplatin has also been evaluated in mice (Mishra et al. 2004). NGAL was up-regulated in the kidney 3 h after a high dose of cisplatin, and interestingly, urinary NGAL concentrations correlated with the dose and duration of cisplatin administration. NGAL urinary concentration can also provide prognostic value for some clinical outcomes, such as initiation of dialysis and mortality (Parikh et al. 2011a). In addition, urinary NGAL level performed well in detecting AKI induced by nephrotoxic agents in humans (Hirsch et al. 2007). An interesting study reported by Haase et al. showed that a cohort of NGAL-positive but normal creatinine patients were 16-fold more likely to undergo dialysis, 3-fold more likely to die during hospitalization, spent 3 more days in the ICU and spent 8 more days at hospital compared with NGAL-negative patients or patients with creatinine elevation (Haase et al. 2011). These findings suggest that NGAL concentration is a biomarker that is capable of detecting subclinical AKI; however, whether subclinical AKI affects prognosis and or long-term effects remains unknown. One disadvantage of the use of this biomarker in the clinical setting is that non-renal NGAL is elevated in response to systemic stress, and thus, urinary NGAL excretion is increased in other pathological conditions or in patients with chronic renal injury without reflecting the presence of AKI (Soni et al. 2010). In fact, serum NGAL is elevated in patients with acute bacterial infections (Alpizar-Alpizar et al. 2009). Although NGAL is an early AKI biomarker, its reduced specificity limits its consistency as an ideal biomarker of AKI.

Kidney injury molecule-1

Kim-1 is a trans-membrane glycoprotein with immunoglobulin and mucin domains. This protein is a phosphatidylserine receptor that recognizes apoptotic cells and confers on epithelial cells the capacity to recognize and phagocytize dead cells that are present after renal ischaemia (Ichimura et al. 2008). Kim-1 is expressed minimally in normal adult rat kidney and is dramatically over-expressed in the S3 segment of the proximal tubule cells after ischaemia/reperfusion (I/R) or nephrotoxic injuries in rat kidneys (Vaidya et al. 2006, 2010). Kim-1 is thought to be expressed in dedifferentiated cells after AKI, as it is also expressed in patients with renal cell carcinoma, a condition that displays cell dedifferentiation (Han et al. 2005). Fortunately, a proteolytically processed ectodomain is easily detected in the urine, facilitating assessment of Kim-1 urinary concentration (Zhang et al. 2007). In fact, in several clinical studies, urinary Kim-1 is higher in patients with AKI than other types of kidney injury, such as CKD (Han et al. 2002; Liangos et al. 2009). Importantly, in patients with recognized AKI, the AUC is 0.90 as is shown in Table 2. However, one study evaluating Kim-1 as an early biomarker reported a poor performance for this protein as is depicted in Table 1 (Han et al. 2008). In spite of the inability of urinary Kim-1 to predict the outcomes after AKI, it has been showed that the urinary Kim-1 and NAG levels could predict the odds for dialysis requirement or hospital death (Liangos et al. 2007). In a population of patients who underwent cardiac surgery, urinary Kim-1 increased significantly compared with non-AKI patients at 2 h after surgery, and after 24 h, the AUC ranged between 0.78 and 0.91 (Table 2). However, Kim-1 performed better in patients with established acute tubular necrosis, with an AUC ranging from 0.9 to 0.95 (Huang & Don-Wauchope 2011). The ability of Kim-1 to predict DGF after kidney transplant has been evaluated by Kim-1 immunohistochemistry. Unexpectedly, the authors did not find any significant correlation between Kim-1 staining and the occurrence of DGF (Schroppel et al. 2010). However, Malyszko et al. (2010) reported that urinary Kim-1 after transplantation provides prognostic information, such as the rate of renal function decline over time, suggesting that although Kim-1 is not an early predictor of DGF, in a long-term context, it may be useful to predict renal dysfunction progression. Kim-1 has also proven successful for diagnosing AKI induced by nephrotoxic agents. In fact, a recent report showed that Kim-1 outperformed serum creatinine, BUN and urinary NAG in multiple rat models of nephrotoxicity, with the best results being observed with cisplatin, gentamicin and kancomycin exposure, suggesting that urinary Kim-1 may facilitate

accurate prediction of human nephrotoxicity in preclinical drug studies (Vaidya et al. 2010). Finally, Kim-1 levels are also valuable for monitoring a renoprotective strategy in an experimental model of chronic cyclosporine nephrotoxicty (Perez-Rojas et al. 2007). Together, these findings indicate that Kim-1 is a better biomarker for diagnosing established AKI than for ascertaining an early diagnosis.

Interleukin-18

IL-18 is a pro-inflammatory cytokine that is up-regulated and cleaved in the proximal tubule during AKI. It is expressed in the intercalated cells of the late distal convoluted tubule, connector and collecting duct. IL-18 is co-expressed with P2X7 and caspase-1, which convert the pro-IL-18 into its active form. Subsequently, IL-18 leaves the cell, and the IL-18 in the tubular epithelium enters the urine (Melnikov et al. 2001; Fantuzzi et al. 1998). Urinary IL-18 level is sensitive in diagnosing established AKI, as its urinary concentration was elevated in patients with acute tubular necrosis, with an AUC of 0.95. However, no elevation is observed in CKD, urinary tract infection, nephrotic syndrome or pre-renal azotaemia (Parikh et al. 2004). For early diagnosis, IL-18 seems to have a low sensitivity but high specificity. However, as is shown in Table 2, inconsistent results have been observed for the ability of IL-18 to predict AKI in post-cardiac surgery patients (Haase et al. 2008; Parikh et al. 2006b; Torregrosa et al. 2012; Parikh et al. 2005; Siew et al. 2010). In a cohort of 1219 adults undergoing cardiac surgery, urinary IL-18 peaked 6 h after the surgery, and the highest urinary IL-18 levels were associated with 6.8-fold increased odds of AKI development, longer hospital and ICU stays and higher risk for dialysis requirement or death (AUC of 0.76 for AKI diagnosis) (Parikh et al. 2011a). The ability of IL-18 to predict DGF was evaluated in 91 transplant patients, in whom DGF was classified as slow graft function or immediate graft function. The median levels of urinary NGAL and IL-18, but not Kim-1, were different between the groups at all time points studied (Hall et al. 2011a). Little is known about the ability of IL-18 to detect AKI induced by nephrotoxic agents. One study reported that IL-18 identified contrast-induced nephropathy (CIN) 24 h earlier than SCr elevation (Ling et al. 2008). All of these data suggest that IL-18 is a suitable biomarker for established AKI but cannot predict AKI after cardiac surgery due to low sensitivity.

Cystatin C

Cystatin C is a cysteine protease inhibitor that is produced by all nucleated cells, is released into the blood at a relatively constant rate, and apparently is not influenced by factors other than GFR. Cystatin C is often considered a marker of GFR because it possesses the main characteristics of an ideal GFR marker: it is freely filtered, completely reabsorbed and not secreted into the renal tubules. In contrast to creatinine, cystatin C levels are not significantly affected by age, gender, race, or muscle mass (Herget-Rosenthal et al. 2004). However, although it is more often recognized as a GFR marker, it seems to be a marker of AKI as well, as renal dysfunction is a main feature of AKI (Zhang et al. 2011; Haase et al. 2009; Nejat et al. 2010; Hall et al. 2011b; Hall et al. 2011a). Indeed, serum cystatin C has been a useful AKI marker in hospitalized patients 24–48 h earlier than serum creatinine elevation but 10 h later than NGAL. Herget-Rosenthal et al. (2004) reported that cystatin C may predict AKI 2 days before serum creatinine elevation in the ICU context. In a post-cardiac surgery paediatric population, increased cystatin C, 6 h after surgery predicted stage 1 and 2 AKI. Moreover, higher cystatin C predicted longer ventilation and ICU stay (Zappitelli et al. 2011). The urinary excretion of cystatin C has shown the ability to predict the requirement for renal replacement therapy in patients with established AKI 2 days earlier than creatinine clearance reduction, with an AUC of 0.72 (Royakkers et al. 2011). However, similar findings were not observed in a paediatric population of kidney transplant recipients because cystatin C was not superior to creatinine for the detection of DGF (Slort et al. 2012). Finally, cystatin C did not show a better performance than serum creatinine in detecting contrast-induced nephropathy (Ribichini et al. 2012). Therefore, cystatin C seems to perform better than serum creatinine in predicting AKI but in lesser proportion than other recently described biomarkers.

N-acetyl-β-D-glucosaminidase

NAG is a lysosomal enzyme found in proximal tubules, and increased activity of this enzyme in the urine suggests injury to tubular cells. Therefore, NAG can serve as specific urinary marker for damaged tubular cells. NAG has proven to be effective for the diagnosis of nephrotoxic renal injury, delayed renal allograft function, chronic glomerular disease, diabetic nephropathy and cardiopulmonary bypass earlier than creatinine elevation (Bazzi et al. 2000; Katagiri et al. 2012). Moreover, higher urinary NAG has been associated with poor outcomes, such as dialysis requirement or death (Liangos et al. 2007). Unfortunately, urinary NAG activity is inhibited by endogenous urea as well as by a number of industrial solvents and heavy metals. Furthermore, increased NAG has been reported in a variety of conditions in the absence of clinically significant AKI, including rheumatoid arthritis, impaired glucose tolerance and hyperthyroidism (Erdener et al. 2005; Tominaga et al. 1989). The insensitivity and non-specificity of NAG may limit its use as a biomarker of AKI. In addition, NAG was reportedly unable to predict the odds of delayed graft function in the transplant context (Moers et al. 2010), but NAG performed better for CIN diagnosis. Ren et al. (2011) reported that amongst 590 patients undergoing diagnostic coronary angiography, a significant increase in urinary NAG was found in 33 patients who developed CIN; this increase occurred 1 or 2 days before serum creatinine elevation. In addition, in an experimental

model of AKI induced by cadmium, Kim-1 increased after 6 weeks of cadmium treatment and continued to increase until 12 weeks; however, no increase of NAG was observed until after 12 weeks of cadmium treatment. Thus, in comparison with Kim-1, NAG performs poorly for diagnosing AKI induced by cadmium (Prozialeck et al. 2009).

Liver fatty acid-binding protein

FABPs are small cytoplasmic proteins of 14 kDa that are abundantly expressed in tissues with active fatty acid metabolism. Two types of FABPs have been isolated from the human kidney: heart-type FABP and liver-type FABP (L-FABP). L-FABP is normally found in the cytoplasm of human proximal tubular cells (Veerkamp et al. 1991). It binds to fatty acids and transports them to mitochondria or peroxisomes, where the fatty acids are β-oxidized, and L-FABP participates in intracellular fatty acid homeostasis. L-FABP is reabsorbed by the proximal tubule via megalin-domain endocytosis and is localized in the cytoplasm of proximal tubular cells, liver cells and small intestine cells (Oyama et al. 2005; Maatman et al. 1992). Recent studies performed in rats have shown that L-FABP is a sensitive biomarker in ischaemic AKI (Negishi et al. 2009). In a cardiovascular surgery setting, Matsui et al. (2011) showed that L-FABP is an early biomarker of AKI and that it is elevated faster than NGAL and NAG, see Table 1. These findings were confirmed by Portilla et al. (2008) in children undergoing cardiac surgery. The increase in urinary L-FABP occurred within 4 h after cardiac surgery and predicted subsequent AKI development with an AUC of 0.81. In the transplant context, urinary L-FABP level correlated well with the ischaemic time of the transplanted kidney and with the length of hospital stay in living related-donor renal transplant recipients (Yamamoto et al. 2007). In addition, Nakamura et al. (2006) reported that baseline urinary L-FABP was significantly higher in those patients who developed contrast nephropathy after coronary angiography; however, the authors did not evaluate the diagnostic performance of urinary L-FABP in predicting AKI. Moreover, a significant elevation of urinary L-FABP was found to exist in established AKI of a variety aetiologies, including acute tubular necrosis, sepsis, and nephrotoxic exposure (Ferguson et al. 2010). In contrast, urinary L-FABP increased proportionally to the dose of cisplatin administrated to the mice and correlated with the tubular injury score.

Heat shock protein 72

Heat shock proteins (Hsps) are up-regulated in response to alterations in cellular homeostasis, as occurs during AKI (Csermely et al. 2007). Particularly, the Hsp70 subfamily are composed of four isoforms: Hsc70 (constitutive isoform), Hsp72 (inducible isoform), mHsp75 and Grp78. Hsp72 is highly induced during AKI such that it constitutes up to 15 % of total cellular protein (Hernadez-Pando et al. 1995; Kelly 2002; Kelly et al. 2001; Molinas et al. 2010). Indeed, Zhang et al. (2008a) reported that Hsp72 is one of the most up-regulated proteins among 30,000 studied proteins in the I/R rat model. This protein is induced in renal tubular cells during AKI, and many of these cells are detached and projected into the urinary space in response to AKI. In a previous study from our laboratory, we reasoned that Hsp72 could be an early and sensitive biomarker to detect AKI (Barrera-Chimal et al. 2011). For this purpose, in rats undergoing different durations of ischaemia (10, 20, 30, 45 or 60 min) to induce different degrees of renal injury, Hsp72 expression progressively increased with the duration of ischaemia. Moreover, in the urine of these animals, Hsp72 concentration increased proportionally to the degree of renal injury, showing a high correlation with the histological injury score, which is the gold standard for monitoring the renal injury induced by I/R. Furthermore, we explored the performance of Hsp72 as an early biomarker of AKI. Rats undergoing to 30 min of ischaemia were randomly sorted into groups of different durations of reperfusion (3–120 h). Urinary Hsp72 was elevated at 3 h of reperfusion, peaked at 18 h and reached normal values at 72 h of reperfusion. Interestingly, this Hsp72 behavior strongly correlated with the histo-pathological findings: starting at 3 h of reperfusion, there was evidence of tubular injury, which peaked at 18 h and began healing after 72 h of reperfusion. These results provide evidence that Hsp72 is an early biomarker of AKI and that it may help in monitoring the regeneration process after AKI. Because we had previously shown that mineralocorticoid receptor blockade with spironolactone or adrenal gland removal is an effective strategy to prevent renal injury induced by spironolactone, we also evaluated the effectiveness of Hsp72 to detect a pharmacological strategy to prevent AKI. A group of animals were pre-treated with different doses of spironolactone 3 days before renal injury induced by renal bilateral ischaemia. Hsp72 was able to monitor the degree of renoprotection conferred by the different doses of spironolactone. In our study, the ability of Hsp72 to monitor the renal injury was compared with NGAL, Kim-1 and IL-18, and we found that Hsp72 was a superior biomarker for the early detection and stratification of AKI, at least in the AKI model induced by renal ischaemia in the rat. Finally, we also showed that Hsp72 seems to be an early biomarker of AKI in humans, because amongst critically ill patients, urinary Hsp72 elevation occurred 24–48 h earlier than serum creatinine elevation in those patients who developed AKI (Barrera-Chimal et al. 2011). Although more clinical studies with more patients are required, Hsp72 seems to be a promising biomarker to detect AKI.

Other biomarkers with potential application in AKI detection

It has been reported that the monocyte chemoattractant protein-1 (MCP-1), a molecule that participates in mediating injury during AKI, can be detected in the urine of mice with AKI induced by maleate and in 10 patients

diagnosed with AKI, in particular this biomarker did not show an overlapping between AKI and no AKI patients (Munshi et al. 2011).

Pro-inflammatory cytokines such as IL-6 and IL-8 were reported to be elevated in serum from patients developing AKI after cardiac surgery and predicted prolonged mechanical ventilation (Liu et al. 2009). In addition, in 25 paediatric patients subjected to CBP, urinary IL-6 increased 6 h after surgery in those patients whom developed AKI with a sensitivity of 88% (Dennen et al. 2010).

Netrin-1 a laminin-like molecule; was observed to be excreted in the urine of mice subjected to I/R or after cisplatin, endotoxin or folic acid nephrotoxicity and in most of the AKI patients included in the study (Reeves et al. 2008). Ramesh et al. (2010) reported that netrin-1 increased 2 h after CBP in patients that developed AKI. The duration and severity of AKI correlated with netrin-1 levels after 6 h of the surgery.

Finally α-Glutathione-S-transferase (α-GST) that is localized in the proximal tubule in the rat and human, was found in the urine of rats after cisplatin induced AKI (Gautier et al. 2010) This enzyme was also assessed in a population of patients after cardiac surgery and it was found that urinary α-GST levels were able to predict the development of AKIN 1 and 3 (Koyner et al. 2010).

Similarity of the performance of various biomarkers in detecting AKI

An ideal biomarker for AKI should exhibit the following characteristics: (i) detect renal injury early, (ii) stratify the degree of renal injury, (iii) screen the effectiveness of a renoprotective intervention and regeneration process, and (iv) help with prognosis prediction. Table 1 compares the performance of the biomarkers discussed here in detecting AKI. Despite many advances in our knowledge about these biomarkers, many features remain to be determined. However, this evaluation allows us to discern how closely the biomarkers fit the ideal performance for detecting AKI. Although Kim-1 seems to be a poor biomarker for early diagnosis of AKI and for monitoring the recovery after renal injury, it appears to be a good biomarker of established AKI. Many issues remain unexplored for IL-18, cystatin C and NAG. Moreover, some studies have shown contradictory results, e.g. regarding cystatin C as an early biomarker of AKI. Although NGAL and L-FABP have shown promise, their ability to monitor a renoprotective intervention remains to be determined. The sensitivity and specificity of each biomarker are variable in the same and in different clinical settings. These discrepancies may be due to the lack of guidelines for cut-off values and standardized testing methods, the timing of the measurements and sample storage protocols. In addition, the AUC analysis sometimes over-estimates a biomarker's performance as a result of its normalisation to urinary creatinine concentration, which is differentially altered under AKI. A summary of the biomarker studies reporting the AUC-ROC analysis in several clinical settings is presented in Table 2. This analysis showed the high variability observed when the same biomarker is used to diagnose AKI in the same clinical context. This issue is reflected in the AUC reported for NGAL in diagnosing AKI after a cardiac surgery, which ranges from 0.5 to 0.95. Despite the variability in AUCs, NGAL seems to be a helpful biomarker because of its early elevation in the patients who will further develop AKI after cardiac surgery and in hospitalized patients in the ICU, as well as its performance in the prediction of DGF after kidney transplant. The performance of the other biomarkers in the early diagnosis of AKI after cardiac surgery seems to be poor compared with NGAL. In the ICU setting, Kim-1 and L-FABP perform well, with AUCs ranging from 0.9 to 0.95. In the kidney transplant field, only one study has reported a low AUC (0.74) for Kim-1. However, other reports studying Kim-1 expression by immunohistochemistry after kidney transplantation have reported opposite results (Schroppel et al. 2010). Zhang et al. (2008b) found that Kim-1 expression correlated with renal function after transplantation whereas Schroppel et al. (2010) showed that Kim-1 did not correlate well. In this regard, IL-18 seems to better predict DGF, and this ability may be due to the inflammatory nature of this clinical condition. Finally, for nephrotoxic AKI, NGAL seems to perform the best. Although other biomarkers have also been studied in different clinical settings, their AUCs were not reported.

All of these studies showed that due to the aetiological diversity, a panel of biomarkers to diagnose AKI may be a better strategy than using a single one. However, cost-effectiveness analyses are also needed to establish whether a panel of biomarkers can be implemented with a favorable clinical-to-economical balance for healthcare systems. Because one of the goals of developing a biomarker is to reduce the extra costs that AKI represents to the health care system in each country (Srisawat et al. 2011). One concern about the sensitivity that a biomarker should have arises from the fact that all biomarkers that display a high sensitivity might identify more patients who are suffering some degree of renal injury (subclinical AKI), but the long-term prognostic value of biomarker results have not been assessed. Thus, the clinical significance of detecting subclinical AKI remains to be determined. Nevertheless, AKI is a risk factor for developing CKD, which underscores the relevance of studying subclinical AKI, given the pandemics of CKD observed in the last few years.

Declaration of interest

The articles cited from our group was supported by research grants No. 112780, 101030 from the Mexican Council of Science and Technology (CONACYT) and by the grant DGAPA IN2009-09-3 from National University of Mexico. The authors report no conflicts of interest.

References

Alpízar-Alpízar W, Laerum OD, Illemann M, Ramírez JA, Arias A, Malespín-Bendaña W, Ramírez V, Lund LR, Borregaard N, Nielsen BS. (2009). Neutrophil gelatinase-associated lipocalin (NGAL/Lcn2) is upregulated in gastric mucosa infected with Helicobacter pylori. *Virchows Arch* 455:225–233.

Bagshaw SM, Gibney RT. (2008). Conventional markers of kidney function. *Crit Care Med* 36:S152–S158.

Barrera-Chimal J, Pérez-Villalva R, Cortés-González C, Ojeda-Cervantes M, Gamba G, Morales-Buenrostro LE, Bobadilla NA. (2011). Hsp72 is an early and sensitive biomarker to detect acute kidney injury. *EMBO Mol Med* 3:5–20.

Bazzi C, Petrini C, Rizza V, Arrigo G, D'Amico G. (2000). A modern approach to selectivity of proteinuria and tubulointerstitial damage in nephrotic syndrome. *Kidney Int* 58:1732–1741.

Bennett M, Dent CL, Ma Q, Dastrala S, Grenier F, Workman R, Syed H, Ali S, Barasch J, Devarajan P. (2008). Urine NGAL predicts severity of acute kidney injury after cardiac surgery: a prospective study. *Clin J Am Soc Nephrol* 3:665–673.

Coca SG, Parikh CR. (2008). Urinary biomarkers for acute kidney injury: perspectives on translation. *Clin J Am Soc Nephrol* 3:481–490.

Cowland JB, Borregaard N. (1997). Molecular characterization and pattern of tissue expression of the gene for neutrophil gelatinase-associated lipocalin from humans. *Genomics* 45:17–23.

Cruz DN, de Cal M, Garzotto F, Perazella MA, Lentini P, Corradi V, Piccinni P, Ronco C. (2010). Plasma neutrophil gelatinase-associated lipocalin is an early biomarker for acute kidney injury in an adult ICU population. *Intensive Care Med* 36:444–451.

Csermely P, Söti C, Blatch GL. (2007). Chaperones as parts of cellular networks. *Adv Exp Med Biol* 594:55–63.

de Geus HR, Bakker J, Lesaffre EM, le Noble JL. (2011). Neutrophil gelatinase-associated lipocalin at ICU admission predicts for acute kidney injury in adult patients. *Am J Respir Crit Care Med* 183:907–914.

Dennen P, Altmann C, Kaufman J, Klein CL, Andres-Hernando A, Ahuja NH, Edelstein CL, Cadnapaphornchai MA, Keniston A, Faubel S. (2010). Urine interleukin-6 is an early biomarker of acute kidney injury in children undergoing cardiac surgery. *Crit Care* 14:R181.

Erdener D, Aksu K, Biçer I, Doganavsargil E, Kutay FZ. (2005). Urinary N-acetyl-beta-D-glucosaminidase (NAG) in lupus nephritis and rheumatoid arthritis. *J Clin Lab Anal* 19:172–176.

Fantuzzi G, Puren AJ, Harding MW, Livingston DJ, Dinarello CA. (1998). Interleukin-18 regulation of interferon gamma production and cell proliferation as shown in interleukin-1beta-converting enzyme (caspase-1)-deficient mice. *Blood* 91:2118–2125.

Ferguson MA, Vaidya VS, Waikar SS, Collings FB, Sunderland KE, Gioules CJ, Bonventre JV. (2010). Urinary liver-type fatty acid-binding protein predicts adverse outcomes in acute kidney injury. *Kidney Int* 77:708–714.

Flower DR, North AC, Sansom CE. (2000). The lipocalin protein family: structural and sequence overview. *Biochim Biophys Acta* 1482:9–24.

Friedewald JJ, Rabb H. (2004). Inflammatory cells in ischemic acute renal failure. *Kidney Int* 66:486–491.

Gautier JC, Riefke B, Walter J, Kurth P, Mylecraine L, Guilpin V, Barlow N, Gury T, Hoffman D, Ennulat D, Schuster K, Harpur E, Pettit S. (2010). Evaluation of novel biomarkers of nephrotoxicity in two strains of rat treated with Cisplatin. *Toxicol Pathol* 38:943–956.

Haase M, Bellomo R, Story D, Davenport P, Haase-Fielitz A. (2008). Urinary interleukin-18 does not predict acute kidney injury after adult cardiac surgery: a prospective observational cohort study. *Crit Care* 12:R96.

Haase M, Bellomo R, Devarajan P, Ma Q, Bennett MR, Möckel M, Matalanis G, Dragun D, Haase-Fielitz A. (2009). Novel biomarkers early predict the severity of acute kidney injury after cardiac surgery in adults. *Ann Thorac Surg* 88:124–130.

Haase M, Devarajan P, Haase-Fielitz A, Bellomo R, Cruz DN, Wagener G, Krawczeski CD, Koyner JL, Murray P, Zappitelli M, Goldstein SL, Makris K, Ronco C, Martensson J, Martling CR, Venge P, Siew E, Ware LB, Ikizler TA, Mertens PR. (2011). The outcome of neutrophil gelatinase-associated lipocalin-positive subclinical acute kidney injury: a multicenter pooled analysis of prospective studies. *J Am Coll Cardiol* 57:1752–1761.

Hall IE, Doshi MD, Poggio ED, Parikh CR. (2011a). A comparison of alternative serum biomarkers with creatinine for predicting allograft function after kidney transplantation. *Transplantation* 91:48–56.

Hall IE, Koyner JL, Doshi MD, Marcus RJ, Parikh CR. (2011b). Urine cystatin C as a biomarker of proximal tubular function immediately after kidney transplantation. *Am J Nephrol* 33:407–413.

Han WK, Alinani A, Wu CL, Michaelson D, Loda M, McGovern FJ, Thadhani R, Bonventre JV. (2005). Human kidney injury molecule-1 is a tissue and urinary tumor marker of renal cell carcinoma. *J Am Soc Nephrol* 16:1126–1134.

Han WK, Bailly V, Abichandani R, Thadhani R, Bonventre JV. (2002). Kidney Injury Molecule-1 (KIM-1): a novel biomarker for human renal proximal tubule injury. *Kidney Int* 62:237–244.

Han WK, Waikar SS, Johnson A, Betensky RA, Dent CL, Devarajan P, Bonventre JV. (2008). Urinary biomarkers in the early diagnosis of acute kidney injury. *Kidney Int* 73:863–869.

Herget-Rosenthal S, Marggraf G, Hüsing J, Göring F, Pietruck F, Janssen O, Philipp T, Kribben A. (2004). Early detection of acute renal failure by serum cystatin C. *Kidney Int* 66:1115–1122.

Hernádez-Pando R, Pedraza-Chaverri J, Orozco-Estévez H, Silva-Serna P, Moreno I, Rondán-Zárate A, Elinos M, Correa-Rotter R, Larriva-Sahd J. (1995). Histological and subcellular distribution of 65 and 70 kD heat shock proteins in experimental nephrotoxic injury. *Exp Toxicol Pathol* 47:501–508.

Herrera J, Rodríguez-Iturbe B. (1998). Stimulation of tubular secretion of creatinine in health and in conditions associated with reduced nephron mass. Evidence for a tubular functional reserve. *Nephrol Dial Transplant* 13:623–629.

Hirsch R, Dent C, Pfriem H, Allen J, Beekman RH 3rd, Ma Q, Dastrala S, Bennett M, Mitsnefes M, Devarajan P. (2007). NGAL is an early predictive biomarker of contrast-induced nephropathy in children. *Pediatr Nephrol* 22:2089–2095.

Huang Y, Don-Wauchope AC. (2011). The clinical utility of kidney injury molecule 1 in the prediction, diagnosis and prognosis of acute kidney injury: a systematic review. *Inflamm Allergy Drug Targets* 10:260–271.

Ichimura T, Asseldonk EJ, Humphreys BD, Gunaratnam L, Duffield JS, Bonventre JV. (2008). Kidney injury molecule-1 is a phosphatidylserine receptor that confers a phagocytic phenotype on epithelial cells. *J Clin Invest* 118:1657–1668.

Jochmans I, Lerut E, van Pelt J, Monbaliu D, Pirenne J. (2011). Circulating AST, H-FABP, and NGAL are early and accurate biomarkers of graft injury and dysfunction in a preclinical model of kidney transplantation. *Ann Surg* 254:784–91; discussion 791.

Katagiri D, Doi K, Honda K, Negishi K, Fujita T, Hisagi M, Ono M, Matsubara T, Yahagi N, Iwagami M, Ohtake T, Kobayashi S, Sugaya T, Noiri E. (2012). Combination of two urinary biomarkers predicts acute kidney injury after adult cardiac surgery. *Ann Thorac Surg* 93:577–583.

Kelly KJ. (2002). Stress response proteins and renal ischemia. *Minerva Urol Nefrol* 54:81–91.

Kelly KJ. (2006). Acute renal failure: much more than a kidney disease. *Semin Nephrol* 26:105–113.

Kelly KJ, Baird NR, Greene AL. (2001). Induction of stress response proteins and experimental renal ischemia/reperfusion. *Kidney Int* 59:1798–1802.

Koyner JL, Vaidya VS, Bennett MR, Ma Q, Worcester E, Akhter SA, Raman J, Jeevanandam V, O'Connor MF, Devarajan P, Bonventre JV, Murray PT. (2010). Urinary biomarkers in the clinical prognosis and early detection of acute kidney injury. *Clin J Am Soc Nephrol* 5:2154–2165.

Liangos O, Perianayagam MC, Vaidya VS, Han WK, Wald R, Tighiouart H, MacKinnon RW, Li L, Balakrishnan VS, Pereira BJ, Bonventre JV, Jaber BL. (2007). Urinary N-acetyl-beta-(D)-glucosaminidase activity and kidney injury molecule-1 level are associated with adverse outcomes in acute renal failure. *J Am Soc Nephrol* 18:904–912.

Liangos O, Tighiouart H, Perianayagam MC, Kolyada A, Han WK, Wald R, Bonventre JV, Jaber BL. (2009). Comparative analysis of urinary biomarkers for early detection of acute kidney injury following cardiopulmonary bypass. *Biomarkers* 14:423–431.

Ling W, Zhaohui N, Ben H, Leyi G, Jianping L, Huili D, Jiaqi Q. (2008). Urinary IL-18 and NGAL as early predictive biomarkers in contrast-induced nephropathy after coronary angiography. *Nephron Clin Pract* 108:c176–c181.

Liu KD, Altmann C, Smits G, Krawczeski CD, Edelstein CL, Devarajan P, Faubel S. (2009). Serum interleukin-6 and interleukin-8 are early biomarkers of acute kidney injury and predict prolonged mechanical ventilation in children undergoing cardiac surgery: a case-control study. *Crit Care* 13:R104.

Maatman RG, van de Westerlo EM, van Kuppevelt TH, Veerkamp JH. (1992). Molecular identification of the liver- and the heart-type fatty acid-binding proteins in human and rat kidney. Use of the reverse transcriptase polymerase chain reaction. *Biochem J* 288 (Pt 1):285–290.

Makris K, Markou N, Evodia E, Dimopoulou E, Drakopoulos I, Ntetsika K, Rizos D, Baltopoulos G, Haliassos A. (2009). Urinary neutrophil gelatinase-associated lipocalin (NGAL) as an early marker of acute kidney injury in critically ill multiple trauma patients. *Clin Chem Lab Med* 47:79–82.

Malyszko J, Koc-Zorawska E, Malyszko JS, Mysliwiec M. (2010). Kidney injury molecule-1 correlates with kidney function in renal allograft recipients. *Transplant Proc* 42:3957–3959.

Matsui K, Kamijo-Ikemori A, Sugaya T, Yasuda T, Kimura K. (2012). Usefulness of urinary biomarkers in early detection of acute kidney injury after cardiac surgery in adults. *Circ J* 76:213–220.

Mehta RL, Chertow GM. (2003). Acute renal failure definitions and classification: time for change? *J Am Soc Nephrol* 14: 2178–2187.

Melnikov VY, Ecder T, Fantuzzi G, Siegmund B, Lucia MS, Dinarello CA, Schrier RW, Edelstein CL. (2001). Impaired IL-18 processing protects caspase-1-deficient mice from ischemic acute renal failure. *J Clin Invest* 107:1145–1152.

Mishra J, Ma Q, Prada A, Mitsnefes M, Zahedi K, Yang J, Barasch J, Devarajan P. (2003). Identification of neutrophil gelatinase-associated lipocalin as a novel early urinary biomarker for ischemic renal injury. *J Am Soc Nephrol* 14:2534–2543.

Mishra J, Mori K, Ma Q, Kelly C, Barasch J, Devarajan P. (2004). Neutrophil gelatinase-associated lipocalin: a novel early urinary biomarker for cisplatin nephrotoxicity. *Am J Nephrol* 24:307–315.

Mishra J, Dent C, Tarabishi R, Mitsnefes MM, Ma Q, Kelly C, Ruff SM, Zahedi K, Shao M, Bean J, Mori K, Barasch J, Devarajan P. (2005). Neutrophil gelatinase-associated lipocalin (NGAL) as a biomarker for acute renal injury after cardiac surgery. *Lancet* 365: 1231–1238.

Moers C, Varnav OC, van Heurn E, Jochmans I, Kirste GR, Rahmel A, Leuvenink HG, Squifflet JP, Paul A, Pirenne J, van Oeveren W, Rakhorst G, Ploeg RJ. (2010). The value of machine perfusion perfusate biomarkers for predicting kidney transplant outcome. *Transplantation* 90:966–973.

Molinas SM, Rosso M, Wayllace NZ, Pagotto MA, Pisani GB, Monasterolo LA, Trumper L. (2010). Heat shock protein 70 induction and its urinary excretion in a model of acetaminophen nephrotoxicity. *Pediatr Nephrol* 25:1245–1253.

Mori K, Lee HT, Rapoport D, Drexler IR, Foster K, Yang J, Schmidt-Ott KM, Chen X, Li JY, Weiss S, Mishra J, Cheema FH, Markowitz G, Suganami T, Sawai K, Mukoyama M, Kunis C, D'Agati V, Devarajan P, Barasch J. (2005). Endocytic delivery of lipocalin-siderophore-iron complex rescues the kidney from ischemia-reperfusion injury. *J Clin Invest* 115:610–621.

Munshi R, Johnson A, Siew ED, Ikizler TA, Ware LB, Wurfel MM, Himmelfarb J, Zager RA. (2011). MCP-1 gene activation marks acute kidney injury. *J Am Soc Nephrol* 22:165–175.

Nakamura T, Sugaya T, Node K, Ueda Y, Koide H. (2006). Urinary excretion of liver-type fatty acid-binding protein in contrast medium-induced nephropathy. *Am J Kidney Dis* 47:439–444.

Nauta FL, Bakker SJ, van Oeveren W, Navis G, van der Heide JJ, van Goor H, de Jong PE, Gansevoort RT. (2011). Albuminuria, proteinuria, and novel urine biomarkers as predictors of long-term allograft outcomes in kidney transplant recipients. *Am J Kidney Dis* 57:733–743.

Negishi K, Noiri E, Doi K, Maeda-Mamiya R, Sugaya T, Portilla D, Fujita T. (2009). Monitoring of urinary L-type fatty acid-binding protein predicts histological severity of acute kidney injury. *Am J Pathol* 174:1154–1159.

Nejat M, Pickering JW, Walker RJ, Westhuyzen J, Shaw GM, Frampton CM, Endre ZH. (2010). Urinary cystatin C is diagnostic of acute kidney injury and sepsis, and predicts mortality in the intensive care unit. *Crit Care* 14:R85.

Oyama Y, Takeda T, Hama H, Tanuma A, Iino N, Sato K, Kaseda R, Ma M, Yamamoto T, Fujii H, Kazama JJ, Odani S, Terada Y, Mizuta K, Gejyo F, Saito A. (2005). Evidence for megalin-mediated proximal tubular uptake of L-FABP, a carrier of potentially nephrotoxic molecules. *Lab Invest* 85:522–531.

Parikh CR, Jani A, Melnikov VY, Faubel S, Edelstein CL. (2004). Urinary interleukin-18 is a marker of human acute tubular necrosis. *Am J Kidney Dis* 43:405–414.

Parikh CR, Abraham E, Ancukiewicz M, Edelstein CL. (2005). Urine IL-18 is an early diagnostic marker for acute kidney injury and predicts mortality in the intensive care unit. *J Am Soc Nephrol* 16:3046–3052.

Parikh CR, Jani A, Mishra J, Ma Q, Kelly C, Barasch J, Edelstein CL, Devarajan P. (2006). Urine NGAL and IL-18 are predictive biomarkers for delayed graft function following kidney transplantation. *Am J Transplant* 6:1639–1645.

Parikh CR, Mishra J, Thiessen-Philbrook H, Dursun B, Ma Q, Kelly C, Dent C, Devarajan P, Edelstein CL. (2006). Urinary IL-18 is an early predictive biomarker of acute kidney injury after cardiac surgery. *Kidney Int* 70:199–203.

Parikh CR, Devarajan P, Zappitelli M, Sint K, Thiessen-Philbrook H, Li S, Kim RW, Koyner JL, Coca SG, Edelstein CL, Shlipak MG, Garg AX, Krawczeski CD. (2011a). Postoperative biomarkers predict acute kidney injury and poor outcomes after adult cardiac surgery. *J Am Soc Nephrol* 22:1748–1757.

Parikh CR, Devarajan P, Zappitelli M, Sint K, Thiessen-Philbrook H, Li S, Kim RW, Koyner JL, Coca SG, Edelstein CL, Shlipak MG, Garg AX, Krawczeski CD. (2011b). Postoperative biomarkers predict acute kidney injury and poor outcomes after pediatric cardiac surgery. *J Am Soc Nephrol* 22:1737–1747.

Pechman KR, De Miguel C, Lund H, Leonard EC, Basile DP, Mattson DL. (2009). Recovery from renal ischemia-reperfusion injury is associated with altered renal hemodynamics, blunted pressure natriuresis, and sodium-sensitive hypertension. *Am J Physiol Regul Integr Comp Physiol* 297:R1358–R1363.

Pérez-Rojas J, Blanco JA, Cruz C, Trujillo J, Vaidya VS, Uribe N, Bonventre JV, Gamba G, Bobadilla NA. (2007). Mineralocorticoid receptor blockade confers renoprotection in preexisting chronic cyclosporine nephrotoxicity. *Am J Physiol Renal Physiol* 292:F131–F139.

Portilla D, Dent C, Sugaya T, Nagothu KK, Kundi I, Moore P, Noiri E, Devarajan P. (2008). Liver fatty acid-binding protein as a biomarker of acute kidney injury after cardiac surgery. *Kidney Int* 73:465–472.

Prabhu A, Sujatha DI, Ninan B, Vijayalakshmi MA. (2010). Neutrophil gelatinase associated lipocalin as a biomarker for acute kidney injury in patients undergoing coronary artery bypass grafting with cardiopulmonary bypass. *Ann Vasc Surg* 24:525–531.

Prozialeck WC, Edwards JR, Vaidya VS, Bonventre JV. (2009). Preclinical evaluation of novel urinary biomarkers of cadmium nephrotoxicity. *Toxicol Appl Pharmacol* 238:301–305.

Ramesh G, Krawczeski CD, Woo JG, Wang Y, Devarajan P. (2010). Urinary netrin-1 is an early predictive biomarker of acute kidney injury after cardiac surgery. *Clin J Am Soc Nephrol* 5:395–401.

Reeves WB, Kwon O, Ramesh G. (2008). Netrin-1 and kidney injury. II. Netrin-1 is an early biomarker of acute kidney injury. *Am J Physiol Renal Physiol* 294:F731–F738.

Ren L, Ji J, Fang Y, Jiang SH, Lin YM, Bo J, Qian JY, Xu XH, Ding XQ. (2011). Assessment of urinary N-acetyl-ß-glucosaminidase as an early marker of contrast-induced nephropathy. *J Int Med Res* 39:647–653.

Ribichini F, Gambaro G, Graziani MS, Pighi M, Pesarini G, Pasoli P, Anselmi M, Ferrero V, Yabarek T, Sorio A, Rizzotti P, Lupo A, Vassanelli C. (2012). Comparison of serum creatinine and cystatin C for early diagnosis of contrast-induced nephropathy after coronary angiography and interventions. *Clin Chem* 58:458–464.

Ronco C, Grammaticopoulos S, Rosner M, de Cal M, Soni S, Lentini P, Piccinni P. (2010). Oliguria, creatinine and other biomarkers of acute kidney injury. *Contrib Nephrol* 164:118–127.

Royakkers AA, Korevaar JC, van Suijlen JD, Hofstra LS, Kuiper MA, Spronk PE, Schultz MJ, Bouman CS. (2011). Serum and urine cystatin C are poor biomarkers for acute kidney injury and renal replacement therapy. *Intensive Care Med* 37:493–501.

Schröppel B, Krüger B, Walsh L, Yeung M, Harris S, Garrison K, Himmelfarb J, Lerner SM, Bromberg JS, Zhang PL, Bonventre JV, Wang Z, Farris AB, Colvin RB, Murphy BT, Vella JP. (2010). Tubular expression of KIM-1 does not predict delayed function after transplantation. *J Am Soc Nephrol* 21:536–542.

Sharfuddin AA, Molitoris BA. (2011). Pathophysiology of ischemic acute kidney injury. *Nat Rev Nephrol* 7:189–200.

Siew ED, Ikizler TA, Gebretsadik T, Shintani A, Wickersham N, Bossert F, Peterson JF, Parikh CR, May AK, Ware LB. (2010). Elevated urinary IL-18 levels at the time of ICU admission predict adverse clinical outcomes. *Clin J Am Soc Nephrol* 5:1497–1505.

Siew ED, Peterson JF, Eden SK, Hung AM, Speroff T, Ikizler TA, Matheny ME. (2012). Outpatient nephrology referral rates after acute kidney injury. *J Am Soc Nephrol* 23:305–312.

Siew ED, Ware LB, Ikizler TA. (2011). Biological markers of acute kidney injury. *J Am Soc Nephrol* 22:810–820.

Slort PR, Ozden N, Pape L, Offner G, Tromp WF, Wilhelm AJ, Bokenkamp A. (2012). Comparing cystatin C and creatinine in the diagnosis of pediatric acute renal allograft dysfunction. *Pediatr Nephrol* 27:843–849.

Soni SS, Cruz D, Bobek I, Chionh CY, Nalesso F, Lentini P, de Cal M, Corradi V, Virzi G, Ronco C. (2010). NGAL: a biomarker of acute kidney injury and other systemic conditions. *Int Urol Nephrol* 42:141–150.

Srisawat N, Wen X, Lee M, Kong L, Elder M, Carter M, Unruh M, Finkel K, Vijayan A, Ramkumar M, Paganini E, Singbartl K, Palevsky PM, Kellum JA. (2011). Urinary biomarkers and renal recovery in critically ill patients with renal support. *Clin J Am Soc Nephrol* 6:1815–1823.

Tominaga M, Fujiyama K, Hoshino T, Tanaka Y, Takeuchi T, Honda M, Mokuda O, Ikeda T, Mashiba H. (1989). Urinary N-acetyl-beta-D-glucosaminidase in the patients with hyperthyroidism. *Horm Metab Res* 21:438–440.

Torregrosa I, Montoliu C, Urios A, Elmlili N, Puchades MJ, Solís MA, Sanjuán R, Blasco ML, Ramos C, Tomás P, Ribes J, Carratalá A, Juan I, Miguel A. (2012). Early biomarkers of acute kidney failure after heart angiography or heart surgery in patients with acute coronary syndrome or acute heart failure. *Nefrologia* 32:44–52.

Tuladhar SM, Püntmann VO, Soni M, Punjabi PP, Bogle RG. (2009). Rapid detection of acute kidney injury by plasma and urinary neutrophil gelatinase-associated lipocalin after cardiopulmonary bypass. *J Cardiovasc Pharmacol* 53:261–266.

Vaidya VS, Ozer JS, Dieterle F, Collings FB, Ramirez V, Troth S, Muniappa N, Thudium D, Gerhold D, Holder DJ, Bobadilla NA, Marrer E, Perentes E, Cordier A, Vonderscher J, Maurer G, Goering PL, Sistare FD, Bonventre JV. (2010). Kidney injury molecule-1 outperforms traditional biomarkers of kidney injury in preclinical biomarker qualification studies. *Nat Biotechnol* 28:478–485.

Vaidya, VS, Ramirez, V, Ichimura, T, Bobadilla, NA, Bonventre, JV. (2006). Urinary kidney injury molecule-1: a sensitive quantitative biomarker for early detection of kidney tubular injury. *Am J Physiol Renal Physiol* 290:F517–F529.

Veerkamp JH, Peeters RA, Maatman RG. (1991). Structural and functional features of different types of cytoplasmic fatty acid-binding proteins. *Biochim Biophys Acta* 1081:1–24.

Wagener G, Gubitosa G, Wang S, Borregaard N, Kim M, Lee HT. (2008). Urinary neutrophil gelatinase-associated lipocalin and acute kidney injury after cardiac surgery. *Am J Kidney Dis* 52:425–433.

Wagener G, Gubitosa G, Wang S, Borregaard N, Kim M, Lee HT. (2009). A comparison of urinary neutrophil gelatinase-associated lipocalin in patients undergoing on- versus off-pump coronary artery bypass graft surgery. *J Cardiothorac Vasc Anesth* 23:195–199.

Wu I, Parikh CR. (2008). Screening for kidney diseases: older measures versus novel biomarkers. *Clin J Am Soc Nephrol* 3:1895–1901.

Yamamoto T, Noiri E, Ono Y, Doi K, Negishi K, Kamijo A, Kimura K, Fujita T, Kinukawa T, Taniguchi H, Nakamura K, Goto M, Shinozaki N, Ohshima S, Sugaya T. (2007). Renal L-type fatty acid–binding protein in acute ischemic injury. *J Am Soc Nephrol* 18:2894–2902.

Zappitelli M, Krawczeski CD, Devarajan P, Wang Z, Snt K, Thiessen-Philbrook H, Li S, Bennett MR, Ma Q, Shlipak MG, Garg AX, Parikh CR; TRIBE-AKI consortium. (2011). Early postoperative serum cystatin C predicts severe acute kidney injury following pediatric cardiac surgery. *Kidney Int* 80:655–662.

Zhang Z, Humphreys BD, Bonventre JV. (2007). Shedding of the urinary biomarker kidney injury molecule-1 (KIM-1) is regulated by MAP kinases and juxtamembrane region. *J Am Soc Nephrol* 18:2704–2714.

Zhang PL, Lun M, Schworer CM, Blasick TM, Masker KK, Jones JB, Carey DJ. (2008a). Heat shock protein expression is highly sensitive to ischemia-reperfusion injury in rat kidneys. *Ann Clin Lab Sci* 38:57–64.

Zhang PL, Rothblum LI, Han WK, Blasick TM, Potdar S, Bonventre JV. (2008b). Kidney injury molecule-1 expression in transplant biopsies is a sensitive measure of cell injury. *Kidney Int* 73:608–614.

Zhang Z, Lu B, Sheng X, Jin N. (2011). Cystatin C in prediction of acute kidney injury: a systemic review and meta-analysis. *Am J Kidney Dis* 58:356–365.

Original Paper

Cellular Physiology and Biochemistry

Cell Physiol Biochem 2010;26:657-668

Accepted: July 30, 2010

Opposite Effect of Hsp90α and Hsp90β on eNOS Ability to Produce Nitric Oxide or Superoxide Anion in Human Embryonic Kidney Cells

Cesar Cortes-González[1,2], Jonatan Barrera-Chimal[1,2], María Ibarra-Sánchez[1,3], Mark Gilbert[1,2], Gerardo Gamba[1,2,4], Alejandro Zentella[1,3], María Elena Flores[1] and Norma A. Bobadilla[1,2]

Molecular Physiology Unit, [1]Instituto de Investigaciones Biomédicas, Universidad Nacional Autónoma de México, Departments of [2]Nephrology and [3]Biochemestry Instituto Nacional de Ciencias Médicas y Nutrición Salvador Zubirán and [4]Instituto Nacional de Cardiología Ignacio Chávez, Mexico City

Key Words

eNOS phosphorylation • Monomer/dimer ratio • AKT/PKB • eNOS dimerization

Abstract

Heat shock protein 90 subfamily is composed by two cytosolic isoforms known as Hsp90α and Hsp90β. Endothelial nitric oxide synthase (eNOS) is regulated by Hsp90, however the specific role of each Hsp90 isoform on NO production has not been established. This study was designed to evaluate the effect of Hsp90α and Hsp90β over-expression on eNOS/NO pathway. Rat Hsp90α and Hsp90β were cloned into pcDNA3.1(+) and transfected in human embryonic kidney cells (HEK-293). Hsp90α and Hsp90β transfection was corroborated by Western blot analysis and their effect on NO production (NO_2/NO_3), eNOS protein and its phosphorylation at Ser1177 and Thr495, as well as Akt/PKB Ser473 phosphorylation was determined. The interaction of Hsp90α and Hsp90β with eNOS and the dimer/monomer ratio of Hsp90, as well as O_2^- generation were also assessed. After transfection, Hsp90α and Hsp90β levels were significantly increased in HEK-293 cells. The Hsp90α over-expression induced a significant increase in NO_2/NO_3 levels, an effect that was associated with increased phosphorylation of eNOS Ser 1177 and Akt/PKB Ser473, as well as with a greater Hsp90α dimerization. Noteworthy, pcHsp90β transfection reduced significantly NO_2/NO_3 and increased O_2^- generation. These effects were associated with a reduction of eNOS dimeric conformation, increased eNOS Thr495 phosphorylation, reduced Akt/PKB phosphorylation, and by a greater amount of monomeric Hsp90β conformation. These data show for first time that Hsp90α and Hsp90β differentially modulate NO and O_2^- generation by eNOS through promoting changes in eNOS conformation and phosphorylation state.

Introduction

The heat shock protein subfamily of 90 kDa belongs to a group of highly conserved stress proteins and it is one of the most abundant proteins in eukaryotic cells, comprising 1-2% of the total protein under non-stress conditions [1]. Five isoforms of Hsp90 have been identified that differ in their cellular localization and abundance. In particular, Hsp90α and Hsp90β are the major cytosolic isoforms, sharing approximately 85% sequence identity

KARGER

Fax +41 61 306 12 34
E-Mail karger@karger.ch
www.karger.com

1015-8987/10/0265-0657$26.00/0

Accessible online at:
www.karger.com/cpb

Norma A. Bobadilla, PhD
Unidad de Fisiología Molecular
Vasco de Quiroga No. 15, Tlalpan, 14000, México City (Mexico)
Tel. 5255-5485-2676, Fax 5255-5655-0382
E-Mail nab@biomedicas.unam.mx or norma.bobadillas@quetzal.innsz.mx

at the protein level. The structure of both Hsp90 isoforms consists of an N-terminal ATP-binding domain and a C-terminal dimerization domain, a middle domain linker region responsible for substrate-protein interactions, and a following charged domain that promotes the dimerization [2, 3]. The ATP binding site is the major target for Hsp90 inhibitors, but until now, specific inhibitors for Hsp90α or Hsp90β have not been developed.

In spite of the molecular similarity of these proteins important differences at the transcriptional and transductional levels have been described, suggesting that Hsp90α and Hsp90β might have differential roles in the cellular processes in which they are involved. Hsp90α transcription is tightly regulated by its promoter region, which contains several heat shock elements (HSEs) that are involved in the inducible gene expression of Hsp90α. However, differences between Hsp90α and Hsp90β are found in the promoter region; for Hsp90β HSEs are found in the first intron of the gene, and is not regarded as a highly inducible protein [4]. Another important difference is that Hsp90α easily dimerizes, whereas Hsp90β is mainly found as a monomer; the regions that facilitate these variations reside at the carboxyl-terminal amino acids of Hsp90 [2]. In this regard, it has been reported that the Hsp90 protein dimer, but not the monomer, stabilizes or activates different proteins known as Hsp90 client proteins in a nucleotide-dependent cycle. The Hsp90 cycle includes the following stages: an open, nucleotide-free form; a closed, ATP-bound structure; and a closed, ADP-bound conformation [5]. The closed conformation had been suggested to form stable client-protein complexes, emphasizing the importance of Hsp90 dimerization for activating the client proteins [6]. Thus, Hsp90 is a crucial regulator of a vast array of cellular processes by interacting with more than 100 client proteins (http://www.picard.ch/downloads/Hsp90interactors). Included among these proteins are steroid hormones, transcription factors, kinases, G proteins subunits, and endothelial nitric oxide synthase (eNOS).

eNOS is the primary source of nitric oxide (NO) in endothelial cells. It has been demonstrated that the interaction between Hsp90 and eNOS increases the activity of this enzyme, with greater NO production as a result. In contrast, the dissociation of these complex is not only associated with a reduction of NO synthesis but also turns eNOS into a superoxide generator [7-9]. Recent studies have shown that Hsp90 binds to the N-terminal oxygenase domain of eNOS present in residues 301-320 [9]. This interaction has a physiological connotation, because eNOS activity is regulated by at least four well-described mechanisms: 1) by enhancing calmodulin binding affinity to eNOS [10, 11]; 2) by facilitating the ability of Ca^{2+}/calmodulin to dissociate the interaction between caveolin-1 and eNOS, which reverses the inhibitory action of caveolin-1 on eNOS [12]; 3) by propitiating eNOS serine 1179/1177 (bovine/human) phosphorylation, a translational modification that activates this enzyme [13]; and 4) by recruiting Akt/PKB, which facilitates eNOS phosphorylation in the serine residue 1179 [14]. However, in the eNOS activation by Hsp90, the specific role of the α or β isoforms has not been completely addressed. To explore the specific participation of each Hsp90 isoform, this study was designed to evaluate the effect of Hsp90α or Hsp90β over-expression on the NO/eNOS pathway in human embryonic kidney (HEK-293) cells.

Materials and Methods

Plasmid constructs

Hsp90α and Hsp90β genes were amplified by PCR from cDNA synthesized from total rat RNA by using the forward primers 5' AAG GAA AAA AGC GGC CGC TCG TCA AGA TGC CTG AGG AA 3' and 5´ AAG GAA AAA AGC GGC CGC CTG CCA AGA TGC CTG AGG AA 3', respectively, and the reverse primers 5' CTA GTC TAG AGA GCC TTT AAT CCA CTT CTT CC 3' and 5' CTA GTC TAG ATT CTG GTG AAG CCT AGT CTA CTT C 5', respectively. In the forward primers, a *Not I* restriction site was included in the sequence, whereas in the reverse primers, a *Xba I* restriction site was introduced. The amplified fragments of 2260 for Hsp90α and 2220 bp for Hsp90β were cloned into the pcDNA3.1 (+) vector (Invitrogen) by using the *Not I* and *Xba I* restriction sites. The identities of the constructions were confirmed by automatic sequencing.

Hsp90 plasmid isolation

The isolation of the plasmids containing Hsp90α or Hsp90β sequences (pc-Hsp90α or pc-Hsp90β, respectively) was performed using the same general strategy for the large-scale isolation described by Qiagen Science (Maryland, USA). The DNA was crudely checked for concentration and purity, using 1% agarose gel electrophoresis against molecular weight markers standards (λ DNA/*Hind* III fragments from Invitrogen, Carlsbad, CA), and it was then corroborated with the molecular weights reported for the Hsp90α or Hsp90β gene. The DNA plasmid yield was 10-15 μg in a 10-ml starting culture.

Cell Culture and Transfection

Human embryonic kidney 293 (HEK-293) cells were maintained in Dulbecco´s Modified Eagle´s Medium (DMEM) (GIBCO) containing 10% fetal bovine serum (FBS) (Life Technology), 100 U/ml penicillin and 100 μg/ml streptomycin at 37°C with 5% CO_2. One day before the transfection, 5 x 10^5 HEK-293 cells were plated in 1 ml of DMEM medium per well in

six-well culture plates until they reached 90% confluence. To determine the amount of plasmid/liposome complex for obtaining the greater Hsp90α or Hsp90β over-expression, 0.5-2 μg of Hsp90α plasmid (pcDNA3.1/Hsp90α) or 4-8 μg of Hsp90β plasmid (pcDNA3.1/Hsp90β) was diluted in 100 μl of Opti-MEM® reduced serum medium (Invitrogen, Carlsbad, CA) and incubated for 15 min at room temperature. Next, 4 μl of Lipofectamine™ 2000 transfection reagent (Invitrogen, Carlsbad, CA) in 100 μl of Opti-MEM reduced serum was added, and the samples were maintained at room temperature for an additional 15 min. Thereafter, 200 μl of each Hsp90 complex was added to each well containing cells. The optimal transfection time for obtaining the higher over-expression of Hsp90α or Hsp90β was assessed at 24, 48 and 72 hours after transfection. Thus, the optimal conditions for Hsp90α and Hs90β over-expression in HEK-293 cells were 1 μg of pc-Hsp90α or 6 μg of pc-Hsp90β and 48 hr after transfection. Cells transfected with the pcDNA3.1(+) empty vector were included as controls in each experiment. All sets of transfections were performed at least in triplicate.

Small-interfering RNA (siRNA) transfection

The silencer pre-designed siRNAs corresponding to the target sequence of Hsp90α (Cat. number 4390818) or Hsp90β (Cat. number AM16831) were purchased from Ambion Inc. (Austin, TX). A silencer negative siRNA was used as a negative control (Cat. Number AM4613). In six-well plates, proliferating HEK-293 cells (at 70-90% confluency) were cultured and transfected with 100 nM of Hsp90α siRNA or Hsp90β siRNA. After 24 hr of transfection, Western blot analysis was carried out to examine the knockdown of targeted proteins and nitric oxide production.

Western Blot Analysis

Proteins from cell cultures transfected with pcDNA3.1/Hsp90α, pcDNA3.1/Hsp90β pcDNA3.1, siRNA-Hsp90α, or siRNA-Hsp90β were extracted using a lysis buffer containing 50 mM HEPES, pH 7.4, 250 mM NaCl, 5 mM EDTA, 0.1% NP-40, a protease inhibitor cocktail (Complete, Roche) and phosphatase inhibitors, followed by centrifugation at 14000 rpm. Thereafter, the supernatants containing the proteins were recovered, and samples containing 20 μg of total protein were resolved by 8.5% SDS-PAGE and electroblotted onto polyvinylidene difluoride membranes (PVDF, Amersham Pharmacia Biotech, Psicataway, NJ, USA). Membranes were then blocked in 5% blotting solution (Bio-Rad) and incubated with their respective specific antibodies, as detailed below. The lower part of the membranes was incubated with a goat anti-actin antibody (1:5000) overnight at 4°C (Santa Cruz Biotechnology, Santa Barbara, CA), whereas the upper membranes were incubated with polyclonal anti-rabbit Hsp90β (1:5000, Abcam Inc. Cambridge, MA), polyclonal anti-rabbit Hsp90α (1:5000, Abcam Inc. Cambridge, MA), anti-rabbit eNOS (1:500, Cell Signalling Technology), polyclonal anti-rabbit phosphorylated eNOS Ser1177 (1:500, Cell Signalling Technology), polyclonal anti-rabbit phospho-eNOS Thr495 (1:500, Cell Signalling Technology), polyclonal anti-human Akt (1:1000, Santa Cruz, Biotechnology), or polyclonal anti-human phospho-Akt Ser473 (1:1000, Santa Cruz, Biotechnology) antibodies. Membranes were then incubated with the secondary HRP-conjugated rat anti-rabbit IgG antibody (1:5000, Alpha Diagnostics, San Antonio, TX). Proteins were detected with an enhanced chemiluminescence kit (GE Healthcare Life Sciences, Amersham) and autoradiography. The bands were scanned for densitometric analysis.

Analysis of dimer and monomer conformation

The Hsp90α and Hsp90β dimer/monomer ratio was evaluated by Western blot for non-denatured proteins. Non-boiled samples containing 10 μg of total protein were resolved in 7.5% PAGE at 4°C. Proteins were transferred to a polyvinylidine difluoride membrane, and Western blot analysis for Hsp90α or Hsp90β was performed as described above. For eNOS dimer/monomer conformation analysis, non-boiled samples containing 50 μg of total protein were resolved in a 6% SDS-PAGE at 4°C. Then, proteins were transferred to a polivinylidine difluoride membrane, and Western blot analysis for eNOS was performed as described above.

Immunoprecipitation (IP) analysis

Subconfluent proliferating cells in 300-mm^2 dishes were harvested, and whole cell extracts were prepared and subjected to IP. After 48 h of transfection, the cells were washed with 2 ml of phosphate buffered saline (PBS), and lysis ELB buffer was added. Cell debris was removed from the cell lysates, and eNOS protein was immunoprecipitated using a protein G immunoprecipitation kit (Sigma Aldrich, Inc. St Louis, MO). Each IP was performed using 3 μg of eNOS antibody (BD Transduction Laboratories) and 1 mg of cell protein. The immunoprecipitated proteins were eluted by boiling in Laemmli sample buffer, separated by 8.5% SDS-PAGE, transferred onto PVDF membranes and subjected to Western blotting. The membrane was blocked with 5% non-fat milk in TBS-Tween (0.1%) and then immunoblotted for eNOS and Hsp90α Abcam Inc., Cambridge, MA), as previously described. Next, the membranes were stripped and reprobed with anti-Hsp90β (1:5000 dilution, Abcam Inc., Cambridge, MA) and eNOS (1:500 dilution) antibodies to demonstrate equal amounts of eNOS immunoprecipitation in all samples.

Hydrogen Peroxide Determination

The amount of hydrogen peroxide was determined in whole cell lysates (WCL) from each group of cells transfected using the Amplex Red Hydrogen Peroxide/Peroxidase Assay kit (Invitrogen 29851 Willow Creek Road), according to the instructions provided. Briefly, 50 μl of each WCL or standard curve (H_2O_2 1- 10 μM) was mixed with 50 μl of the Amplex Red reagent/HRP in a microplate. The samples were incubated for 30 minutes protected from light to allow the reaction between H_2O_2 and the Amplex reagent to occur. The plate was read at 560 nm. The amount of H_2O_2 detected in the samples is expressed as nM/μg of protein.

Measurement of NO release or NO Assay

NO production was indirectly determined in WCL from each transfected group using the colorimetric Nitric Oxide Assay

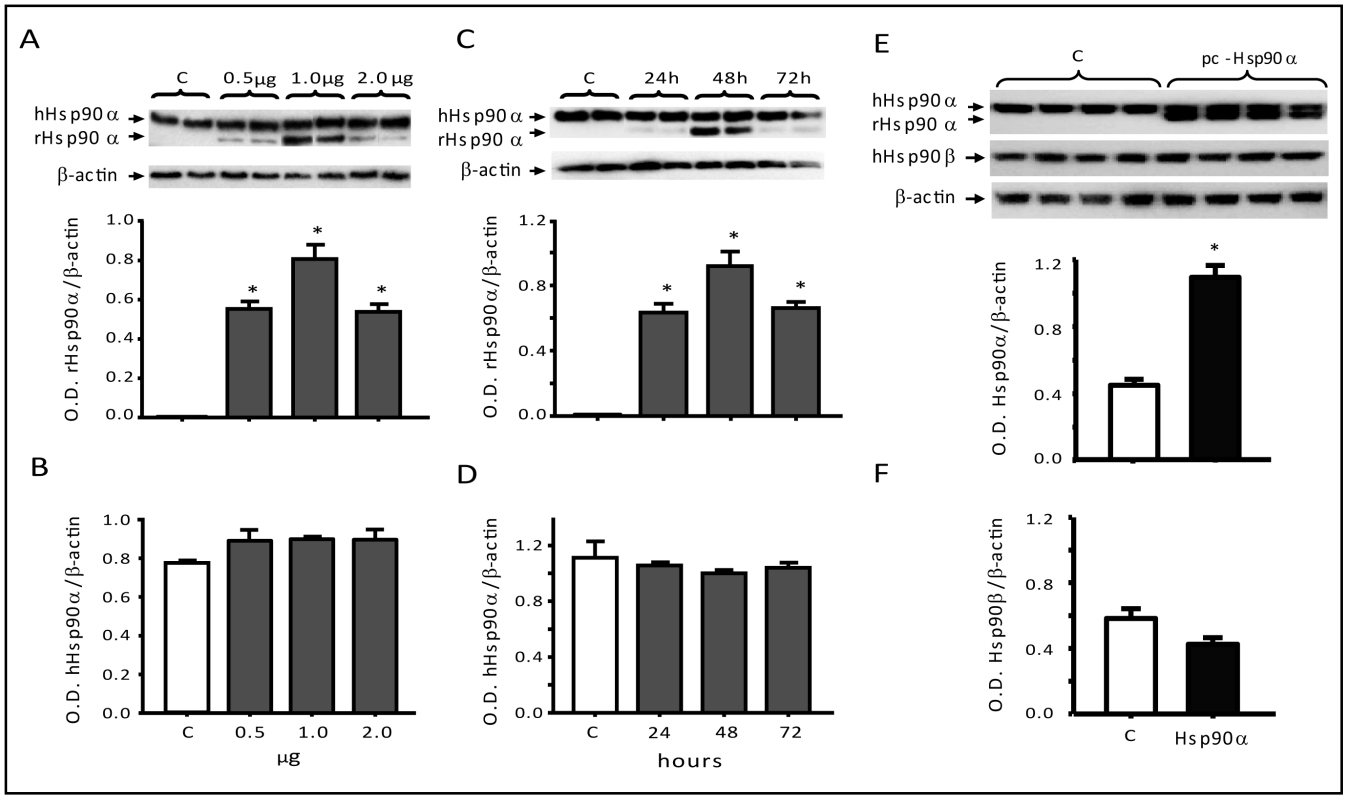

Fig. 1. A) Hsp90α protein levels in HEK-293 cells transfected with different amounts of pc-Hsp90α construct (black bars) compared with liposome-treated HEK-293 cells (white bars). Greater over-expression was obtained with 1 µg of pc-Hsp90α, B) without modifying endogenous Hsp90α. C) Western blot analysis of Hsp90α, showing that the higher efficiency of over-expression was obtained after 48 h of pc-Hsp90α transfection, D) without modifying endogenous Hsp90α. E) After 48h of transfection using 1µg of pc-Hsp90α, Hsp90α protein levels were significantly increased, F) without modifying basal Hsp90β expression. These experiments were performed in at least three different cell transfected cultures. *p<0.05 vs. empty vector-transfected cells.

Kit (Oxford Biomedical Research Inc., Oxford, MI). This assay consists of reducing the sample nitrates to nitrites with the use of nitrate reductase, followed by nitrite quantification with the Griess reaction and detection at 540 nm. The protein concentration in each WCL was determined by the Lowry assay (Bio Rad, Hercules, CA) and in duplicate. The concentration of nitrites in the WCL is expressed as µM/µg of protein.

Superoxide anion detection

Intracellular superoxide detection was assessed by hydroethidine staining (Polysciences, Inc., Warrington, PA). A stock solution of hydroethidine (HE) was prepared by dissolving 7 mg of HE in 1 mL of N,N-dymethylacetamide. The working solution was prepared by the addition of 20 µl of HE to 10 ml of PBS, and this mixture was filtered through a 0.22-mM Millipore filter. After 48 h of transfection, the medium was removed, and the cells were washed three times with PBS. The staining solution was added, and the cultures were incubated for 15 minutes at room temperature and protected from the light. Thereafter, the staining solution was removed, and the cells were washed three times. The cells were re-suspended in PBS for flow cytometry analysis. Ten thousand cells from each transfection group were analyzed in a FACScan cytometer (Becton Dickinson), and the fluorescence intensity was determined using an excitation of 535 nm and an emission of 610 nm. The data were analyzed using the Cell Quest program.

Statistical analysis

Results are presented as means ± SE. The significance of the differences among groups was tested by ANOVA using Bonferroni's correction for multiple comparisons and between two groups by the un-paired T test. Statistical significance was defined as a p value <0.05.

Results

Hsp90α cloning and HEK-293 transfection

The Hsp90α gene was amplified from rat kidney cDNA using specific primers, as detailed above. After the proper purification of PCR product of ≈ 2260 bp, rat Hsp90α (rHsp90α) was cloned into the pcDNA3.1(+) expression vector via a multi-cloning site by using *Xba I* and *Not I* sites. After *Xba I* and *Not I* digestion, two

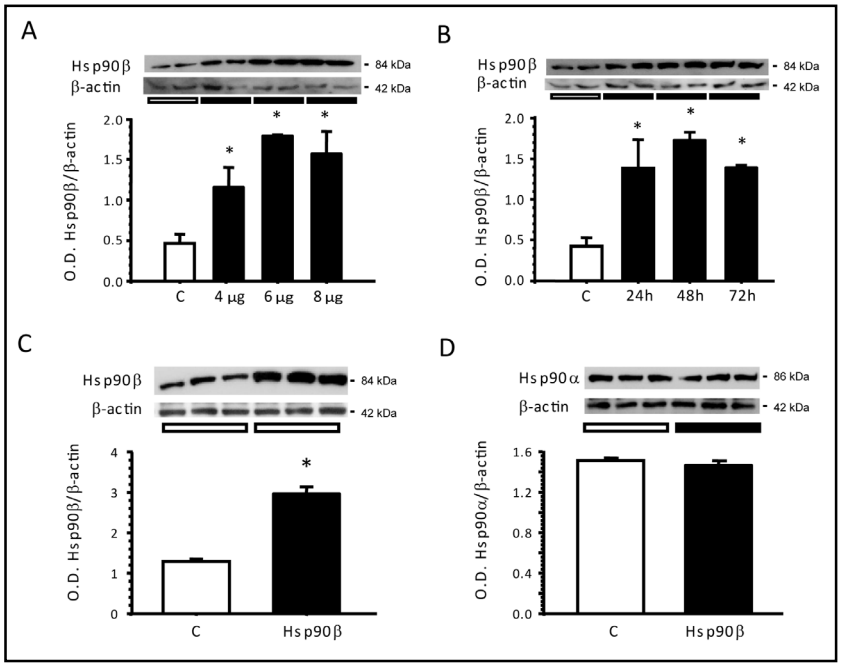

Fig. 2. A) Hsp90β protein levels in HEK-293 cells transfected with different amounts of pc-Hsp90β construct (black bars) compared with liposome-treated HEK-293 cells (white bars). The greater over-expression was obtained with 6 μg of pc-Hsp90β. B) Western blot analysis of Hsp90β showing that the higher efficiency of over-expression was obtained after 48 h of pc-Hsp90β transfection. C) After 48h of transfection using 6 μg of pc-Hsp90β, Hsp90β protein levels were significantly increased, D) without modifying basal Hsp90α expression. These results were obtained from at least two different experiments *p<0.05 vs. empty vector-transfected cells.

fragments were obtained, with the larger corresponding to the pcDNA3.1 vector and the smaller to the Hsp90α sequence (data not shown). The sequence of Hsp90α was corroborated by automatic sequencing that revealed 99% identity with the rat sequence reported for Hsp90α in GenBank (number AJ428213.1). Similarly, Hsp90α was cloned in the expression vector pcDNA3.1/NT-GFP (which codifies for the green fluorescent protein). Epifluorescence inverted microscopy was employed to detect the transfection efficiency. It was shown that 80% of HEK-293 cells were able to express the GFP (data not shown).

Different concentrations of Hsp90α plasmid were transfected into HEK-293 cells to determine the optimal conditions for pcDNA 3.1/Hsp90α transfection. The upper panel of Fig. 1A shows the insets of the Western blot analysis for Hsp90α and β actin. Two bands in the Hsp90α Western blot were detected. The larger band corresponds to the human endogenous Hsp90α that is expressed in HEK-293 cells, and the lower band corresponds to the transfected rat Hsp90α. Greater rat Hsp90α over-expression was detected when the cells were transfected with 1 μg of pcDNA 3.1/Hsp90α without changes in the endogenous Hsp90α expression, as shown in Fig. 1B. In addition, different times after transfection were assessed to determine the greatest Hsp90α over-expression. As shown in Fig. 1C, the higher rat Hsp90α expression was obtained after 48 h, without changes in human Hsp90α expression (Fig. 1D). Other groups of cells were transfected with the optimal conditions, then Hsp90α and Hsp90β protein levels were detected by

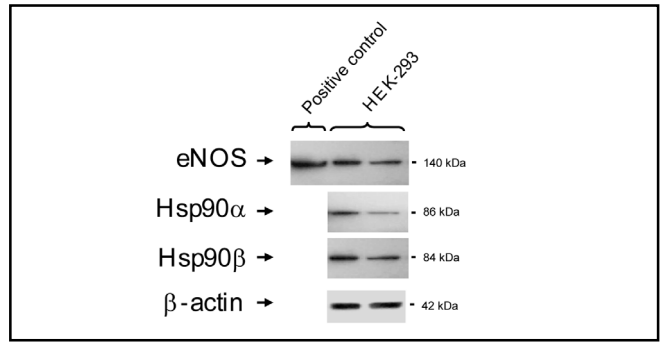

Fig. 3. Western blot analysis showing basal protein levels of eNOS, Hsp90α, Hsp90β and β-actin in HEK-293 intact cells.

Western blot analysis. As expected, pcDNA3.1/Hsp90α transfection increased Hsp90α protein levels, as shown in Fig. 1E, without altering Hsp90β protein levels as is represented in Fig. 1F. These results shown that Hsp90α and Hsp90β antibodies were specific to detect each Hsp90 isoform studied.

Hsp90β cloning and HEK-293 transfection

The Hsp90β gene was also amplified from rat kidney cDNA using specific primers, as detailed above. The PCR product of ≈2220 bp was purified and cloned into pcDNA3.1(+) using *Not I* and *Xba I* restriction sites. The Hsp90β sequence was first corroborated by restriction analysis; for this, the vector was digested with Xba I and *Not I*, *Xba I*, *Sac I*, *EcoR I*, *Kpn I*, and *Mfe I*. When the vector was digested with Xba I and Not I, two fragments were obtained, with the larger corresponding

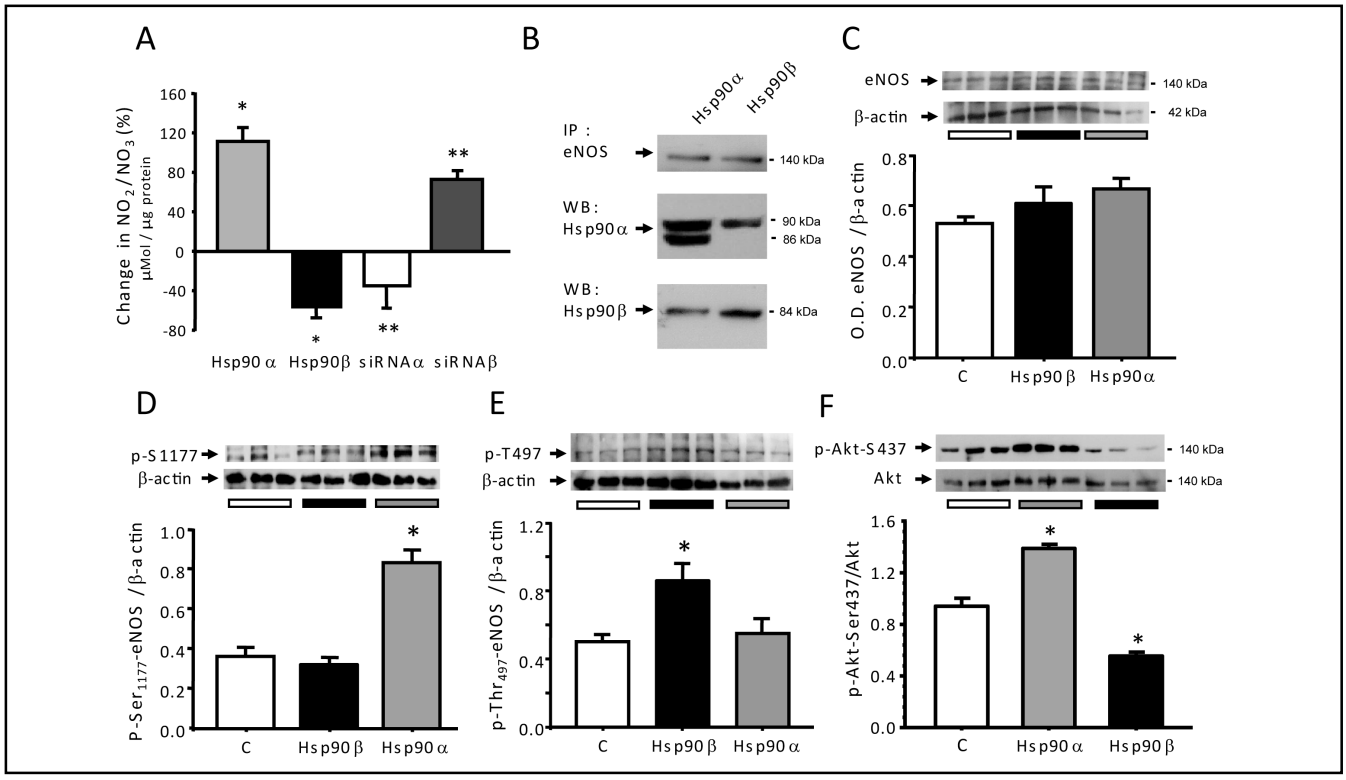

Fig. 4. Effects of pc-Hsp90α and pc-Hsp90β transfection on eNOS/NO pathway. A) Change in percentages of NO2/NO3 levels in the lysates of HEK-293 cells transfected with pc-Hsp90α (gray bars), pc-Hsp90β (black bars), siRNAHsp90α (white bars), and siRNA Hsp90β (dark gray bars). B) Co-immunoprecipitation of eNOS and Hsp90α or Hsp90β from HEK-293 cell lysates transfected with either Hsp90α or Hsp90β respectively. C) eNOS expression detected by Western blot analysis from HEK-293 cells transfected with empty vector, Hsp90α or Hsp90β. D) eNOS Ser1177 phosphorylation, E) eNOS Thr495 phosphorylation, and F) Akt expression and phosphorylation at residue Ser437, determined by Western blot analysis using specific phospho-antibodies in the studied groups of HEK-293 cells. The proteins were isolated from at least three different cell transfected cultures *p<0.05 vs. liposome-transfected cells. **p<0.05 vs. pc-Hsp90α or pc-Hsp90β-transfected cells.

to the pcDNA3.1 vector and the smaller to Hsp90β (data not shown). With the rest of the enzymes, we obtained the expected specific size fragments for Hsp90β (these size fragments are not obtained when Hsp90α was digested with these enzymes). The sequence was also corroborated by automatic sequencing, which revealed 100% identity with the rat sequence reported for Hsp90β in GenBank (number DQ022068.2). To determine the optimal conditions for Hsp90β over-expression, HEK-293 cells were transfected with different plasmid concentrations. As shown in Fig. 2A, maximum over-expression was detected when cells were transfected with 6 µg of pcDNA 3.1/Hsp90β a unique band of Hsp90β was detected corresponding to both human endogenous and rat transfected sequence. In addition, the best period of time to obtain maximum over-expression with 6 µg of plasmid was at 48 h after transfection (Fig. 2B). Independent groups of cells were transfected with the optimal conditions, and Hsp90α and Hsp90β protein levels were detected by Western blot analysis. As expected, pcDNA3.1/Hsp90β transfection increased Hsp90β by ≈2-fold, as shown in Fig. 2C, without modifying the Hsp90α protein levels (Fig. 2D).

Effects of Hsp90α and Hsp90β over-expression on the eNOS/NO pathway

Because it has been shown that Hsp90 regulates eNOS activity [10-13, 15] , we studied the specific role of Hsp90α and Hsp90β over-expression in nitric oxide production. First we assessed eNOS protein levels in un-transfected HEK-293, as Fig. 3 shows these cells do express eNOS, as well as Hsp90α and Hsp90β. This finding was further confirmed by the measurement of NO_2/NO_3 levels in these cells. Figure 4A shows the percentage changes in NO_2/NO_3 levels in groups transfected with Hsp90α or Hsp90β, compared with the cells that were transfected with the empty pcDNA vector. Hsp90α over-expression produced a significant increase

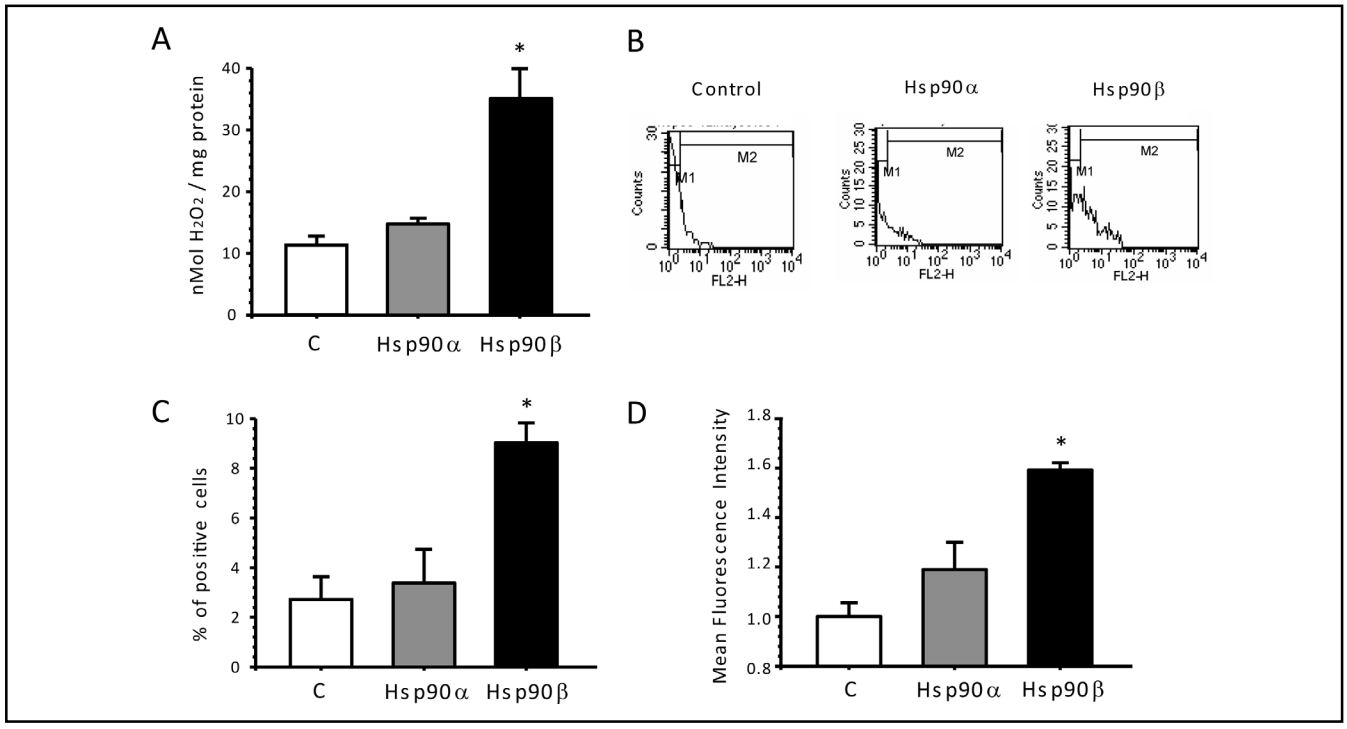

Fig. 5. Effects of Hsp90α and Hsp90β over-expression on oxidative stress in HEK-293 cells. A) Hydrogen peroxide levels in lysates of HEK-293 cells transfected with empty vector (white bars), pc-Hsp90α (dark gray bars), and pc-Hsp90β (black bars). Hydroethidine staining was assessed as a measure of superoxide anion production and was quantified by flow cytometry. B) Upper panel, representative histograms of the three groups of transfected HEK-293 cells, showing a greater hydroethidine staining in the group that was transfected with pc-Hsp90β. C) The percentage of HEK-293 cells positive for hydroethidine staining and D) Fold increase in the Mean Fluorescence Intensity (FMI). These results were performed with at least three different transfected cultures. *$p<0.05$ vs. empty vector-transfected cells.

in NO metabolites (from 0.29 ± 0.01 to 0.61 ± 0.03 μM/μg of protein) that represented an increase of 113.3%. Intriguingly, Hsp90β over-expression produced the opposite effect, such that NO_2/NO_3 levels were significantly reduced in transfected HEK-293 cells (0.13 ± 0.01 μM/μg of protein). The specificity of the observed effects was studied by reducing the endogenous Hsp90α and Hsp90β expression by using specific siRNAs for these proteins. Therefore, other groups of cells were transfected with the corresponding siRNA/Hsp90α or siRNA/Hsp90β. We assessed the Hsp90α and Hsp90β expression after 24 to 72 h after respective siRNAs transfection and from these results the experiments with siRNAs were performed after 48h (data not shown). When the NO_2/NO_3 levels were evaluated, we observed that siRNA/Hsp90α transfection produced a significant reduction in NO metabolites, by 36.5 % as is depicted in Fig. 4A. In contrast, siRNA/Hsp90β transfection was associated with a significant increase in NO_2/NO_3 levels, by 74.7%. These data strongly suggest that Hsp90α and Hsp90β have differential roles in regulating eNOS activity.

We examined whether these differences were propagated by changes in the interaction of Hsp90α or Hsp90β with eNOS. As shown in Fig. 4B, it was not the case, as the IP-Western blotting analysis revealed that eNOS was able to associate with both Hsp90α and Hsp90β, suggesting that the reduction of eNOS activity by Hsp90β did not result from an inability of this chaperone to associate with eNOS.

To evaluate if the differential modification of NO production induced by Hsp90α and Hsp90β over-expression was mediated by changes in eNOS expression and its phosphorylation, eNOS protein levels and the phosphorylation of serine 1177 and threonine 497 residues of eNOS were evaluated in transfected HEK-293 cells by Western blot analysis using the corresponding phospho-antibodies. The eNOS protein levels in HEK-293 cell cultures was not modified by either Hsp90α or Hsp90β transfection, as evident in the top inset and by the densitometric analysis shown in Fig. 4C. A significant increase in the immune-detection signal of phosphorylated Ser1177 was observed in the cells that over-expressed

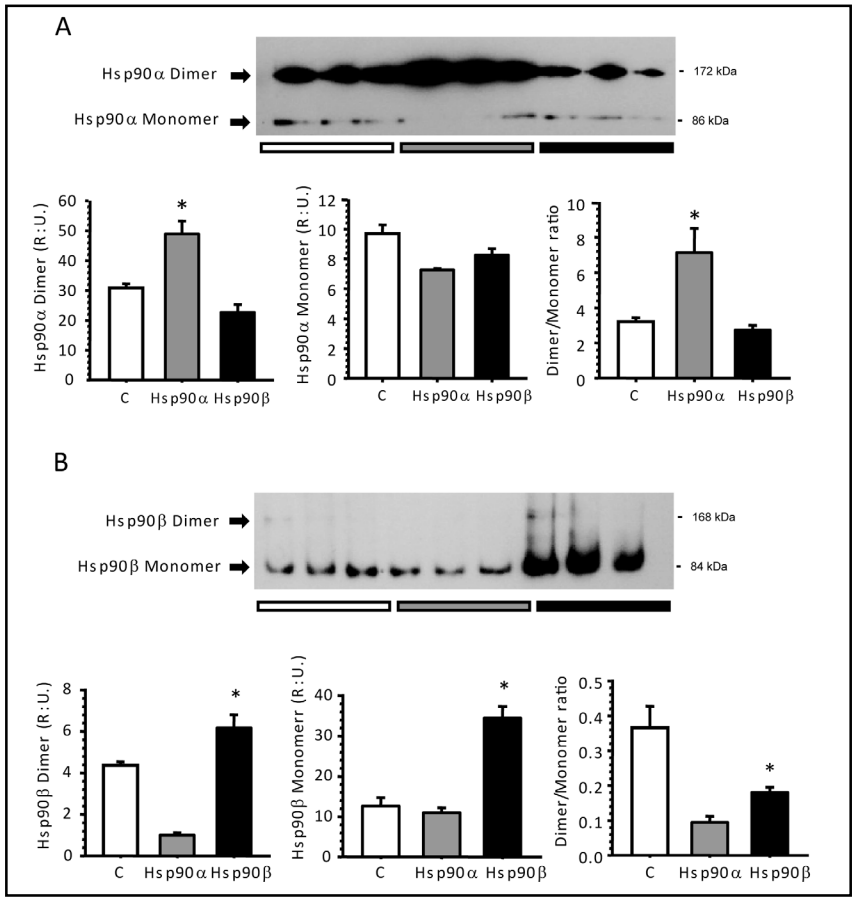

Fig. 6. Effects of Hsp90α or Hsp90β overexpression on the monomer and dimer conformations. A) Hsp90α Western blot analysis of non-denatured proteins extracted from HEK-293 cells transfected with empty vector (white bars) pc-Hsp90α (dark gray bars), and pc-Hsp90β (black bars). The upper panel shows a representative image of the Hsp90α Western blot, and the lower panel shows graphical representations of the dimers, monomers and dimer/monomer ratios of Hsp90α. B) Hsp90β Western blot analysis of non-denatured proteins extracted from HEK-293 cells transfected with empty vector (white bars), pc-Hsp90α (dark gray bars), and pc-Hsp90β (black bars). The proteins were extracted from three different HEK-293 transfected cell cultures. *p<0.05 versus empty transfected cells.

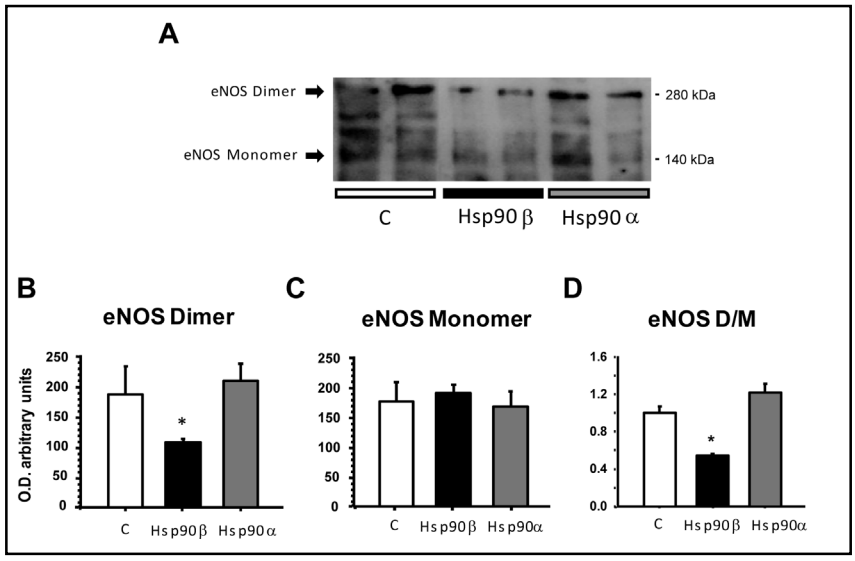

Fig. 7. Effect of Hsp90α and Hsp90β overexpression on eNOS dimer/monomer conformation. A) A representative image of eNOS Western blot from total proteins extracted from HEK-293 cells transfected with empty vector (open bars), Hsp90β (black bars), and Hsp90α (gray bars), respectively. Two bands were detected: 280kDa and 140kDa, corresponding to eNOS dimeric and monomeric conformations, respectively. B and C) dimeric and monomeric eNOS densitometric analysis, and D) eNOS dimer/monomer ratio (D/M). The results reported here were repeated two times with similar results. *p<0.05 vs. empty vector transfected cells.

Hsp90α, an effect that was not seen in Hsp90β-transfected cells (Fig. 4D). The mean ratio of phosphorylated Ser1177 eNOS/β-actin in pc-Hsp90α-transfected cells was 0.83 ± 0.08, compared to 0.32 ± 0.04 and 0.36 ± 0.05 AU for pc-Hsp90β and pcDNA3.1 empty vector, respectively. In contrast, the transfection of pc-Hsp90β significantly increased Thr495 eNOS phosphorylation (Fig. 4E), but overexpression of Hsp90α did not modify the phosphorylation of this eNOS residue. The mean ratio of phosphorylated Thr495-eNOS/β-actin in Hsp90β and pcDNA3.1-transfected cells was 0.86 ± 0.1, compared to 0.50 ± 0.05 and 0.55 ± 0.09 in liposomes and Hsp90α-transfected cells, respectively.

Because it has been reported that Hsp90 plays an important role in the activation of p-Akt/PKB [16] and because this kinase it is able to phosphorylate Ser1177 of eNOS [17, 18], we evaluated the effect of over-expressing Hsp90α or Hsp90β on Akt/PKB activation. As shown in Figure 4F, the transfection of either Hsp90α or Hsp90β did not modify the Akt/PKB protein levels, but a different effect was observed for the phosphorylation of this kinase. Thus, Hsp90α over-expression was associated with a significant increase in Akt/PKB phosphorylation, whereas Hsp90β over-expression induced a significant reduction in the amount of phosphorylated Akt/PKB.

Moreover, it has been previously shown that eNOS is able to generate superoxide anion when it is phosphorylated at Thr-497; thus, we assessed the effect of Hsp90α or Hsp90β over-expression on the cellular oxidative stress state by measuring the hydrogen peroxide levels in HEK-293 cell cultures. Figure 5A shows the H_2O_2 levels in WCL, expressed as nmol/μg of protein. It is noteworthy that the H_2O_2 levels increased by two-fold when Hsp90β was over-expressed, an effect that was not observed when pc-Hsp90α was transfected. To further confirm these findings, we performed hydroethidine (HE) staining to detect intracellular superoxide anion generation by flow cytometry analysis. Figure 5B shows the representative histograms of each transfected group, and Figure 5C and 5D show the percentage of stained cells and the quantification of the mean fluorescence intensity (MFI), respectively. The HE staining confirmed that Hsp90β over-expression induced a higher generation of superoxide anion, as shown by the increase in the percentage of cells positive for HE staining (from 2.7 ± 0.9 to 9.0 ± 0.8 %, p=0.002) and by the MFI measurement (from 1 ± 0.06 to 1.6 ± 0.03 AU, p=0.002).

Because the dimeric Hsp90 conformation has been shown to be necessary for interactions with the client proteins, the monomeric/dimeric ratio in HEK-293 cells transfected with Hsp90α and Hsp90β was evaluated. The insets in Fig. 6A and Fig. 6B show Westerns blot under non-denaturing conditions of proteins extracted from Hsp90α and Hsp90β-transfected cells, respectively. Typically, most of the Hsp90α was found in its dimeric conformation (Fig. 6A), in contrast with the Hsp90β which was found mainly in the monomeric conformation (cells transfected with the empty vector) as is shown in Fig. 6B. When the monomeric/dimeric ratio was evaluated in cells transfected with either pc-Hsp90α or pc-Hsp90β most of the Hsp90α was found in its dimeric conformation. In addition, a greater amount of this protein was detected in the cells that were transfected with pc-Hsp90α. In contrast, when Hsp90β was over-expressed, most of the protein was found in its monomeric conformation, and again, more monomeric Hsp90 was observed in the cells that were transfeceted with pc-Hsp90β (Fig. 6B).

It has been previously reported that dimeric eNOS conformation is required for a suitable NO production [19], thus we evaluated if Hsp90α and Hsp90β over-expression modify the dimeric/monomeric eNOS conformation. The upper panel of Figure 7 shows the inset of eNOS Western blot analysis in non-denaturating conditions from HEK-293 cells transfected with empty vector, pcHsp90α and pcHsp90β respectively. The lower panel depicts the densitometric analysis of dimeric and monomeric bands of eNOS, together with the resulting dimeric/monomeric ratio. The reduction of NO synthesis induced by Hsp90β over-expression was associated with a significant decrease in eNOS dimeric conformation, with the concomitant eNOS dimeric/monomeric ratio reduction. This effect was not seen in pcHsp90α transfected cells.

Discussion

Hsp90 plays a key role in cellular signal transduction networks, as it is essential for maintaining the activity of numerous signaling proteins. One of the most studied Hsp90 interactions is that established with eNOS. Several studies have shown that Hsp90 regulates eNOS activity through modulations of the following processes: helping to activate eNOS by dissociating it from caveolin-1; enhancing eNOS enzymatic activity by promoting its dimerization; facilitating the activating eNOS phosphorylation; and modulating the release of NO vs. superoxide by eNOS [10-13]. Furthermore, Hsp90 has also been proposed to facilitate the calcineurin-dependent dephosphorylation of the residue Thr495 site of eNOS, which contributes to enhance its enzymatic activity [15]. Therefore, Hsp90 plays a critical role in vascular NO synthesis through the regulation of eNOS activity. In this regard, we have recently shown that Hsp90 inhibition with radicicol, that reduced Hsp90 interaction with their client proteins, produced a significant reduction in renal plasma flow and glomerular filtration rate, an effect that was associated with a decreased urinary excretion of nitrites and nitrates (NO_2/NO_3), suggesting that the disruption of eNOS-Hsp90 complex reduced renal NO synthesis [20]. In addition, previous studies have shown that the disruption of eNOS/Hsp90 complex promotes not only the reduction

of NO but also the generation of O_2^- anion by eNOS [8, 9, 21, 22]. Even though there is enough evidence about the Hsp90/eNOS coupling and uncoupling in NO and O_2^- generation, respectively, the specific role of Hsp90α and Hsp90β in this pathway have not been completely addressed. Two previous studies [7, 23] suggested that transfection of Hsp90β induces an increase in NO production in COS and pulmonary arterial endothelial cells (PAEC). However, results from these studies are hard to evaluate because the Hsp90 antibody that was used recognizes both isoforms and thus Hsp90β over-expression was not demonstrated. In addition, in one of the studies [23], the effect of empty adenovirus transfection was not evaluated. Other studies in which the interaction between eNOS and Hsp90 was enhanced by a transient Hsp90 transfection, did not specified which isoform of Hsp90 was used for the transfection [15, 24].

In the present study, the participation of Hsp90α or Hsp90β in the eNOS/NO/O_2^- pathway was evaluated by inducing the over-expression of each isoform in HEK-293 cells. For this issue, we cloned Hsp90α and Hsp90β into an expression vector and the over-expression was gotten by transitory transfection. The pc-Hsp90α transfection produced a significant elevation in Hsp90α without modifing Hsp90β protein levels. Similarly, in cells transfected with pc-Hsp90β, the levels of this protein were significantly enhanced, whereas the endogenous Hsp90α protein levels were not affected. Therefore, the effects seen in this study on the NO/eNOS pathway were solely induced by the transitory over-expresion of each Hsp90 isoform.

Accordingly, we observed that Hsp90α over-expression was associated with a significant increase in NO_2/NO_3 levels. Quite interestingly, pc-Hsp90β transfection produced the opposite effect; thus, NO metabolites were significantly reduced in HEK-293 cells. These findings were supported by results using respective siRNAs of Hsp90α or Hsp90β. Consequently, when Hsp90α expression was reduced by this strategy, the NO metabolites were significantly decreased. In contrast, when HEK-293 cells were transfected with Hsp90β siRNA, the NO_2/NO_3 levels were significantly enhanced. In this regard, these results suggest that cystosolic Hsp90 isoforms exert distintive functions in the NO pathway, in which Hsp90α positively regulates NO synthesis whereas Hsp90β has a contrary effect.

To begin to understand the mechanisms by which Hsp90α and Hsp90β have differential roles in NO production, we evaluated the eNOS protein levels and the eNOS phosphorylation of two main residues that are implicated in this enzyme activity. We found that eNOS protein levels were not modified when the HEK-293 cells were transfected with either Hsp90α or Hsp90β, however, profound changes in its phosphorylation state were observed. Hsp90α over-expression was associated with a significant increase in eNOS-activating phosphorylation (Ser1177), whereas Hsp90β over-expression produced an increase in the eNOS-inactivating phosphorylation (Thr495). In this regard, previous studies have shown that increased eNOS phosphorylation at Thr495, as caused by eNOS-Hsp90 uncoupling, resulted in lesser NO production [20, 25, 26]. In support of this, Lin et al. [27] reported that the T495A eNOS mutant, which cannot be phosphorylated at this site, was able to enhance eNOS activity. The immunoprecipitation analysis performed in this study revealed that both Hsp90α and Hsp90β are able to associate with eNOS, suggesting that these two Hsp90 isoforms exert differential eNOS regulation through modulating eNOS phosphorylation. Incidentally, it has been shown that eNOS activation by Hsp90 is mediated, in part, by a scaffolding effect that enhances the interaction between eNOS and the active serine/threonine kinase Akt/PKB [10], which, in turn, promotes eNOS Ser1177 phosphorylation. Intriguingly, Akt/PKB activity is also regulated by Hsp90 through the prevention of PP2A-mediated Akt dephosphorylation [16]. Consequently with these previous findings, we observed that pc-Hsp90α transfection increased Akt/PKB phosphorylation, suggesting that the greater NO synthesis observed in these transfected cells was in part due to an enhanced Akt/PKB activity, resulting in eNOS Ser1177 phosphorylation. Of note, pc-Hsp90β transfection induced a significant reduction of Akt/PKB phosphorylation, which was associated with an increase in the inactivating eNOS phosphorylation (Thr495), and these findings were associated with a significant reduction in NO production. Thus, our results suggest that another way by which Hsp90α and Hsp90β differentially regulate eNOS is by modifying Akt/PKB phosphorylation.

Several studies have shown that eNOS Thr495 phosphorylation promotes the superoxide anion (O_2^-) generation instead of NO [8, 9, 23, 28, 29]. To explore the significance of the increased eNOS Thr495 phosphorylation induced by pc-Hsp90β transfection on O_2^- generation, the levels of peroxide hydrogen and O_2^- anion were evaluated in transfected HEK-293 cells. The reduction of NO induced by Hsp90β over-expression was associated with a significant increase in hydrogen peroxide, suggesting a greater O_2^- generation. These results were confirmed by measuring cellular O_2^- by

cytofluorometry, in which a significant increase in the generation of this anion was observed in HEK-293 cells transfected with pc-Hsp90β, an effect that was not seen following transfection with pc-Hsp90α. Altogether, these results suggest that Thr 497 phosphorylation switches the ability of eNOS to produce O_2^-, and, interestingly, this effect seems to be promoted by the association of Hsp90β with eNOS.

The dimeric molecular conformation of Hsp90 is required for the activation and stabilization its client proteins. Hsp90 consists of a C-terminal dimerization domain, a middle domain (which may interact with substrate proteins), and an N-terminal ATP-binding domain. The activation process depends on the hydrolysis of ATP by Hsp90. Thus, the ability of Hsp90 to interact with its client proteins is strongly determined by its conformational state [3, 30, 31]. In this sense, Hsp90β human and mouse is less frequently found as a dimer than Hsp90α. The impeded ability of Hsp90β to dimerize is related to the 16 amino acid substitutions located in the 561-685 amino acid region of the C-terminal dimerization domain [32]; specifically, Thr566 and Ala629 seem to be responsible for the reduced ability of Hsp90β to dimerize [33]. Here, we evaluated the monomer/dimer ratio of Hsp90α and Hsp90β in HEK-293 cells before and after pc-Hsp90α or pc-Hs90β transfection. As has been previously reported, we found that Hsp90α was predominantly in its dimeric molecular conformation, whereas Hsp90β persisted in a monomeric conformation in the cells that were transfected with the empty vector. When Hsp90α was over-expressed, most of the protein was found in the dimeric form, without changes in the Hsp90β monomer form. In contrast, the over-expression of Hsp90β rendered a greater proportion of the monomeric conformation. These results suggest that both Hsp90 isoforms are able to associate with eNOS, but the conformation state of Hsp90 seems to be a regulator of eNOS ability to produce NO or O_2^-. Because Hsp90 is also able to interact with neuronal and inducible NOS [34-36], we can not exclude the participation of other NOS isoforms in the NO production seen when Hsp90α or Hsp90β were over-expressed.

The differential regulation of eNOS by Hsp90α and Hsp90β seems not only to be explained by changes in eNOS phosphorylation or Hsp90 conformation, but also, Hsp90β over-expression induced a significant reduction in eNOS active conformation. Thus, the reduction in NO synthesis observed in HEK-293 cells transfected with pcHsp90β was associated with a lesser dimeric conformation of eNOS, suggesting that this is another mechanism by which Hsp90β differentially regulates eNOS activity.

Taken together, our results suggest that to obtain a suitable NO synthesis, the formation of the dimeric conformation of Hsp90α is required, which not only allows eNOS dimerization, but also helps to eNOS phosphorylation at Ser1177 by Akt/PKB. In contrast, when Hsp90β is predominantly found as a monomer, it affects eNOS pathway through two different mechanisms: by reducing Akt/PKB phosphorylation/activity and by propitiating the inactive eNOS conformation which in turns is associated with eNOS phosphorylation at Thr495, an effect that causes eNOS to produce O_2^- instead of NO. These findings could have important implications for abnormal vascular physiology in which the generation of the superoxide anion is increased and nitric oxide availability is reduced.

Acknowledgments

We thank to Rosalba Pérez for her technical assistance and all members of the Molecular Physiology Unit for their enthusiastic comments. The results presented in this paper have not been published previously in whole or in part, except for the abstracts, which were presented at the ASN 42nd and 43rd Annual Meetings & Scientific Expositions, 2008 and 2009 (Philadelphia, PA, and San Diego, CA, respectively). This project was supported by grants from the Mexican Council of Science and Technology 48483 and 101030 to NAB, from the National University of Mexico IN200909-3 to NAB, and DK64635 from NIDDK to GG.

References

1 Lindquist S, Craig EA: The heat-shock proteins. Annu Rev Genet 1988;22:631-677.

2 Csermely P, Schnaider T, Soti C, Prohaszka Z, Nardai G: The 90-kDa molecular chaperone family: structure, function, and clinical applications. A comprehensive review. Pharmacol Ther 1998;79:129-168.

3 Hainzl O, Lapina MC, Buchner J, Richter K: The charged linker region is an important regulator of Hsp90 function. J Biol Chem 2009;284:22559-22567.

4 Sreedhar AS, Kalmar E, Csermely P, Shen YF: Hsp90 isoforms: functions, expression and clinical importance. FEBS Lett 2004;562:11-15.
5 Richter K, Hendershot LM, Freeman BC: The cellular world according to Hsp90. Nat Struct Mol Biol 2007;14:90-94.
6 Wandinger SK, Richter K, Buchner J: The Hsp90 chaperone machinery. J Biol Chem 2008;283:18473-18477.
7 Garcia-Cardena G, Fan R, Shah V, Sorrentino R, Cirino G, Papapetropoulos A, Sessa WC: Dynamic activation of endothelial nitric oxide synthase by Hsp90. Nature 1998;392:821-824.
8 Pritchard KA, Jr., Ackerman AW, Gross ER, Stepp DW, Shi Y, Fontana JT, Baker JE, Sessa WC: Heat shock protein 90 mediates the balance of nitric oxide and superoxide anion from endothelial nitric-oxide synthase. J Biol Chem 2001;276:17621-17624.
9 Xu H, Shi Y, Wang J, Jones D, Weilrauch D, Ying R, Wakim B, Pritchard KA Jr: A Heat Shock Protein 90 Binding Domain in Endothelial Nitric-oxide Synthase Influences Enzyme Function. J Biol Chem 2007;282:37567-37574.
10 Takahashi S, Mendelsohn ME: Synergistic activation of endothelial nitric-oxide synthase (eNOS) by HSP90 and Akt: calcium-independent eNOS activation involves formation of an HSP90-Akt-CaM-bound eNOS complex. J Biol Chem 2003;278:30821-30827.
11 Takahashi S, Mendelsohn ME: Calmodulin-dependent and -independent activation of endothelial nitric-oxide synthase by heat shock protein 90. J Biol Chem 2003;278:9339-9344.
12 Gratton JP, Fontana J, O'Connor DS, Garcia-Cardena G, McCabe TJ, Sessa WC: Reconstitution of an endothelial nitric-oxide synthase (eNOS), hsp90, and caveolin-1 complex in vitro. Evidence that hsp90 facilitates calmodulin stimulated displacement of eNOS from caveolin-1. J Biol Chem 2000;275:22268-22272.
13 Papapetropoulos A, Fulton D, Lin MI, Fontana J, McCabe TJ, Zoellner S, Garcia-Cardena G, Zhou Z, Gratton JP, Sessa WC: Vanadate is a potent activator of endothelial nitric-oxide synthase: evidence for the role of the serine/threonine kinase Akt and the 90-kDa heat shock protein. Mol Pharmacol 2004;65:407-415.
14 Fontana J, Fulton D, Chen Y, Fairchild TA, McCabe TJ, Fujita N, Tsuruo T, Sessa WC: Domain mapping studies reveal that the M domain of hsp90 serves as a molecular scaffold to regulate Akt-dependent phosphorylation of endothelial nitric oxide synthase and NO release. Circ Res 2002;90:866-873.
15 Kupatt C, Dessy C, Hinkel R, Raake P, Daneau G, Bouzin C, Boekstegers P, Feron O: Heat shock protein 90 transfection reduces ischemia-reperfusion-induced myocardial dysfunction via reciprocal endothelial NO synthase serine 1177 phosphorylation and threonine 495 dephosphorylation. Arterioscler Thromb Vasc Biol 2004;24:1435-1441.
16 Sato S, Fujita N, Tsuruo T: Modulation of Akt kinase activity by binding to Hsp90. Proc Natl Acad Sci U S A 2000;97:10832-10837.
17 Fulton D, Gratton JP, McCabe TJ, Fontana J, Fujio Y, Walsh K, Franke TF, Papapetropoulos A, Sessa WC: Regulation of endothelium-derived nitric oxide production by the protein kinase Akt. Nature 1999;399:597-601.
18 Wei Q, Xia Y: Roles of 3-phosphoinositide-dependent kinase 1 in the regulation of endothelial nitric-oxide synthase phosphorylation and function by heat shock protein 90. J Biol Chem 2005;280:18081-18086.
19 Bauersachs J, Schafer A: Tetrahydrobiopterin and eNOS dimer/monomer ratio-a clue to eNOS uncoupling in diabetes? Cardiovasc Res 2005;65:768-769.
20 Ramirez V, Mejia-Vilet JM, Hernandez D, Gamba G, Bobadilla NA: Radicicol, a heat shock protein 90 inhibitor, reduces glomerular filtration rate. Am J Physiol Renal Physiol 2008;295:F1044-F1051.
21 Pritchard KA, Jr., Ackerman AW, Gross ER, Stepp DW, Shi Y, Fontana JT, Baker JE, Sessa WC: Heat shock protein 90 mediates the balance of nitric oxide and superoxide anion from endothelial nitric-oxide synthase. J Biol Chem 2001;276:17621-17624.
22 Li Z, Carter JD, Dailey LA, Huang YC: Vanadyl sulfate inhibits NO production via threonine phosphorylation of eNOS. Environ Health Perspect 2004;112:201-206.
23 Sud N, Sharma S, Wiseman DA, Harmon C, Kumar S, Venema RC, Fineman JR, Black SM: Nitric oxide and superoxide generation from endothelial NOS: modulation by HSP90. Am J Physiol Lung Cell Mol Physiol 2007;293:L1444-L1453.
24 Brouet A, Sonveaux P, Dessy C, Balligand JL, Feron O: Hsp90 ensures the transition from the early Ca2+-dependent to the late phosphorylation-dependent activation of the endothelial nitric-oxide synthase in vascular endothelial growth factor-exposed endothelial cells. J Biol Chem 2001;276:32663-32669.
25 Sugimoto M, Nakayama M, Goto TM, Amano M, Komori K, Kaibuchi K: Rho-kinase phosphorylates eNOS at threonine 495 in endothelial cells. Biochem Biophys Res Commun 2007;361:462-467.
26 Sessa WC: eNOS at a glance. J Cell Sci 2004;117:2427-2429.
27 Lin MI, Fulton D, Babbitt R, Fleming I, Busse R, Pritchard KA Jr, Sessa WC: Phosphorylation of threonine 497 in endothelial nitric-oxide synthase coordinates the coupling of L-arginine metabolism to efficient nitric oxide production. J Biol Chem 2003;278:44719-44726.
28 Konduri GG, Ou J, Shi Y, Pritchard KA Jr: Decreased association of HSP90 impairs endothelial nitric oxide synthase in fetal lambs with persistent pulmonary hypertension. Am J Physiol Heart Circ Physiol 2003;285:H204-H211.
29 Ou J, Ou Z, Ackerman AW, Oldham KT, Pritchard KA Jr: Inhibition of heat shock protein 90 (hsp90) in proliferating endothelial cells uncouples endothelial nitric oxide synthase activity. Free Radic Biol Med 2003;34:269-276.
30 Richter K, Soroka J, Skalniak L, Leskovar A, Hessling M, Reinstein J, Buchner J: Conserved conformational changes in the ATPase cycle of human Hsp90. J Biol Chem 2008;283:17757-17765.
31 Hessling M, Richter K, Buchner J: Dissection of the ATP-induced conformational cycle of the molecular chaperone Hsp90. Nat Struct Mol Biol 2009;16:287-293.
32 Nemoto T, Ohara-Nemoto Y, Ota M, Takagi T, Yokoyama K: Mechanism of dimer formation of the 90-kDa heat-shock protein. Eur J Biochem 1995;233:1-8.
33 Kobayakawa T, Yamada S, Mizuno A, Nemoto TK: Substitution of only two residues of human Hsp90alpha causes impeded dimerization of Hsp90beta. Cell Stress Chaperones 2008;13:97-104.
34 Yoshida M, Xia Y: Heat shock protein 90 as an endogenous protein enhancer of inducible nitric-oxide synthase. J Biol Chem 2003;278:36953-36958.
35 Bender AT, Silverstein AM, Demady DR, Kanelakis KC, Noguchi S, Pratt WB, Osawa Y: Neuronal nitric-oxide synthase is regulated by the Hsp90-based chaperone system in vivo. J Biol Chem 1999;274:1472-1478.
36 Bachmann S, Bosse HM, Mundel P: Topography of nitric oxide synthesis by localizing constitutive NO synthases in mammalian kidney. Am J Physiol 1995;268:F885-F898.

OPEN ACCESS Freely available online

PLoS one

Gene Expression Analysis Reveals the Cell Cycle and Kinetochore Genes Participating in Ischemia Reperfusion Injury and Early Development in Kidney

Tae-Min Kim[1☯], Victoria Ramírez[2,4☯], Jonatan Barrera-Chimal[3,4], Norma A. Bobadilla[3,4], Peter J. Park[1], Vishal S. Vaidya[2,5*]

1 Center for Biomedical Informatics, Harvard Medical School, Boston, Massachusetts, United States of America, **2** Renal Division, Department of Medicine, Brigham and Women's Hospital, Harvard Medical School, Boston, Massachusetts, United States of America, **3** Molecular Physiology Unit, Instituto de Investigaciones Biomédicas, Universidad Nacional Autónoma de México, Mexico City, Mexico, **4** Departamento de Nefrología y Metabolismo Mineral, Instituto Nacional de Ciencias Médicas y Nutrición Salvador Zúbiran, Mexico City, Mexico, **5** Department of Environmental Health, Harvard School of Public Health, Boston, Massachusetts, United States of America

Abstract

Background: The molecular mechanisms that mediate the ischemia-reperfusion (I/R) injury in kidney are not completely understood. It is also largely unknown whether such mechanisms overlap with those governing the early development of kidney.

Methodology/Principal Findings: We performed gene expression analysis to investigate the transcriptome changes during regeneration after I/R injury in the rat (0 hr, 6 hr, 24 hr, and 120 hr after reperfusion) and early development of mouse kidney (embryonic day 16 p.c. and postnatal 1 and 7 day). Pathway analysis revealed a wide spectrum of molecular functions that may participate in the regeneration and developmental processes of kidney as well as the functional association between them. While the genes associated with cell cycle, immunity, inflammation, and apoptosis were globally activated during the regeneration after I/R injury, the genes encoding various transporters and metabolic enzymes were down-regulated. We also observed that these injury-associated molecular functions largely overlap with those of early kidney development. In particular, the up-regulation of kinases and kinesins with roles in cell division was common during regeneration and early developmental kidney as validated by real-time PCR and immunohistochemistry.

Conclusions: In addition to the candidate genes whose up-regulation constitutes an overlapping expression signature between kidney regeneration and development, this study lays a foundation for studying the functional relationship between two biological processes.

Citation: Kim T-M, Ramírez V, Barrera-Chimal J, Bobadilla NA, Park PJ, et al. (2011) Gene Expression Analysis Reveals the Cell Cycle and Kinetochore Genes Participating in Ischemia Reperfusion Injury and Early Development in Kidney. PLoS ONE 6(9): e25679. doi:10.1371/journal.pone.0025679

Editor: Christos A. Ouzounis, The Centre for Research and Technology, Hellas, Greece

Received May 16, 2011; **Accepted** September 8, 2011; **Published** September 28, 2011

Funding: Vaidya laboratory is supported by National Institutes of Environmental Health Sciences' Pathway to Independence Grant [ES016723]. TMK and PJP are supported by a grant from National Institute of General Medical Sciences (R01 GM082798). The funders had no role in study design, data collection and analysis, decision to publish, or preparation of the manuscript.

Competing Interests: The authors have declared that no competing interests exist.

* E-mail: vvaidya@partners.org

☯ These authors contributed equally to this work.

Introduction

Acute kidney injury represents a common clinical problem leading to high rates of morbidity and mortality [1]. Identification of accurate diagnostic markers or effective targets for therapeutic intervention is challenging and it would benefit from a comprehensive understanding about the molecular programs governing renal injury-regeneration processes [2,3]. Kidney regeneration after ischemic injury represents a complicated but highly coordinated process, which involves a diverse set of molecular functions. For example, animal studies using micro-array-based expression analysis revealed that various molecular functions (e.g., cell cycle, inflammation and apoptosis) were perturbed in ischemic-reperfusion (I/R) injury [4–7]. It has also been proposed that the transcriptional reprogramming induced by I/R injury may recapitulate those of kidney organogenesis in which the kidney injury induces the re-expression of various nephrogenic genes such as Vimentin, Pax-2 and Bmp-7 [8–10]. Considering that these two biological processes (kidney regeneration and development) require tightly regulated cellular processes that control cell proliferation and differentiation, a comparison between the transcriptional programs associated with these processes may provide a better understanding about the underlying molecular mechanisms, as exemplified in other organogenesis model (e.g., liver) [11,12].

In this study, we performed microarray-based gene expression analysis to investigate changes in the transcriptome during kidney I/R injury and early development using animal models. Pathway analysis of the transcriptome changes revealed that a wide spectrum of molecular functions may be involved in these

biological processes. A detailed examination on the relationship between regeneration- and development-related genes in terms of their enrichment to known functional gene categories further showed that some molecular functions are common to kidney regeneration and development. Among the shared functions, we focused on a number of cell cycle and kinetochore genes that were over-expressed during I/R injury and embryonic kidneys with experimental verification.

Results

Adult kidney injury model using bilateral ischemia-reperfusion injury

Kidney injury was induced by 20 minutes of bilateral renal ischemia followed by reperfusion that resulted in kidney dysfunction, characterized by elevation of serum creatinine (SCr) and blood urea nitrogen (BUN), (Figure 1A and 1B) at 24 hr of reperfusion followed by a recovery at 120 hr. Kidney Injury Molecule-1 (Kim-1) mRNA levels , recently identified as sensitive indicator in monitoring tubular kidney injury [3] and Vimentin mRNA levels, a marker of mesenchymal phenotype and dedifferentiation of tubular cells [13] also showed peak expression at 24 hr after injury while the expression decreased to control levels after 120 hr (Figure 1C and 1D). The histopathological examination showed typical lesions caused by renal ischemia at 24 hr characterized by proximal tubular necrosis and apoptosis that resulted in substantial loss in epithelial brush border and cell debris accumulation in luminal area at 24 hr with a structural and functional recovery by 120 hr due to an efficient kidney regeneration response (Figure 2A). The immunohistochemistry of Ki-67 showed a marked staining level at 72 hr and 120 hr after I/R injury (Figure 2B), which indicates the enhanced cellular proliferation during these regenerative time points.

Animal model for embryonic kidney development and comparative gene expression profiling

To take into account the differential expression pattern between renal cortex and medulla, we isolated total RNA from rat renal cortices and medullas and performed gene expression profiling at 6 hr, 24 hr and 120 hr which correspond to early, intermediate and late-regeneration phase after I/R injury ($n = 3$ for each). To explore the expression profiles of kidney development, we also collected RNA from mouse kidney at embryonic day 16 postcoitum or p.c. (E16d) and at postnatal day 1 and 7 (PN1d and PN7d; $n = 5$ for each), respectively. We selected E16d since this time point is critical in early kidney development (e.g., distinction of cortex versus medulla and the beginning of differentiation of functional proximal tubule) and PN1d and PN7d represent the immediate and early postnatal period, respectively.

The hierarchical clustering of highly variable genes showed that the expression profiles of renal cortex and medulla are largely distinguishable from each other and the profiles from kidneys subjected to I/R injury are also distinguishable from those of sham (Figure 3A). The hierarchical clustering also clearly separated the expression profiles of embryonic mouse kidney from those of postnatal kidneys (Figure 3B). We also combined the expression profiles of rat I/R injury and mouse developmental kidneys and performed hierarchical clustering using highly variable orthologous genes (Figure 3C). The segregating pattern observed when two species were separately analyzed (e.g., three main clusters in each profile) was preserved in the combined analysis. The clustering of merged dataset further reveals the expression similarities between two species such as sham (rat) and PN7d (mouse) as well as E16d (mouse)-ischemic medulla (rat) and PN1d (mouse)-ischemic cortex (rat).

Next, we performed pathway analysis to explore the coordinated expression changes of functionally related genes during kidney I/R injury and development. Parametric analysis of gene

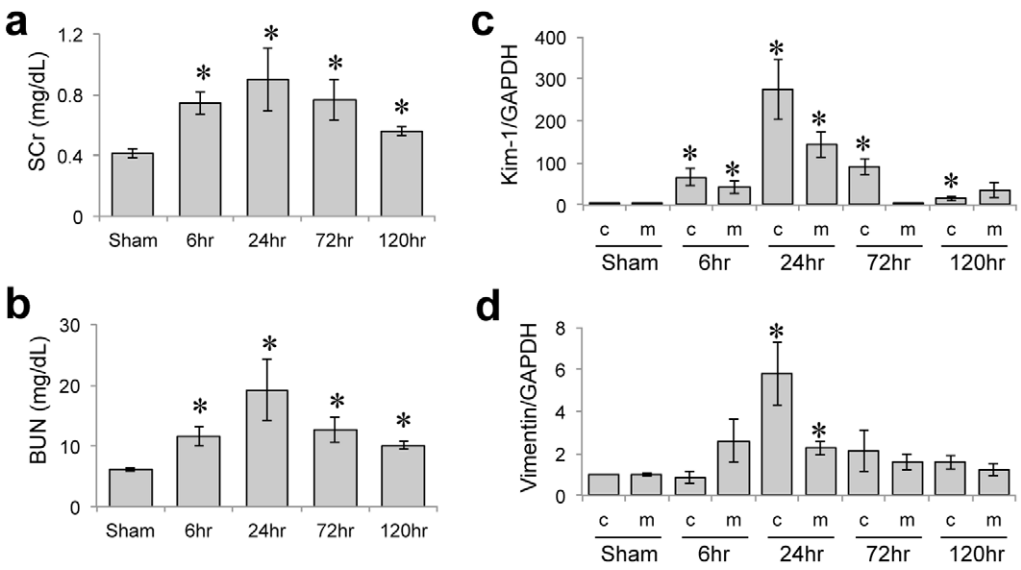

Figure 1. Temporal profiles of kidney biomarkers in ischemic-reperfusion kidney model. A. SCr levels are measured after 6 hr, 24 hr, 72 hr, and 120 hr of reperfusion after I/R injury in rat. Significant difference of SCr level compared to Sham is shown with asterisk ($P<0.05$). **B.** The temporal changes in BUN levels are shown. Renal mRNA levels of Kim-1 (**C**) and Vimentin (**D**) are shown for cortex and medulla. The mRNA levels were normalized using GAPDH as control gene (denoted as c and m, respectively). * represents $P<0.05$ as determined by one way ANOVA in comparison with sham rats.
doi:10.1371/journal.pone.0025679.g001

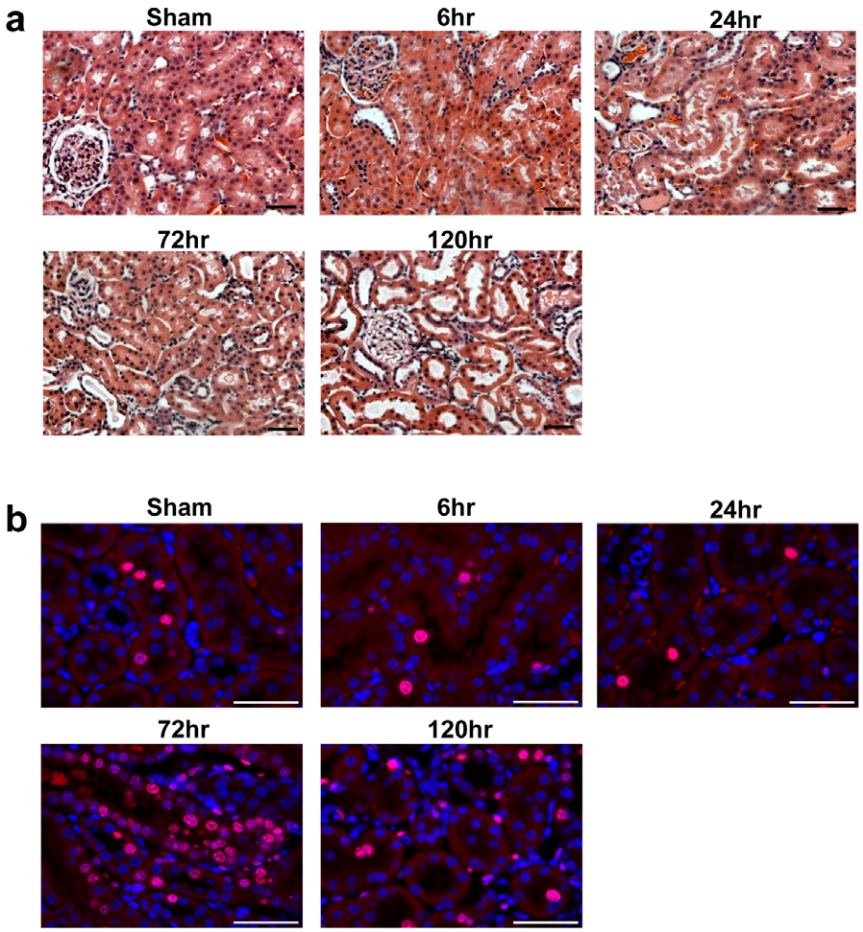

Figure 2. Histological and immunohistochemical examination of kidney tissue injury and repair following I/R injury. Representative formalin fixed paraffin embedded kidney tissue sections of sham male Wistar rats and those undergone 20 min bilateral ischemia reperfusion over time stained by (**A**) Hematoxylin and Eosin (40× magnification) and (**B**) Ki-67 (60× magnification). $n = 5$/group. Bar represents 50 μm.
doi:10.1371/journal.pone.0025679.g002

expression (PAGE) [14] was used to measure the enrichment of Gene Ontology (GO) functional categories [15] between two phenotypes (e.g., sham versus 6-hr in renal cortex). We collected GO annotations with significant enrichment ($P<0.05$, Bonferroni adjusted) across eight comparisons, i.e., six for I/R injury (6 hr, 24 hr and 120 hr for cortex and medulla; each compared to sham) and two for development (PN1d and PN7d; each compared to E16d). Figure 4 shows the representative functional categories in each comparison (full lists of significant functions are available in Tables S1,S2,S3). We observed that the molecular functions representing immunity, inflammation and apoptosis are globally up-regulated across all time points measured after I/R injury (6 hr, 24 hr and 120 hr) in cortex and medulla indicating that these functions are characteristic transcriptional features of kidney regeneration after ischemic injury. In addition, the molecular functions associated with metabolism or ion transport are commonly down-regulated during kidney regeneration.

We observed that some molecular functions are observed both during kidney regeneration and development. For example, cell cycle and chromosome-related functions are up-regulated at 24 hr after I/R injury, while down-regulated in postnatal kidneys compared to embryonic ones. Also, the up-regulated functions such as ion transporters or metabolism in postnatal kidney (or down-regulated in embryonic kidney) largely overlap with those observed in ischemic-regeneration profiles.

We further constructed a functional network comprising the up- and down-regulated genes in the two processes and their enriched GO categories as nodes (Figure 5A). Their associations (significant gene overlap between gene sets) are illustrated as edges. The subnetwork on the left (Figure 5A) includes six up-regulated gene sets during kidney ischemic-regeneration (red rectangles) and one down-regulated gene set (one green rectangle) in postnatal kidney compared to embryonic kidney. This subnetwork also includes multiple GO categories representing cell cycle/mitosis, cytoskeleton and immune/inflammation. The other subnetwork is largely associated with functional categories of transport/membrane and metabolism and composed of regeneration-down-regulated and postnatal-up-regulated genes (Figure 5A, right). Thus, our pathway analysis reveals that the differentially expressed genes in both regenerative and developmental time points share common functional gene sets, highlighting the similarity in the two processes.

When the GO nodes are removed (the differentially expressed genes in regeneration or development are compared directly), a substantial overlap among datasets becomes clearer (Figure 5B). Among the significant gene overlap between differentially expressed genes, we focused on those between regenerative- and developmental profiles and their overlapping genes (listed in Figure 5B). For example, we observed significant gene overlap between PN7d (down-regulated) and 24 hr I/R (up-regulated;

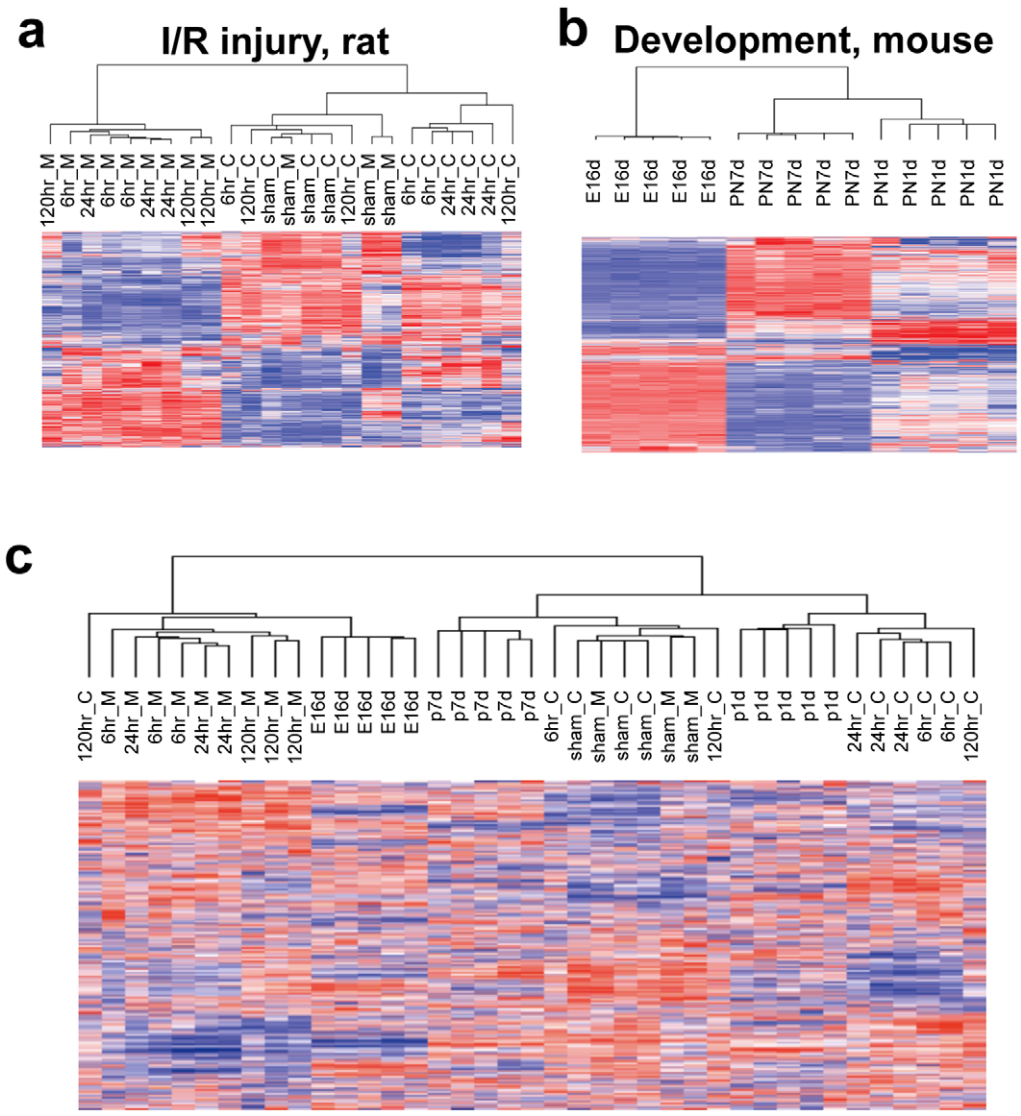

Figure 3. Hierarchical clustering of kidney regeneration after ischemic injury and development. A. Hierarchical clustering of top variable 2000 genes segregates the expression profiles of renal cortex (C) and medulla (M) after ischemic injury while sham samples are also distinguished from injury-associated profiles. **B.** The expression profiles of fetal mouse kidney (E16d) are clearly distinguished from those of postnatal kidney (PN1d and PN7d) by hierarchical clustering. C. The rat I/R injury- and mouse development expression profiles were merged and hierarchically clustered for top variable 2000 orthologous genes.
doi:10.1371/journal.pone.0025679.g003

both in cortex and medulla) and the overlapping genes largely represent kinase and kinetochore-encoding genes. The up-regulated genes in PN1d and PN7d were enriched in the down-regulated genes of 6 hr and 24 hr after I/R injury in medulla. These genes largely represent membrane-associated or ion-transport molecules (e.g., solute carrier gene families, Nox4, Mep1A, Apom, and Anpep). The functional annotations of overlapping genes are consistent with the enriched functional categories between two biological processes also highlighting the overlapping genes as candidates for molecular validation.

Confirmation of overlapping genes

For experimental validation, we focused on the overlapping genes between those down-regulated at postnatal 7 day (PN7d) kidney and those up-regulated at 24 hr after I/R injury in renal cortex and medulla (Figure 5A; two edges indicated by arrows). Eight genes were observed in either edge. Aurkb, Kif22 (or Kid), Cdc2A (or Cdk1), Tpx2, and Mcm6 were observed in both edges while Cdca3, Plk1 (in medulla only) and Ranbp1 (in cortex only) were observed in single edge. These genes are primarily associated with celldivision functions as essential components of kinetochore.

We selected 4 candidate genes (Aurkb, Plk1, Mcm6, and Kif22) for experimental verification (Figure 6). We confirmed the transcriptional up-regulation of Aurkb, Plk1, Mcm6, and Kif22 after 24 hr of ischemic injury (both in renal cortex and medulla) and also in rat embryonic kidneys (E17d; $n = 6$, each). We also isolated total RNA from 6 day embryo (E16d) and 60-day-old (P60d) BALB/c mice ($n = 4$, each) to confirm the relative up-regulation of these genes in embryonic kidneys. In order to localize these proteins post I/R injury and during development, we performed immunofluorescence analysis using specific antibodies for each protein. While Aurkb and Plk1 staining was absent in

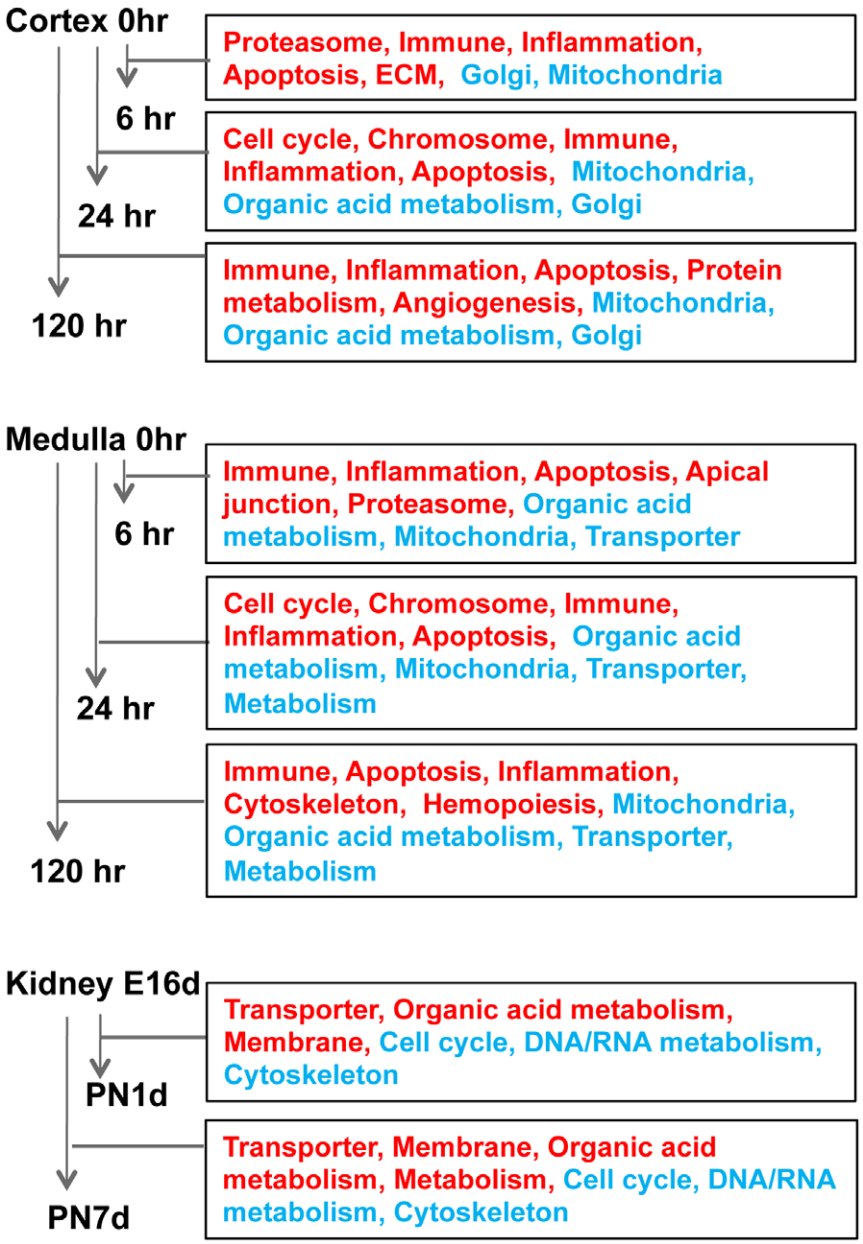

Figure 4. Pathway analysis of expression changes associated with kidney regeneration after ischemic injury and development. Pathway analysis shows the significantly up- and down-regulated GO functional categories (red- and blue-coded in the corresponding rectangles, respectively) in each time point measured after ischemic induction (cortex and medulla of rat kidney) or in the corresponding developmental time points (mouse kidney). Only representational functional categories are shown from a list of significantly enriched GO categories. Full list of observed GO categories are available in Tables S1,S2,S3.
doi:10.1371/journal.pone.0025679.g004

sham rats, Mcm6 was localized in the nucleus. At 24 hr post I/R, we observed a marked nuclear staining in the kidney for Aurkb, Plk1 and Mcm6. This effect was also observed in the E17d rat kidneys. The mRNA level of Kif22 also showed significant increased expression at 24 hr after I/R injury while clear decrease was observed after 72 hr and 120 hr. Immunofluorescence analysis shows that Kif proteins are normally located in the nucleus, as confirmed by DAPI nuclear staining. After I/R injury, we observed the increase in Kif staining in the cortico-medullary area of the kidney, where primary ischemic injury occurs. A slight increase in cytoplasmic staining post ischemia for Kif22 was also noted.

Discussion

Our analysis provides a comprehensive understanding of the functional overlap between the transcriptional programs governing the regenerative and developing kidney processes. These biological processes are regulated by a cascading activation of various molecular functions, which can be inferred from the coordinated expression of functionally related genes [e.g., Gene ontology (GO) annotations]. Among the observed functions, the cell cycle functions were commonly up-regulated during peak of injury (24 hr after I/R injury) and embryonic kidneys (compared to postnatal kidneys) and we validated the transcriptional up-

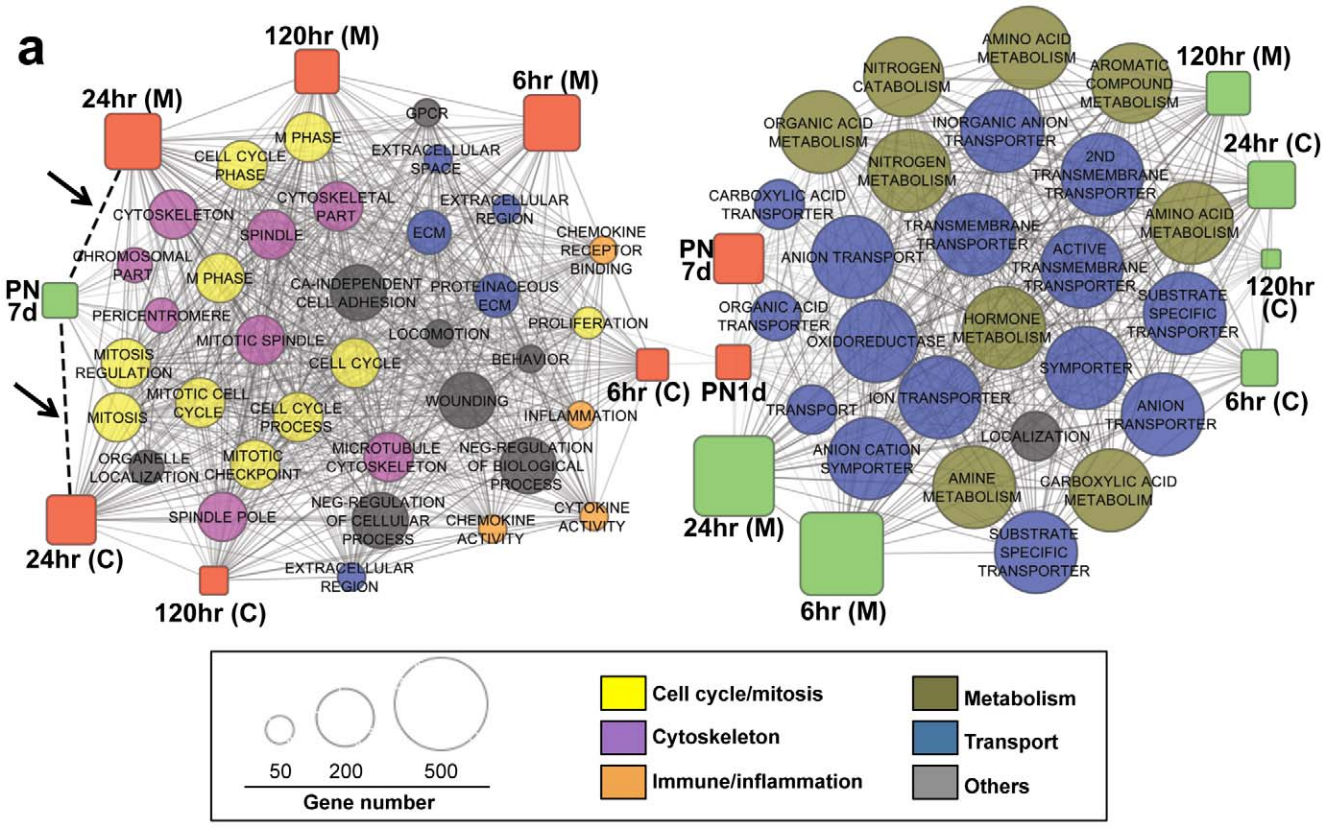

Figure 5. Functional association network. A. The differentially expressed genes during regeneration or development of kidney (the up- and down-regulated genes as red and green rectangles, respectively) and GO categories (circles) are shown as nodes. The significant enrichment between two gene sets is shown as edge between two corresponding nodes. The size of node is proportional to the gene size and GO categories were classified into six major functions as shown in the color scheme. Two dashed lines with arrows represent the significant association between PN7d (genes down-regulated compared to E16d) and 24 hr I/R (genes up-regulated compared to sham). **B.** The significant associations between gene sets are shown after removing GO categories. The overlapping genes are shown for pairs between I/R injury and development. Experimentally validated four genes are bold. * and ** represent the genes only observed with 6 hr/medulla and 24 hr/medulla, respectively. Number of overlapping genes are shown in parenthesis for significant pairs between I/R injury gene sets.
doi:10.1371/journal.pone.0025679.g005

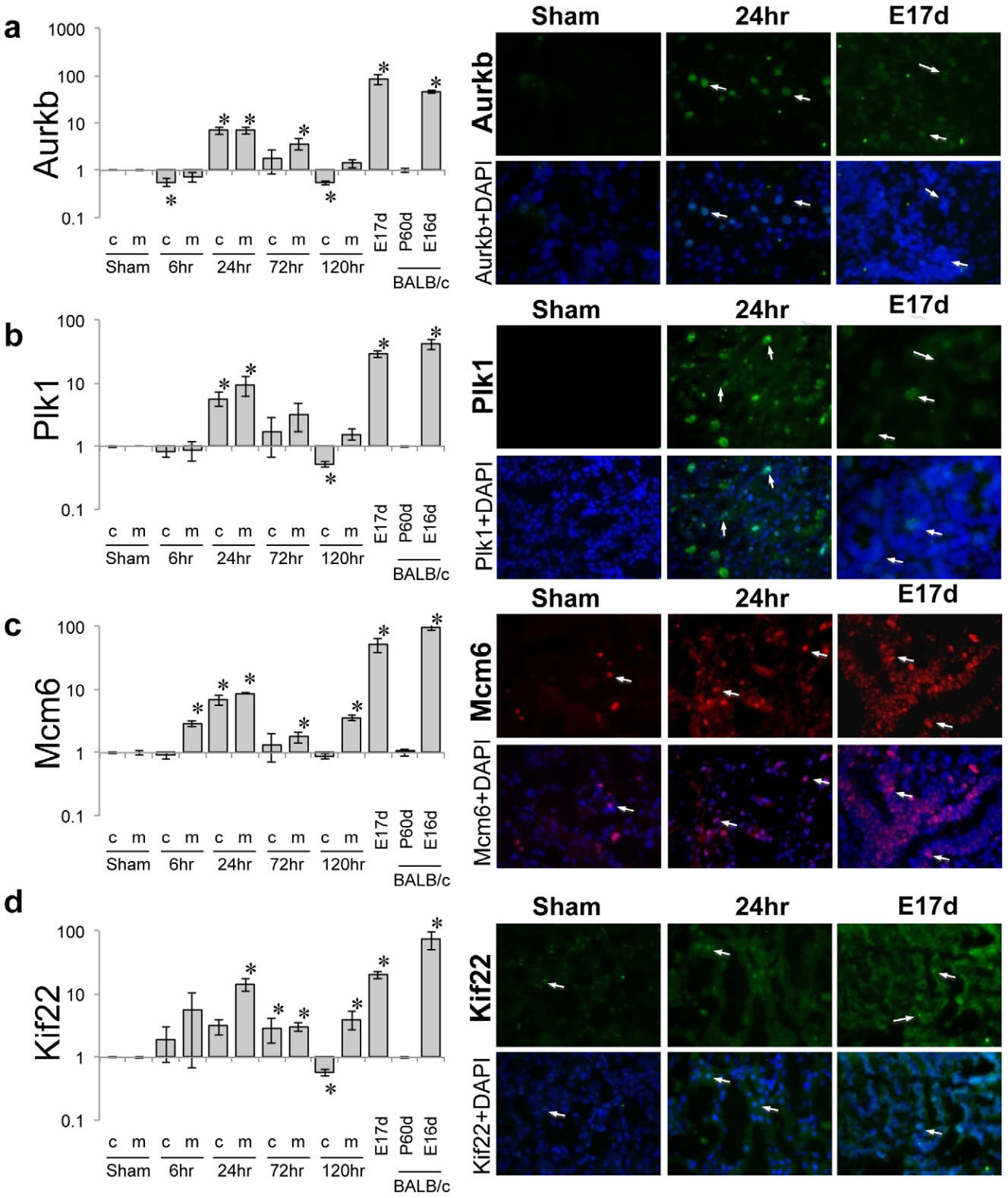

Figure 6. Quantitative mRNA levels. A. mRNA levels of Aurkb were measured by real-time quantitative PCR in rat and mouse kidney (left). Rat kidneys collected at 0 hr (shame), 6 hr, 24 hr, 72 hr, and 120 hr after ischemic injury are shown for cortex (c) and medulla (m), respectively. The expression levels are shown for embryonic rat kidney (embryonic day 17; E17d) along with those of mouse kidney (E16d and P60d as embryonic day 16 and postnatal day 60, respectively). All data were normalized using GAPDH as a control gene. Immune fluorescence analysis shows the absence of Aurkb expression in sham rat kidney; however, embryonic kidneys and those after 24 hr of ischemic injury show increased Aurkb expression, the nuclear co-localization of which were confirmed by DAPI staining (right). **B**, **C**, **D** are similarly shown for Plk1, Mcm6 and Kif22. 40× magnification.
doi:10.1371/journal.pone.0025679.g006

regulation of cell cycle-associated kinases and kinetochore genes, *Aurkb, Plk1, Mcm6, and Kif22*.

Aurkb, Plk1 and Cdc2A are among the chief kinases involving kinetochore assembly and formation of kinetochore-microtubue attachment [16]. The inhibition of Aurkb is associated with a failure in cytokinesis and complete segregation of chromosomes, which leads to polyploidy and cell death in cell culture [17]. *Tpx2* encodes cofactor of Aurora kinases, which is required for correct spindle assembly [18]. *Plk1* also encodes kinase that is essential for cell division [19] and the phosphorylation of this kinase or its substrates by Cdc2A helps the interactions between them [20]. In addition, *Kif22* encodes a chromokinesin involved in chromosome arm orientation on the spindle [21] and similar roles have been reported for Cdca3, Mcm6 and Ranbp1 [22–24]. Some studies have proposed the putative roles of kinetochore genes involved in both renal regeneration and development [25]. Our results provide supporting evidences for cell cycle/mitosis-associated molecules as potential markers in evaluating the developing and regenerating kidney. These findings are consistent with the need to proliferate while maintaining fully differentiated function that is shared by the developing and regenerating kidney. Furthermore, genes involved in mitosis checkpoints such as Aurkb and Plk1, are likely to be related to the need for increased surveillance system required in both renal regeneration process and early kidney development.

Prior studies have largely focused on conducting gene expression analysis focusing on one model at-a-time using either regenerating kidney following I/R injury alone or early development of kidney alone and hence have not provided a context to compare two biological processes in terms of expression or functional similarity [4–7]. For example, Perco et al observed that the 89 proteins reported in previous I/R injury studies largely represent six functional categories of immunity, cell cycle, apoptosis, cell structure, proliferation, and transporter/carrier [26]. Stuart et al performed expression analysis during the development of rat kidneys [27]. They classified genes associated with different developmental stages into five functional categories, e.g., DNA replication/cell cycle (early embryonic kidney) and transporter/metabolism/oxidative stress functions (adult kidney). Our results are largely consistent with these previous reports; however, we focused on the similarity between I/R injury and developmental kidney expression profiles in terms of enriched GO categories and overlapping genes between the profiles. For example, some of the enriched molecular functions are consistently activated (e.g., cell cycle/apoptosis, immunity/inflammation) or repressed (e.g., membrane-associated enzymes or transporters) during the kidney regeneration or in embryonic kidneys. The similarity of functional annotations between two processes suggests that kidney regeneration after ischemic injury may accompany the reactivation of developmental regulatory programs.

We also observed that hierarchical clustering largely segregates the expression profiles of renal cortex and medulla and the pathway analysis also revealed that some molecular functions are restricted to specific time points or anatomical segments (e.g., the up-regulation of angiogenesis (cortex) and hemopoiesis genes (medulla) in late regenerative phase). The hierarchical clustering of merged dataset also showed that regenerative cortex and medulla resemble the postnatal kidneys of 1 and 7 days, respectively.These findings suggest that these renal segments may have different compensatory mechanism to cope with I/R injury, which are worthy of further investigation. In addition, our analysis involves cross-species comparison (i.e., I/R injury- and development-associated profiles were obtained from rat and mouse, respectively). The expression profiles obtained from rat and mouse would form separate clusters if there were potential batch effects or substantial gene expression differences [28]. However, the hierarchical clustering of merged expression profiles shows that the expression patterns of sham (rat) and postnatal kidneys (PN7d; mouse) are more similar with each other than the remaining expression profiles from the corresponding species. This suggests that the batch effects or the cross-species differences are not substantial compared to I/R injury- or development-associated expression changes.

In summary, the candidate genes identified in this analysis could potentially act as differentiation/dedifferentiation markers and the elucidation of functional significance of their up-regulation in kidney injury and development could offer new therapeutic strategies to enhance kidney regeneration.

Materials and Methods

Animals

Male Wistar rats (280–300 g, 8–9 weeks old) were purchased from Harlan Laboratories (Indianapolis, IN) andwere maintained in central animal facility over wood chips free of any known chemical contaminants under conditions of $21\pm1^{\circ}$C and 50–80% relative humidity at all times in an alternating 12 hr light-dark cycle. Animals were fed with commercial rodent chow (Teklad rodent diet # 7012), given water ad lib, and were acclimated for 1-week prior to use. All animal maintenance and treatment protocols were in compliance with the Guide for Care and Use of Laboratory animals as adopted and promulgated by the National Institutes of Health and were approved by the Harvard Medical School Animal Care and Use Committees (IACUC).

Experimental design

Nine male Wistar rats underwent I/R surgery and three rats underwent sham surgery simulating I/R. In order to perform I/R surgery, the rats were anesthetized using pentobarbital sodium (30 mg/kg, ip) and renal ischemia was induced by nontraumatic vascular clamps over the pedicles for 20 min as described before [3,29]. Upon release of the clamps, the incision was closed in two layers with 2–0 sutures. The sham rats underwent anesthesia and a laparotomy only and were sacrificed after 24 hr. The rats in I/R group were further divided in subgroups of three rats each and sacrificed after 6 hr, 24 hr, and 120 hr of reperfusion. To confirm the results of gene expression analysis twenty male Wistar rats underwent 20 minutes bilateral I/R surgery and five rats underwent sham surgery as described above and were sacrificed at 6 hr, 24 hr, 72 hr and 120 hr following reperfusion ($n = 5$, each timepoint). At the time of sacrifice, kidneys were macroscopically divided into renal cortex and medulla, frozen in liquid nitrogen, and maintained at -80°C until use as previously described [30]. We also included rat embryos at embryonic day 17 p.c. for kidney development analysis (E17d). Kidney was collected from male BALBc mice embryos at embryonic day 16 p.c. (E16d) as well as those from 1, 7 and 60 postnatal days (PN1d, PN7d and P60d, respectively). The E17d rat embryonic kidneys were collected from Sprague-Dawleyrats from Charles River Laboratories, Inc. (Raleigh, NC).

Blood Chemistry

At sacrifice of rats following renal I/R injury, blood was collected from dorsal aorta in heparinized tubes. Serum creatinine (SCr) concentrations were measured using a Beckman Creatinine Analyzer II. Blood urea nitrogen (BUN) was measured spectrophotometrically at 340 nm using a commercially available kit (Thermo Scientific, Rockford, IL) as described before [3].

RNA isolation and Real Time-Polymerase Chain Reaction (RT-PCR)

Total RNA was isolated from each kidney cortex, medulla, and embryonic kidney following the manufacturer's protocol for Trizol extraction method (Invitrogen, Carisbad, CA). The density of total RNA was measured by spectrophotometer, and subsequently checked for integrity by 1% agarose gel electrophoresis. All RNA samples were treated with DNase I (Invitrogen, Carisbad; CA) to avoid DNA contamination followed by reverse transcription with 1 μg of total RNA using iScriptcDNA synthesis (BIO-RAD. Hercules; CA). The mRNA levels of Kim-1, Vimentin, Kif22, Mcm6, Aurkb, Plk1 and GAPDH as the internal control were determined using the iQ SYBR Green super mix kit (Bio-rad, Hercules, CA) following the manufacturer's instructions. We performed the assay in an iCycler PCR System (BIO-RAD, Hercules, CA) with the cycling protocol as follows: 3′94°C, 15″55°C, and 72°C for 35″ for 45 cycles. The primer pair sequence of each assay is detailed in Table 1. The relative quantification of gene expression was performed using the comparative CT method.

Separation of cortex and medulla

To confirm that there was no contamination between cortex and medulla, the mRNA levels for sodium chloride cotransporter (NCC) as a specific gene expressed in cortex was quantified by real-time PCR on the ABI Prism 7300 Sequence Detection System (*Taq*Man, ABI, Foster City, CA, assay number assay number Rn00571074_m1). As an endogenous control, we used eukaryotic 18S rRNA (predesigned assay reagent, external run, ABI). The relative quantification of expression was performed using the comparative CT method [31] Results revealed that mRNA levels of NCC were abundantly expressed in renal cortex (1 ± 0.07) as compared to renal medulla (0.001 ± 0.0001) demonstrating that there was no contamination of the cortex with medulla (Figure S1).

Microarray analysis

Biotin-16-UTP was used during in vitro transcription. Microarray analysis was performed in biological triplicates. Labeled RNAs were hybridized onto Gene chip array RatRef-12 V1.0 (BD-202-0202 Illumina San Diego CA.), which contains 22,523 genes for rat. For mouse RNA, we used MouseRef-8 V1.1 (AMIL1791 Illumina San Diego; CA.) with 24,854 genes following the manufacturer's instructions. After washing and blocking, streptavidin-Cy3 was used to crosslink the amplified RNA, which were scanned by the Illumina bead reader. The data was analyzed using Illumina bead studio software (Illumina San Diego; CA). The scanned intensity values were quantile normalized for subsequent analysis. The expression microarray data can be accessed from Gene Expression Omnibus (GEO) with accession number of GSE27274 (rat) and GSE28054 (mouse).

Pathway analysis

Agglomerative hierarchical clustering was performed for the highly variable 2000 genes from expression profiles ofrenal I/R injury (rat) and nephrogenic models (mouse). For clustering, 1 minus Pearson correlation coefficient was used as distance with average linkage [32]. For functional gene set, we obtained GO categories from MSigDB database (http://www.broadinstitute.org/gsea/msigdb/index.jsp; c5 GO category) [33]. Pathway analysis was performed using parametric analysis of gene expression (PAGE) method [14]. For individual GO categories, the significance of enrichment was measured by converting the mean fold change of genes belonging to the GO category into $\mathcal{Z}$ score. The significance of enrichment was measured across 6 comparisons (3 time points after I/R injury against sham, cortex and medulla, respectively) and 2 comparisons (PN1d and PN7d against E16d). Significantly (Bonferroni corrected $P<0.05$) enriched GO categories were collected with leading edge gene subsets (fold change >1.5 or <-1.5). A full list of enriched GO categories are available in Tables S1,S2,S3 (I/R injury in cortex and medulla as well as mouse developmental kidney). To construct functional network of gene sets or association map, we first collected genes showing highly up- or down-regulation (fold change >1.5 or <-1.5, respectively) for 8 time scales (6 for rat kidney and 2 for mouse kidney) [34]. Sixteen sets of differentially expressed genes were then measured for the significant of enrichment with GO categories by Fisher's exact test and 57 GO categories showing significant enrichment (Bonferroni corrected $P<0.05$) with any of 16 gene sets were selected. We ignored the down-regulated genes in PN1d in network since they do not show significant association with other gene sets. The selected GO categories were manually curated into 6 functional categories (cell cycle/mitosis, immune/inflammation, transport, metabolism, cytoskeleton, and others). The collected 72 gene sets (57 GO categories and 15 regeneration-/development-associated gene sets) were measured for the significance of enrichment in a pairwise manner. We used CytoScape software to construct a network using organic layout [35]. In the network, the gene sets are represented as nodes and the significant association between the gene sets was shown as edge.

Table 1. The primer pairs for RT-PCR.

Gene	Forward primer	Reverse primer
Kim-1 (rat)	5′ CCACAACTACAAGACCCACAACCAC 3′	5′ GGATGTCACAGTGCCATTCCAG 3′
Kim-1 (mouse)	5′ GGAAGTAAAGGGGGTAGTGGG 3′	5′ AAGCAGAAGATGGGCATTGC 3′
Vimentin	5′ ACCGCTTCGCCAACTACATC 3′	5′ GCAACTCCCTCATCTCCTCC 3′
Kif22	5′ CTAAGCAAGGGAGGAGTCAGC 3′	5′ TTGGCTACTTCAAGAGAGCAGC 3′
Mcm6	5′ CCGAATCTCTAACCTCATCGTGC 3′	5′ GCTCTCGCTTCCTTCACTGGAG 3′
Aurkb	5′ GATGATTGAAGGGCGGATGC 3′	5′ AAAGGGCAGAGGGAGGCAGAAC 3′
Plk1 (rat)	5′ TGCTCAAGCCCCATCAGAAG 3′	5′ AGTCGCTGTCCTCAAAAAAGC 3′
Plk1 (mouse)	5′ CCCCACCAGAAGGAGAAGATG 3′	5′ AAATACAAATACAAAGTCGCTGTCC 3′
GAPDH	5′ TCCGCCCCTTCTGCCGATG 3′	5′ CACGGAAGGCCATGCCAGTGA 3′

doi:10.1371/journal.pone.0025679.t001

Immunofluorescence

After perfusion, the kidneys were isolated, frozen and later sectioned in slides of 5 μm thickness. For single staining, cryosections from 4 rats of each group and three E17d tissues were fixed in 10% formaldehyde for 5 min, followed by 5 min 0.1% Triton-X permeabilization, and then blocking with BSA 3% for 60 min. After washing, the sections were incubated overnight with rabbit monoclonal anti-Ki67 (Vector Laboratories, Burlingame, CA), rabbit anti Kif22 1:1000 (Abcam, Cambridge MA), rabbit anti Plk1 antibody 1:500 (Cell Signaling Technology Inc), and rabbit anti Aurkb (1:500) (Cell Signaling Technology Inc, Danvers.MA). Goat anti-mcm6 antibody 1:1000 (Abcam, Cambridge MA.) at 4°C was used. After washing, sections were incubated at room temperature with secondary antibody Cy3 conjugated goat anti rabbit 1:600 (Jackson Immune research, West Grove Pa) or alexafluor 488 conjugated donkey anti goat 1:500 (Invitrogen) for 60 min and washed again. The images were captured by Nikon DS-QiMc camera attached to Nikon eclipse 90i flourescence microscope using oil immersion objectives (40× magnification) by Nikon NIS elements AR ver3.2 software.

Statistics

Data are expressed as average+standard error. Statistical difference ($P<0.05$) as calculated by one way ANOVA or student's t-test. $P<0.05$ was considered significant and represented by '*' where applicable. All graphs were generated by GraphPad Prism (GraphPad, Inc., La Jolla, CA).

Supporting Information

Figure S1 Realtime PCR analysis confirming no cross contamination between kidney cortex and medulla. Real time-PCR for sodium chloride cotransporter (NCC) that is expressed only in the cortex was conducted. Results were normalized to eukaryotic 18S rRNA as control gene. * represents $p<0.05$ determined by t test with respect to renal cortex.
(TIF)

Table S1 The GO functional categories significantly (Bonferroni corrected P<0.05) enriched in cortex I/R injury profiles. The functions up- and down-regulated in each time scale (6 hr, 24 hr and 120 hr) compared to Sham are shown. The gene size and uncorrected significance level are also shown. Leading edge genes represent genes highly up- and down-regulated (fold change >1.5 and <−1.5) among the genes belonging to the corresponding GO categories.
(PDF)

Table S2 The GO functional categories significantly enriched in medulla I/R injury profiles.
(PDF)

Table S3 The GO functional categories significantly enriched in developing kidney. The expression profiles from postnatal day 1 and 7 (PN1d and PN7d) are compared to that of embryonic kidney (E16d).
(PDF)

Acknowledgments

We thank Dr. Edie Sloter from WIL Research laboratories for help with rat embryonic kidneys and we also thank Drs. Jacqueline Ho and Jordan Kriedberg from Children's Hospital, Harvard Medical School for help with embryonic mouse kidneys.

Author Contributions

Conceived and designed the experiments: TMK VR VSV. Performed the experiments: TMK VR JBC. Analyzed the data: TMK VR PJP NAB VSV. Contributed reagents/materials/analysis tools: NAB. Wrote the paper: TMK VSV.

References

1. Thadhani R, Pascual M, Bonventre JV (1996) Acute renal failure. N Engl J Med 334: 1448–1460.
2. Bonventre JV, Vaidya VS, Schmouder R, Feig P, Dieterle F (2010) Next-generation biomarkers for detecting kidney toxicity. Nat Biotechnol 28: 436–440.
3. Vaidya VS, Ozer JS, Dieterle F, Collings FB, Ramirez V, et al. (2010) Kidney injury molecule-1 outperforms traditional biomarkers of kidney injury in preclinical biomarker qualification studies. Nat Biotechnol 28: 478–485.
4. Yoshida T, Tang SS, Hsiao LL, Jensen RV, Ingelfinger JR, et al. (2002) Global analysis of gene expression in renal ischemia-reperfusion in the mouse. Biochem Biophys Res Commun 291: 787–794.
5. Kieran NE, Doran PP, Connolly SB, Greenan MC, Higgins DF, et al. (2003) Modification of the transcriptomic response to renal ischemia/reperfusion injury by lipoxin analog. Kidney Int 64: 480–492.
6. Supavekin S, Zhang W, Kucherlapati R, Kaskel FJ, Moore LC, et al. (2003) Differential gene expression following early renal ischemia/reperfusion. Kidney Int 63: 1714–1724.
7. Yuen PS, Jo SK, Holly MK, Hu X, Star RA (2006) Ischemic and nephrotoxic acute renal failure are distinguished by their broad transcriptomic responses. Physiol Genomics 25: 375–386.
8. Maeshima A, Maeshima K, Nojima Y, Kojima I (2002) Involvement of Pax-2 in the action of activin A on tubular cell regeneration. J Am Soc Nephrol 13: 2850–2859.
9. Villanueva S, Cespedes C, Vio CP (2006) Ischemic acute renal failure induces the expression of a wide range of nephrogenic proteins. Am J Physiol Regul Integr Comp Physiol 290: R861–R870.
10. Vukicevic S, Basic V, Rogic D, Basic N, Shih MS, et al. (1998) Osteogenic protein-1 (bone morphogenetic protein-7) reduces severity of injury after ischemic acute renal failure in rat. J Clin Invest 102: 202–214.
11. Jochheim-Richter A, Rudrich U, Koczan D, Hillemann T, Tewes S, et al. (2006) Gene expression analysis identifies novel genes participating in early murine liver development and adult liver regeneration. Differentiation 74: 167–173.
12. Kelley-Loughnane N, Sabla GE, Ley-Ebert C, Aronow BJ, Bezerra JA (2002) Independent and overlapping transcriptional activation during liver development and regeneration in mice. Hepatology 35: 525–534.
13. Witzgall R, Brown D, Schwarz C, Bonventre JV (1994) Localization of proliferating cell nuclear antigen, vimentin, c-Fos, and clusterin in the postischemic kidney. Evidence for a heterogenous genetic response among nephron segments, and a large pool of mitotically active and dedifferentiated cells. J Clin Invest 93: 2175–2188.
14. Kim SY, Volsky DJ (2005) PAGE: parametric analysis of gene set enrichment. BMC Bioinformatics 6: 144.
15. Ashburner M, Ball CA, Blake JA, Botstein D, Butler H, et al. (2000) Gene ontology: tool for the unification of biology. The Gene Ontology Consortium. Nat Genet 25: 25–29.
16. Cheeseman IM, Desai A (2008) Molecular architecture of the kinetochore-microtubule interface. Nat Rev Mol Cell Biol 9: 33–46.
17. Ditchfield C, Johnson VL, Tighe A, Ellston R, Haworth C, et al. (2003) Aurora B couples chromosome alignment with anaphase by targeting BubR1, Mad2, and Cenp-E to kinetochores. J Cell Biol 161: 267–280.
18. Giubettini M, Asteriti IA, Scrofani J, De LM, Lindon C, et al. (2011) Control of Aurora-A stability through interaction with TPX2. J Cell Sci 124: 113–122.
19. Strebhardt K, Ullrich A (2006) Targeting polo-like kinase 1 for cancer therapy. Nat Rev Cancer 6: 321–330.
20. Elia AE, Rellos P, Haire LF, Chao JW, Ivins FJ, et al. (2003) The molecular basis for phosphodependent substrate targeting and regulation of Plks by the Polo-box domain. Cell 115: 83–95.
21. Levesque AA, Compton DA (2001) The chromokinesin Kid is necessary for chromosome arm orientation and oscillation, but not congression, on mitotic spindles. J Cell Biol 154: 1135–1146.
22. Ayad NG, Rankin S, Murakami M, Jebanathirajah J, Gygi S, et al. (2003) Tome-1, a trigger of mitotic entry, is degraded during G1 via the APC. Cell 113: 101–113.
23. Forsburg SL (2004) Eukaryotic MCM proteins: beyond replication initiation. Microbiol Mol Biol Rev 68: 109–131.
24. Rensen WM, Roscioli E, Tedeschi A, Mangiacasale R, Ciciarello M, et al. (2009) RanBP1 downregulation sensitizes cancer cells to taxol in a caspase-3-dependent manner. Oncogene 28: 1748–1758.
25. Witzgall R, O'Leary E, Gessner R, Ouellette AJ, Bonventre JV (1993) Kid-1, a putative renal transcription factor: regulation during ontogeny and in response to ischemia and toxic injury. Mol Cell Biol 13: 1933–1942.

26. Perco P, Pleban C, Kainz A, Lukas A, Mayer B, et al. (2007) Gene expression and biomarkers in renal transplant ischemia reperfusion injury. Transpl Int 20: 2–11.
27. Stuart RO, Bush KT, Nigam SK (2001) Changes in global gene expression patterns during development and maturation of the rat kidney. Proc Natl Acad Sci U S A 98: 5649–5654.
28. Lu Y, Huggins P, Bar-Joseph Z (2009) Cross species analysis of microarray expression data. Bioinformatics 25: 1476–1483.
29. Vaidya VS, Waikar SS, Ferguson MA, Collings FB, Sunderland K, et al. (2008) Urinary biomarkers for sensitive and specific detection of acute kidney injury in humans. Clin Transl Sci 1: 200–208.
30. Vaidya VS, Ramirez V, Ichimura T, Bobadilla NA, Bonventre JV (2006) Urinary kidney injury molecule-1: a sensitive quantitative biomarker for early detection of kidney tubular injury. Am J Physiol Renal Physiol 290: F517–529.
31. Ramirez V, Uribe N, Garcia-Torres R, Castro C, Rubio J, et al. (2004) Upregulation and intrarenal redistribution of heat shock proteins 90alpha and 90beta by low-sodium diet in the rat. Cell Stress Chaperones 9: 198–206.
32. Eisen MB, Spellman PT, Brown PO, Botstein D (1998) Cluster analysis and display of genome-wide expression patterns. Proc Natl Acad Sci U S A 95: 14863–14868.
33. Subramanian A, Tamayo P, Mootha VK, Mukherjee S, Ebert BL, et al. (2005) Gene set enrichment analysis: a knowledge-based approach for interpreting genome-wide expression profiles. Proc Natl Acad Sci U S A 102: 15545–15550.
34. Tomlins SA, Mehra R, Rhodes DR, Cao X, Wang L, et al. (2007) Integrative molecular concept modeling of prostate cancer progression. Nat Genet 39: 41–51.
35. Shannon P, Markiel A, Ozier O, Baliga NS, Wang JT, et al. (2003) Cytoscape: a software environment for integrated models of biomolecular interaction networks. Genome Res 13: 2498–2504.

Nephrol Dial Transplant (2012) 27: 3160–3169
doi: 10.1093/ndt/gfs014
Advance Access publication 19 April 2012

Recovery from ischemic acute kidney injury by spironolactone administration

Katy Sánchez-Pozos[1,2], Jonatan Barrera-Chimal[1,2], Juan Garzón-Muvdi[1,2], Rosalba Pérez-Villalva[1,2], Roxana Rodríguez-Romo[1,2], Cristino Cruz[2], Gerardo Gamba[1,2] and Norma A. Bobadilla[1,2]

[1]Unidad de Fisiología Molecular, Departamento de Medicina Genómica, Instituto de Investigaciones Biomédicas, Universidad Nacional Autónoma de México, Mexico City, Mexico and [2]Unidad de Fisiología Molecular, Departamento de Nefrología y Metabolismo Mineral, Instituto Nacional de Ciencias Médicas y Nutrición Salvador Zubirán, Mexico City, Mexico

Correspondence and offprint requests to: Norma A. Bobadilla; E-mail: nab@biomedicas.unam.mx

Abstract

Background. Prophylactic mineralocorticoid receptor (MR) antagonism with spironolactone (Sp) in rats completely prevents renal damage induced by ischemia. Because acute renal ischemia cannot typically be predicted, this study was designed to investigate whether Sp could prevent renal injury after an ischemic/reperfusion insult.

Methods. Six groups of male Wistar rats were studied: rats that received a sham abdominal operation (S); rats that underwent 20 min of ischemia and reperfusion for 24 h (I/R) and four groups of rats treated with Sp (20 mg/kg) 0, 3, 6 or 9 h after ischemia.

Results. As expected, I/R resulted in renal dysfunction characterized by a fall in renal blood flow and glomerular filtration rate and severe tubular injury which was confirmed by a significant increase in tubular damage biomarkers including kidney injury molecule-1, heat shock protein 72 and urinary protein excretion. The renal injury induced by I/R was in part due to Rho-kinase, endothelin and angiotensin II type 1 receptor upregulation. Interestingly, Sp administration at 0 and 3 h after ischemia completely reversed and prevented the damage induced by I/R. The protection induced by Sp given 6 h after ischemia was partial, but no protection was observed by administering Sp 9 h after ischemia.

Conclusion. Our results show that MR antagonism administered, either immediately or 3 h after I/R, effectively prevented ischemic acute renal injury, indicating that spironolactone is a promising agent for preventing acute kidney injury once an ischemic insult has occurred.

Keywords: AKI treatment; endothelin; renal dysfunction; Rho-kinase

Introduction

Acute kidney injury (AKI) is characterized by an abrupt and sustained decline in the glomerular filtration rate (GFR) that leads to a wide spectrum of acute alterations in kidney function and structure. One prominent cause of AKI is renal ischemia that occurs in patients with low blood pressure as result of a complication of several common clinical situations, such as severe cardiac failure or arrhythmia, generalized sepsis or excessive loss of blood or fluid during surgery or as a consequence of trauma. Thus, ischemic and nephrotoxic injuries are the major causes of AKI in native and transplanted kidneys [1]. AKI occurs in ∼5% of hospitalized patients and up to 40–60% of intensive care unit patients [2]. Despite technical improvements in dialysis and clinical care, the prevalence of AKI has risen significantly in the last 15 years due to aging population and the rising pandemics of obesity, diabetes and hypertension [3, 4]. In addition to high morbidity and mortality during the AKI episode, once resolved, AKI may also lead to the development of chronic kidney disease (CKD) or increases the transition rate from pre-existing CKD to end-stage renal disease [5–8]. In addition, even a small change in kidney function due to a minor AKI is associated with a higher long-term mortality rate [9].

In addition to its renal effects as a mineralocorticoid hormone, aldosterone plays a prominent role in the pathophysiology of renal diseases [10–19]. Recent evidence suggests that aldosterone is a potent renal vasoconstrictor [20–22]. Supporting that, aldosterone modulates the tone of the renal vasculature, we have shown that a mineralocorticoid receptor (MR) blockade with spironolactone not only reduces the structural renal damage associated with cyclosporine (CsA) but also prevents renal dysfunction due to afferent and efferent vasoconstriction [23–25]. We have also shown that prophylactic treatment with spironolactone completely prevents renal dysfunction and histological signs of tubular injury from ischemia–reperfusion (I/R) injuries [26]. To determine whether the protective effect of spironolactone during ischemia is due to blocking MR or to an unknown effect of this drug, we demonstrated that adrenalectomy had similar effects to those observed with spironolactone treatment [27]. Altogether, these results support the hypothesis that spironolactone prevents AKI after I/R by blocking the MR and therefore suggest that aldosterone plays a central role in promoting renal damage induced by a renal ischemic insult.

At present, there are no specific treatments for AKI caused by ischemia or nephrotoxic agents for use in the common clinical practice. In hypotension, once ischemia has damaged the kidney, other than restoring renal perfusion pressure and avoiding nephrotoxics, there is nothing that can currently be done to help prevent further damage or repair what has already occurred in the tubular cells. Therefore, prevention is a challenge clinicians face. In this regard, several treatments and experimental strategies have been advanced for the prevention of AKI, with different degrees of effectiveness, depending on the patient's other risk factors and the strategy used. However, most of these treatments are only effective when they are prophylactically administered [28–33]. Unfortunately, the development of renal ischemia cannot be predicted. Because we previously observed that giving spironolactone several hours before an ischemic insult completely prevents the histological and biochemical consequences of I/R, we designed the present study to investigate whether MR antagonism could reverse the renal injury induced by ischemia/reperfusion once ischemia has already been established and to better understand the molecular mechanisms of the renoprotection involved.

Materials and methods

All experiments involving animals were conducted in accordance with the Guide for the Care and Use of Laboratory Animals (National Academy Press, Washington, DC, 1996) and were approved by our Institutional Animal Care and Use Committee. Sixty-two male Wistar rats (270–315 g) were divided into six groups: sham-operated rats (S); animals subjected to bilateral renal ischemia for 20 min and 24 h of reperfusion (I/R) and four groups of rats that underwent bilateral renal ischemia for 20 min and reperfusion for 24 h, but also received one dose of spironolactone at 20 mg/kg by gastric gavage immediately after or at 3, 6 or 9 h after ischemia (Sp0, Sp3, Sp6 and Sp9, respectively). Two hours after ischemia, the animals were placed in metabolic cages at 22°C with a 12:12-h light–dark cycle and were allowed free access to water. All animals were studied after 24 h of reperfusion. At least six animals per group were used for renal functional and biochemical studies, and the rest were used for molecular studies.

Renal ischemia/reperfusion (I/R) injury (surgical procedure)

The rats were anesthetized by intraperitoneal injections of sodium pentobarbital (30 mg/kg) and underwent abdominal incision and the dissection of bilateral renal pedicles. Renal ischemia was induced by using nontraumatic vascular clamps; placed on each pedicle for 20 min. After the clamps were released, the incision was sutured, and the animals were allowed to recover. Sham abdominal operated rats underwent anesthesia and renal pedicle dissection only.

Functional studies

After recovery, the animals were placed in metabolic cages with 12:12-h light–dark cycle and were allowed free access to water. Twenty-four hours after ischemia, the rats were anesthetized with an intraperitoneal injection of sodium pentobarbital and placed on a homeothermic table. The trachea, jugular veins, femoral arteries and bladder were catheterized with polyethylene tubing (PE-240, PE-50 and PE-90). During surgery, the rats were maintained under euvolemic conditions by infusing 10 mL/kg body weight of isotonic rat plasma followed by an infusion of 5% low calorie commercial sugar (METCO, Mexico City, Mexico) at 1.6 mL/h as a marker of the GFR. We have previously shown that this compound has sufficient sensitivity to measure GFR under normal and pathophysiological conditions to a similar extent as the gold standard inutest [34]. The mean arterial pressure was continuously monitored with a pressure transducer (model p23 db; Gould) and recorded on a polygraph (Grass Instruments, Quincy, MA). The left renal artery was exposed via a midline abdominal incision, and an ultrasound transit-time flow probe (1RB; Transonic, Ithaca, NY) was placed around the left renal artery and filled with ultrasonic coupling gel (HR Lubricating Jelly; Carter–Wallace, New York, NY) to record the renal blood flow (RBF). Therefore, GFR was determined by using the Davidson method [35].

In addition, the urine protein excretion was measured from 24-h urine collections by using the trichloroacetic acid (TCA)-turbidimetric method [36]. Serum aldosterone was quantitatively determined by enzyme-linked immunosorbent assay (ELISA) following the procedures described by the manufacturer (EIA-4128; DRG International Inc.). Urine and serum creatinine concentrations were measured with QuantiChrom creatinine assay kit (DICT-500), and renal creatinine clearance was calculated.

Urinary Hsp72 protein levels

Urinary heat shock protein 72 (Hsp72) protein levels were analyzed using a commercially available high-sensitivity ELISA (Assay Designs EKS-715, MI). Briefly, samples and standards were added to wells coated with a mouse monoclonal antibody. Hsp72 was captured by the antibody and then detected by adding a rabbit polyclonal detection antibody. Both antibodies are specific for inducible Hsp72 and do not react with other members of the HSP70 family. A horseradish peroxidase (HRP) conjugate bound to the detection antibody and color development was accomplished by the addition of tetramethylbenzidine substrate and stopped with an acidic stop solution. The optical density of samples was read at 450 nm by a plate reader and was compared to a standard curve generated from known concentrations of recombinant Hsp72 that ranged from 0.1 to 12.5 ng/mL.

Histological studies

At the end of the experiment, one kidney was removed and quickly frozen for molecular studies. The other kidney was perfused with phosphate buffer through the femoral catheter, preserving the mean arterial pressure. The kidney was fixed with 4% formaldehyde. After appropriate dehydration, kidney slices were embedded in paraffin, sectioned at 3 μm and stained with routine periodic acid-Schiff and hematoxylin. Ten subcortical and juxtamedullary fields were recorded from each kidney slice using a digital camera mounted on a Nikon microscope (Nikon Instruments Inc., Japan). Digital microphotographs were recorded for each rat slide to assess the number of tubules with cast formation per field. We counted at least 400 tubules on each slide per animal. The damaged tubular area was expressed as the percentage of tubules with cast formation.

Oxidative stress determination

Renal lipoperoxidation. Malondialdehyde (MDA), a measure of lipid peroxidation, was assayed as previously reported [26]. Briefly, after homogenization of the tissue, the reaction was performed in a 15.4 mM solution of *N*-methyl-2-phenylindole in 15% of hydrochloride acid and heated at 45°C for 40 min. The mixtures were centrifuged at 3000 *g* for 15 min. The supernatant absorbance was read at 586 nm. MDA was quantified using an extinction coefficient of 1.1×10 [4] M^{-1}/cm^{-1} and expressed as nanomoles of MDA per milligram of protein. The tissue protein composition was estimated using the Lowry method.

Urinary hydrogen peroxide assay. The amount of hydrogen peroxide (H_2O_2) in urine was determined with an Amplex Red Hydrogen Peroxide/Peroxidase Assay Kit (Invitrogen, Eugene, OR) according to the manufacturer's instructions. The assay employed a standard curve of H_2O_2 (1–10 μM). A 50 μL of each urine standard was placed in a microplate; 50 μL of Amplex red reagent/HRP was then added, and the samples were incubated for 30 min at room temperature, protected from the light. In the presence of peroxidase, the Amplex reagent reacts with H_2O_2 to produce resorufin, a red-fluorescent oxidation product. Therefore, the plate was read at 560 nm. The H_2O_2 concentration in the samples was expressed as nanomoles per 24 h.

Molecular studies

RNA isolation and real-time reverse transcription–polymerase chain reaction. The total RNA was isolated from the kidneys using the TRIzol method (Invitrogen, Carlsbad, CA) and checked for integrity using 1% agarose gel electrophoresis. To avoid DNA contamination, total RNA samples were treated with DNAase (DNAase I; Invitrogen). Reverse transcription was conducted with 1.0 μg of total RNA using 200 U of

the Moloney murine leukemia virus reverse transcriptase (Invitrogen). The messenger RNA (mRNA) levels of kidney injury molecule-1 (Kim-1), Rho-kinase, angiotensinogen and angiotensin II type 1 (AT1) receptor as well as prepro-endothelin and ETA and ETB endothelin receptors were quantified by real-time polymerase chain reaction on the ABI Prism 7300 Sequence Detection System (TaqMan; ABI, Foster City, CA). Primers and probes were ordered as kits: Rn00597703_m1 for Kim-1, Mm00485745_m1 for Rho-kinase, Rn00593114_m1 for angiotensinogen, Rn00578456_m1 for AT1 receptor, Rn00560677_s1 for AT2, Rn00561129_m1 for prepro-endothelin, for the ETA receptor and Rn00569139_m1 for the ETB receptor (Assays-on-Demand; ABI). As an endogenous control, we used eukaryotic 18S ribosomal RNA (predesigned assay reagent, external run; ABI). The relative quantification of all gene expression was performed using the comparative 2[-Delta Delta C(t)] method [37].

Western blot analysis

To obtain a pool of cell homogenized kidneys cells, proteins from the cortex of four kidneys in each group were isolated by homogenization with a lysis buffer. The denatured proteins were separated with a sodium dodecyl sulfate (SDS)–polyacrylamide gel and transferred to polyvinylidine fluoride membranes (Millipore). The membranes were blocked and then incubated overnight at 4°C with goat anti-Rho-kinase antibody (1:2500; Santa Cruz Biotechnology, Santa Cruz, CA), rabbit anti-endothelin A receptor antibody (1:5000; Abcam Inc. Cambridge, MA), rabbit anti-endothelin B receptor antibody (1:5000; Abcam Inc.) or goat anti-angiotensin AT1 receptor (1:500; Abcam Inc.). Then, the membranes were incubated with a secondary antibody donkey anti-goat IgG-HRP (Santa Cruz Biotechnology) or rat anti-rabbit IgG HRP (Alpha Diagnostics, San Antonio, TX). To control protein loading and transfer, all membranes were probed with an actin antibody (1:5000) and a secondary antibody, donkey anti-goat IgG-HRP (1:5000; Santa Cruz Biotechnology). For this purpose, the membranes were stripped and re-probed. For stripping, the membranes were submerged in stripping buffer (100 mM 2-mercaptoethanol, 2% SDS, 62.5 mM Tris–HCL, pH 6.7) and incubated at 50°C for 30 min, then the membranes were washed three times with large volumes of wash buffer and were blocked and incubated with the antibodies as described previously. In the case of Rho-kinase, the lower part of the membrane was used for actin blotting. Proteins were detected with an enhanced chemiluminescence kit (Millipore) and autoradiography, following the manufacturer's recommendations. All western blot analyses were performed within the linear range of protein loads and antibody use. The bands were scanned for densitometric analysis.

Tissue levels of endothelin-1

Endothelin-1 levels were analyzed using a commercially available ELISA kit [Endothelin-1 (1-31) Assay kit; Immuno-Biological Laboratories Inc.] according to the manufacturer's instructions. Tissue homogenates and standards were added to the pre-coated wells and incubated overnight at 4°C. Endothelin-1 was captured by the antibody and then detected by adding the labeled antibody and the chromogen. The optical density of the samples was read at 450 nm by a plate reader and was compared to a standard curve generated from known concentrations of endothelin-1 that ranged from 1.56 to 200 pg/mL. The protein concentration in the tissue homogenates was determined by the Lowry method (BioRad). The endothelin-1 concentration was normalized by the amount of protein added to the well.

Statistical analysis

Results are presented as the means ± Standard error. The significance of the differences among groups was tested by analysis of variance (ANOVA) using Bonferroni's correction for multiple comparisons. Statistical significance was defined as having a P-value <0.05.

Results

Figure 1 depicts results of several physiological parameters analyzed in the studied groups. Neither I/R or spironolactone administration modified the mean arterial pressure values among the groups (Figure 1A). As we previously reported [26, 27], renal ischemia induced a significant increase in the serum aldosterone. A similar increase was observed in all experimental groups receiving spironolactone after the renal I/R insult (Figure 1B). After 24 h of ischemia, rats exposed to I/R exhibited renal hypoperfusion, as demonstrated by a significant decrease in RBF, and hypofiltration, as shown by the reduction in the

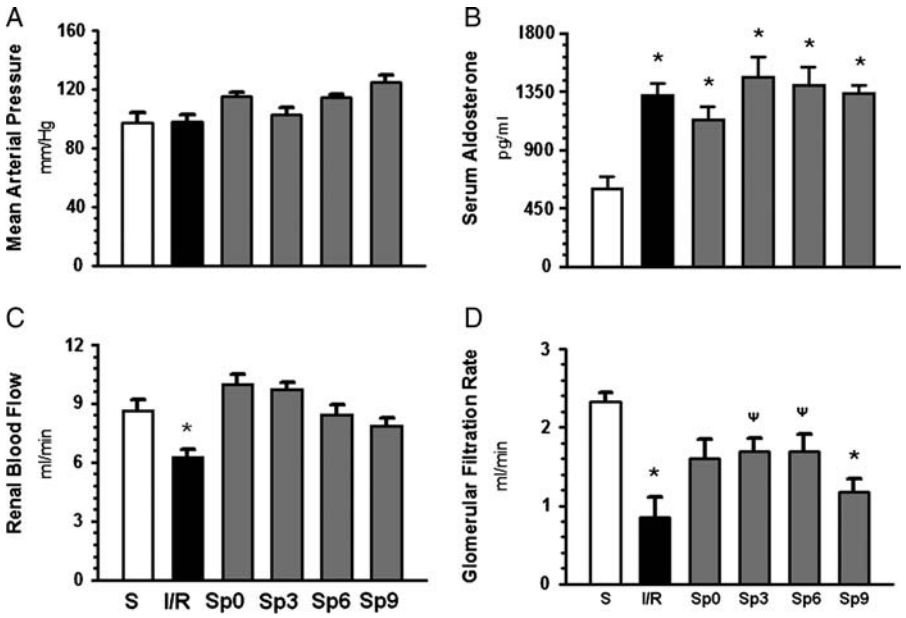

Fig. 1. Functional parameters in rats that underwent I/R and treated with spironolactone after the ischemic insult. (**A**) Mean arterial pressure, (**B**) Serum aldosterone levels, (**C**) RBF and (**D**) GFR in sham-operated rats (white bars), in rats that underwent 20 min of bilateral renal ischemia and 24 h of reperfusion (black bars) and in rats that received spironolactone immediately, 3, 6 or 9 h after renal ischemia (gray bars, Sp0, Sp3, Sp6 and Sp9, respectively). Error bars represent the Standard error. *P < 0.05 versus sham-operated rats, ψP < 0.05 versus the I/R group.

GFR (Figure 1C and D, respectively) and creatinine clearance (from 1.65 ± 0.13 to 0.86 ± 0.13 mL/min, $P < 0.05$). RBF reduction was not observed in the groups that received a single dose of spironolactone at 0, 3, 6 or 9 h after renal ischemia. The fall in GFR was partially prevented by spironolactone administration at 0, 3 and 6 h after ischemia as is depicted by GFR mean values (Figure 1D) and creatinine clearances (1.28 ± 0.12, 1.36 ± 0.15 and 1.79 ± 0.44 mL/min, respectively, although only in Sp6 group, the difference was statically different by ANOVA). Even though the renal plasma flow was corrected in the 9-h group, the renal function did not recover.

The upper panel of Figure 2 shows representative images of renal histological slides from the rats that underwent I/R alone (Figure 2A cortex, Figure 2B medulla) and from rats that underwent I/R followed by spironolactone at 0, 3, 6 and 9 h after bilateral renal ischemia (Figure 2C–J, respectively). Light microscopy revealed that renal I/R produced severe tubular damage characterized by lumen dilatation or collapse, loss of the brush border, cellular detachment from tubular basement membranes observed in the renal cortex (Figure 2A, magnification ×400) and extensive cast formation in renal medulla (Figure 2B, magnification ×100). All these lesions were practically absent in rats exposed to spironolactone at 0, 3 and 6 h after ischemic insult (Figure 2C–H, respectively). Consistent with the functional data, at the histological level, no protection was observed when spironolactone was administrated 9 h after ischemia was induced (Figure 2I and J).

Quantitative analysis of the histological images revealed that the percentage of tubules with cast formation in the I/R group was 23.9 ± 5.7%. In contrast, due to spironolactone administration, this percentage was reduced to 2.5 ± 1.3, 6.2 ± 2.2, 11.4 ± 3.7 and 8.7 ± 3.7 in the groups Sp0, Sp3, Sp6 and Sp9, respectively (Figure 2K), but only the values for Sp0 were significantly different from the I/R group, when ANOVA analysis was performed.

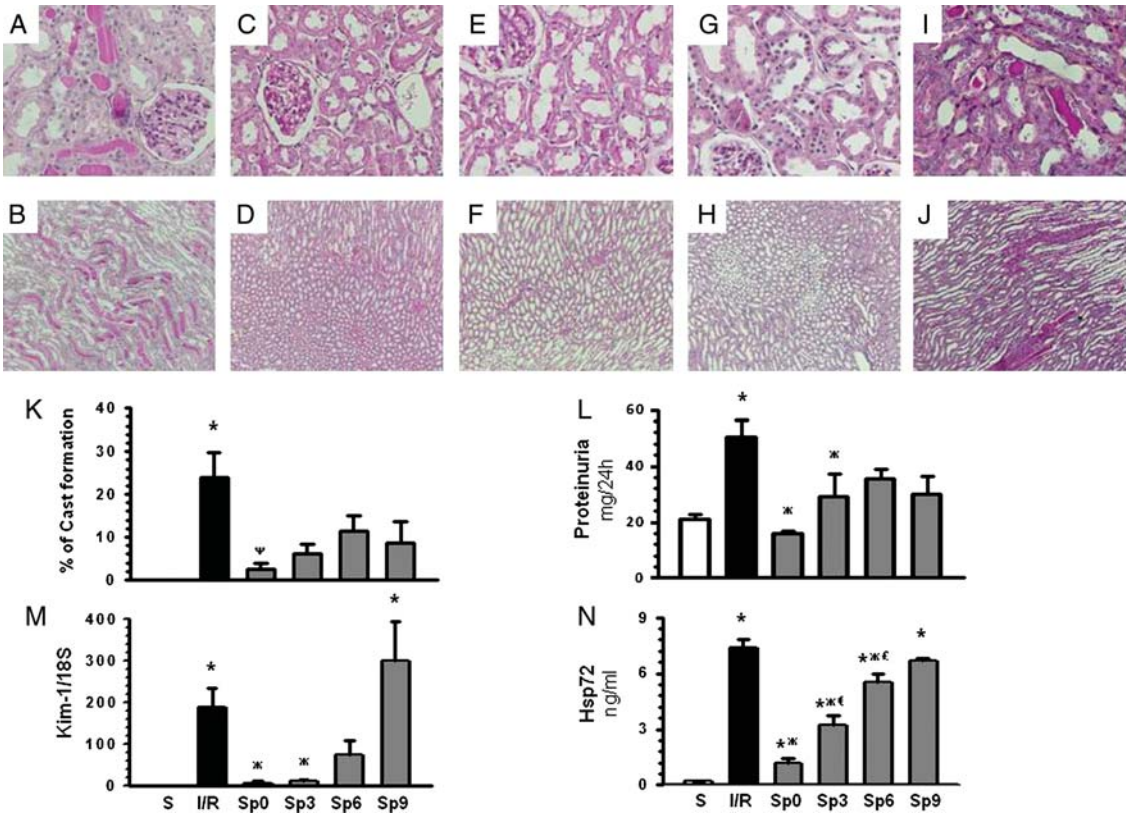

Fig. 2. Effect of spironolactone administration on tubular injury after an ischemic insult induced by I/R. Subcortical and medullary histological sections of kidneys stained with periodic acid-Schiff from studied groups. (**A**) and (**B**) Kidney histology from an untreated I/R rat with detachment of the basement membrane of tubular epithelial cells, tubular dilation, loss of brush border, flattened epithelial cells and the presence of hyaline casts (magnification ×400 and ×100, respectively). (**C**) and (**D**) Representative images of cortical and medullary sections from rats treated with spironolactone immediately after bilateral renal ischemia (magnification ×400 and ×100, respectively). (**E**) and (**F**) Representative images of cortical and medullary sections from rats treated with spironolactone 3 h after bilateral renal ischemia (magnification ×400 and ×100, respectively). (**G**) and (**H**) Representative images of kidney sections from rats treated with spironolactone 6 h after bilateral renal ischemia, (magnification ×400 and ×100, respectively). (**I**) and (**J**) Representative images of kidney sections from rats treated with spironolactone 9 h after bilateral renal ischemia, (magnification ×400 and ×100, respectively). (**K**) Quantification of the tubular percentage of tubules with casts formation, in sham-operated rats (white bars), in rats that underwent 20 min of bilateral renal ischemia and 24 h of reperfusion (black bars) and in I/R rats that received spironolactone immediately, 3, 6 or 9 h after renal ischemia (gray bars, Sp0, Sp3, Sp6 and Sp9, respectively); at least 400 tubules on each histological slide were counted. (**L**) Urinary protein excretion levels. (**M**) Kim-1 mRNA levels and (**N**) Urinary Hsp72 excretion. Error bars represent the Standard error. *$P < 0.05$ versus sham-operated rats, ж$P < 0.05$ versus the I/R group, €$P < 0.05$ versus Sp0 and £$P < 0.05$ versus Sp3.

The biomarkers of tubular injury were consistent with the functional and histological observations. In the I/R group, urinary protein excretion increased by ∼4-fold, when compared with sham-operated rats (Figure 2L). In the rats that underwent I/R and were treated with spironolactone after 0 h, the increase in urinary protein excretion was completely prevented. In the Sp3, Sp6 and Sp9 groups, proteinuria developed, but the levels were significantly lower than those observed in the I/R group; however, only the Sp3 group showed levels that were significantly different. As shown in Figure 2M, Kim-1 mRNA levels increased by ∼150-fold in the I/R group, whereas in the Sp0 and Sp3 groups, Kim-1 mRNA levels were similar to the normal values. Although Kim-1 mRNA levels were increased in the Sp6 group, these values were significantly lower than those of the I/R group. In contrast, in the Sp9 group, Kim-1 upregulation was not prevented. We also assessed the urinary concentration of the Hsp72 because recent observations from our laboratory suggest that this protein is a sensitive and early biomarker of AKI induced by renal ischemia [38]. Accordingly, urinary Hsp72 excretion was significantly increased in the I/R group compared to the sham-operated rats (7.3 ± 1.3 versus 0.1 ± 0.03 ng/mL, respectively, $P < 0.0001$). Spironolactone administrated immediately after bilateral renal ischemia induction prevented Hsp72 upregulation (1.1 ± 0.3 ng/mL), but this upregulation was partially prevented when the mineralocorticoid blocker was administrated 3 or 6 h after the insult (3.2 ± 0.6 and 5.5 ± 1.1 ng/mL, respectively). The decrease in urinary Hsp72 excretion was not observed in the Sp9 group (7.0 ± 0.5 ng/mL).

The renoprotection conferred by early spironolactone administration after renal ischemia was also supported by the measurement of kidney malondialdehyde and urinary H_2O_2 excretion as markers of oxidative stress (Figure 3A and B, respectively). As we previously reported [26, 27], renal injury induced by I/R was associated with an ∼5-fold increase in oxidative stress in both tissue and urine. This increase in oxidative stress was not observed in the groups that received spironolactone at 0 or 3 h after kidney ischemia and this effect was observed in lesser

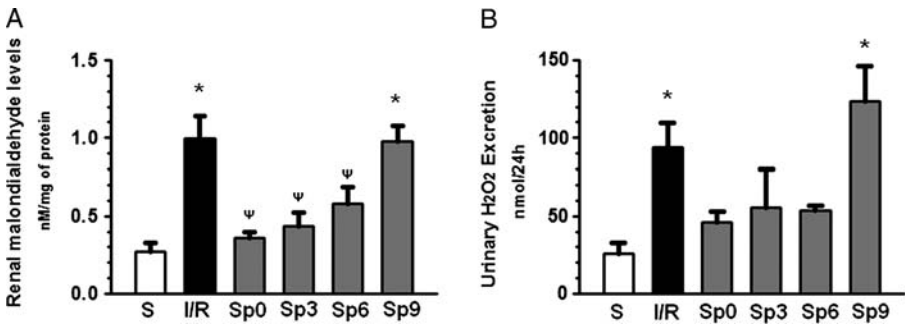

Fig. 3. Effect of spironolactone administration after ischemic insult on oxidative stress induced by I/R. (**A**) Renal malondialdehyde levels in sham-operated rats (white bars), in rats that underwent 20 min of bilateral renal ischemia and 24 h of reperfusion (black bars) and in I/R rats that received spironolactone immediately, 3, 6 or 9 h after renal ischemia (gray bars, Sp0, Sp3, Sp6 and Sp9, respectively). (**B**) Urinary H_2O_2 excretion in all studied groups. *$P < 0.05$ versus sham-operated rats, ψ$P < 0.05$ versus the I/R group.

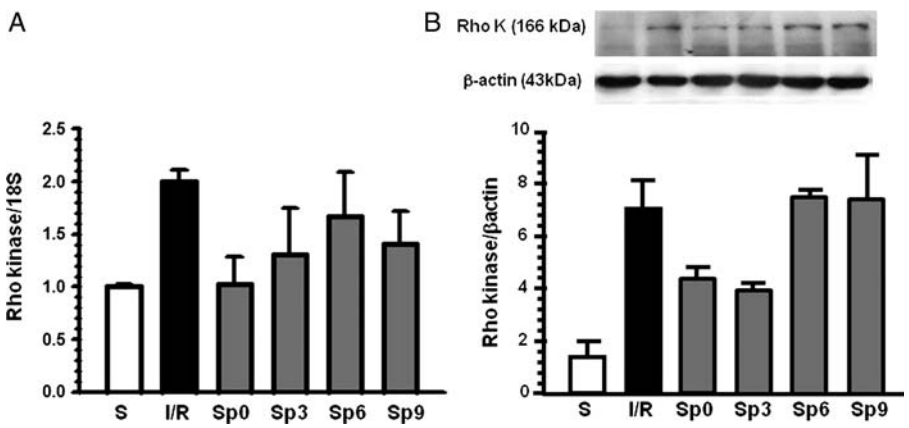

Fig. 4. Ischemia/reperfusion injury is associated with Rho-kinase upregulation and is partially prevented by early spironolactone administration. (**A**) Rho-kinase mRNA levels determined by real-time reverse transcription–polymerase chain reaction in total renal cortex RNA extracted from sham-operated rats (white bars), in rats underwent 20 min of bilateral renal ischemia and 24 h of reperfusion (black bars) and in I/R rats that received spironolactone immediately, 3, 6 or 9 h after renal ischemia (gray bars, Sp0, Sp3, Sp6 and Sp9, respectively). (**B**) The upper inset is a representative autoradiography image obtained from a western blot analysis of all studied groups. The graph represents the densitometry analysis. Error bars represent the Standard error.

proportion in the rats treated after 6 h. This renoprotective effect was not observed in the Sp9 group.

Recent studies have shown that Rho-kinase is involved in signaling pathways that mediate vasoconstriction [39]. Therefore, its induction by aldosterone might contribute to the renal hypoperfusion and hypoxia observed after an ischemic insult. To determine whether these effects are another potential renoprotective mechanism of spironolactone, the expression levels of Rho-kinase were assessed. Figure 4A shows the mRNA levels of Rho-kinase and Figure 4B the Rho-kinase protein expression. In the kidneys from rats with ischemia and reperfusion, the mRNA and protein levels of Rho-kinase were increased compared to those of the sham-operated rats; however, the differences did not reach significance by ANOVA analysis. Of note, this upregulation was partially prevented in the groups treated with spironolactone immediately and 3 h after renal ischemia, but not in the groups that received spironolactone 6 or 9 h afterward.

Endothelin is a potent vasoconstrictor in renal vasculature; thus, we also assessed the mRNA levels of prepro-endothelin, the tissue endothelin levels by ELISA and the levels of ETA and ETB receptors by western blot analysis. In accordance with our previous observations [27], prepro-endothelin mRNA levels increased by ~9-fold in the I/R group, as is shown in Figure 5A. The increase in prepro-endothelin transcripts was partially prevented by spironolactone administration, even after 9 h. An increase in endothelin after renal ischemia was also observed by using ELISA and was prevented by the administration of spironolactone immediately after ischemia, the differences between I/R rats and those treated at 3, 6 or 9 h were not significant by ANOVA (Figure 5B). This is probably due to the similarity between the I/R group and most of the groups treated with spironolactone; however, it is evident that endothelin was increased by ischemia, indeed *t*-test was significant when this group was compared with sham-operated values, and that this increase was prevented by spironolactone administered at time 0. Renal ischemia had no effect upon the expression of the ETA receptor (Figure 5C). In contrast, the level of the vasodilatory ETB receptor was significantly reduced in the I/R group (Figure 5D). This effect was partially prevented by spironolactone at 0, 3 and 6 h, but not at 9 h.

Angiotensinogen and the AT1 receptor mRNA levels were measured in the total RNA extracted from the kidneys in each study group. No changes in angiotensinogen mRNA levels were observed (Figure 6A), but the I/R

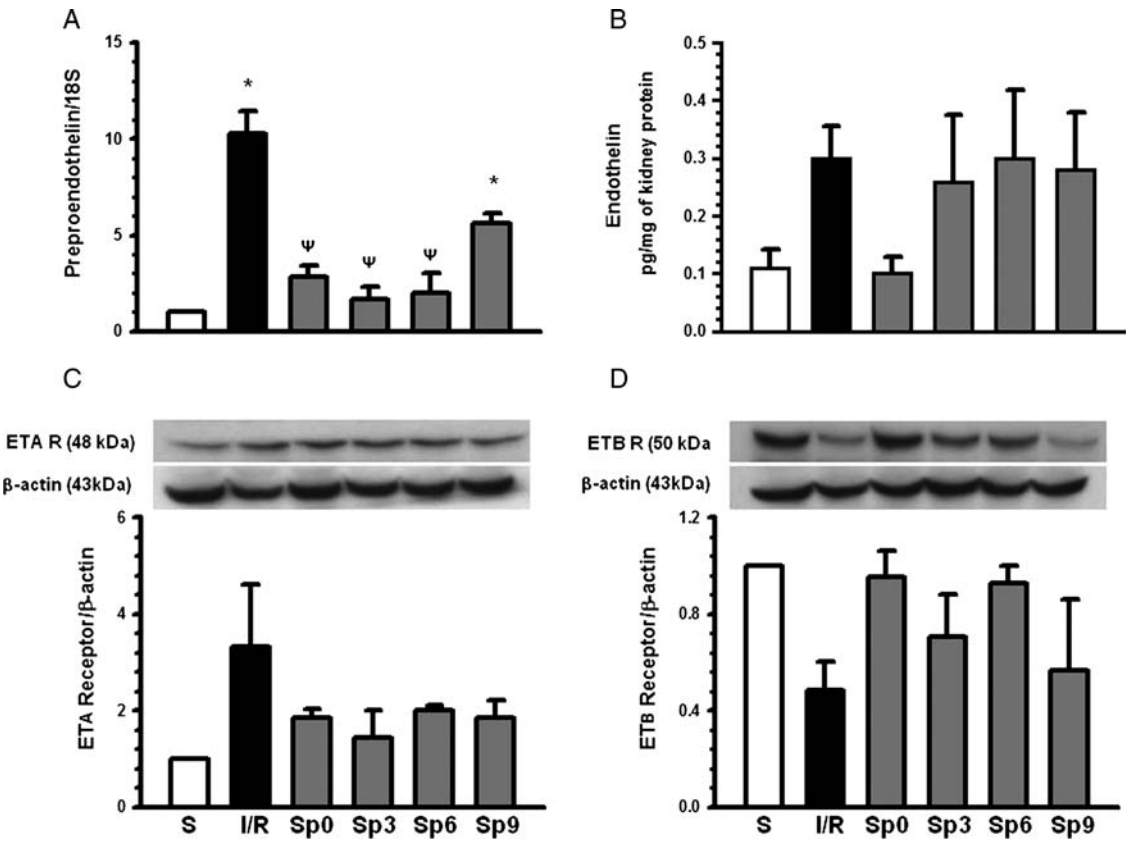

Fig. 5. Ischemia/reperfusion injury is associated with endothelin upregulation and is partially prevented by spironolactone administration. (**A**) Prepro-endothelin mRNA levels determined by real-time reverse transcription–polymerase chain reaction in total renal cortex RNA extracted from sham-operated rats (white bars), in rats underwent 20 min of bilateral renal ischemia and 24 h of reperfusion (black bars) and rats that received spironolactone immediately, 3, 6 or 9 h after renal ischemia (gray bars, Sp0, Sp3, Sp6 and Sp9, respectively). (**B**) Renal cortex endothelin levels assessed by ELISA in all studied groups. (**C**) and (**D**) ETA and ETB protein levels by western blot analysis; the upper insets are representative images of this chemilumiescent analysis and the lower graphs are the corresponding densitometric analysis. *$P < 0.05$ versus sham-operated rats, ψ$P < 0.05$ versus the I/R group.

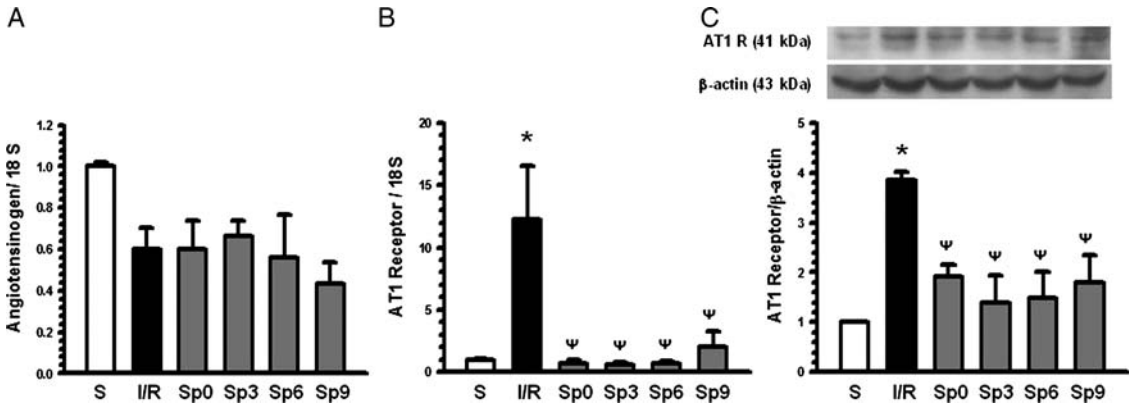

Fig. 6. Ischemia/reperfusion injury is associated with AT1 receptor mRNA levels upregulation and prevented by spironolactone administration. (**A**) The mRNA levels of angiotensinogen assessed by real-time reverse transcription–polymerase chain reaction in total renal cortical RNA extracted from sham-operated rats (white bars), from rats underwent 20 min of bilateral renal ischemia and 24 h of reperfusion (black bars) and from I/R rats that received spironolactone immediately, 3, 6 or 9 h after renal ischemia (gray bars, Sp0, Sp3, Sp6 and Sp9, respectively). (**B**) The mRNA levels of the AT1 receptor. (**C**) AT1 receptor protein levels by western blot analysis, the upper insets are representative images of this chemiluminescent analysis and the lower graph is the corresponding densitometric analysis. *$P < 0.05$ versus sham-operated rats, ψ$P < 0.05$ versus I/R group.

group exhibited more than a 10-fold upregulation of AT1 mRNA, and this effect was completely mitigated in all of the groups treated with spironolactone after the ischemic insult, as depicted in Figure 6B. In accordance with these findings, western blot analysis depicted in Figure 6C, showed that AT1 receptor protein level was significantly increased in the I/R group by 3-fold. In contrast, AT1 receptor upregulation was significantly reduced in all the groups treated with spironolactone.

Discussion

In this study, we show that blocking the MR with spironolactone immediately after or even 3 h after renal bilateral ischemia completely prevented renal dysfunction, tubular injury and oxidative stress. The expected increase in sensitive biomarkers of renal injury was also prevented. A direct relationship between renal protection and the blockage of MR is also supported by the fact that spironolactone conferred partial renoprotection when administered after 6 h and did not confer protection after 9 h.

AKI is characterized by vascular and tubular abnormalities that take place after ischemia and during the reperfusion process. Intra-renal vasoconstriction that leads to a reduction in GFR, together with vascular congestion in the outer medulla and activation of tubulo-glomerular feedback constitute part of the vascular defects, which are likely caused by the increased release of vasoconstrictor factors (mainly endothelin, adenosine and angiotensin II) and decreased production of vasodilators (such as nitric oxide, prostaglandin, acetylcholine and bradykinin) (for a review [40]). Considering that hypoperfusion is a major stimulus of the renin–angiotensin–aldosterone system and that we previously showed that both prophylactic spironolactone administration and adrenals removal prevented renal dysfunction induced by I/R [26, 27], our data suggest that aldosterone plays a primary role in sustaining renal vasoconstriction in this model of ischemic damage. In our previous study using I/R as a model of AKI, the effects of aldosterone were blocked before the ischemic insult took place, and the resulting prevention of AKI was so remarkable that we reasoned that it is possible that spironolactone given after renal ischemia could be helpful to reduce or prevent functional and structural injury. Considering that renal ischemia often occurs unexpectedly in the clinical setting, we evaluated the ability of spironolactone to protect the kidney after establishing an ischemic insult. We found that the decline in RBF with the subsequent reduction in GFR induced by I/R was completely prevented when spironolactone was administrated immediately or 3 h after the renal ischemic insult had occurred. Administering spironolactone 6 h after the ischemic insult produced a lower degree of protection, which, however, was still significant. In this study, we used a low calorie commercial sugar as a GFR marker since we previously showed that this compound has enough sensitivity to measure GFR in normal and pathophysiological conditions to a similar extent of the gold standard polyfructosan [34, 41]. Moreover, our data were further confirmed when the renal function was assessed by creatinine clearance.

It is well known that the tubular epithelium suffers functional and morphological alterations as a consequence of renal hypoperfusion induced by ischemia. Hence, the I/R group exhibited the classical picture of acute tubular necrosis that was accompanied by increased urinary protein excretion, together with upregulation of sensitive biomarkers such as Kim-1 and Hsp72 [38, 42–44]. The morphological alterations and the elevation of sensitive tubular markers of renal injury were also prevented or reduced when spironolactone was administrated immediately and until 6 h after renal ischemia had occurred. Hsp72 was the most consistent biomarker with the time-dependence protection of spironolactone evidenced by the histological injury. These discrepancies among the biomarkers used could be due to a greater sensitivity of Hsp72 to stratify renal injury than Kim-1 or proteinuria, as we previously reported [38] or with different kinetics of induction of each biomarker because it has been

reported that some biomarkers are induced very quickly and returned to normal values after 24 h of renal injury or contrariwise [45]. Taken together, our observations provide evidence about the potential effect that the mineralocoriticoid blockade may have on the improvement of renal function and structure when spironolactone is administrated immediately or even 6 h after an ischemic insult is established. This action spectrum might be more notable in humans, considering the short life of the rats.

As expected [46], the extensive tubular damage observed in the I/R group was associated with a significant increase in oxidative stress, as was evidenced by the increase in renal thiobarbituric acid reactive substances and in the urinary excretion of H_2O_2. This was also prevented by the MR blockade 0, 3 or even 6 h after renal ischemia, suggesting that aldosterone promotes a cellular oxidative milieu. In support of these findings, a specific role for aldosterone in mediating oxidative stress has become apparent [47], specifically; it has been shown that aldosterone induced reactive oxygen species generation by inducing the activation of NADPH oxidase in cultured mesangial cells [48] and by decreasing glucose-6-phosphate dehydrogenase activity [22].

Recent advances in vascular cell biology have demonstrated the substantial involvement of the small GTPase Rho and its downstream effector Rho-kinase in promoting vascular smooth muscle cell contraction by inactivating myosin phosphatase and subsequently increasing myosin light chain phosphorylation (for a review, see [39]). Specifically for AKI, during renal I/R, Rho-kinase mRNA and protein levels increase [27, 49]. Renal injury induced by long-term aldosterone administration has also been associated with increases in myosin phosphate target subunit-1, a marker of Rho-kinase activity [50]. Thus, the Rho/Rho-kinase pathway has recently attracted great attention in various research fields, due to its participation in vascular tone regulation [51] and more recently, due to its role in mediating both extensive foot-process effacement and histologic features of focal segmental glomerulosclerosis [52]. In the present study, we detected that in kidneys isolated from I/R rats that exhibited considerable increases in aldosterone, Rho-kinase mRNA and protein levels were significantly upregulated. This effect was partially prevented when spironolactone was administrated at 0 and 3 h after renal insult. Consistent with this observation, adrenalectomy prevents the Rho-kinase upregulation induced by I/R [27], and eplerenone was able to reduce the Rho-kinase mRNA upregulation observed in salt-induced hypertension in Dahl salt-sensitive (DS) rats [53]. Moreover, the Rho-kinase inhibitor fasudil attenuated the renal injury induced by I/R [54]. All these studies together suggest that aldosterone mediates Rho-kinase upregulation and may mediate, at least in part, the renal vasoconstriction and dysfunction induced by I/R. Even though the GFR was partially recovered in the Sp6 group, it was not associated with the restoration of Rho-kinase levels, suggesting that the possible induction of this kinase by aldosterone occurred very early after ischemia, pointing out that blocking angiotensin and endothelin pathways (Figures 5 and 6) are also involved in the beneficial effect of spironolactone.

As was previously mentioned, the reduction in RBF is primarily mediated by an imbalance in vasoactive substance release. Endothelin is a largely vasoconstrictive peptide that has been implicated in renal pathophysiology [55]. An increase in endothelin levels during I/R-induced renal injury has been observed by us as well as by others [27, 56]. Here, we corroborated that I/R-induced renal injury was related with an upregulation of prepro-endothelin mRNA levels and renal endothelin level. These transcriptional changes were prevented in the animals that underwent ischemia and received spironolactone at 0, 3 and 6 h, suggesting that aldosterone mediates this transcriptional effect. In fact, several studies have demonstrated an increase in both endothelin-1 transcript and protein in response to aldosterone in vascular smooth muscle [57], cardiac [58] and renal [56] tissues as well as in inner medullary collecting duct cells [59]. Interestingly, responsive elements to MRs have been identified in the endothelin promoter [60]. Moreover, endothelin upregulation may also increase Rho-kinase activity [58], prolonging the vicious cycle that contributes to the adverse effects of aldosterone under pathophysiological conditions.

As mentioned above, angiotensin II is a mediator of renal injury induced by I/R. We previously showed that blocking AT1 receptor with losartan partially prevents renal dysfunction in rats that have undergone ischemia [61], suggesting that this peptide partially participates in the renal vasoconstriction observed in this model of renal damage. Although we did not observe changes in the angiotensionogen mRNA levels, the AT1 receptors were upregulated at the mRNA and protein levels in rats that underwent ischemia/repefusion, an effect that was completely prevented by spironolactone.

We recently observed that the prophylactic treatment with MR blocker spironolactone completely prevented I/R-induced AKI in rats [26]. Here, we showed a similar degree of protection when spironolactone was administrated after the ischemic insult had been established. The renoprotection conferred by spironolactone was mediated by slowing down endothelin, AT1 receptor and Rho-kinase renal levels that contributed to preventing renal hypoperfusion and the concomitant generation of free radicals. These data together with our previous findings show that MR antagonism should be further studied as a strategy for preventing AKI following renal ischemia.

Acknowledgements. We are grateful to the members of the Molecular Physiology Unit for their suggestions and to Dr Octavio Villanueva for his help with animal care.

The results presented in this paper have not been published previously in whole or in part, except as an abstract presented at the Annual Meetings and Scientific Exposition 2008 of the *American Society of Nephrology* (Philadelphia, PA.). This project was supported by grants from the Mexican Council of Science and Technology (CONACyT) (101030 and 112780 to N.A.B. and 59992 to G.G.), from the National University of Mexico (IN200909-3 and IN203412-3 to N.A.B.) and from the Pfizer Institute of Science to G.G. K.S.P. was supported by a scholarship from CONACYT-Mexico and is a graduate student in the Biochemistry Science PhD Program of the Universidad Nacional Autónoma de México.

Conflict of interest statement. None declared.

References

1. Friedewald JJ, Rabb H. Inflammatory cells in ischemic acute renal failure. *Kidney Int* 2004; 66: 486–491
2. Kelly KJ. Acute renal failure: much more than a kidney disease. *Semin Nephrol* 2006; 26: 105–113
3. Liano F, Pascual J. Epidemiology of acute renal failure: a prospective, multicenter, community-based study. Madrid Acute Renal Failure Study Group. *Kidney Int* 1996; 50: 811–818
4. Waikar SS, Curhan GC, Wald R *et al*. Declining mortality in patients with acute renal failure, 1988 to 2002. *J Am Soc Nephrol* 2006; 17: 1143–1150
5. Cerda J, Lameire N, Eggers P *et al*. Epidemiology of acute kidney injury. *Clin J Am Soc Nephrol* 2008; 3: 881–886
6. Mosier MJ, Pham TN, Klein MB *et al*. Early acute kidney injury predicts progressive renal dysfunction and higher mortality in severely burned adults. *J Burn Care Res* 2010; 31: 83–92
7. Block CA, Schoolwerth AC. Acute renal failure: outcomes and risk of chronic kidney disease. *Minerva Urol Nefrol* 2007; 59: 327–335
8. Hsu CY, Ordonez JD, Chertow GM *et al*. The risk of acute renal failure in patients with chronic kidney disease. *Kidney Int* 2008; 74: 101–107
9. Chertow GM, Burdick E, Honour M *et al*. Acute kidney injury, mortality, length of stay, and costs in hospitalized patients. *J Am Soc Nephrol* 2005; 16: 3365–3370
10. Pitt B, Zannad F, Remme WJ *et al*. The effect of spironolactone on morbidity and mortality in patients with severe heart failure. Randomized Aldactone Evaluation Study Investigators. *N Engl J Med* 1999; 341: 709–717
11. Pitt B, Remme W, Zannad F *et al*. Eplerenone, a selective aldosterone blocker, in patients with left ventricular dysfunction after myocardial infarction. *N Engl J Med* 2003; 348: 1309–1321
12. Rocha R, Chander PN, Khanna K *et al*. Mineralocorticoid blockade reduces vascular injury in stroke-prone hypertensive rats. *Hypertension* 1998; 31: 451–458
13. Rocha R, Chander PN, Zuckerman A *et al*. Role of aldosterone in renal vascular injury in stroke-prone hypertensive rats. *Hypertension* 1999; 33: 232–237
14. Rocha R, Stier CT, Jr, Kifor I *et al*. Aldosterone: a mediator of myocardial necrosis and renal arteriopathy. *Endocrinology* 2000; 141: 3871–3878
15. Hollenberg NK. Aldosterone in the development and progression of renal injury. *Kidney Int* 2004; 66: 1–9
16. Aldigier JC, Kanjanbuch T, Ma LJ *et al*. Regression of existing glomerulosclerosis by inhibition of aldosterone. *J Am Soc Nephrol* 2005; 16: 3306–3314
17. Bianchi S, Bigazzi R, Campese VM. Antagonists of aldosterone and proteinuria in patients with CKD: an uncontrolled pilot study. *Am J Kidney Dis* 2005; 46: 45–51
18. Sato A, Hayashi K, Naruse M *et al*. Effectiveness of aldosterone blockade in patients with diabetic nephropathy. *Hypertension* 2003; 41: 64–68
19. Boldyreff B, Wehling M. Non-genomic actions of aldosterone: mechanisms and consequences in kidney cells. *Nephrol Dial Transplant* 2003; 18: 1693–1695
20. Arima S, Kohagura K, Xu HL *et al*. Nongenomic vascular action of aldosterone in the glomerular microcirculation. *J Am Soc Nephrol* 2003; 14: 2255–2263
21. Gros R, Ding Q, Armstrong S *et al*. Rapid effects of aldosterone on clonal human vascular smooth muscle cells. *Am J Physiol Cell Physiol* 2007; 292: C788–C794
22. Leopold JA, Dam A, Maron BA *et al*. Aldosterone impairs vascular reactivity by decreasing glucose-6-phosphate dehydrogenase activity. *Nat Med* 2007; 13: 189–197
23. Feria I, Pichardo I, Juarez P *et al*. Therapeutic benefit of spironolactone in experimental chronic cyclosporine A nephrotoxicity. *Kidney Int* 2003; 63: 43–52
24. Perez-Rojas JM, Derive S, Blanco JA *et al*. Renocortical mRNA expression of vasoactive factors during spironolactone protective effect in chronic cyclosporine nephrotoxicity. *Am J Physiol Renal Physiol* 2005; 289: F1020–F1030
25. Perez-Rojas J, Blanco JA, Cruz C *et al*. Mineralocorticoid receptor blockade confers renoprotection in preexisting chronic cyclosporine nephrotoxicity. *Am J Physiol Renal Physiol* 2007; 292: F131–F139
26. Mejia-Vilet JM, Ramirez V, Cruz C *et al*. Renal ischemia-reperfusion injury is prevented by the mineralocorticoid receptor blocker spironolactone. *Am J Physiol Renal Physiol* 2007; 293: F78–F86
27. Ramirez V, Trujillo J, Valdes R *et al*. Adrenalectomy prevents renal ischemia-reperfusion injury. *Am J Physiol Renal Physiol* 2009; 297: F932–F942
28. Matsumoto M, Makino Y, Tanaka T *et al*. Induction of renoprotective gene expression by cobalt ameliorates ischemic injury of the kidney in rats. *J Am Soc Nephrol* 2003; 14: 1825–1832
29. Pedraza-Chaverri J, Tapia E, Bobadilla N. Ischemia-reperfusion induced acute renal failure in the rat is ameliorated by the spin-trapping agent alpha-phenyl-N-tert-butyl nitrone (PBN). *Ren Fail* 1992; 14: 467–471
30. Fujii T, Sugiura T, Ohkita M *et al*. Selective antagonism of the postsynaptic alpha(1)-adrenoceptor is protective against ischemic acute renal failure in rats. *Eur J Pharmacol* 2007; 574: 185–191
31. Sadis C, Teske G, Stokman G *et al*. Nicotine protects kidney from renal ischemia/reperfusion injury through the cholinergic anti-inflammatory pathway. *PLoS ONE* 2007; 2: e469.
32. Chatterjee PK, Patel NS, Sivarajah A *et al*. GW274150, a potent and highly selective inhibitor of iNOS, reduces experimental renal ischemia/reperfusion injury. *Kidney Int* 2003; 63: 853–865
33. Suzuki S, Maruyama S, Sato W *et al*. Geranylgeranylacetone ameliorates ischemic acute renal failure via induction of Hsp70. *Kidney Int* 2005; 67: 2210–2220
34. Perez-Rojas JM, Blanco JA, Gamba G *et al*. Low calorie commercial sugar is a sensitive marker of glomerular filtration rate. *Kidney Int* 2005; 68: 1888–1893
35. Davidson DW, Sackner MA. Simplification of the anthrone method for the determination of inulin in clearance studies. *J Lab Clin Med* 1963; 62: 351–356
36. Henry RJ, Sobel C, Segalove M. Turbidimetric determination of proteins with sulfosalicylic and tricholoroacetic acids. *Proc Soc Exp Biol Med* 1956; 92: 748–751
37. Livak KJ, Schmittgen TD. Analysis of relative gene expression data using real-time quantitative PCR and the 2(-Delta Delta C(T)) Method. *Methods* 2001; 25: 402–408
38. Barrera-Chimal J, Perez-Villalva R, Cortes-Gonzalez C *et al*. Hsp72 is an early and sensitive biomarker to detect acute kidney injury. *EMBO Mol Med* 2011; 3: 5–20
39. Shimokawa H, Takeshita A. Rho-kinase is an important therapeutic target in cardiovascular medicine. *Arterioscler Thromb Vasc Biol* 2005; 25: 1767–1775
40. Devarajan P. Update on mechanisms of ischemic acute kidney injury. *J Am Soc Nephrol* 2006; 17: 1503–1520
41. Ramirez V, Mejia-Vilet JM, Hernandez D *et al*. Radicicol, a heat shock protein 90 inhibitor, reduces glomerular filtration rate. *Am J Physiol Renal Physiol* 2008; 295: F1044–F1051
42. Vaidya VS, Ozer JS, Dieterle F *et al*. Kidney injury molecule-1 outperforms traditional biomarkers of kidney injury in preclinical biomarker qualification studies. *Nat Biotechnol* 2010; 28: 478–485
43. Vaidya VS, Ford GM, Waikar SS *et al*. A rapid urine test for early detection of kidney injury. *Kidney Int* 2009; 76: 108–114
44. Vaidya VS, Ramirez V, Ichimura T *et al*. Urinary kidney injury molecule-1: a sensitive quantitative biomarker for early detection of kidney tubular injury. *Am J Physiol Renal Physiol* 2006; 290: F517–F529
45. Han WK, Wagener G, Zhu Y *et al*. Urinary biomarkers in the early detection of acute kidney injury after cardiac surgery. *Clin J Am Soc Nephrol* 2009; 4: 873–882
46. Jassem W, Heaton ND. The role of mitochondria in ischemia/reperfusion injury in organ transplantation. *Kidney Int* 2004; 66: 514–517
47. Fiebeler A, Luft FC. The mineralocorticoid receptor and oxidative stress. *Heart Fail Rev* 2005; 10: 47–52

48. Miyata K, Rahman M, Shokoji T *et al*. Aldosterone stimulates reactive oxygen species production through activation of NADPH oxidase in rat mesangial cells. *J Am Soc Nephrol* 2005; 16: 2906–2912
49. Caron A, Desrosiers RR, Beliveau R. Kidney ischemia-reperfusion regulates expression and distribution of tubulin subunits, beta-actin and rho GTPases in proximal tubules. *Arch Biochem Biophys* 2004; 431: 31–46
50. Sun GP, Kohno M, Guo P *et al*. Involvements of rho-kinase and tgf-Beta pathways in aldosterone-induced renal injury. *J Am Soc Nephrol* 2006; 17: 2193–2201
51. Yao L, Romero MJ, Toque HA *et al*. The role of RhoA/Rho kinase pathway in endothelial dysfunction. *J Cardiovasc Dis Res* 2010; 1: 165–170
52. Zhu L, Jiang R, Aoudjit L *et al*. Activation of RhoA in podocytes induces focal segmental glomerulosclerosis. *J Am Soc Nephrol* 2011; 22: 1621–1630
53. Kobayashi N, Hara K, Tojo A *et al*. Eplerenone shows renoprotective effect by reducing LOX-1-mediated adhesion molecule, PKCepsilon-MAPK-p90RSK, and Rho-kinase pathway. *Hypertension* 2005; 45: 538–544
54. Prakash J, de Borst MH, Lacombe M *et al*. Inhibition of renal rho kinase attenuates ischemia/reperfusion-induced injury. *J Am Soc Nephrol* 2008; 19: 2086–2097
55. Barton M, Yanagisawa M. Endothelin: 20 years from discovery to therapy. *Can J Physiol Pharmacol* 2008; 86: 485–498
56. Wong S, Brennan FE, Young MJ *et al*. A direct effect of aldosterone on endothelin-1 gene expression in vivo. *Endocrinology* 2007; 148: 1511–1517
57. Wolf SC, Schultze M, Risler T *et al*. Stimulation of serum- and glucocorticoid-regulated kinase-1 gene expression by endothelin-1. *Biochem Pharmacol* 2006; 71: 1175–1183
58. Doi T, Sakoda T, Akagami T *et al*. Aldosterone induces interleukin-18 through endothelin-1, angiotensin II, Rho/Rho-kinase, and PPARs in cardiomyocytes. *Am J Physiol Heart Circ Physiol* 2008; 295: H1279–H1287
59. Gumz ML, Popp MP, Wingo CS *et al*. Early transcriptional effects of aldosterone in a mouse inner medullary collecting duct cell line. *Am J Physiol Renal Physiol* 2003; 285: F664–F673
60. Stow LR, Gumz ML, Lynch IJ *et al*. Aldosterone modulates steroid receptor binding to the endothelin-1 gene (edn1). *J Biol Chem* 2009; 284: 30087–30096
61. Molinas SM, Cortes-Gonzalez C, Gonzalez-Bobadilla Y *et al*. Effects of losartan pretreatment in an experimental model of ischemic acute kidneyinjury. *Nephron Exp Nephrol* 2009; 112: e10–e19

Received for publication: 3.11.2011; Accepted in revised form: 10.1.2012

Nephrol Dial Transplant (2012) 27: 3169–3175
doi: 10.1093/ndt/gfs033
Advance Access publication 15 March 2012

ARB protects podocytes from HIV-1 nephropathy independently of podocyte AT1

Akihiro Shimizu[1,2], Jianyong Zhong[3,4,5], Yoichi Miyazaki[2], Tatsuo Hosoya[2], Iekuni Ichikawa[6,7] and Taiji Matsusaka[1,3]

[1]Department of Internal Medicine, Tokai University School of Medicine, Isehara, Kanagawa, Japan, [2]Division of Kidney and Hypertension, Department of Internal Medicine, The Jikei University School of Medicine, Tokyo, Japan, [3]Department of Metabolic System Medicine, Institute of Medical Science, Tokai University School of Medicine, Isehara, Kanagawa, Japan, [4]Department of Pediatrics, Vanderbilt University Medical Center, Nashville, TN, USA, [5]Department of Nephrology, Huashan Hospital, Fudan University, Shanghai, China, [6]Department of Bioethics, Tokai University School of Medicine, Isehara, Kanagawa, Japan and [7]Department of Medicine, Vanderbilt University Medical Center, Nashville, TN, USA

Correspondence and offprint requests to: Akihiro Shimizu; E-mail: akihiro@jikei.ac.jp

Abstract

Background. Angiotensin I-converting enzyme inhibitors and angiotensin receptor blockers protect podocytes more effectively than other anti-hypertensive drugs. Transgenic rats overexpressing angiotensin II Type 1 (AT1) receptor selectively in podocytes have been shown to develop glomerulosclerosis. The prevailing hypothesis is that angiotensin II has a capacity of directly acting on the AT1 receptor of podocytes to induce injury. We therefore investigated the mechanism of reno-protective effect of AT1 receptor in a mouse model of HIV-1 nephropathy.

Methods. We generated transgenic mice carrying the HIV-1 gene (control/HIV-1) or both HIV-1 gene and podocyte-selectively nullified AT1 gene (AT1KO/HIV-1). In these mice, we measured urinary protein or albumin excretion and performed histological analysis.

Results. At 8 months of age, AT1KO/HIV-1 ($n = 13$) and control/HIV-1 ($n = 15$) mice were statistically indistinguishable with respect to urinary albumin/creatinine ratio (median 2.5 versus 9.1 mg/mg), glomerulosclerosis (median 0.63 versus 0.45 on 0–4 scale) and downregulation of nephrin (median 6.90 versus 7.02 on 0–8 scale). In contrast to the observed lack of effect of podocyte-specific AT1KO, systemic AT1 inhibition with AT1 blocker (ARB) significantly attenuated proteinuria and glomerulosclerosis in HIV-1 mice.

Original Report: Patient-Oriented, Translational Research

American Journal of Nephrology

Am J Nephrol
DOI: 10.1159/000350539

Received: January 1, 2013
Accepted: March 6, 2013
Published online: ■■■

Mineralocorticoid Receptor Blockade Reduced Oxidative Stress in Renal Transplant Recipients: A Double-Blind, Randomized Pilot Study

Marcos Ojeda-Cervantes[a, b] Jonatan Barrera-Chimal[a, c] Josefina Alberú[b]
Rosalba Pérez-Villalva[a, c] Luis Eduardo Morales-Buenrostro[a, b]
Norma A. Bobadilla[a, c]

[a]Nephrology and [b]Transplantation Departments, Instituto Nacional de Ciencias Médicas y Nutrición Salvador Zubirán, and [c]Molecular Physiology Unit, Instituto de Investigaciones Biomédicas Universidad Nacional Autónoma de México, Mexico City, Mexico

Key Words
Acute kidney injury · Aldosterone · Oxidative stress · Slow graft function · Urinary biomarkers level

Abstract
Background: Previous experimental studies from our laboratory have demonstrated that aldosterone plays a central role in renal ischemic processes. This study was designed to evaluate the effect of mineralocorticoid receptor blockade in renal transplant recipients from living donors. ***Methods:*** 20 adult kidney transplant recipients from living donors were included a double-blind, randomized, placebo-controlled clinical pilot study that compared spironolactone and placebo. Placebo or spironolactone (25 mg) was administered 1 day before and 3 days posttransplantation. Renal function and urinary kidney injury molecule-1, interleukin-18, and heat-shock protein 72 as well as urinary hydrogen peroxide (H_2O_2) levels were quantified. ***Results:*** No significant differences were seen between the groups studied regarding age, gender, indication for kidney transplantation, residual renal function, renal replacement therapy, or warm and cold ischemia periods. In contrast, spironolactone administration significantly reduced the oxidative stress assessed by the urinary H_2O_2 excretion, in spite of no differences in renal function or reduction in tubular injury biomarkers. ***Conclusions:*** The findings of this exploratory study strongly suggest that aldosterone promotes oxidative stress and that the administration of spironolactone reduces the production of urinary H_2O_2 as a result of lesser formation of surrogate reactive oxygen species secondary to the ischemia-reperfusion phenomenon.

Introduction

Ischemia/reperfusion (I/R) is the major cause of acute kidney injury (AKI) in recipients of renal allograft that often results in different degrees of early posttransplant renal dysfunction [1]. The participation of I/R injury in early function recovery after renal transplantation in both deceased and living donors, as well as its role in the immunogenicity of the graft and its long-term outcome, has recently been receiving considerable attention. Thus it has been demonstrated that renal dysfunction associated with ischemic AKI has a potential role in the pathogenesis of delayed graft function [2]. Several studies have shown that delayed graft function is not only associated with decreased graft survival in the follow-up, but also

KARGER

E-Mail karger@karger.com
www.karger.com/ajn

0250–8095/13/0000–0000$38.00/0

Norma A. Bobadilla-Sandoval
Vasco de Quiroga No. 15
Tlalpan, Mexico City 14000 (Mexico)
E-Mail nab@biomedicas.unam.mx

with acute and chronic graft rejection [3, 4]. Accordingly, a major challenge that faces nephrologists and transplant surgeons is to prevent renal injury induced by I/R.

The abrupt drop in blood circulation is recognized as key player in the initiation and subsequent damage to the kidney structures. Following ischemia, renal hypoxia may directly damage the vascular endothelium and increase leukocyte adhesion and permeability [5, 6]. These alterations induce the activation of the inflammatory process and the generation of reactive oxygen species (ROS) with the subsequent damage to essential structures of the cells such as lipids, carbohydrates, proteins and nucleic acids that lead to a loss of cell viability mediated by either necrosis or apoptosis [7]. It has also been demonstrated that an impaired nitric oxide system intensifies renal hypoxia and vasoconstriction [8, 9]. These complex pathophysiological interactions and perhaps other mediators, that have not been completely elucidated, result in serious disturbances in the kidney function and structure.

Aldosterone has traditionally been recognized as a mediator that maintains water and sodium homeostasis through its signaling on mineralocorticoid receptor (MR) by mediating genomic actions on renal tubular cells. Nevertheless, there is enough evidence in humans and experimental models of disease that aldosterone is capable of inducing pathophysiological effects in cardiovascular, renal and other organs [10–18]. Indeed, the vasculature is now considered as a direct target of aldosterone [19]. Certainly, MR is expressed in the endothelium and in the smooth muscle vascular cells [20]. As a result of this location, aldosterone pathway activation affects endothelial function and vascular tone [21–24]. Supporting that aldosterone modulates the tone of the renal vasculature, previous experimental studies from our laboratory showed that a MR blockade with spironolactone prevents renal dysfunction and reduced renal damage associated with cyclosporine administration in the rat [25–27]. In addition, we have also shown that spironolactone administration before or after bilateral renal ischemia prevented renal dysfunction and structural injury in the rat [28, 29]. In addition, we have also demonstrated that adrenalectomized rats had similar effects to those observed with spironolactone treatment [30]. Altogether these results support the hypothesis that spironolactone prevents ischemic AKI by blocking the MR and therefore suggest that aldosterone plays a central role in promoting renal damage induced by a renal ischemic insult.

Taking all this evidence into consideration, we decided to perform a translational study to evaluate whether spironolactone can reduce tubular damage and oxidative stress in renal transplant patients from a living donor.

Material and Methods

Patients

We carried out a double-blind, randomized, and placebo-controlled clinical pilot study in adult kidney transplant recipients from living donors. This study was approved by the Ethical Committee of the Instituto Nacional de Ciencias Médicas y Nutrición, Salvador Zubiran. All patients included in this study signed the informed consent.

Enrollment of the patients started in March 2009 and was completed in March 2010. Inclusion criteria comprised the enrolment of patients aged ≥18 years, recipients of a live donor kidney and with identical and non-identical HLA match. Exclusion criteria were multiorgan transplant or deceased donor kidney. Eligible patients were randomized to receive either 25 mg of spironolactone daily or placebo orally. The caplets were administered 24 h prior to transplant surgery and 3 consecutive days posttransplantation. Furthermore, all donors of each group also received a single dose of the assigned treatment the night before nephrectomy.

The patients included in the present study received the same institutional immunosuppressive regimen with basiliximab or daclizumab + tacrolimus, mycophenolate mofetil and prednisone.

All recipients had negative cross-matches assessed by the Anti-human Globulin (AHG)-enhanced complement-dependent cytotoxicity assay (T-cell AHG-CDC) before transplantation. Because there are no previous studies, the sample size was not probabilistic for a pilot study and will allow to generate a hypothesis for further studies.

Previous to the transplant surgery, a 24-hour urine sample was collected from all patients (day 0) and 5 consecutive days posttransplantation. Urine samples were homogenized and five aliquots were stored at –70°C. Additionally, serum creatinine (Scr), potassium and urine volume were measured at baseline (just before kidney transplantation), and daily during the 5 consecutive days.

Urinary Biomarkers Measurement

Urinary kidney injury molecule-1 (Kim-1) and interleukin-18 (IL-18) levels were analyzed using commercially available enzyme-linked immune absorbent assay (ELISA) kits: human Kim-1 ELISA kit (90785; USCN Life Science, Inc.) and human IL-18 ELISA Kit (KHC0181; Invitrogen). All procedures were performed according to the manufacturer's instructions. Because we recently showed that heat-shock protein 72 (Hsp72) is a sensitive biomarker of AKI [31], urinary Hsp72 levels were analyzed by using a commercially available high-sensitivity ELISA (ADI-EKS-715; Assay Designs, Ann Arbor, Mich., USA). Briefly, samples and standards were added to wells coated with a mouse monoclonal antibody. Hsp72 was captured by the antibody and then detected by adding a rabbit polyclonal detection antibody. Both antibodies are specific for inducible Hsp72 and do not react with other members of the HSP70 family. A horseradish peroxidase conjugate (HRP) bound to the detection antibody and color development was accomplished by the addition of tetramethylbenzidine substrate and stopped with an acid stop solution. The optical density of samples was read at 450 nm by a plate reader and was overlapped with the standard curve generated from known concentrations of recombinant Hsp72 that ranged from 0.1 to 12.5 ng/ml.

Table 1. General characteristics of renal transplant recipients

Characteristics	Spironolactone n = 10	Placebo n = 10
Age (median), years	31.50 (24.75–37.5)	32 (23.25–43.75)
Male/female	4/6	6/4
Previous transplant	0	1
Hemodialysis	5	3
Peritoneal dialysis	4	4
Preemptive renal transplant	1	3
Chronic kidney disease duration (median), years	1 (1–3)	1 (1–6.25)
ACEi or ARBs before transplant	6	5
Etiology		
Diabetes mellitus	2	1
Other	4	0
Unknown	4	9
HLA identical	2	1
Induction		
Without induction	2	1
Antilymphocyte globulin	1	0
Basiliximab/daclizumab	1/6	2/7
Immunosuppressive therapy	TAC/Pred/MMF	TAC/Pred/MMF
Serum tacrolimus levels, ng/ml	3.65 (1.2–11.7)	6.05 (1.7–10.1)
Laparoscopic surgery	10	10
Conversion to open surgery	1	0

TAC = Tacrolimus; Pred = prednisone; MMF = mycophenolate mofetil. Values are expressed as median and IQR.

Oxidative Stress Evaluation

Urinary hydrogen peroxide (H_2O_2) excretion was determined to evaluate oxidative stress. The amount of H_2O_2 was quantified with the use of the Amplex® Red Hydrogen Peroxide/Peroxidase Assay according to the manufacturer's instructions. Briefly, a standard curve from 1 to 10 mM of H_2O_2 was used. 50 µl of the urine or standard samples were loaded onto a microplate, 50 µl of the Amplex red reagent-HRP was added, and the samples incubated for 30 min. The plate was read at 560 nm. The accuracy of this assay to detect H_2O_2 in urine sample has been previously validated [32].

Statistical Analysis

Statistics was performed using GraphPad PRISM software (GraphPad Software, La Jolla, Calif., USA) and the SPSS package (SPSS, Inc., Chicago, Ill., USA). Numerical variables were expressed as the median with interquartile range (IQR) and were compared using the Mann-Whitney U test. Categorical variables were shown using frequencies and compared with Fisher's exact test. Differences were considered to be significant at p values <0.05.

Results

Characteristics of Renal Transplant Recipients

From 2009 to 2010, 39 adult renal transplants from living donors were performed in our institution. 19 patients refused to participate in this study and the rest of the recipients with HLA identical and non-identical HLA match were included. One half of the patients received spironolactone and the other half received placebo blindly. The general characteristics of both patient groups are given in table 1. No significant differences were seen between the groups studied regarding age, gender, and indication for kidney transplantation, residual renal function, treatment with angiotensin-converting enzyme inhibitors (ACEi) or angiotensin II receptor blockers (ARBs) before the transplant or renal replacement therapy. The induction therapy was basiliximab or daclizumab, except in 3 patients because they shared two haplotypes with their donors. The maintenance immunosuppressive therapy was based on tacrolimus, mycophenolate mofetil and prednisone. Tacrolimus was started when Scr levels reduced at least 50% after renal transplant and in accordance with our institutional guidelines. No differences in the first determination of serum tacrolimus levels between both groups were observed. None of the patients received ACEi or ARBs after renal transplant. After the codes were opened, we noticed that 4 patients underwent preemptive renal transplantation – 1 patient belonged to the placebo

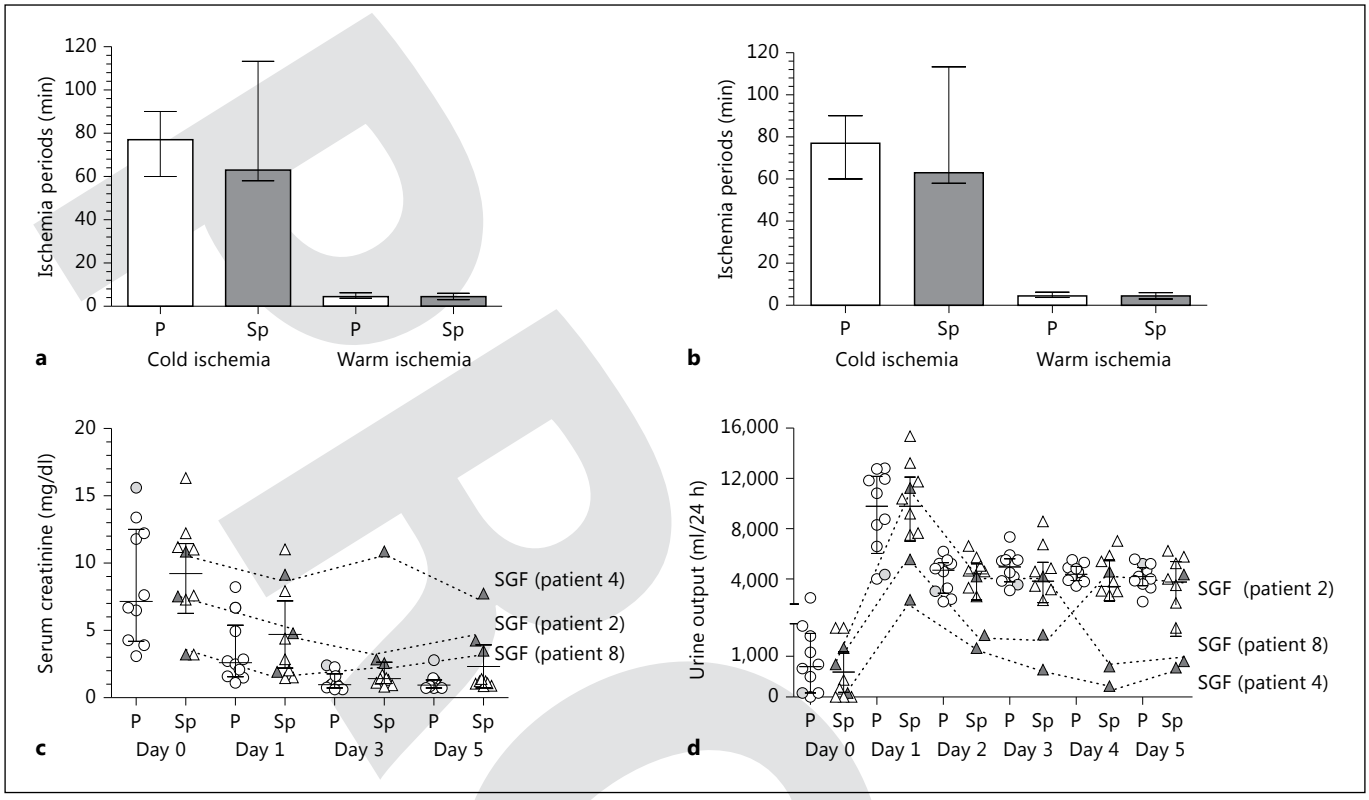

Fig. 1. Effect of spironolactone treatment on serum potassium levels, Scr, and urine output in renal transplant recipients from living donors: (**a**) periods of warm and cold ischemia in placebo- (white bars) and spironolactone-treated recipients (gray bars); (**b**) serum potassium levels, (**c**) Scr, and (**d**) urine output along with the study for placebo- (white circles) and spironolactone-treated recipients (gray circles). The 3 patients treated with spironolactone who exhibited slow graft function are shown. Individual values together with the median and IQR are also depicted.

group and the other 3 to the spironolactone group. All kidneys were obtained by hand-assisted laparoscopic nephrectomy, but 1 patient belonged to the spironolactone group and required conversion to open surgery.

Taking in account that ischemic warm and cold periods may affect the graft function, both periods were recorded and analyzed. As shown in figure 1a, the grafts of the spironolactone and placebo groups exhibited similar periods of warm ischemia, 4.5 and 4.5 min, respectively ($p = 0.969$), or cold ischemia of 63 and 77 min, respectively ($p = 0.589$). The spironolactone effect on renal function or oxidative stress was therefore not related with smaller periods of warm or cold ischemia.

Serum Potassium Levels

Because hyperkalemia is a frequent concern when spironolactone is used, serum potassium levels were measured every day for 5 consecutive days posttransplant as depicted in figure 1b. There were no episodes of severe hyperkalemia, defined as serum potassium >6.0 mEq/dl, and none of the patients required withdrawal of spironolactone. Serum potassium levels >5.0 mEq/dl occurred in only 1 patient from the spironolactone group, however after 5 days of treatment the serum potassium concentration was 3.9 mEq/dl. Similarly, 1 patient from the placebo group exhibited serum potassium levels >5.0 mEq/dl at days 2 and 4 posttransplantation, but serum potassium levels were normal at day 5 (4.8 mEq/l). Accordingly, the mean serum potassium level in the spironolactone group did not differ from the control group throughout the period studied.

Effect of Spironolactone Administration on Renal Graft Function

Figure 1c depicts the behavior of Scr levels before and after renal transplant. Before the transplant the placebo and spironolactone groups had a similar degree of renal dysfunction that tended to be greater in the group with

MR blockade (7.2 and 9.2 mg/dl, respectively; p = 0.879). As expected, renal transplant gradually eased renal function. On the first day posttransplant the SCr in the placebo- and spironolactone-treated groups exhibited a reduction in SCr that was reduced even more at the fifth day. Accordingly, urine output improved posttransplant, as shown in figure 1d. The highest urine volume recorded on the first day resulted from the vigorous hydration. We noticed that 3 of the 4 patients had delayed graft function and exhibited the higher levels of SCr and lower urine output. The 4 patients who underwent renal biopsy and histological analysis within the 5 days posttransplant showed that one half of them exhibited acute rejection and both were from the spironolactone group. The other half exhibited acute tubular necrosis, 1 from the placebo-treated group and 1 from the spironolactone-treated group.

Urinary Tubular Biomarkers in Renal Transplant Recipients

The effect of MR blockade in the tubular damage induced by the I/R phenomenon was evaluated by assessing urinary Kim-1, IL-18 and Hsp72 levels. Figure 2 shows absolute concentrations of each biomarker in 24-hour timed collections at 1, 3, and 5 days posttransplant. Urinary Kim-1 levels were similar in the placebo and spironolactone groups and were not modified during the follow-up as depicted in figure 2a. Similar behavior was observed with the other two biomarkers IL-18 and Hsp72. Thus no differences in the urinary biomarkers were found in any period observed when spironolactone was compared with the placebo group (fig. 2a–c). We noticed however a substantial dispersion that could be influenced by different biological variables and with the number of patients included. As expected, the greater urinary levels of IL-18 and Hsp72 after 5 days of renal transplant were seen in those patients who exhibited slow graft function.

Effect of Spironolactone on Oxidative Stress

We simultaneously measured urinary H_2O_2 levels, a surrogate marker of oxidative stress at 1, 3 and 5 days after renal transplant as depicted in figure 3. On the first day, increased oxidative stress was observed in both groups, although the values in the spironolactone group tended to be lower than the placebo-treated group (1,665.42 vs. 2,484.55 pmol/ml, respectively; p = 0.247). This behavior was also observed at the third day. Interestingly, after 5 days of transplantation the placebo group remained with higher urinary H_2O_2 levels (1,164.382 pmol/ml), in

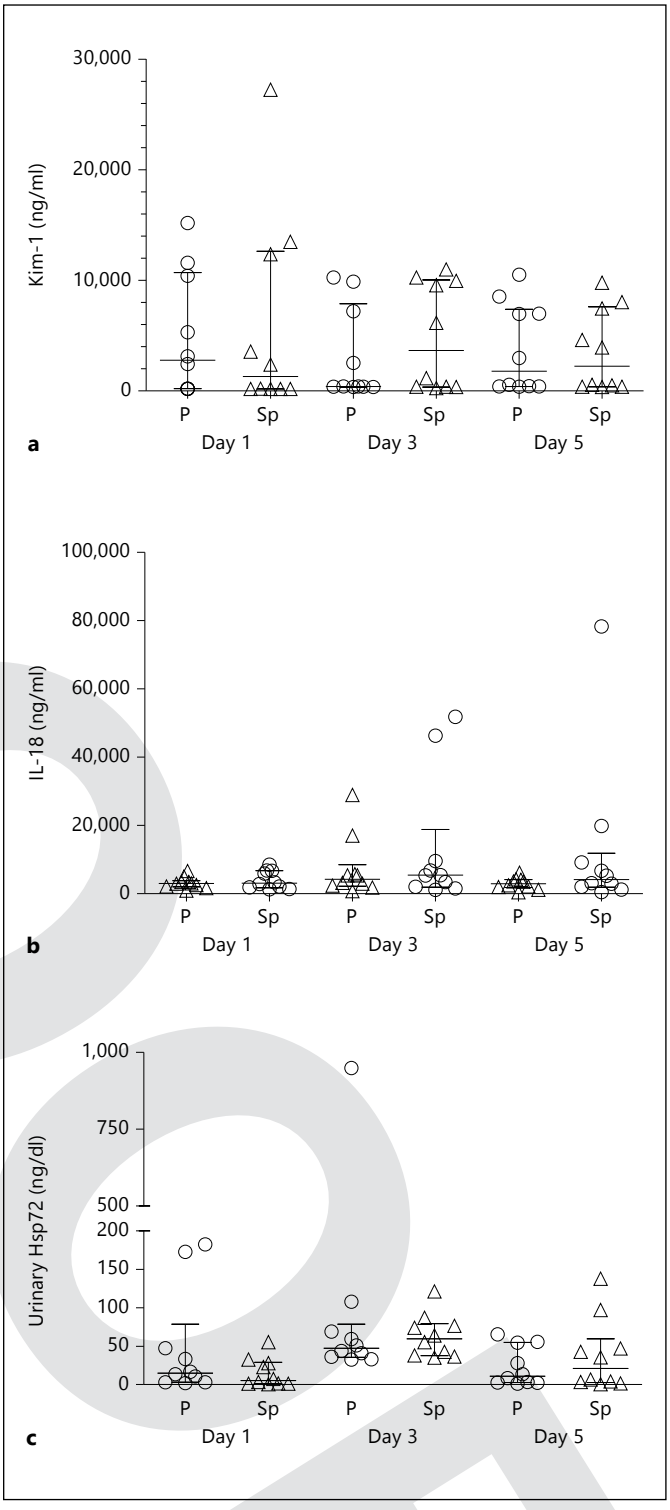

Fig. 2. Behavior in the excretion of tubular injury biomarkers in renal transplant recipients treated with placebo or spironolactone: (**a**) Kim-1, (**b**) IL-18, and (**c**) Hsp72 at days 1, 3 and 5 posttransplant from placebo- (white circles) and spironolactone-treated recipients (gray circles). Individual values, median and IQR are depicted.

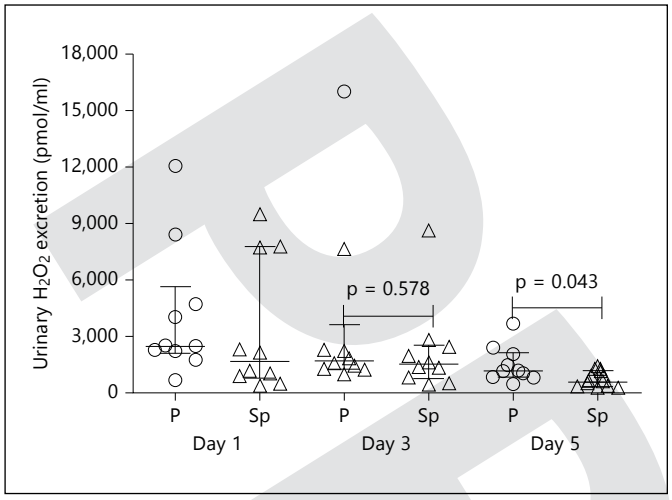

Fig. 3. Effect of spironolactone treatment on oxidative stress in renal transplant recipients from living donors. Urinary H_2O_2 levels were assessed at days 1, 3 and 5 after renal transplant in placebo- (white circles) and spironolactone-treated recipients (gray circles). Individual values, median and IQR are represented. * $p < 0.05$ vs. placebo group at day 5 posttransplant.

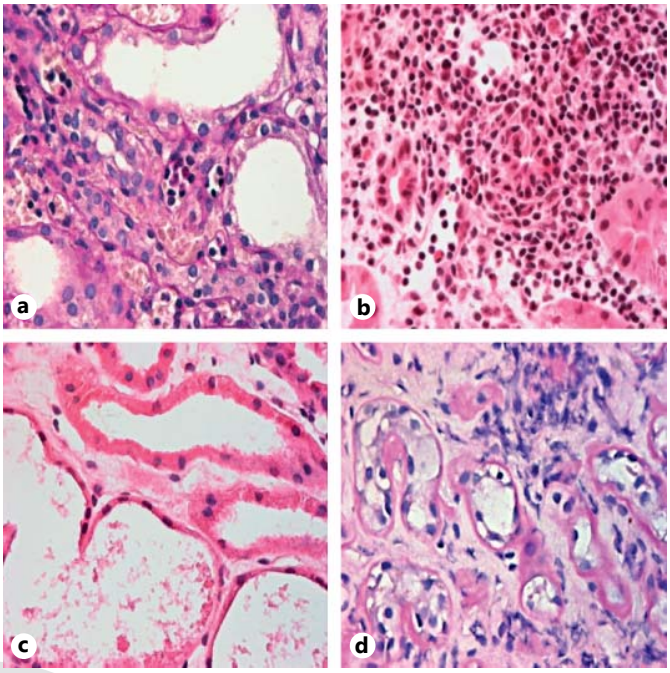

Fig. 4. Histopathological aspect of cases with slow graft function. **a** There are abundant inflammatory cells with margination, within peritubular capillaries, corresponding to acute humoral rejection. PAS. ×60. **b** There is a dense interstitial inflammatory infiltrate that surrounds a tubule with intense tubulitis in acute cellular rejection. HE. ×60. **c** Patchy tubular damage, some tubules are denuded, with attenuated epithelium, there is cellular debris within the tubular lumen, corresponding to acute tubular necrosis. HE. ×60. **d** A specimen showing interstitial fibrosis and moderate tubular atrophy. A few tubules exhibit mild tubulitis in a case of borderline alterations. PAS. ×60.

contrast, the spironolactone-treated group exhibited a significant reduction (575.089 pmol/ml, $p = 0.0307$). The urinary H_2O_2 levels from the patients who developed slow graft function were included in both groups.

Other Outcomes Related to Renal Transplant

Table 2 shows some adverse events not related with the use of spironolactone or placebo. Four patients experienced renal graft dysfunction posttransplantation and only 1 of them belonged to the placebo group. These patients underwent renal biopsy into the first 5 days. Light microscopy findings showed that 3 patients with slow graft function from the spironolactone group exhibited acute humoral rejection (fig. 4a), acute cellular rejection (fig. 4b), and acute tubular necrosis (fig. 4c), respectively, whereas the patients from the placebo group exhibited borderline alterations such as mild tubulitis, moderate tubular atrophy and interstitial fibrosis (fig. 4d).

Discussion

In this study we showed that MR antagonism with spironolactone administered 1 day before and 3 days posttransplant, with an accumulative dose exposure of spironolactone of 100 mg, reduced oxidative stress induced by the renal I/R phenomenon.

I/R injury is an inevitable consequence of renal transplantation and other organ solid transplants. During the organ procurement and the kidney transplant process, the graft suffered periods of warm and cold ischemia followed by a period of reinstitution of blood flow into the kidney after vascular anastomosis. In consequence, the variability in the periods of renal ischemia results in different degrees of renal injury [for review, see 33]. In this regard, Mehrotra et al. [34] demonstrated that renal transplant recipients who developed AKI, without dialysis requirement, had both an increased risk of graft loss (hazard ratio 2.74, 95% CI 2.56–2.92) and an increased risk of death (hazard ratio 2.36, 95% CI 2.14–2.60), whereas in patients with severe AKI and dialysis requirement, the hazard ratio for graft loss increased to 7.35 (95% CI 6.32–8.54).

In addition, studies from both humans and animals have demonstrated that I/R injury may contribute to

Table 2. Characteristics of the patients with slow graft function

No.	Gender	Age	Group	SCr (basal) mg/dl	SCr (at day 5) mg/dl	Biopsy findings (Banff 2011)	Adverse events
1	female	18	spironolactone	3.20	3.49	mixed rejection	urinary tract infection (*E. coli* BLEE); graft compression venous
2	male	30	spironolactone	7.53	4.24	acute cellular rejection	ventilator associated pneumonia
3	male	54	spironolactone	10.85	7.74	acute tubular necrosis	
4	male	21	placebo	15.60	2.80	borderline alterations	

graft rejection secondary to an increased expression of major histocompatibility complex (MHC) class II, acute tubular necrosis, and to the progressive renal dysfunction [4, 35, 36].

The main events described after renal ischemic injury are a consequence of the cessation of arterial blood flow and include depletion of adenosine 5′-triphosphate [37], phospholipase A_2 activation which initiates the arachidonic acid cascade, alteration in the autoregulation of blood flow [38, 38], activation of local inflammation [39–42], generation of ROS [43–46], reduction in vascular density [47, 48], epithelial cell cycle arrest in G2/M [49], epigenetic changes in fibroblast [50], among others.

The improvement in the understanding of molecular basis of I/R pathophysiology has contributed to the development of therapeutic interventions in preventing or ameliorating the deleterious effects of this phenomenon. However, it is still necessary to explore new interventions with a greater impact on the graft survival in the long term.

Several experimental studies from our laboratory and others have shown that aldosterone plays an important role in the physiopathology of the ischemic process, such as acute and chronic cyclosporine nephrotoxicity or in the I/R model [25–30, 51–53]. Interestingly, we have shown that spironolactone treatment before [28] or after ischemia [29], as well as adrenal gland removal [30], completely prevents AKI in rats undergoing bilateral renal ischemia, suggesting that aldosterone is a key molecule in mediating renal injury by an ischemic process and that the MR antagonism, even after ischemia, is a helpful strategy to prevent AKI.

In this exploratory randomized and double-blind study performed in renal transplant patients, spironolactone administration before and after renal transplant was not able to improve renal function or modify the urinary biomarker levels of tubular injury. In addition, we observed that 4 patients, 1 from the placebo group and 3 from the spironolactone group, exhibited slow graft function. This finding was unexpected and because 2 patients exhibited acute humoral and cellular rejection as was clearly shown by the histopathological analysis, we believe that these events are not related with the use of spironolactone, but could be in part explained by the fact that this protocol just started a few weeks after the surgical team changed from open nephrectomy to a hand-assisted laparoscopic technique, evidencing the effect of the learning curve on the development of slow graft function (unusual for living donor transplant). The slow graft function cases were not necessarily associated with longer periods of ischemia, but possibly related with a greater vascular manipulation and higher gas pressure (pneumoperitoneum). Additionally, we believe that the slow graft function events may contribute to overexpress HLA antigen and may favor the acute rejection episodes, because in these particular cases, calcineurin inhibitor administration was delayed and when we compared the first determination of serum tacrolimus levels posttransplant, the spironolactone group had lower tacrolimus levels than the placebo group (table 1).

It has been suggested that during the ischemic process aldosterone binding influences endothelial function and vascular tone [20, 21, 25, 30], thus we believe the lack of a spironolactone effect on renal function in these renal transplant recipients could in part be explained by either insufficient MR blockade or by the short period of treatment. This hypothesis is supported by recent studies in humans and mice in which a protective effect was reached when higher doses of eplerenone or spironolactone were used [54, 55]. Indeed,

Zhao et al. [54] recently demonstrated that the administration of 50 mg eplerenone during 2 weeks efficiently resolved retinal detachment and choroidal vasodilation in patients with central serous chorioretinopathy. Similarly, Quin et al. [55] showed that a high dose of eplerenone, around 200 mg/kg, reduced cardiac hypertrophy in transgenic mice overexpressing 11β-hydroxysteroid dehydrogenase type 2 in cardiomyocytes, a model that enhances aldosterone binding to the MRs in the heart.

There is enough evidence showing that another deleterious effect of aldosterone is mediated by its ability to promote ROS formation. In fact, in chronically infused aldosterone rats a significant increase in renal oxidative stress was clearly demonstrated [24, 56]. Moreover, Hayashi et al. [57] confirmed that the addition of aldosterone to rat cardiomyocytes increases both ROS and apoptotic cell death – effects that were prevented by the administration of eplerenone. Similarly, in kidney epithelial cells in culture (MMDD1) incubation with aldosterone increased superoxide production, an effect that was also blocked by the antagonism of MRs [58]. The increase in ROS induced by aldosterone appears to be mediated by the reduction in the expression of glucose-6-phosphate dehydrogenase (G6PDH), a cytosolic enzyme in the pentose phosphate pathway which maintains the adequate levels of reduced nicotinamide adenine dinucleotide phosphate (NADPH). Therefore, a decrease in G6PD activity renders a decrease in nitric oxide and an increase in ROS generation, exposing the cellular components to the oxidative damage [24]. Another mechanism by which aldosterone increases oxidative stress is through enhancing NADPH oxidase levels [59]. Accordingly, with all this evidence, in this study we found that transplant patients treated with spironolactone exhibited lower levels of oxidative stress. This renoprotective effect of spironolactone however was not reflected by a reduction in any of the tubular injury biomarkers assessed. It is possible that the low performance of the biomarkers to detect a lesser injury by ROS in spironolactone-treated patients may result from: (1) an excessive dilution on the biomarker concentration, because of the high urine output in the first 3 postoperative days; (2) by the low period of follow-up together with a little and limited exposure to the investigation drug, and (3) the sensitivity of the biomarker may be profoundly affected by the variability in the flow urine rate observed. Moreover, we decided to not normalize the urinary biomarker concentration by urinary creatinine for several reasons: rapid changes in the concentration of urinary creatinine in the posttransplant period, oliguria or polyuria that is observed in these transplant patients, and for differences in urinary flow rate, age, sex, weight and race.

We recognize that the major limitation of this study was the low number of randomized subjects included. This is an exploratory study because it is the first study to explore the MR blockade in renal transplant recipients and the aim was to obtain enough information to generate a new hypothesis for a larger collaborative study. Our findings suggest that oxidative stress observed in transplant patients is in part mediated by aldosterone and that MR antagonism was effective to reduce ROS generation. However, the long-term beneficial impact of this renoprotective effect must be evaluated in further and larger studies in recipients of a renal transplant from both living and deceased donors.

Acknowledgments

The authors are grateful to the members of the Molecular Physiology Unit for their suggestions and Dr. Norma Uribe for her comments about graft renal biopsies. The results presented here have not been published previously in whole or in part, except as an abstract presented at the American Transplant Congress 2012 (Boston, Mass., USA). This project was supported by grants from the Mexican Council of Science and Technology (CONACyT) (112780 and 181267 to N.A.B.) and from the National University of Mexico (IN203412-3 to N.A.B.). J.B.C. and M.O.C. are graduate students in the Biomedical Science and Medical Science PhD Program at Universidad Nacional Autónoma de México and were supported by a scholarship from CONACyT-Mexico.

References

1 Perico N, Cattaneo D, Sayegh MH, Remuzzi G: Delayed graft function in kidney transplantation. Lancet 2004;364:1814–1827.

2 Yarlagadda SG, Coca SG, Formica RN Jr, Poggio ED, Parikh CR: Association between delayed graft function and allograft and patient survival: a systematic review and meta-analysis. Nephrol Dial Transplant 2009;24:1039–1047.

3 Tilney NL, Guttmann RD: Effects of initial ischemia/reperfusion injury on the transplanted kidney. Transplantation 1997;64:945–947.

4 Goes N, Urmson J, Ramassar V, Halloran PF: Ischemic acute tubular necrosis induces an extensive local cytokine response. Evidence for induction of interferon-γ, transforming growth factor-β_1, granulocyte-macrophage colony-stimulating factor, interleukin-2, and interleukin-10. Transplantation 1995;59:565–572.

5 Schwarz C, Regele H, Steininger R, Hansmann C, Mayer G, Oberbauer R: The contribution of adhesion molecule expression in donor kidney biopsies to early allograft dysfunction. Transplantation 2001;71:1666–1670.
6 Koo DD, Welsh KI, Roake JA, Morris PJ, Fuggle SV: Ischemia/reperfusion injury in human kidney transplantation: an immunohistochemical analysis of changes after reperfusion. Am J Pathol 1998;153:557–566.
7 Saikumar P, Dong Z, Weinberg JM, Venkatachalam MA: Mechanisms of cell death in hypoxia/reoxygenation injury. Oncogene 1998;17:3341–3349.
8 Kourembanas S, Marsden PA, McQuillan LP, Faller DV: Hypoxia induces endothelin gene expression and secretion in cultured human endothelium. J Clin Invest 1991;88:1054–1057.
9 Bachmann S, Mundel P: Nitric oxide in the kidney: synthesis, localization, and function. Am J Kidney Dis 1994;24:112–129.
10 Pitt B, Zannad F, Remme WJ, et al: The effect of spironolactone on morbidity and mortality in patients with severe heart failure. Randomized Aldactone Evaluation Study Investigators. N Engl J Med 1999;341:709–717.
11 Rocha R, Stier CT Jr, Kifor I, et al: Aldosterone: a mediator of myocardial necrosis and renal arteriopathy. Endocrinology 2000;141:3871–3878.
12 Pitt B, Remme W, Zannad F, et al: Eplerenone, a selective aldosterone blocker, in patients with left ventricular dysfunction after myocardial infarction. N Engl J Med 2003;348:1309–1321.
13 Chrysostomou A, Pedagogos E, MacGregor L, Becker GJ: Double-blind, placebo-controlled study on the effect of the aldosterone receptor antagonist spironolactone in patients who have persistent proteinuria and are on long-term angiotensin-converting enzyme inhibitor therapy, with or without an angiotensin II receptor blocker. Clin J Am Soc Nephrol 2006;1:256–262.
14 Chrysostomou A, Becker G: Spironolactone in addition to ACE inhibition to reduce proteinuria in patients with chronic renal disease. N Engl J Med 2001;345:925–926.
15 Hostetter TH, Ibrahim HN: Aldosterone in chronic kidney and cardiac disease. J Am Soc Nephrol 2003;14:2395–2401.
16 Joffe HV, Adler GK: Effect of aldosterone and mineralocorticoid receptor blockade on vascular inflammation. Heart Fail Rev 2005;10:31–37.
17 Rocha R, Chander PN, Khanna K, Zuckerman A, Stier CT Jr: Mineralocorticoid blockade reduces vascular injury in stroke-prone hypertensive rats. Hypertension 1998;31:451–458.
18 Greene EL, Kren S, Hostetter TH: Role of aldosterone in the remnant kidney model in the rat. J Clin Invest 1996;98:1063–1068.
19 Schiffrin EL: Effects of aldosterone on the vasculature. Hypertension 2006;47:312–318.
20 Nguyen Dinh CA, Griol-Charhbili V, Loufrani L, et al: The endothelial mineralocorticoid receptor regulates vasoconstrictor tone and blood pressure. FASEB J 2010;24:2454–2463.
21 Griol-Charhbili V, Fassot C, Messaoudi S, Perret C, Agrapart V, Jaisser F: Epidermal growth factor receptor mediates the vascular dysfunction but not the remodeling induced by aldosterone/salt. Hypertension 2011;57:238–244.
22 Arima S, Kohagura K, Xu HL, et al: Nongenomic vascular action of aldosterone in the glomerular microcirculation. J Am Soc Nephrol 2003;14:2255–2263.
23 Gros R, Ding Q, Armstrong S, O'Neil C, Pickering JG, Feldman RD: Rapid effects of aldosterone on clonal human vascular smooth muscle cells. Am J Physiol Cell Physiol 2007;292:C788–C794.
24 Leopold JA, Dam A, Maron BA, et al: Aldosterone impairs vascular reactivity by decreasing glucose-6-phosphate dehydrogenase activity. Nat Med 2007;13:189–197.
25 Feria I, Pichardo I, Juarez P, et al: Therapeutic benefit of spironolactone in experimental chronic cyclosporine A nephrotoxicity. Kidney Int 2003;63:43–52.
26 Perez-Rojas JM, Derive S, Blanco JA, et al: Renocortical mRNA expression of vasoactive factors during spironolactone protective effect in chronic cyclosporine nephrotoxicity. Am J Physiol Renal Physiol 2005;289:F1020–F1030.
27 Perez-Rojas J, Blanco JA, Cruz C, et al: Mineralocorticoid receptor blockade confers renoprotection in preexisting chronic cyclosporine nephrotoxicity. Am J Physiol Renal Physiol 2007;292:F131–F139.
28 Mejia-Vilet JM, Ramirez V, Cruz C, Uribe N, Gamba G, Bobadilla NA: Renal ischemia-reperfusion injury is prevented by the mineralocorticoid receptor blocker spironolactone. Am J Physiol Renal Physiol 2007;293:F78–F86.
29 Sanchez-Pozos K, Barrera-Chimal J, Garzon-Muvdi J, et al: Recovery from ischemic acute kidney injury by spironolactone administration. Nephrol Dial Transplant 2012;27:3160–3169.
30 Ramirez V, Trujillo J, Valdes R, et al: Adrenalectomy prevents renal ischemia-reperfusion injury. Am J Physiol Renal Physiol 2009;297:F932–F942.
31 Barrera-Chimal J, Perez-Villalva R, Cortes-Gonzalez C, et al: Hsp72 is an early and sensitive biomarker to detect acute kidney injury. EMBO Mol Med 2011;3:5–20.
32 Ramirez V, Mejia-Vilet JM, Hernandez D, Gamba G, Bobadilla NA: Radicicol, a heat-shock protein 90 inhibitor, reduces glomerular filtration rate. Am J Physiol Renal Physiol 2008;295:F1044–F1051.
33 Simmons MN, Schreiber MJ, Gill IS: Surgical renal ischemia: a contemporary overview. J Urol 2008;180:19–30.
34 Mehrotra A, Rose C, Pannu N, Gill J, Tonelli M, Gill JS: Incidence and consequences of acute kidney injury in kidney transplant recipients. Am J Kidney Dis 2012;59:558–565.
35 Loutfi I, Batchelor JR, Lavender JP: Imaging and quantitation of renal transplant rejection in the rat by in vivo use of ^{111}In-labelled antilymphocyte and anti-class I and II major histocompatibility complex monoclonal antibodies. Transplant Proc 1991;23:2143–2146.
36 Azuma H, Nadeau K, Takada M, Mackenzie HS, Tilney NL: Cellular and molecular predictors of chronic renal dysfunction after initial ischemia/reperfusion injury of a single kidney. Transplantation 1997;64:190–197.
37 Green CJ, Gower JD, Healing G, Cotterill LA, Fuller BJ, Simpkin S: The importance of iron, calcium and free radicals in reperfusion injury: an overview of studies in ischaemic rabbit kidneys. Free Radic Res Commun 1989;7:255–264.
38 Conger JD, Robinette JB, Hammond WS: Differences in vascular reactivity in models of ischemic acute renal failure. Kidney Int 1991;39:1087–1097.
39 Donnahoo KK, Meng X, Ayala A, Cain MP, Harken AH: Meldrum DR. Early kidney TNF-α expression mediates neutrophil infiltration and injury after renal ischemia-reperfusion. Am J Physiol 1999;277:R922–R929.
40 Donnahoo KK, Meldrum DR, Shenkar R, Chung CS, Abraham E, Harken AH: Early renal ischemia, with or without reperfusion, activates NF-κB and increases TNF-α bioactivity in the kidney. J Urol 2000;163:1328–1332.
41 Lopez-Hernandez FJ, Lopez-Novoa JM: Role of TGF-β in chronic kidney disease: an integration of tubular, glomerular and vascular effects. Cell Tissue Res 2012;347:141–154.
42 Stroo I, Stokman G, Teske GJ, et al: Chemokine expression in renal ischemia/reperfusion injury is most profound during the reparative phase. Int Immunol 2010;22:433–442.
43 Basile DP, Leonard EC, Beal AG, Schleuter D, Friedrich JL: Persistent oxidative stress following renal ischemia reperfusion injury increases Ang II hemodynamic and fibrotic activity. Am J Physiol Renal Physiol 2012;302:F1494–F1502.
44 Schneider MP, Sullivan JC, Wach PF, et al: Protective role of extracellular superoxide dismutase in renal ischemia/reperfusion injury. Kidney Int 2010;78:374–381.
45 Xie J, Guo Q: Apoptosis antagonizing transcription factor protects renal tubule cells against oxidative damage and apoptosis induced by ischemia-reperfusion. J Am Soc Nephrol 2006;17:3336–3346.
46 Li C, Jackson RM: Reactive species mechanisms of cellular hypoxia-reoxygenation injury. Am J Physiol Cell Physiol 2002;282:C227–C241.

47 Basile DP, Friedrich JL, Spahic J, et al: Impaired endothelial proliferation and mesenchymal transition contribute to vascular rarefaction following acute kidney injury. Am J Physiol Renal Physiol 2011;300:F721–F733.
48 Basile DP, Donohoe D, Roethe K, Osborn JL: Renal ischemic injury results in permanent damage to peritubular capillaries and influences long-term function. Am J Physiol Renal Physiol 2001;281:F887–F899.
49 Yang L, Besschetnova TY, Brooks CR, Shah JV, Bonventre JV: Epithelial cell cycle arrest in G2/M mediates kidney fibrosis after injury. Nat Med 2010;16:535–543.
50 Bechtel W, McGoohan S, Zeisberg EM, et al: Methylation determines fibroblast activation and fibrogenesis in the kidney. Nat Med 2010; 16:544–550.
51 Macunluoglu B, Arikan H, Atakan A, et al: Effects of spironolactone in an experimental model of chronic cyclosporine nephrotoxicity. Transplant Proc 2008;40:273–278.
52 Thomson AW, McAuley FT, Whiting PH, Simpson JG: Angiotensin-converting enzyme inhibition or aldosterone antagonism reduces cyclosporine nephrotoxicity in the rat. Transplant Proc 1987;19:1242–1243.
53 Bobadilla NA, Gamba G: New insights into the pathophysiology of cyclosporine nephrotoxicity: a role of aldosterone. Am J Physiol Renal Physiol 2007;293:F2–F9.
54 Zhao M, Celerier I, Bousquet E, et al: Mineralocorticoid receptor is involved in rat and human ocular chorioretinopathy. J Clin Invest 2012;122:2672–2679.
55 Qin W, Rudolph AE, Bond BR, et al: Transgenic model of aldosterone-driven cardiac hypertrophy and heart failure. Circ Res 2003; 93:69–76.
56 Nishiyama A, Yao L, Nagai Y, et al: Possible contributions of reactive oxygen species and mitogen-activated protein kinase to renal injury in aldosterone/salt-induced hypertensive rats. Hypertension 2004;43:841–848.
57 Hayashi H, Kobara M, Abe M, et al: Aldosterone nongenomically produces NADPH oxidase-dependent reactive oxygen species and induces myocyte apoptosis. Hypertens Res 2008;31:363–375.
58 Zhu X, Manning RD Jr, Lu D, et al: Aldosterone stimulates superoxide production in macula densa cells. Am J Physiol Renal Physiol 2011;301:F529–F535.
59 Iwashima F, Yoshimoto T, Minami I, Sakurada M, Hirono Y, Hirata Y: Aldosterone induces superoxide generation via Rac1 activation in endothelial cells. Endocrinology 2008; 149:1009–1014.

Response to How confirm the specific effect of spironolactone in chronic kidney disease caused by ischemic acute kidney injury?

Journal:	*Kidney International*
Manuscript ID:	KI-03-13-0345
Manuscript Type:	Response Letter to the Editor
Date Submitted by the Author:	12-Mar-2013
Complete List of Authors:	Barrera-Chimal, Jonatan; Instituto de Investigaciones Biomedicas, Universidad Nacional Autónoma de México e Instituto Nacional de Ciencias Médicas y Nutrición Salvador Zubirán, Unidad de Fisiología Molecular Bobadilla, Norma; Instituto de Investigaciones Biomedicas, Universidad Nacional Autónoma de México e Instituto Nacional de Ciencias Médicas y Nutrición Salvador Zubirán, Unidad de Fisiología Molecular
Keywords:	acute kidney injury, chronic kidney disease, aldosterone
Subject Area:	Acute Kidney Injury, Chronic Kidney Injury

Response to: How to confirm the specific effect of spironolactone in chronic kidney disease caused by ischemic acute kidney injury?

by

Jonatan Barrera-Chimal and Norma A. Bobadilla

Molecular Physiology Unit,

Instituto de Investigaciones Biomédicas, Universidad Nacional Autónoma de México and

Instituto Nacional de Ciencias Médicas y Nutrición Salvador Zubirán,

Mexico City, Mexico

Corresponding author:
Norma A. Bobadilla, PhD
Unidad de Fisiología Molecular
Vasco de Quiroga No. 15,
Tlalpan, 14000
México City
Tel.: 5255-5485-2676
Fax: 5255-5655-0382
nab@biomedicas.unam.mx
norma.bobadillas@quetzal.innsz

We thank Drs. Chow and Lin for their observation (1)that allowed us to further expand the results of our findings. Previously, we showed that mineralocorticoid receptor blockade (MRB) or adrenalectomy prevented renal damage induced by a mild ischemic period (20 min) (2) (3). In our recently published study (4), rats were exposed to a severer ischemic injury (45 min) observing that MRB before or after the ischemic insult prevented CKD development, which was associated with a reduction in AKI severity, as was evidenced by a lower proteinuria 24-h after reperfusion (Figure 1A, (4)). Here, we added a new set of rats underwent 45 min of bilateral ischemia and studied after 24-h, as is shown in Figure 1. The prophylactic MRB only partially protected these animals as is exhibited by Hsp72 urinary levels (Figure 1D) (5). These results emphasize that the degree of AKI was lower than in untreated rats. In spite of the complete restoration of renal function observed after 10 days of ischemia, MRB was effective enough to prevent the increased signaling of inflammation and fibrosis pathways (Figure 1E and 1F, (4)) that is not seen in ischemic untreated rats. So, we believe MRB not only reduced the severity of AKI, but also it avoided other aldosterone detrimental effects. We agree with Drs. Chow and Lin that will be necessary to see the time course of these pathways to know with more precision the effects of aldosterone leading to long-term development of CKD. Indeed this is a part of another ongoing project in our laboratory.

Figure legend:

Severe ischemic injury is partially prevented by prophylactic spironolactone administration. A) Renal blood flow, in the sham (o), bilateral renal ischemia (•), and rats receiving spironolactone (20 mg/K of BW) three days before ischemia (•), B) serum creatinine and C) urinary protein excretion, and D) urinary heat shock protein 72 (Hsp72). *p<0.05 vs. the sham group and ¥p<0.05 vs. the I/R untreated group.

References

1. Chou YH and Lin SL How to confirm the specific effect of spironolactone in chronic kidney disease caused by ischemic acute kidney. Kidney Int. This issue.

2. Mejia-Vilet JM, Ramirez V, Cruz C *et al.* Renal ischemia-reperfusion injury is prevented by the mineralocorticoid receptor blocker spironolactone. *Am J Physiol Renal Physiol* **293**(Issue):F78-F86, 2007
3. Ramirez V, Trujillo J, Valdes R *et al.* Adrenalectomy prevents renal ischemia-reperfusion injury. *Am J Physiol Renal Physiol* **297**(Issue):F932-F942, 2009
4. Barrera-Chimal J, Perez-Villalva R, Rodriguez-Romo R *et al.* Spironolactone prevents chronic kidney disease caused by ischemic acute kidney injury. *Kidney Int* **83**(Issue):93-103, 2013
5. Barrera-Chimal J, Perez-Villalva R, Cortes-Gonzalez C *et al.* Hsp72 is an early and sensitive biomarker to detect acute kidney injury. *EMBO Mol Med* **3**(Issue):5-20, 2011

Figure 1

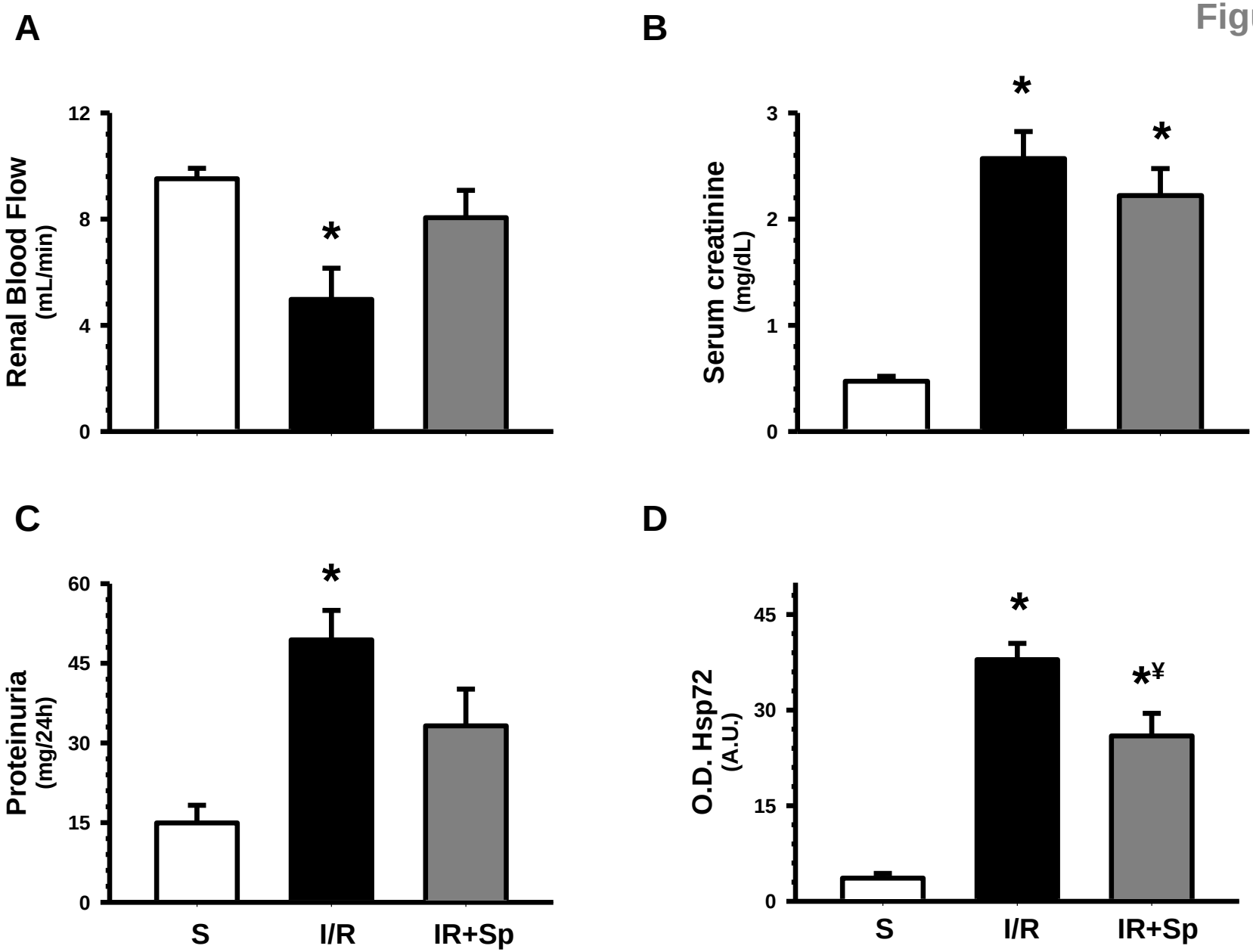
A
Renal Blood Flow
(mL/min)
12
8
4
0
*
B
Serum creatinine
(mg/dL)
3
2
1
0
*
*
C
Proteinuria
(mg/24h)
60
45
30
15
0
*
D
O.D. Hsp72
(A.U.)
45
30
15
0
*
*¥
S
I/R
IR+Sp
S
I/R
IR+Sp

VIII. ARTÍCULOS EN REVISIÓN

American Journal of Transplantation

Intra-renal transfection of heat shock protein 90 alpha or beta (Hsp90α or Hsp90β) protects against ischemia/reperfusion injury

Journal:	*American Journal of Transplantation*
Manuscript ID:	AJT-O-13-00468
Wiley - Manuscript type:	O - Original Article
Date Submitted by the Author:	08-Apr-2013
Complete List of Authors:	Barrera-Chimal, Jonatan; Instituto de Investigaciones Biomédicas, Universidad Nacional Autónoma de México and Instituto Nacional de Ciencias Médicas y Nutrición Salvador Zubirán, Molecular Physiology Unit, Pérez-Villalva, Rosalba; Instituto de Investigaciones Biomédicas, Universidad Nacional Autónoma de México and Instituto Nacional de Ciencias Médicas y Nutrición Salvador Zubirán, Molecular Physiology Unit, Ortega-Trejo, Juan Antonio; Instituto de Investigaciones Biomédicas, Universidad Nacional Autónoma de México and Instituto Nacional de Ciencias Médicas y Nutrición Salvador Zubirán, Molecular Physiology Unit, Uribe-Uribe, Norma; Instituto Nacional de Ciencias Médicas y Nutrición Salvador Zubirán, Pathology Gamba, Gerardo; Instituto de Investigaciones Biomédicas, Universidad Nacional Autónoma de México and Instituto Nacional de Ciencias Médicas y Nutrición Salvador Zubirán, Molecular Physiology Unit, Cortés-González, Cesar; Instituto Nacional de Cancerología, Unidad de Investigación Biomédica en Cáncer Bobadilla, Norma; Instituto de Investigaciones Biomédicas, Universidad Nacional Autónoma de México and Instituto Nacional de Ciencias Médicas y Nutrición Salvador Zubirán, Molecular Physiology Unit,
Keywords:	nitric oxide, renal injury, renal ischemia reperfusion injury, animal models, renal blood flow

American Journal of Transplantation

Urinary Neutrophil Gelatinase-Associated Lipocalin Predicts Graft Loss after Acute Kidney Injury in Kidney Transplant

Journal:	*American Journal of Transplantation*
Manuscript ID:	AJT-B-13-00357
Wiley - Manuscript type:	B - Brief Communication
Date Submitted by the Author:	17-Mar-2013
Complete List of Authors:	Ramirez-Sandoval, Juan Carlos; Instituto Nacional de Ciencias Médicas y Nutrición Salvador Zubirán, Nephrology and Mineral Metabolism Barrera-Chimal, Jonatan; Instituto de Investigaciones Biomédicas, Universidad Nacional Autónoma de México, ; Instituto Nacional de Ciencias Médicas y Nutrición Salvador Zubirán, Nephrology and Mineral Metabolism Simancas, Perla E.; Instituto Nacional de Ciencias Médicas y Nutrición Salvador Zubirán, Nephrology and Mineral Metabolism Rojas-Montaño, Alejandro; Instituto Nacional de Ciencias Médicas y Nutrición Salvador Zubirán, Nephrology and Mineral Metabolism Correa-Rotter, Ricardo; Instituto Nacional de Ciencias Médicas y Nutrición Salvador Zubirán, Nephrology and Mineral Metabolism Bobadilla, Norma A.; Instituto de Investigaciones Biomédicas, Universidad Nacional Autónoma de México, ; Instituto Nacional de Ciencias Médicas y Nutrición Salvador Zubirán, Nephrology and Mineral Metabolism Morales-Buenrostro, Luis E.; Instituto Nacional de Ciencias Médicas y Nutrición Salvador Zubirán, Nephrology and Mineral Metabolism
Keywords:	allograft loss, biomarker, kidney injury, graft outcome, prognostic factors, acute graft failure

IX. Artículos en preparación

1) Aguilar-Carrasco JC, Pérez-Villalva R, Barrera-Chimal J, Reyna J and Bobadilla NA. Hsp72 is an early and sensitive biomarker of acute kidney injury induced by cisplatin and acetaminophen.

2) Salas-Nolasco O, Barrera-Chimal J, Casas-Aparicio G, Irizar-Santana S, Pérez-Villalva R, Correa-Rotter R, Bobadilla NA and Morales-Buenrostro LE. Heat shock protein 72 (Hsp72) is a novel biomarker to predict acute kidney injury in critical care patients.

3) Rodríguez-Romo R, Barrera-Chimal J, Benítez K, Pérez-Villalva R, Gamba G and Bobadilla NA. Losartan retards the developmemnt of chronic kidney disease after an acute kidney injury episode